Some kinetic and equilibrium studies of -adduct formation and proton transfer in the reactions of aromatic nitro-compounds with bases

Paul James Routledge

SOME KINETIC AND EQUILIBRIUM STUDIES OF σ-ADDUCT FORMATION AND PROTON TRANSFER IN THE REACTIONS OF AROMATIC NITRO-COMPOUNDS WITH BASES

by

PAUL JAMES ROUTLEDGE, B.Sc. (Durham)

(Graduate Society)

A thesis submitted for the degree of Doctor of Philosophy in the University of Durham, 1983

DECLARATION

The material in this thesis is the result of research carried out in the Department of Chemistry, University of Durham, between October 1980 and June 1983. It has not been submitted for any other degree, and is the author's own work, except where acknowledged by reference.

ABSTRACT

Some Kinetic and Equilibrium Studies of σ-Adduct Formation and Proton Transfer in the Reactions of Aromatic Nitro-compounds with Bases.

by Paul James Routledge.

Comparison of kinetic and equilibrium data for the cyclisation of 1-(2,2-dimethyl-3-hydroxypropoxy)-2,4-dinitronaphthalene in alkaline media with those for the cyclisation of 1-(3-hydroxypropoxy)-2,4-dinitronaphthalene indicates the absence of a marked gem-dimethyl effect.

^{1}H n.m.r. and visible spectral measurements show that alkoxide addition to 2,2′,4,4′,6,6′-hexanitrobibenzyl (HNBB) and 2,2′,4,4′,6,6′-hexanitrostilbene (HNS) gives σ-adducts. Formation of the 3-(3′-) adduct is kinetically preferred but the 1-(1′-) adduct is thermodynamically more stable. In media of high basicity the 1:2 adduct with alkoxide addition at the 1- and 1′- positions is observed. For HNS a third interaction occurs which may be alkoxide addition at the olefinic bond. Kinetic and equilibrium data are reported for the reactions with methoxide ions in methanol and ethoxide ions in ethanol and compared with data for related compounds.

The interactions of aliphatic amines with 2,4,6-trinitrobenzyl chloride (TNBCl), HNBB, HNS and 2,4,6-trinitrophenetole (TNP) in dimethyl sulphoxide have been investigated using visible and ^{1}H n.m.r. spectroscopic methods. Kinetic and equilibrium data are reported for the various processes observed.

The reversible reactions of TNBCl with primary amines are found to be: rapid formation of the 3-adduct, followed by isomerisation to the thermodynamically more stable 1-adduct, follow

by equilibration with the conjugate base formed by transfer of a side-chain proton. With the secondary amines piperidine and pyrrolidine, σ-adduct formation at the 1-position is not observed because the presence of two bulky groups at the 1-position is sterically unfavourable. The σ-adduct forming reactions occur *via* zwitterionic intermediates and it is shown that proton transfers between these species and amines may be kinetically significant.

The reactions of HNBB and HNS with amine also involve the initial formation of 3-adducts and 1-adducts. At high amine concentrations di-adducts may be formed by reaction of the 1- and 1′- or 3- and 3′- positions. A slow reaction of HNBB with amines gives a blue species which is shown to be a dianion formed by loss of two methylene protons. The slow step in this reaction is shown to be rate limiting proton transfer from the substrate or from 1:1 σ-adducts.

TNP reacts with primary and secondary amines to give isomeric σ-adducts at the 3-position and 1-position. Nucleophilic substitution involves general acid catalysed expulsion of the ethoxy group and yields N-substituted picramides.

Data are also reported for the reactions of TNBCl with hydroxide ions in water and 30:70 (v/v) DMSO-water, of TNBCl with hydroxide ions in mixed (methanol-water-tetrahydrofuran) solvents, of HNBB with sulphite ions and of 1,3,5-trinitrobenzene with thioglycollic acid in water.

PUBLICATIONS

Some of the work reported in this thesis has been the subject of the following papers:

The Stabilities of Meisenheimer Complexes. Part 27. The Effects of gem-Dimethyl Substitution and Ring Size on Spiro-complex Formation.

J.Chem.Res., 1981, (S) 152; (M) 1972.

(with Dr. M.R. Crampton and P.M. Wilson)

The Stabilities of Meisenheimer Complexes. Part 28. The Reactions of 2,2′,4,4′,6,6′-Hexanitrobibenzyl with Alkoxides.

J.Chem.Soc., Perkin Trans.2, 1982, 31.

(with Dr. M.R. Crampton, Dr. G.C. Corfield, R.M. King and Dr. P. Golding).

The Stabilities of Meisenheimer Complexes. Part 31. The Reactions of 2,2′,4,4′,6,6′-Hexanitrostilbene with Alkoxides.

J.Chem.Soc., Perkin Trans.2, 1982, 1621.

(with Dr. M.R. Crampton and Dr. P. Golding).

The stabilities of Meisenheimer Complexes. Part 33. Kinetic Studies of the Formation of Isomeric σ-Adducts from 2,4,6-Trinitrobenzyl Chloride and Aliphatic Amines in Dimethyl Sulphoxide.

J.Chem.Soc., Perkin Trans.2, 3/1038.

(With Dr. M.R. Crampton and Dr. P. Golding).

The Stabilities of Meisenheimer Complexes. Part 34. Kinetic Studies of σ-Adduct Formation and Nucleophilic Substitution in the Reactions of 2,4,6-Trinitrophenetole with Aliphatic Amines in Dimethyl Sulphoxide.

J.Chem.Soc., Perkin Trans.2, 3/1336.

(with Dr. M.R. Crampton).

The stabilities of Meisenheimer Complexes. Part 35. Dianion Formation by Proton Transfer from 2,2′,4,4′,6,6′-Hexanitrobibenzyl to Amines.

J.Chem.Res., in the press.

(with Dr. M.R. Crampton and Dr. P. Golding).

The Stabilities of Meisenheimer Complexes. Part 36. The Reaction of 2,4,6-Trinitrobenzyl Chloride with Sodium Hydroxide in water.

In preparation.

(with Dr. M.R. Crampton and Dr. P. Golding).

The Stabilities of Meisenheimer Complexes. Part 37. Kinetic and Equilibrium Studies of the Reactions of 2,2′,4,4′,6,6 Hexanitrobibenzyl with Aliphatic Amines in Dimethyl Sulphoxide.

J.Chem.Soc., Perkin Trans.2, to be submitted.

(with Dr. M.R. Crampton and Dr. P. Golding).

The Stabilities of Meisenheimer Complexes. Part 38. Kinetic and Equilibrium Studies of the Reactions of 2,2′,4,4′,6,6′-Hexanitrostilbene with Aliphatic Amines in Dimethyl Sulphoxide.

J.Chem.Soc., Perkin Trans.2, to be submitted

(with Dr. M.R. Crampton and Dr. P. Golding).

ACKNOWLEDGEMENTS

I would like to thank my supervisor, Dr. M.R. Crampton, for his constant help and guidance during this work and in the preparing of this thesis. Thanks are also due to Dr. P. Golding, Ministry of Defence, P.E.R.M.E., for the many informative discussions I had with him throughout my three years of research.

I would also like to thank the academic, technical and student members of the department who have helped in any way.

I thank the Ministry of Defence for providing the maintenance grant that enabled me to do this research.

Finally, I would like to thank Mrs. Marion Wilson for typing this thesis and her invaluable help with its preparation, and also to my brother Martin for his help with the proof reading.

To My Family

and

West Ham United Football Club

"Any fool can measure rates of reactions,
but it sometimes takes a genius to
interpret the results."

Professor Charles Vernon,
University College, London.

PREFACE

The work reported in this thesis was instigated by the Propellants, Explosives and Rocket Motor Establishment (P.E.R.M.E.), Waltham Abbey, which is part of the Ministry of Defence. Using a continuous production process based on the Shipp-Kaplan reaction[2], they are commercially producing the heat resistant explosive 2,2´,4,4´,6,6´-hexanitrostilbene (HNS) from 2,4,6-trinitrotoluene (TNT). The complete reaction mechanism by which the Shipp-Kaplan reaction proceeds is unknown. However, because intense colours are observed during the reaction one possibility is that Meisenheimer complexes are involved as intermediates. In the hope of elucidating the Shipp-Kaplan reaction mechanism it was therefore of interest to study the mode or modes of interaction of bases with HNS and also with 2,2´,4,4´,6,6´-hexanitrobibenzyl (HNBB), a major by-product of the Shipp-Kaplan reaction. (The interaction of bases with TNT have already been studied[82,83]). This is one reason why the study of the compounds HNS and HNBB forms such a prominent part in this thesis.

The other aromatic nitro-compounds, reported in this thesis, have been studied because their interactions with base can be directly compared with those of HNS and HNBB to give a more complete understanding of the processes involved, or because they are of interest in other areas of Meisenheimer complex chemistry, or for both the above reasons.

It should be noted that the introduction consists of two unequal parts. The first part will give some background information on the Shipp-Kaplan reaction and the second part

should provide the reader with a basic knowledge of Meisenheimer complex chemistry, which will help in the understanding of the experimental data reported in the rest of the thesis.

CONTENTS

Page No.

Page No.

CHAPTER ONE

INTRODUCTION

1.1 The Shipp-Kaplan Reaction

Shipp[1] first unequivocally synthesised 2,2´,4,4´,6,6´-hexanitrostilbene (HNS) from 2,4,6-trinitrotoluene (TNT) and m-hydroxybenzaldehyde using a five stage process. The Shipp-Kaplan reaction[2] is a continuous process used commercially to synthesise HNS from TNT using aqueous sodium hypochlorite in a 2:1:2 tetrahydrofuran/methanol/water solvent at 0-15°C. The yield of HNS obtained by this process is limited to about 50% due to several concurrent reactions producing a large number of by-products in the complex reaction mixture. The major by-product is 2,2´,4,4´,6,6´-hexanitrobibenzyl (HNBB) which, in the appropriate conditions, can become the principle product.

HNS has two important properties. It is a heat resistant explosive, used by the aerospace industry for the explosive components of high speed aircraft and spacecraft, and it is a crystal modifying agent used in melt cast TNT-based explosive compositions.[3] The Apollo 17 Lunar Seismic Profiling Experiment used HNS for its explosive charges.[4]

The reaction mechanism postulated by Shipp and Kaplan[2] for the formation of HNS from TNT by alkaline hypochlorite is shown in Scheme 1.1. The first stage is the formation of 2,4,6-trinitrobenzyl chloride (TNBCl) from TNT. This has been shown by quenching the reaction mixture after 90 seconds with acid and obtaining yields of TNBCl of 85%.[68] The second stage is the formation of HNS from TNBCl. This involves postulating the formation of the TNBCl anion which then undergoes a nucleophilic displacement-elimination reaction with a molecule of TNBCl to form HNS. Scheme 1.2 shows this part of the reaction

Scheme 1.1

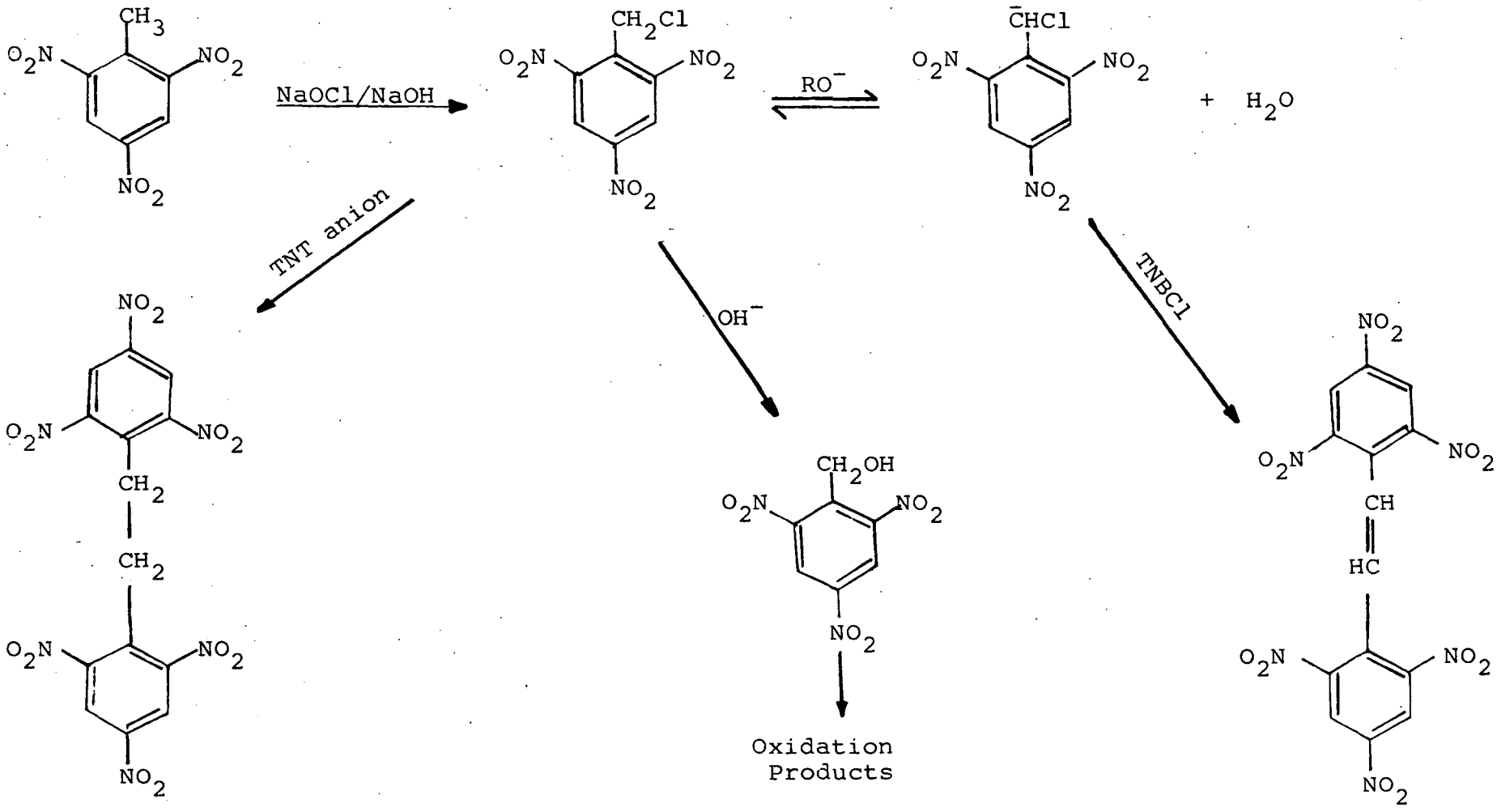
NaOCl/NaOH
RO⁻
+ H2O
TNT anion
OH⁻
TNBCl
Oxidation Products
HNBB
HNS

Scheme 1.2

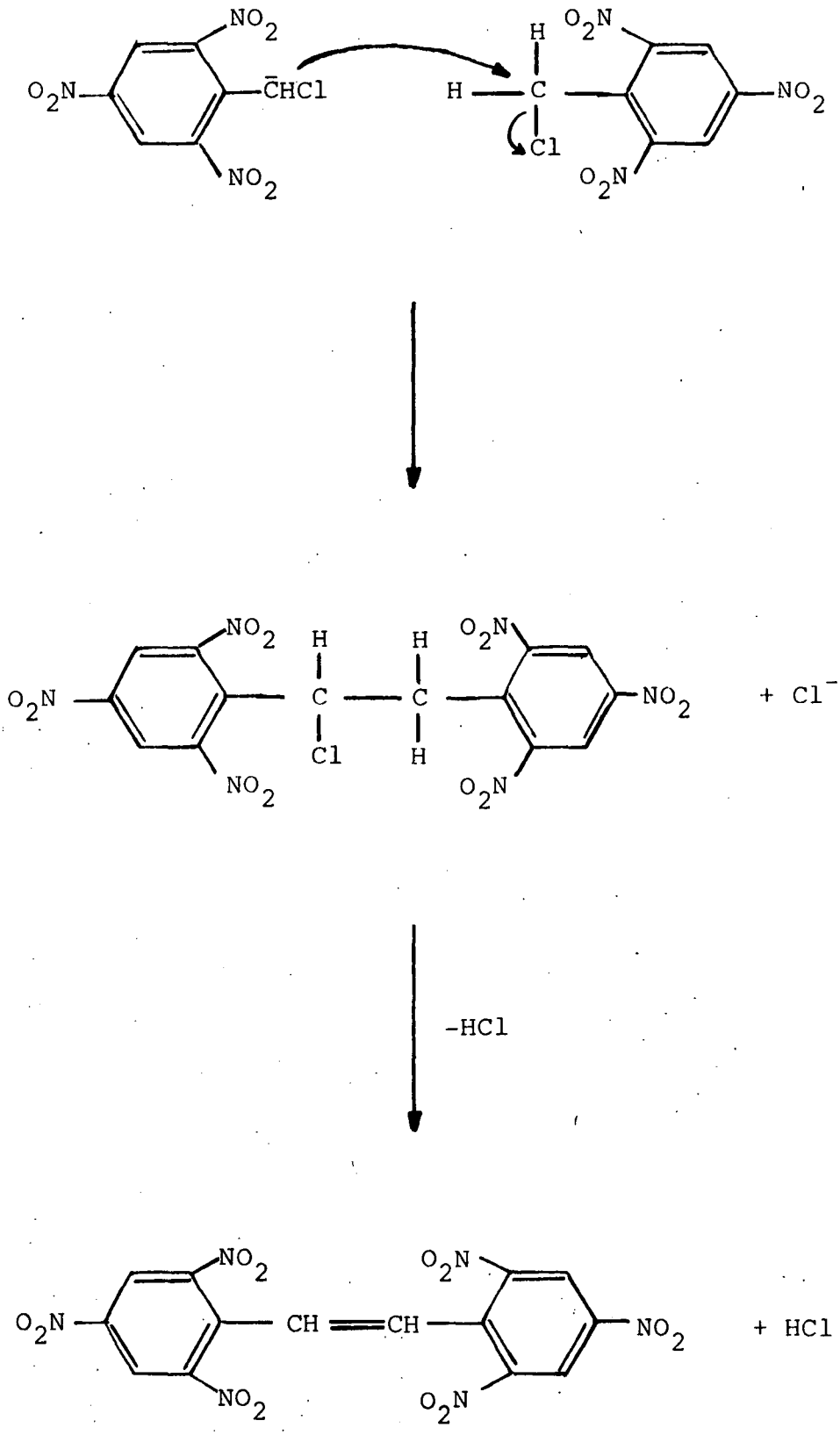
NO2
O2N
CHCl
NO2
H
C
Cl
O2N
NO2
O2N
H
C
H
C
Cl
H
NO2
O2N
NO2
O2N
+ Cl−
-HCl
NO2
O2N
CH
CH
NO2
O2N
NO2
O2N
+ HCl

more clearly. The TNBCl anion displaces a molecule of TNBCl to form α-chlorohexanitrobibenzyl. This then immediately eliminates hydrogen chloride to produce HNS. Also present in the reaction mixture are TNT anions and other nucleophiles such as hydroxide ions. These can also undergo displacement reactions with a molecule of TNBCl to produce HNS and trinitrobenzyl alcohol respectively, and thereby reduce the yield of HNS.

To support the nucleophilic displacement-elimination reaction Shipp and Kaplan presented evidence[2] that the yield of HNS was dependent on the mole ratio of alkali to trinitrobenzyl chloride while all other conditions were maintained constant. They also showed HNS could be made by adding base to TNBCL but could not isolate any α-chlorohexanitrobibenzyl. α-Chlorohexanitrobibenzyl would be expected to be very unstable as even unnitrated α-chlorobibenzyl readily eliminates hydrogen chloride to form the stilbene.[5]

A free radical mechanism has been suggested as was found for the synthesis of 4,4´-dinitrostilbene from 4-nitrobenzyl chloride.[6] However, free radical intermediates of aromatic trinitro-compounds are rare as they prefer to form anions.[7]

Kinetic evidence for a nucleophilic displacement-elimination mechanism has been reported[8] but the study was carried out in a 50/50 dioxalan-water solvent with hydroxide as the base. Below it will be shown that by changing the solvent the type of reaction can be changed and also it is known that it is critical for an alcohol to be present in the Shipp-Kaplan reaction.[9]

Further study of the Shipp-Kaplan reaction has shown the yield of HNS is profoundly effected by changing the pH and water content of the reaction mixture, and to a lesser extent by changing the temperature and time of the reaction.

Maximum yields of HNS are achieved at a pH of 10.2.[10] It has also been found[11] yields of HNS are maximised by the presence of organic amine bases, with pK_a values of 10 to 11, in the reaction mixture, irrespective of their steric structure. Sollot[12] believes the reason why these organic amine bases are good at maximising yields is that they regulate the concentration of hydroxide ions in a constant and controlled manner.

If the initial temperature of the exothermic reaction is kept below 5°C for the first minute and then allowed to rise to 15-20°C maximum yields of HNS are obtained.[9] If kept below 5°C for the whole reaction the yields of HNS are usually low.

A study[9] of HNS yield versus time has shown the yield of HNS increases with time up to 120 minutes and thereafter falls steadily.

The concentration of water present in the reaction mixture has a profound effect on the yield of HNS.[9] Shipp patented her reaction with what was later found to be the preferred water content.[2]

The addition of alkaline oxides,[13] in particular calcium oxide, may slow down the Shipp-Kaplan reaction considerably but pure HNS is produced, the formation of which increases with time. The need for critical pH control is also removed. It is postulated that the function of calcium oxide is in stabilising key intermediates by complexation.

1.2 A Survey of Meisenheimer Complex Chemistry

1.2.1 A Short History

Hepp[14] over one hundred years ago observed that intense colours are produced on the addition of base to solutions of aromatic trinitro-compounds. A little later it was found[15-18] that in favourable cases highly coloured solids could be isolated. By 1900 Jackson and Gazzolo[19] had postulated that the quinonoid structure (1.1) was responsible for the coloured species. But it was Meisenheimer,[20] in 1902, who first produced strong chemical evidence which supported the quinonoid structure for the complex (1.1; R = Me, R′= Et),

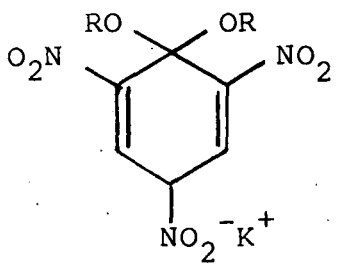

(1.1)

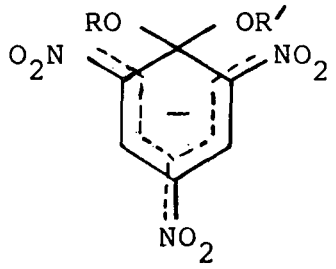

(1.2)

followed a year later by Jackson and Earle[21] when they prepared (1.1; R = Et, R′ = Isonyl). Since then modern spectroscopic and crystallographic methods (see later) have confirmed this general structure for the coloured complexes, although today they are usually represented as having the negative charge delocalised around the ring, as shown by (1.2).

It is chemically correct to refer to a species such as (1.2) as an anionic σ-adduct, but they are popularly referred

to in the literature as Meisenheimer complexes in deference to Meisenheimer's original evidence.[20] However, over the years they have also been called Jackson-Meisenheimer complexes, cyclohexadienate ions, σ-adducts, and for σ-adducts such as (1.4), where nucleophilic attack has occurred at an unsubstituted ring position, Servis complexes.

After Meisenheimer and Jackson there was little interest in Meisenheimer complexes until the ninteen fifties when Bunnett[22,23] proposed that most nucleophilic aromatic substitution (S_NAr) reactions involving activated substrates and good leaving groups should proceed by a two step mechanism *via* an intermediate analogous to (1.2). This stimulated interest in Meisenheimer complexes again and from the mid-nineteen fifties techniques were developed, or invented, to allow investigations into the structures, the stabilities and the kinetics of Meisenheimer complexes. Since the early nineteen sixties there has been an accelerating growth in the reports of kinetic and thermodynamic studies of Meisenheimer complexes.

All the complexes in Figure 1.1 have now been reported for benzene derivatives containing three electron withdrawing groups (EWG); their formation and stability depending on the following factors:

(i) The type of nucleophile

e.g. Nu = MeO^-, SO_3^{2-}, or $RR'NH_2$

(ii) The concentration of nucleophiles.

(iii) The type of solvent used

e.g. aprotic, protic or aprotic/protic mixtures

Figure 1.1

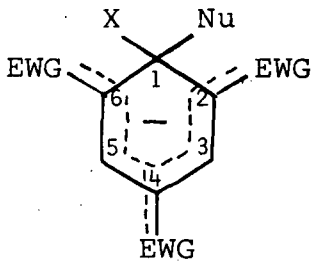

(1.3)

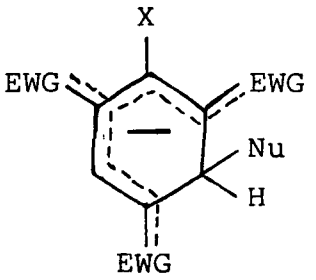

(1.4)

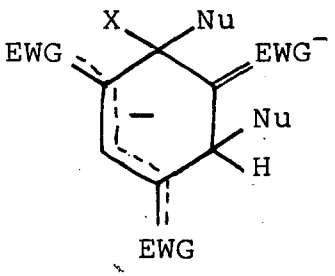

(1.5)

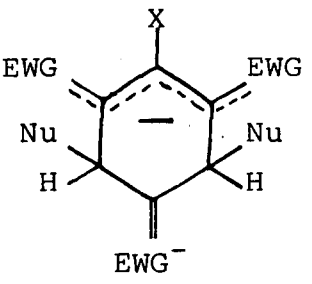

(1.6)

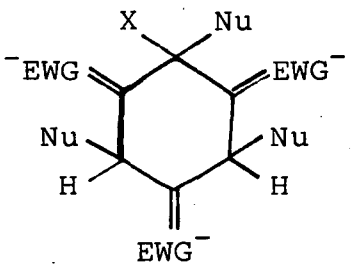

(1.7)

(iv) The type of substituent on the benzene ring

e.g. X = H, Me, or MeO^-.

(v) The type of electron withdrawing group

e.g. E.W.G. = NO_2, CF_3SO_2, CN or various combinations.

The Meisenheimer complexes in Figure 1.2 are known as spiro-complexes. They are formed by intramolecular nucleophilic attack. Z and Y may consist of O, S or NR groups. Again their formation and stability is dependent on the factors (iii), (iv) and (v) given above, and the concentration of base.

The rest of this chapter will be mainly concerned with the Meisenheimer complexes formed between aromatic trinitro-compounds and nucleophiles. A fuller description of the numerous Meisenheimer complexes that are formed, by the reaction of nucleophiles with a variety of activated homoaromatic and heteroaromatic substrates, is contained in several excellent reviews[24-28] on Meisenheimer complexes, the most recent of which are by Terrier[27] and Beletskaya *et al.*[28] Also to be published shortly is a book[29] on Meisenheimer complexes by some of the most distinguished workers in this area of chemistry today.

Figure 1.2

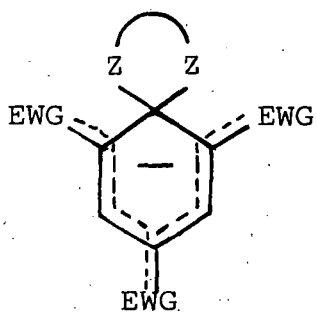

(1.8)

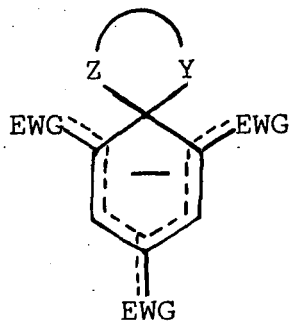

(1.9)

1.2.2 Nomenclature

To differentiate between isomeric σ-adducts the position of nucleophilic addition to the substrate is used. The aromatic carbons of the substrate are numbered in the conventional way (see (1.3)) with the substituent X at the 1-position. For example, if Nu = OR then (1.3) is the 1-alkoxy adduct while its isomer (1.4) is the 3-alkoxy adduct. Because the complexes (1.3) and (1.4) are formed from the addition of one molecular equivalent of nucleophile to substrate they are also referred to as 1:1 or mono-adducts. Where complexes are formed from the addition of two or three equivalents of nucleophile they are referred to as 1:2 or di-adducts and 1:3 or tri-adducts respectively. It is also possible for di-adducts such as (1.5) and (1.6) to exhibit cis/trans isomerism while there are four possible steroisomers for the tri-adduct (1.7).

In this thesis substrates where two picryl rings are separated by a hydrocarbon link have been studied. Here it is possible to have a 1:2 or di-adduct such as (1.10) or (1.11) where there is one equivalent of nucleophile per ring of the substrate. The complex (1.10) will be referred to as a 1,1′-di-adduct and (1.11) as the 3,3′-di-adduct, and it is possible for both to exhibit cis/trans isomerism.

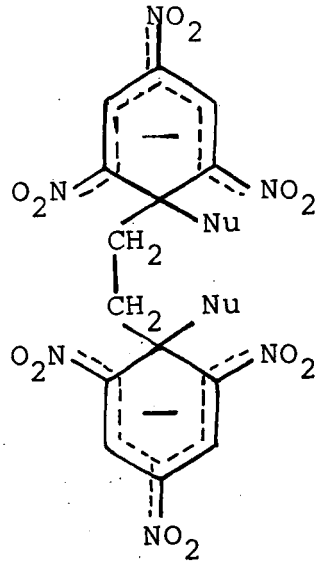

(1.10)

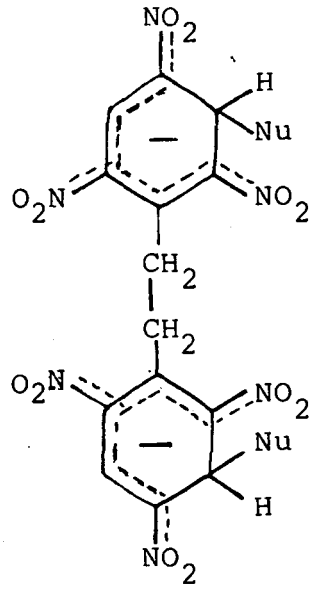

(1.11)

1.2.3 Theoretical Studies

A number of workers have now reported molecular orbital (MO) calculations of the electronic structures of Meisenheimer complexes and these have been summarised previously.[26,29,30] Some of the general features will be described briefly in this section.

It should be remembered that Meisenheimer complexes are usually produced in solution but M.O calculations refer to molecules in the gas phase and therefore take no account of solvation nor of ion association, which are important interactions in solution. Also the majority of calculations are based on the cyclopentadienyl system (1.12) or the hydride adduct (1.13), as it is assumed that varying the substituent on the tetrahydral carbon will have little effect.

(1.12)

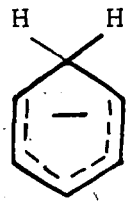

(1.13)

Simple Hückel Molecular Orbital (HMO) treatments of nucleophilic aromatic substitution have been given by Simonetta *et al.*[31] More detailed HMO treatments[32,33] have taken account of the steric crowding between alkoxy and ortho-nitro groups in the parent picryl ethers, and in the 1-alkoxy adducts formed from them. These studies indicate an increase in the charge on the nitro groups and a decrease in the charge on the ring carbons of the adduct compared to the parent. More sophisticated calculations[34,35] have been made using the method of composite molecules (CM), or using Pariser-Parr-Pople (PPP) type self consistent field (SCF) calculations, and differen conclusions have been reached to those given above. They indicate that the adduct has higher π electron density on both the ring and the nitro groups. PPPSCF calculations predict a greater share of π-charge on the nitro groups than on the ring carbons while CM calculations predict it is *vice versa*.

A few of the more interesting applications of M O calculations to Meisenheimer complexes will now be discussed briefly.

M O calculations can be used to predict electronic transitions and therefore the u.v.-visible spectra of Meisenheimer complexes. For example, PPPSCF calculations[35] have provided reasonably good agreement between the predicted and experimentally observed electronic transitions of Meisenheimer complexes.

The use of SCF-MO-CI type calculations[36] has provided confirmation that the nitro group is more effective than the cyano group at delocalising negative charge. It has also been shown,[37] using *ab initio* calculations[38] with STO-3G basis set of Pople *et al*,[39] that the electron withdrawing ability of the nitro group is constant and independent of any substituent in the ring. Using ^{17}O n.m.r. this has been found[37] experimentally. *Ab initio* calculations[40-42] have also been used with reasonable success to determine the relative stabilities of intermediates in S_NAr reactions. Calculations using MINDO/3[43] can also give reasonable quantitative rationalisation of the rates of S_NAr reactions in terms of the effects of the substituents on the stabilities of the Meisenheimer complexes.

Another interesting feature of the *ab initio* calculations[40], with STO-3G basis set is that the bond lengths and angles indicate a planar structure for cyclohexadienyl anions. However, there is a possibility that the ring can pucker, as shown by (1.15), up to 20° for an increase of only 9.2kJ. This is known as homoconjugation. Experimental ^{1}H and ^{13}C n.m.r.

studies have shown that all C_6 aromatics and C_5X aromatics, where $X \neq C$, are planar. But n.m.r. measurements[44] have shown that the 1,6-dihydro-1,2,4,5-tetrazines and their conjugated acids and bases (1.16) are homoconjugated.

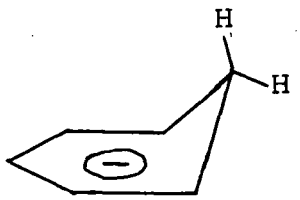

(1.15)

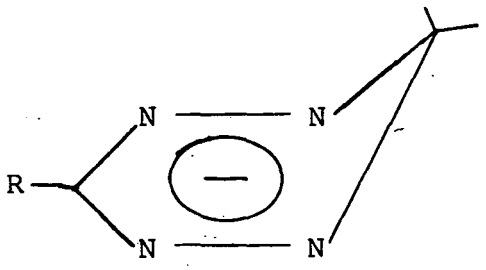

(1.16)

1.2.4 Techniques used for Structural Determination

(a) Crystallography

Crystallography supplies information on isolable crystalline Meisenheimer complexes and generally this information can be applied to Meisenheimer complexes in solution (confirmed by ^1H n.m.r.). Conformational information obtained on crystals was not necessarily applicable to complexes in solution as crystal conformations are usually subject to large intermolecular forces, which are not present in solution.

The crystal structures of the methoxy adducts of 2,4,6-trinitroanisole[33] (TNA) and 2,4,6-trinitrophenetole (TNP)[45] have been reported, as has that of the methoxy adduct of 4-methoxy-5,7-dinitrobenzofuran.[46] Common to all these adducts are the following features which will be explained with reference to the 1-ethoxy adduct of TNP shown in Figure 1.3. Firstly, the majority of the negative charge is located on the

oxygen atoms of the para-nitro group. This is indicated by the C4-N2 bond length of the para-nitro group being considerably shorter than the C2-N1 and C6-N3 bond lengths of the ortho-nitro groups. As the C6-C5 and C2-C3 bond lengths are much shorter than the other C-C ring bonds this also supports the above conclusion, and shows the adduct to be quinonoid as in the structure postulated by Jackson and Gazzolo.[1]

Figure 1.3 Pertinent Structural Parameters for 1-ethoxy adduct of TNP (from reference 26). All bond lengths in Angstroms.

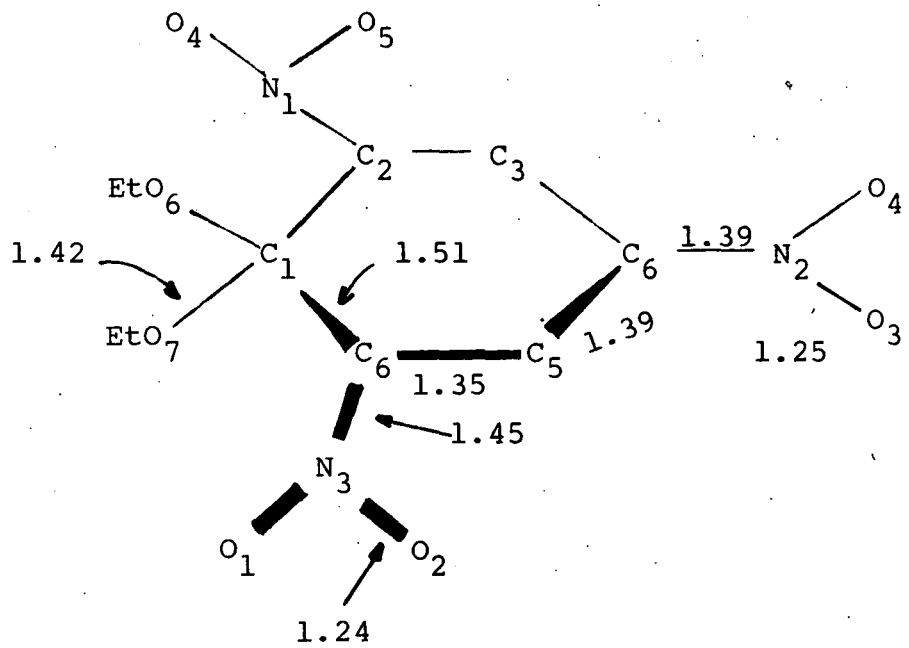

Secondly, the ring is planar and the resulting C2-C1-C6 bond angle is under considerable strain. Thirdly, the ethoxy oxygens lie in a plane perpendicular to the ring. Also as the C-O bond length is close to that found for aliphatic ethers[33] instead of the much longer bond length found in TNP. These observations suggest that C1 has considerable sp^3 character. Fourthly, the ortho-nitro groups in the adduct are nearly planar to the ring. In TNP itself dihedral angles up to 62° have

been observed between the exthoxyl group and the ortho-nitro groups[47] which is presumably due to steric compression between these functions. The release of steric compression in the 1-ethoxy adduct could be a primary reason for its greater stability compared to that of the 3-ethoxy adduct.

The crystal structure determinations provide evidence which concurs with the theoretical M O calculations described in the previous section.

(b) Infra Red Spectroscopy

Infra red spectroscopy is a poor technique for the structural studies of Meisenheimer complexes and consequently has been little used. Its use was reported[24,48-57] for a short time mainly in the mid-nineteen sixties. The most useful information that was gained was about the aromatic nitro groups; as these groups give strong absorptions, for asymmetric and symmetric stretches, at 1530-1550 and 1345-1350 cm^{-1} respectively. However complete band assignment was never easy and therefore rarely unequivocal.

I.R. spectroscopy is not totally redundant in its application to Meisenheimer complexes as Russian workers[58] have recently used it to show that O-2,4,6-trinitroaryl derivatives of hydroxy aldehydes, and their imines may exist in tautomeric equilibrium with spirocyclic forms such as (1.17).

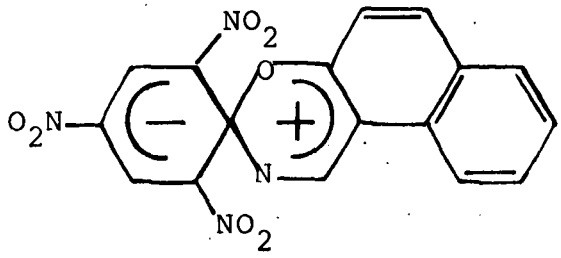

(1.17)

(c) N.m.r. Spectroscopy

^{1}H n.m.r. spectroscopy has been the most widely used technique for the determination of the structures of Meisenheimer complexes since Crampton and Gold[59] first used it to unequivocally determine the structure of the 1-methoxy adduct of TNA.

The experimental technique is simple. Usually the spectra are recorded in a solvent consisting of [$^2H_6$] dimethyl sulphoxide (DMSO) or one partially composed of [$^2H_6$] DMSO. This is because DMSO has been found to be a particularly good solvent for promoting adduct formation. First a spectrum of the substrate is recorded followed by spectra of the substrate with several different molecular equivalents of base. Usually the chemical shifts are measured with reference to internal tetramethylsilane.

The most sophisticated theory to date, using CM or PPPSCF calculations,[34,35] predicts that on complex formation there is an increase in electron charge on the ring carbons. This would be expected to cause the ring protons in the complex to resonate at higher field than in the parent. Experimentally this is observed. For example, consider the σ-adduct formed by TNA with potassium methoxide in [$^2H_6$] DMSO which Crampton and Gold originally studied.[59] TNA produces two bands, one at δ9.07 due to the ring protons and one at δ4.07 due to the methoxyl protons, in the intensity ratio of 2:3 respectively. On addition of base these bands are shifted upfield to δ8.65 (ring protons) and δ3.03 (methoxyl protons) in the intensity ratio 2:6. This indicates that the methoxyl protons are equivalent and the structure of the adduct is (1.18). In addition the upfield shift is compatible with the change in

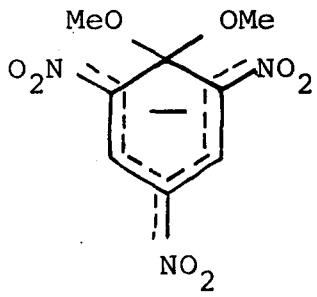

(1.18)

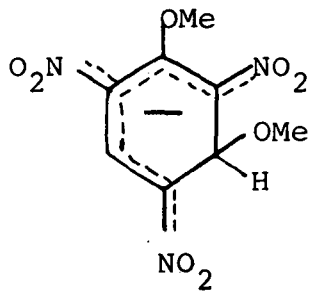

(1.19)

hybridisation from sp^2 to sp^3 at the 1-position, which has been observed for the solid complex using crystallography.

In general, n.m.r. allows the determination of the ring position or positions at which addition has occurred since the change in hybridisation from sp^2 to sp^3 is invariably accompanied by a large shift to high-field of the attacked substituent. For example, Servis[7] using more concentrated base found that on base addition two doublets (J=1-2Hz) were observed at δ6.17 and δ8.42. These observations are attributable to the ring protons and are consistent with (1.19). With time these bands were replaced by the band at δ8.65 as shown above. It can be deduced that (1.19) is the kinetically preferred adduct while (1.18) is the thermodynamically preferred adduct. Crampton and Gold[60] showed that the conversion of (1.19) to (1.18) is catalysed by methoxide ions and this indicates an intermolecular mechanism. At high base concentrations the 1:2 σ-adduct (1.20) is observed,[61,62] the ring protons producing bands at δ6.13 and δ8.8.

(1.21) shows the 1:2 σ-adduct produced by the reaction of TNA with the bulky sulphite ion which has been observed[63] by

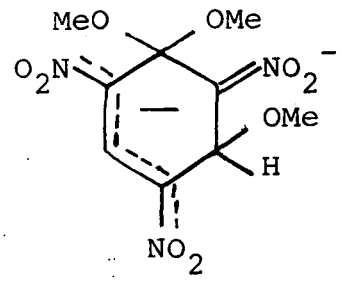

(1.20)

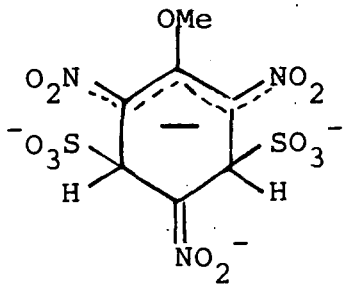

(1.21)

^{1}H n.m.r. In this example the nucleophile has added at unsubstituted ring positions in contrast to (1.20).

Finally, ^{1}H n.m.r. has been of considerable use in determining the structures of spiro-complexes such as (1.22). For (1.22) an A_2B_2 pattern is observed for the four methylene protons.

In some cases the lifetimes of Meisenheimer complexes are too short for conventional ^{1}H n.m.r. spectroscopy to be used to determine their structures. For such complexes a rapid mixing system is required. Stopped-flow n.m.r. spectroscopy is one such technique and rapid injection (R.I.) n.m.r. is another. R.I. n.m.r. has a shortest acquisition time of 72ms and has been used to observe[64] the intermediates (1.23) and (1.24), formed during the reaction of TNA with methylamine in 1:1 [$^2H_6$] DMSO-[$^2H_4$] methanol at -40°C.

More recent investigations of the structures of Meisenheimer complexes have involved ^{13}C, ^{15}N, ^{17}O and ^{19}F n.m.r. spectroscopy of which an example of each will be given.

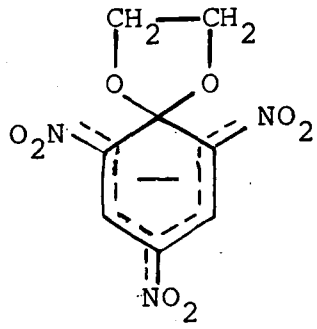

(1.22)

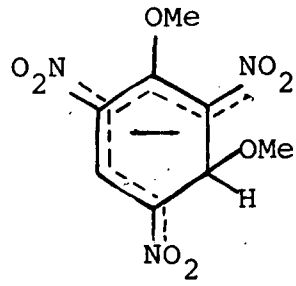

(1.23)

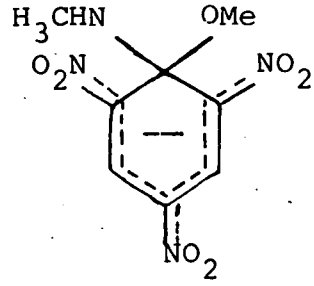

(1.24)

A series of 2,4-dinitro-6-X-anisoles and their 1-methoxy adducts[65] have been studied using ^{13}C n.m.r. It has been found that on formation of the 1-adducts the resonances of the 2, 4 and 6 ring carbons move to higher field while the resonances of the 3 and 5 ring carbons move to lower field. This is interpreted as showing more charge is localised on the 2, 4 and 6 ring carbons and less charge is localised on the 3 and 5 ring carbons, which is in agreement with theoretical calculations.[35] However, it has been noted[65] that ^{13}C shifts may not be simply related to charge effects.

^{13}C together with ^{1}H n.m.r. spectroscopy,[33] as mentioned in the theoretical studies section, has always shown that Meisenheimer complexes formed from trinitrobenzenes are planar, there is no experimental evidence for homoconjugation.

^{17}O n.m.r. spectroscopy has been used[46] to show that the electron density on the oxygen atoms of the nitro groups does not vary with the changing of substituents on the ring of neutral disubstituted nitrobenzenes.

Both ^{13}C and ^{15}N n.m.r. spectra have shown[66] that the adduct formed between pentane-2,4-dione and TNB exists in the enol form (1.25).

^{19}F n.m.r. spectroscopy has been used[67] in studying the adduct formed between 1,3,5-tris(trifluoromethylsulphonyl)-benzene with diethylamine in moist DMSO. It has been shown that under these conditions the hydroxide adduct is favoured.

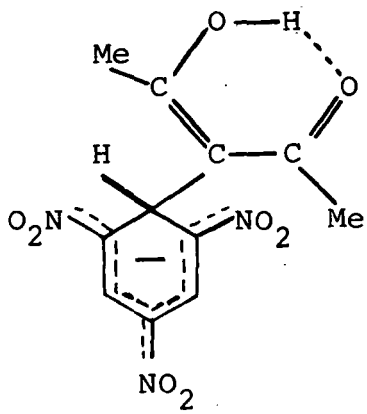

(1.25)

(d) Raman Spectroscopy

Raman spectroscopy gives essentially the same structural information, though with generally less well resolved spectra, as I.R. spectroscopy. Its major advantage over I.R. spectroscopy is that it can be used for molecules which produce no dipole change.

In the last few years Raman spectroscopy has been applied to study Meisenheimer complexes. In particular it has been used to examine the interactions of picryl chloride with

alkoxide ions,[69] the effects of solvation on σ-adduct structures[70] and solvent effects on the dissociation of alkali metal salts of 1,1-dimethoxy-2,4,6-trinitrocyclohexadienates.[71]

(e) Visible Spectroscopy

Visible spectroscopy is of limited value in determining the structure of Meisenheimer complexes. It can be used to differentiate between 1:1, 1:2 and 1:3 σ-adducts by the shape of their visible spectra. Abe[72,73] has shown using simple HMO calculations that a visible spectrum can be explained qualitatively by the transitions between the highest occupied molecular orbital and the lowest unoccupied molecular orbital in the delocalised anion. From these calculations he has shown that in the visible region of 350-700nm the 1:1 σ-adduct has two absorption maxima, with the maximum at higher wavelength being twice as intense as the maximum at lower wavelength, the 1:2 σ-adduct has one absorption maximum, and the 1:3 σ-adduct has no absorption maximum. These are illustrated in Figure 1.4. Experimental visible spectra agree with the general conclusions of the theoretical calculations but differ in the precise wavelength of the absorption maxima, also the absorption maxima of a 1:1 σ-adduct are found to have an intensity ratio of less than 2:1. Figure 1.5 shows a typical experimentally measured spectrum of 1:1 and 1:2 σ-adducts.

However, visible spectroscopy often is unable to distinguish between different Meisenheimer complex structures where there is geometric isomerism. For example, the visible spectrur for the 1:1 σ-adduct (1.3) formed by addition of the nucleophile at the unsubstituted position. Also the visible spectra of a variety of complexes like (1.3) where X=Nu or X=H are all

Figure 1.4 Visible absorption spectra of (A) cyclohexadienate and (B) propenide complexes (from reference 26).

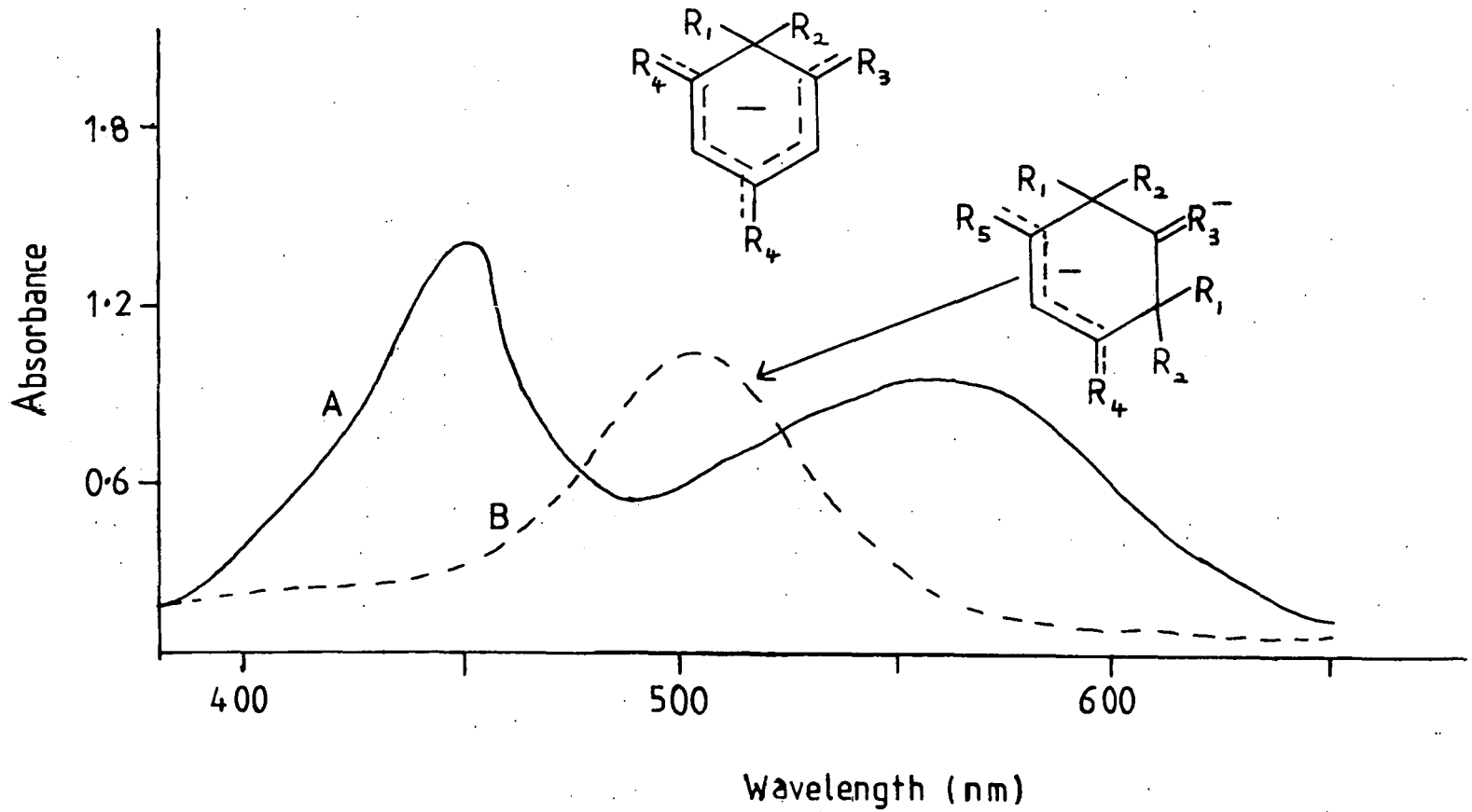

Figure 1.5 Visible spectra of (A) the 1:1 adduct and (B) the 1:2 adduct formed by the reaction of TNB (4×10^{-5} M) and thioethoxide (2.5×10^{-3} M and 0.5 M respectively) in methanol (from reference 25).

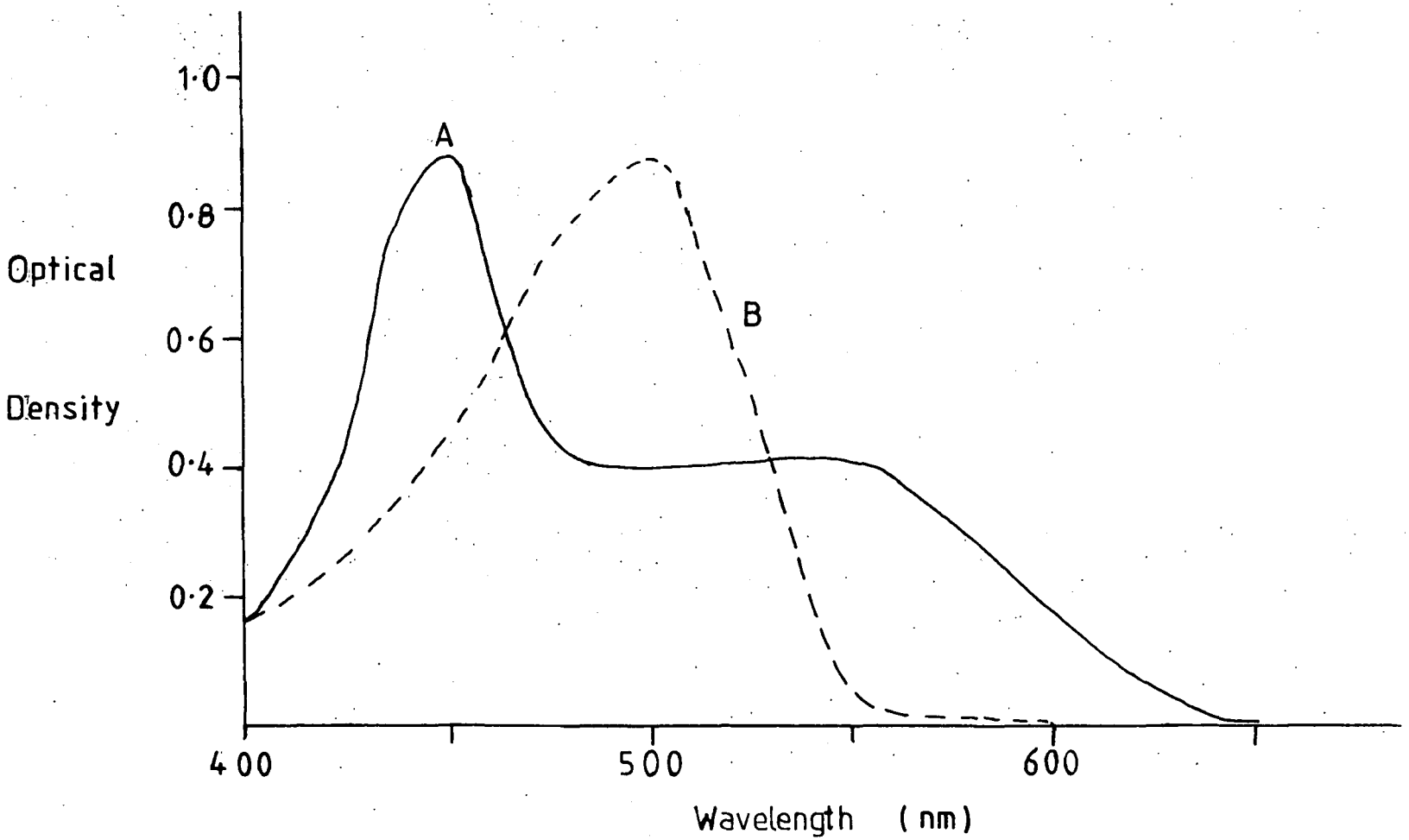

very similar[62] with absorption maxima at *ca* 415 and 500 nm.

1.2.5 Techniques for Kinetic and Equilibrium Studies

Meisenheimer complexes are highly coloured species, generally formed rapidly, (half lives of the order of a few milliseconds to several seconds), and can be of low stability, especially in protic solvents. The technique most widely used for their kinetic and equilibrium studies is stopped-flow spectrophotometry,[74] but relaxation techniques[75] such as the temperature jump method have also been used. When Meisenheimer complex formation is slow conventional spectrophotometry may be used.

Stopped-flow spectrophotometry was originally used by Caldin *et al*[117,118] in the mid-nineteen fifties to study the reactions of 1,3,5-trinitrobenzene (TNB) derivatives with ethoxide ions in ethanol, but it is only since about nineteen seventy that commercial stopped-flow spectrophotometers have been readily available.

Kinetic data can only be simply obtained by monitoring, with respect to time, the change of absorption at a suitable wavelength. The Benesi-Hildebrand method,[76] or a modification of it, is often used for the calculation of equilibrium data. The method uses optical density measurements at the completion of complex formation at different base concentrations, measured at a suitable wavelength.

1.2.6 The Stability of Meisenheimer Complexes

The stability of Meisenheimer complexes depends on several factors which are closely related. To assist with

the explanation of how these factors influence the stability of Meisenheimer complexes they will be discussed under the two general headings; structural effects and medium effects.

(a) Structural Effects

The type, number and position (ortho or para to the reaction centre) of the electron withdrawing groups in the aromatic ring has a major effect on the stability of Meisenheimer complexes. The trifluoromethylsulphonyl group is the strongest neutral electron withdrawing group known.[77] It is found that the 1-methoxy adduct of 2,4,6-tris(trifluoromethylsulphonyl)-benzene is 10^6 times more stable than its TNB analogue.[78] The stability of a Meisenheimer complex is increased with the increasing number of electron withdrawing groups added onto the ring, though the effect is not additive.[79] The electron withdrawing group gives its maximum electronic effect if it is para to the reaction centre rather than ortho to the reaction centre.[80,81] But when the electron withdrawing group is ortho to the reaction centre there can also be a steric effect.[23]

Table 1.1 gives kinetic and equilibrium data for the σ-adduct formation reactions of three aromatic trinitro-compounds with methoxide in methanol. By use of this data the effect of substituents in the picryl ring on the stability of the σ-adducts formed can be illustrated. By inference similar explanations can be applied to other activated aromatic compounds.

The σ-adduct formation reaction of TNB with methanolic methoxide ions can be used as a standard as there is only one type of reaction site, an unsubstituted site, for nucleophilic

attack. TNT, however, offers a choice of reaction sites. The nucleophile can attack at the substituted, or 1-position, or at the unsubstituted, or 3-position. Only formation of the 3-methoxy adduct of TNT is observed and this is much less stable than the methoxy adduct of TNB. The explanation of this observation is as follows. The $-CH_3$ group is a bulky and relative to hydrogen, an electron releasing substituent. Lack of formation of the 1-methoxy adduct is therefore due to unfavourable electronic effects. The low stability of the 3-methoxy adduct is caused by steric and electronic effects. The $-CH_3$ group being an electron releasing group, relative to hydrogen, tends to destabilise the negatively charged σ-adduct. Also because the $-CH_3$ group is bulky the nitro groups are twisted out of the ring plane, where they exert their maximum electron withdrawing ability, so that they are not as efficient at delocalising the negative charge.[33]

TNBCl like TNT offers a choice of reaction sites with both the 1-methoxy and 3-methoxy adduct being formed with methanolic methoxide ions. The 3-methoxy adduct is again less stable than the TNB analogue but more stable than the

Table 1.1 Kinetic and equilibrium data for TNB derivatives with methoxide ions in methanol at 25°C

	k_3 ($l\ mol^{-1} s^{-1}$)	k_{-3} (s^{-1})	K_3 ($l\ mol^{-1}$)	k_1 ($l\ mol^{-1} s^{-1}$)	k_{-1} (s^{-1})	K_1 ($l\ mol^{-1}$)
TNB[a]	7300	300	20			
TNT[b]	280	3000	0.07			
TNBCl[c]			<20	770	2.2	350

a. Ref. 78
b. Ref. 83
c. Ref. 82

TNT analogue. This can be rationalised by the dominance of the steric effect of the bulky $-CH_2Cl$ group causing the ortho nitro groups to twist out of the ring plane. The $-CH_2Cl$ group is electron withdrawing, relative to hydrogen. amd therefore should assist in the stabilising the negatively charged σ-adduct. The 1-methoxy adduct of TNBCl is more thermodynamically stable than the 3-methoxy adduct. This increased stability arises partly from the fact that the reaction centre is attached to an electron withdrawing group, and, partly from the relief of steric strain as the bulky $-CH_2Cl$ group is twisted from the ring plane. The kinetic preference for the 3-methoxy adduct is due to there being no bulky substituent at this position allowing for easier access to the reaction site for the methoxide ion.

The type of nucleophile attacking a given substrate in a particular solvent is also important for the stability of Meisenheimer complexes. The steric requirements[26] of the nucleophile can determine the type of Meisenheimer complex it will form when reacting with an unsymmetrical aromatic trinitro-compound. For example, TNA will form σ-adducts at the 1-position with azide ions and diethylamine, but only σ-adducts at the 3-position with sulphite and acetonate ions. Also the carbon basicity of the nucleophile, often different to its proton basicity,[84] has an effect on the Meisenheimer complex.

(b) Medium Effects

The formation of Meisenheimer complexes have generally been studied in protic solvents, such as water or alcohols, or dipolar aprotic solvents, such as DMSO. The stability of

1:1 σ-adducts is enhanced in aprotic solvents relative to protic solvents. This is because aprotic solvents are good at solvating large polarisable ions, like σ-adducts, but not so good at solvating small polar ions. Hence, transfer from protic to dipolar aprotic solvents causes desolvation of the nucleophile increasing the reaction rate. It has been shown that 1:2 σ-adducts may be stabilised in protic solvents and this has been attributed to the high negative charge localised on nitro groups in these adducts making them resemble inorganic salts.[26]

The effect of micelles on Meisenheimer complex stability has been studied.[85] It was found Meisenheimer complex stability was increased by cationic micelles, decreased by anionic micelles while neutral micelles had no effect. The results were interpreted in terms of incorporation of the aromatic substrates into the micelle which, depending on its charge type, attracts or repels the anionic nucleophile.

Salt effects on Meisenheimer complex formation and decomposition processes have been reported for a number of systems. Ion pairing has been reported as increasing Meisenheimer complex stability.[86] In particular ion pairing has been found to be important in the stability of 1,1-dialkoxy complexes.[85]

1.2.7 Reactions of Aromatic Trinitro-Compounds

There are a variety of ways in which the highly activated aromatic trinitro compounds may react with bases.[87] Therefore only the more important reactions will be described here. These are:- proton abstraction, electron transfer and σ-adduct formation which may lead to nucleophilic substitution

if the substrate carries a leaving group.

Abstraction of a ring proton was first suggested by Meyer[88] as an explanation for the highly coloured species observed by Hepp[14] and others. It has been shown[89-91] that in basic solutions TNB and dinitrobenzene do exchange ring hydrogens for deuterium or tritium in the solvent. However, the plausible carbanion intermediate (1.26) for this exchange

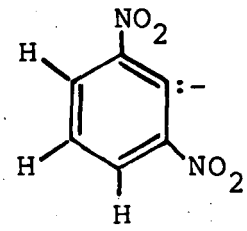

(1.26)

reaction has been found[91] to be present only in small concentrations and therefore carbanion formation is not the explanation for the presence of colour. When an aromatic trinitrocompound has a substituent containing a hydrogen atom, *e.g.* TNT,[82] then it is possible for the base to remove a proton from it to produce the conjugate base as shown in Scheme 1.3. The conjugate base of TNT would be (1.27; X=Y=H) and has been observed[83,92,93,117,118] by ^{1}H n.m.r. Kinetic evidence that the anion of TNT is formed has also been provided by a kinetic isotope study,[94] which compared the deprotonation of TNT with that of TNT-d_3 (*i.e.* the methyl group is deuterated) and found a large primary isotope effect. If this type of proton transfe reaction is studied in solvents where ion association is negligible, *e.g.* D.M.S.O., then the equilibrium constant for proton

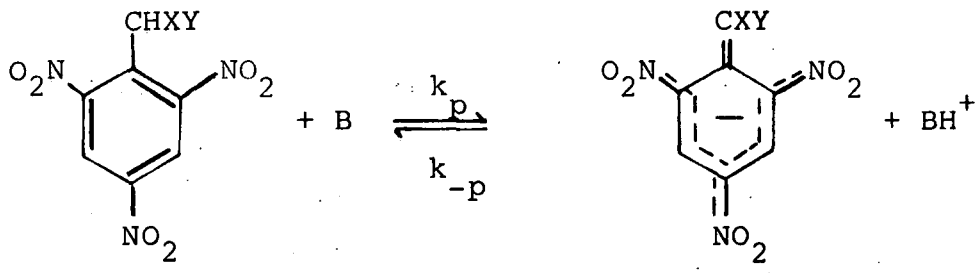

(1.27)

Scheme 1.3

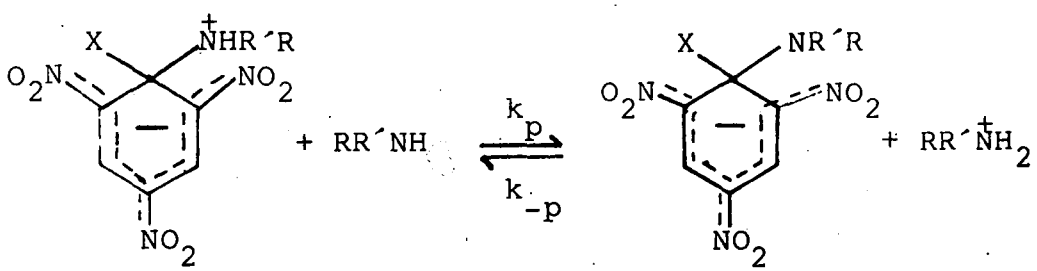

Scheme 1.4

---

transfer, k_p, reflects the basicity of the bases used.[82] There are also examples of proton transfer reactions between the nitrogen atoms of primary and secondary amines and zwitterionic intermediates, as depicted in Scheme 1.4, which are not diffusion controlled. The slowness of these proton transfer reactions is generally attributed to steric factors. The base has to be able to remove a proton from a position in close proximity to two bulky ortho nitro groups. Therefore the bulkier the base the slower the proton transfer.

There are two types of electron transfer reactions. One type involves partial electron transfer, (1.28), as observed by Mulliken[95] in the very weak charge transfer reactions of aromatic nitro-compounds with hydrocarbons and aromatic amines.[96,97] The second type involves complete transfer to give radical anions, such as (1.29).

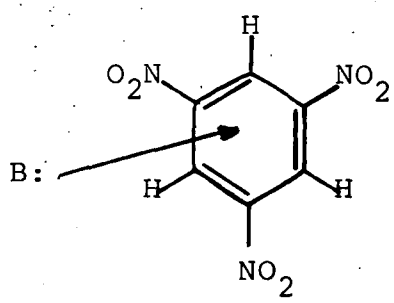

(1.28)

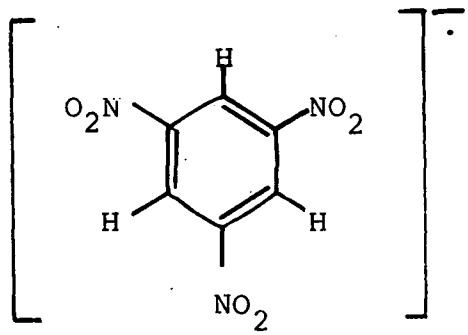

(1.29)

Radical anions are easily detected using e.s.r. spectroscopy. Generally radicals are found in large concentrations in reactions between aromatic mononitro- or aromatic dinitrobenzenes and bases.[98-100] When bases react with trinitrobenzenes generally less than 1% of radicals are detected. Servis has shown,[7] using a M O description of these molecules, that due to the symmetry of the anti-bonding molecular orbitals a third nitro group on the benzene ring will greatly increase the stability of the cyclohexadienate type anion (1.13), but not greatly increase the stability of the radical anion. Exceptions where aromatic trinitro-compounds have been postulated to react *via* electron transfer processes are known, *e.g.* the reactions of picryl chloride with amines like piperidine.[101]

The decomposition of Meisenheimer adducts can also proceed *via* electron transfer.

S_NAr reactions are of great interest to many chemists and involve Meisenheimer complexes as intermediates. Schemes 1.5 and 1.6 show two types of intermolecular S_NAr reactions involvi anionic nucleophiles and neutral nucleophiles respectively. It should also be noted that X, the nucleofuge or leaving group, can be neutral or positively charged before displacement. Also where the nucleofuge is a poor leaving group, *i.e.* has a small nucleofugacity, then these S_NAr reactions can terminate at the intermediate (1.30) or (1.31). For schemes 1.5 and 1.6 there are many reactions known where nucleophilic attack at the 3-position to form the 3-adduct precedes nucleophilic attack at the 1-position. For certain bases, *e.g.* secondary amines, only the 3-adduct, formed by nucleophilic attack at the 3-position, is known. For the reaction in scheme 1.6 Bunnett[22,23,102,103] has shown the final step to give the product is *via* a specific base-general acid (SB-GA) mechanism.

Scheme 1.7 shows an intramolecular S_NAr reaction to form a spiro-complex. This type of reaction can then be followed by an intermolecular S_NAr reaction if there is a nucleophile present (perhaps the base itself) in the reaction mixture, or by an intramolecular displacement of a nitro group.

There is no unique reactivity order for all the possible substrate/nucleophile/solvent combinations that have been studied for S_NAr reactions. The type of substituent is known to strongly influence the rate of reaction but the magnitude of the rate depends on the position of the substituent to the reaction centre, the nucleophile, the solvent and the leaving group.

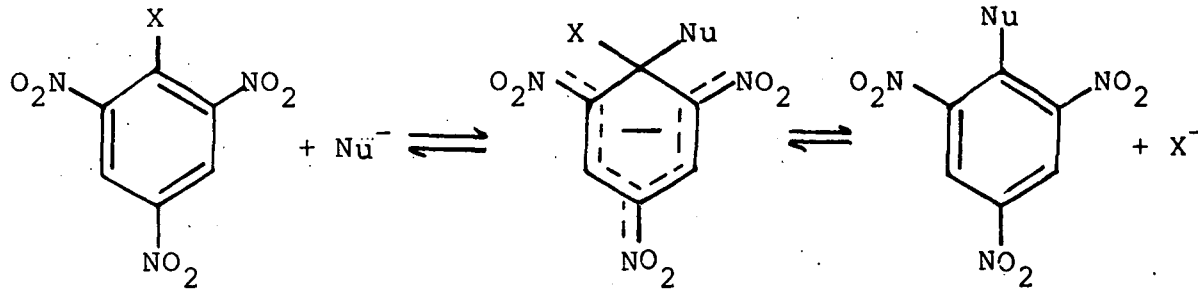

(1.30)

Scheme 1.5

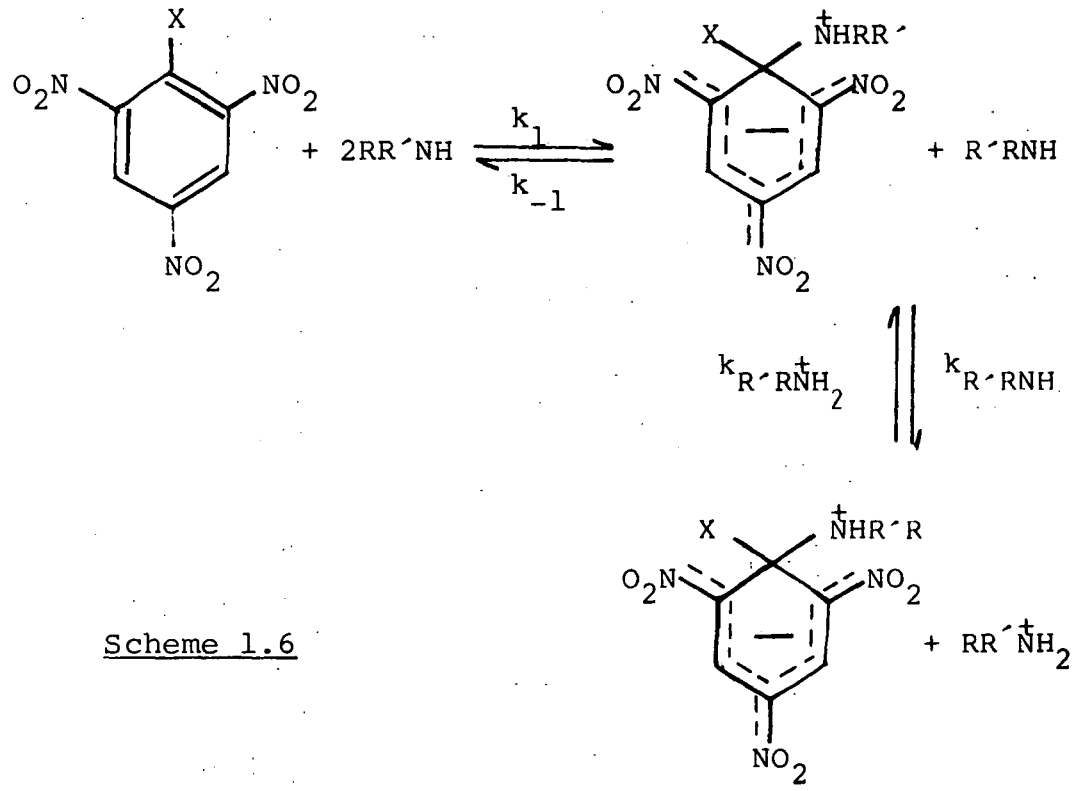

(1.31)

Scheme 1.6

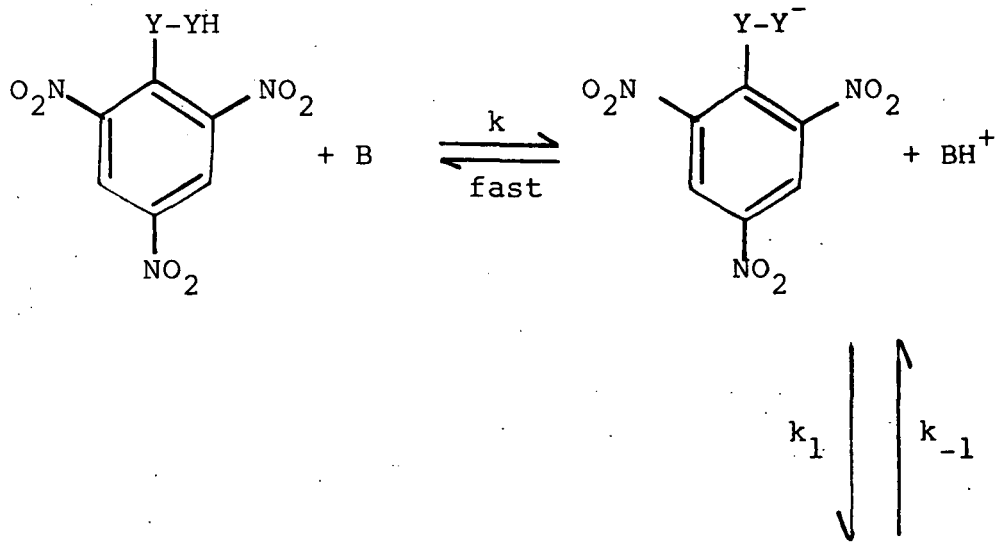

Scheme 1.7

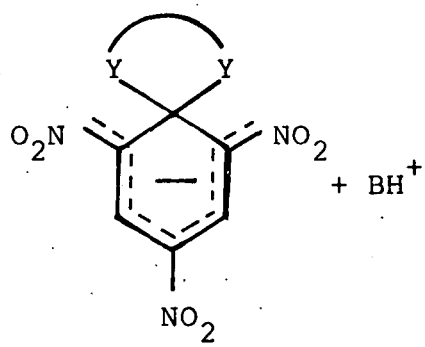

Generally throughout this chapter examples of Meisenheimer complexes involving oxygen or nitrogen centres have been given. So in conclusion one or two examples will be given for nucleophiles that contain and σ-bond through atoms which are not oxygen or nitrogen.

(a) Sulphur bonded σ-complexes

Sulphur containing nucleophiles react in an analogous way to oxygen containing nucleophiles except that there are no examples of the formation of the conjugate base by removal of a side chain proton from the substrate. Presumably this is due to sulphur nucleophiles being soft bases. Examples of sulphur containing nucleophiles are sulphite, thioethoxide and thiophenoxide ions. With 1-X-2,4,6-trinitrobenzenes sulphite ions tend to form 1:1 (1.32) and 1:2 (1.33) complexes with addition at the unsubstituted positions. Sulphite ions are bulky and when there is a bulky group at the 1-position steric effects may stop formation of the 1-adduct.[25] There are exceptions such as the sulphite adduct (1.34) of 2,4,6-trinitrobenzaldehyde.[104]

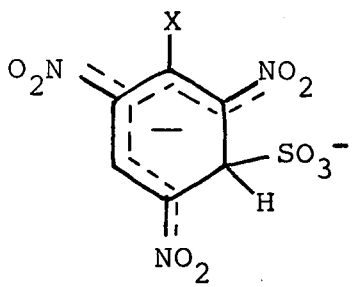

(1.32)

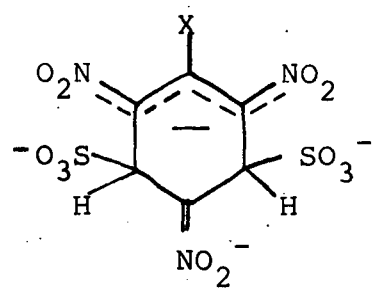

(1.33)

When rate data for the formation of σ-adducts with sulphur and oxygen containing nucleophiles are compared, it is suggested[1] the order EtS^- > MeO^- > PhS^- > PhO^- is that of "thermodynamic affinity" to aromatic carbons.

Sulphur containing spiro complexes, such as (1.35) formed from 1-[(2-Mercaptoethyl)thio]-2,4,6-trinitrobenzene, are more stable than their oxygen analogues when formed in water. This may be explained by the higher acidity of the thiols relative to the alcohols, the first equilibrium in scheme 1.6 (Y=S), rather than larger K values for the internal cyclisation, the second equilibrium in scheme 1.6 (Y=S).

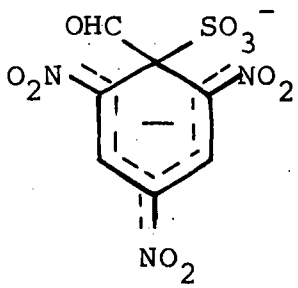

(1.34)

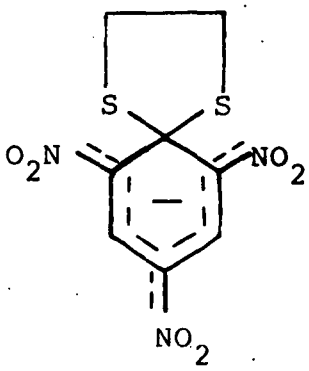

(1.35)

(b) Phosphorous bonded σ-complexes

A number of phosphorous compounds react with trinitro-aromatics to form σ-complexes[106] but the most studied are those containing trialkyl phosphites. Phosphorous compounds react in DMSO in essentially an analogous way to amines. For example, alkyl phosphites react with TNB in DMSO to form the σ-adduct (1.36) behaving like a secondary amine. One difference is that unlike tertiary amines the trialkyl phosphites yield stable

zwitterionic complexes[107] (1.37) with TNB in DMSO. In reactions with 1-X-2,4,6-trinitrobenzenes the phosphorous nucleophiles presumably due to their bulk only form adducts at the unsubstituted position.[108]

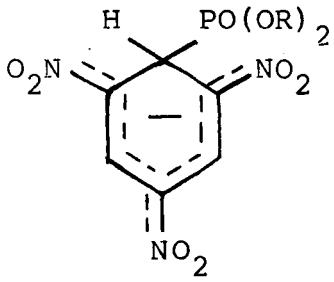

(1.36)

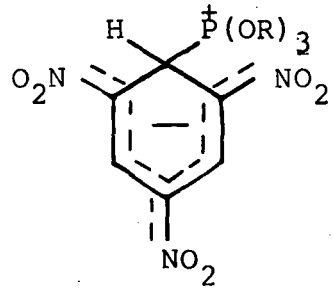

(1.37)

(c) Carbon bonded σ-complexes

There have been numberous reports of carbon bonded σ-complexes.[109] Cyanide ions form σ-adducts with TNB (1.38) in a variety of solvents. All cyanide complexes are found to have a much higher stability than would be expected from the hydrogen basicity of cyanide ions. Enolate complexes, also known as Janowsky complexes, such as (1.39) are formed between enolate carbanions of ketones, aldehydes, keto esters, esters and amides. The formation of some of these complexes have become important in a variety of pharmaceutical colour tests.[110] In such cases there are two steps, the first being rapid formation of the carbanion followed by the rate determining complex formation. A recent report[111] has described

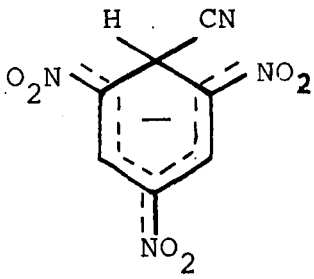

(1.38)

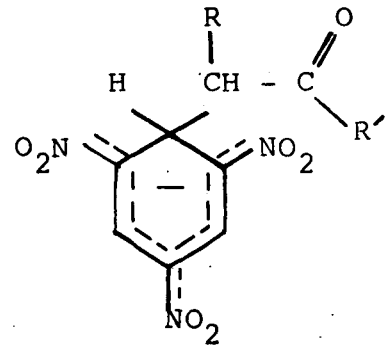

(1.39)

has described the use of TNB to trap CX_3^- ions to form the complex (1.40) when trihalocetic acid rapidly decomposes in DMSO. As (1.40) is highly coloured it allows the rate of trihaloacetic acid decomposition to be measured spectrophotometrically. An interesting Janowsky complex is that formed between TNB and the conjugate base of TNT.[112,113]

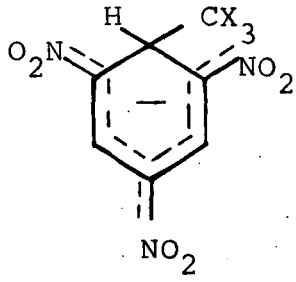

(1.40)

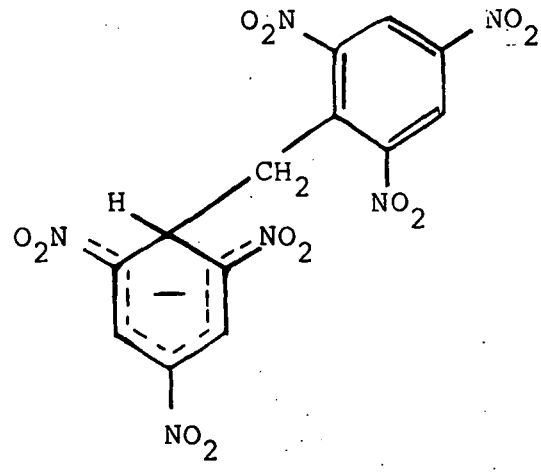

(1.41)

(d) Halide σ-complexes

Only two σ-complexes have been reported from the reaction of halogens and trinitro-aromatics. In acetonitrile containing 18-crown-6-ether the adduct (1.42) has been observed,[105]

using ^{1}H and ^{19}F n.m.r., for the reaction of picryl fluoride and potassium fluoride. It is quite stable until trace amounts of water are added. The adduct (1.43) was isolated in the reaction between TNB and tetramethylammonium fluoride in tetrahydrofuran [114] (THF).

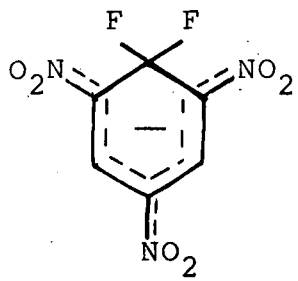

(1.42)

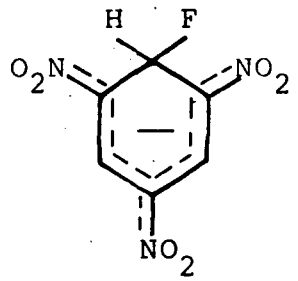

(1.43)

(e) Hydride σ-complexes

One of the many preparations of the σ-adduct (1.44) is by the reaction of TNB with tetramethylammonium tetrahydroborate in acetonitrile.[115]

(f) Organometallic complexes

Complexes of the type (1.45) have been isolated as solids when TNB reacts with R_3EM (R_3E=Me_3Si, Et_3Ge, Me_3Sn, Ph_3Sn; M=Li, K, Cs) in organic media, *e.g.* DMSO, THF, at -5 to -10°C, under argon or in a vacuum.[116] They are stable for several days unless they are exposed to oxygen when they decompose in twenty to thirty minutes.

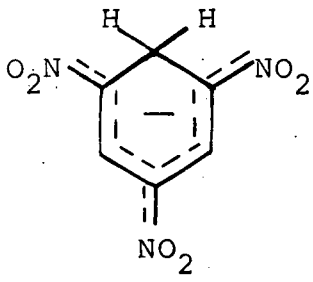

(1.44)

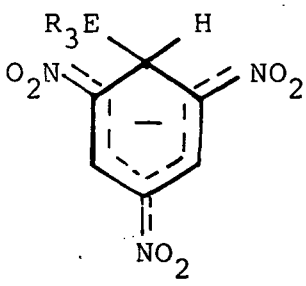

(1.45)

CHAPTER TWO

EXPERIMENTAL

2.1 Chemicals Used

2.1.1 Solvents

Acetonitrile: puriss grade, degassed under a hard vacuum.

Dimethyl sulphoxide: puriss grade, generally used without further treatment. If dry dimethyl sulphoxide was required then it was refluxed over calcium hydride, fractionally distilled under reduced pressure and kept protected from moisture.

$[^2H_6]$ - Dimethyl sulphoxide: commercial sample (isotopic purity 99.9%) containing 1% tetramethylsilane, used as supplied.

Deuterium oxide: commercial sample (isotopic purity 99.8%), used as supplied.

Ethanol: AnalaR grade, used without further treatment, or boiled and stored as for water (see below).

Tetrahydrofuran: AnalaR grade, dried over sodium.

Methanol: AnalaR grade, used as supplied.

$[^2H_4]$ - Methanol: Commercial sample (isotopic purity 99.5%), used as supplied.

Water: distilled water was boiled for fifteen minutes to expel dissolved carbon dioxide, and then protected from air by a soda lime guard tube.

2.1.2 Substrates

1-(2,2-dimethyl-3-hydroxypropoxy)-2,4-dinitronaphthalene: orange crystalline solid. Prepared from the reaction of 1-chloro-2,4-dinitronaphthalene with sodium 2,2-dimethyl-3-hydroxypropoxide[119] by Penelope M. Wilson, m.p. 114°C.

2,2´,4,4´,6,6´ - hexanitrobibenzyl: yellow powdery crystalline solid. Samples supplied wet by P.E.R.M.E., Waltham Abbey, and dried in air. ^{1}H n.m.r. spectra showed no trace of impurities, m.p. 218-220°C (Lit.[2], 218-220°C).

2,2´,4,4´,6,6´ - hexanitrostilbene: pale yellow crystalline solid. Samples supplied wet by P.E.R.M.E., Waltham Abbey, and dried in air, or prepared by Shipp-Kaplan reaction.[2] HNS exists as the trans isomer in two crystalline forms; HNS I, m.p. 316°C (Lit.[2], 316°C) and HNS II, m.p. 324°C. ^{1}H n.m.r. spectra showed no trace of impurities and no difference between HNS I or HNS II in solution.

1,3,5 - trinitrobenzene: light brown crystalline solid. Dried reagent grade, m.p. 123°C (Lit.[121], 122.5°C).

2,4,6 - trinitrobenzyl chloride: pale yellow crystalline solid. Samples supplied wet by P.E.R.M.E., Waltham Abbey, and dried in air. Then recrystallised twice from benzene/pentane to remove any trace of 2,4,6-trinitrotoluene. ^{1}H n.m.r. spectra showed no trace of impurities, m.p. 82°C (Lit.[2], 82°C).

2,4,6 - trinitrophenetole: green crystalline solid. Prepared from the reaction of 1-chloro-2,4,6-trinitrobenzene with one equivalent of sodium ethoxide in ethanol by Mr. Brian Eddy. Recrystallised from ethanol. ^{1}H n.m.r. spectra showed no trace of impurities, m.p. 80°C (Lit.[122], 78.5°C).

2.1.3 Nucleophiles

1,4-Diazabicyclo[2,2,2]octane: reagent grade, used as supplied.

Benzylamine: commercial pure sample, used as supplied.

n-Butylamine: commercial reagent grade, used as supplied.

Piperidine: puriss A.R. grade, used as supplied.

Pyrrolidine: puriss grade, used as supplied.

Sodium deuterioxide: prepared by dissolving freshly cut pieces of sodium in deuterium oxide. Samples of the solution were diluted and titrated against standard acid.

Sodium ethoxide: prepared by dissolving freshly cut pieces of sodium metal in AnalaR ethanol under nitrogen. Samples of the solution (usually around 1$\underline{\underline{M}}$) were diluted with ethanol and titrated against standard acid.

Sodium hydroxide: all sodium hydroxide solutions were made up by diluting a 1$\underline{\underline{M}}$ A.V.S. sodium hydroxide stock solution, which was manufactured from AnalaR reagents.

Sodium methoxide: freshly cut pieces of sodium were cleaned in methanol before being dissolved in AnalaR methanol under nitrogen. If necessary the solution was centrifuged and decanted to remove any solid particles formed. Samples of the solution (usually around 3$\underline{\underline{M}}$) were then diluted with methanol and titrated against standard acid.

Sodium $[^2H_3]$-methoxide: prepared by dissolving freshly cut pieces of sodium in AnalaR $[^2H_4]$-methanol under nitrogen. Samples of the solution were diluted in methanol and titrated against standard acid.

Sodium sulphite: AnalaR sodium sulphite heptahydrate was dried at 200^{o}C overnight, then stored in an airtight container.

Thioglycollic acid: commercial sample used as supplied.

2.1.4 Salts

Benzylammonium chloride: commercial "99% pure" sample was used as supplied.

Benzylammonium perchlorate: prepared in DMSO solution from weighed amounts of amine and perchloric acid; the p.H. value of the solution was measured after reaction, and if necessary small quantities of acid or base were added until the theoretically calculated p.H. was obtained. The salt solution so prepared contained less than 0.1% of free acid or free amine.

n-Butylammonium chloride: originally prepared from bubbling HCl gas into an ether solution of amine, and white crystalline solid immediately falls out of solution. More easily prepared by the addition of the proper amount of concentrated hydrochloric acid to an ethanol solution of amine and isolating the precipitated white solid.[123] Acetonitrile was used for recrystallisation of the salt.

n-Butylammonium perchlorate: prepared in an analogous way to benzylammonium perchlorate.

1,4-Diazabicyclo[2,2,2]octane perchlorate: stock solutions prepared by mixing the appropriate weights of amine and 60% aqueous perchloric acid in a known volume of DMSO. N.B. Only one nitrogen atom per molecule is protonated.

Piperidinium chloride: a commercial "pure" sample was used as supplied.

Piperidinium perchlorate: prepared in analogous way to benzylammonium perchlorate.

Sodium chloride: AnalaR sodium chloride was used.

Sodium perchlorate: AnalaR sodium perchlorate monohydrate was heated to 60°C under a vacuum for three hours. The anhydrous sodium perchlorate was stored in an airtight container, kept in a dessicator over silica gel.

2.1.5 Buffers

p-Bromophenol: a commercial sample was used as supplied m.p. 64°C (Lit.[124], 66.4°C).

Phenol: AnalaR phenol was dried by heating it above 100°C and then left to cool and recrystallise protected from atmospheric moisture by a calcium chloride guard. m.p. 40-41°C (Lit.[124], 43°C).

Sodium bicarbonate: a commercial sample was used as supplied.

2.1.6 Free Radical Inhibitors

Di-tert-butyl-nitroxide: a commercial sample was used as supplied.

Oxygen: bubbled into DMSO as compressed air.

2.2 Measurement Techniques

2.2.1 Rates

Reaction rates with half lives smaller than 30 seconds, or larger than 10^{-2} seconds, were measured using either a Canterbury SF-3A or Hi-Tech SF-3L stopped-flow spectrophotometer. Each machine was thermostated at 25°C and contained a silica cell with 2mm path length. First order kinetics were measured by always keeping base concentrations well in excess of substrate concentrations. The rate coefficients are quoted as a mean of at least five separate measurements and are precise to ±5%. The principles of the stopped-flow spectrophotometer's design and use have been thoroughly reported previously.[74,120]

Rate measurements were made from an oscilloscope trace. The actual technique employed depended on the number of processes observed. Figures 2.1(a) to 2.1(d) show examples of the types of traces observed for the reactions reported in this thesis. Figure 2.1(a) shows the simplestcase of a colour forming reaction producing a stable species, with a stable infinity voltage, V_∞. The measurements of values for ΔV_t, the voltage at a time t, are easily made. Figure 2.1(b) shows a trace of a colour forming species followed by its subsequent decay. If the decay process is much slower than the formation process, then the start of the decay process is generally linear. This linear trace can be extrapolated back to zero time allowing values of ΔV_t to be measured, and also allowing the calculation of ΔV ($=V_\infty - V_c$) which can be related to optical density for the completion of the measured process (see Section 2.2.2). This procedure has been described previously

FIGURE 2.1

Examples of types of oscilloscope traces observed.

ΔV_t $(=V_\infty - V_t)$ The difference in voltage at time t.

ΔV The difference in voltage when the process is complete.

V_c Voltage in the absence of the absorbing species.

V_∞ Maximum voltage in the presence of the absorbing species.

m This shows how the mixing time *ca* 5ms can be observed on an oscilloscope for a fast process.

g Grid lines that appear on the oscilloscope to enable measurement of ΔV_t and t. They are only shown on Figure 2.1(a).

by Bernasconi.[78] The same technique is used for the trace shown in Figure 2.1(c) except in this case a rapid colour forming process followed by a slower colour forming process. Figure 2.1(d) shows how using a slower time base the second slower process becomes measurable while the first process is too fast for measurement.

In all the above examples several values (generally *ca* 6) of ΔV_t at time t are measured over one to two half lives of the reaction. Then a plot of ln ΔV_t versus t allows the observed rate constant, k_{obs}, to be calculated from the slope. For these plots the slope is determined by eye, this being as accurate as any other method.

When an infinity value cannot be accurately measured then techniques not requiring an infinity value, such as the Guggenheim method[125,126] and the Kezdy-Swinbourne method,[126-128] were used to calculate k_{obs}.

To Measure reaction rates for the reactions with half lives larger than thirty seconds the following conventional recording spectrophotometers were used; the Pye-Unicam SP-8100 and the Beckman No. 25. Also the non-recording Unicam SP-800 spectrophotometer was used. k_{obs} was calculated using the same techniques which were described above for the fast reactions except Δ O.D., the change in optical density, values were used instead of ΔV values.

2.2.2 Equilibria

Optical density measurements, used for calculating equilibrium constants from Benesi-Hildebrand plots,[76] were measured using the same conventional spectrophotometers used

FIGURE 2.1

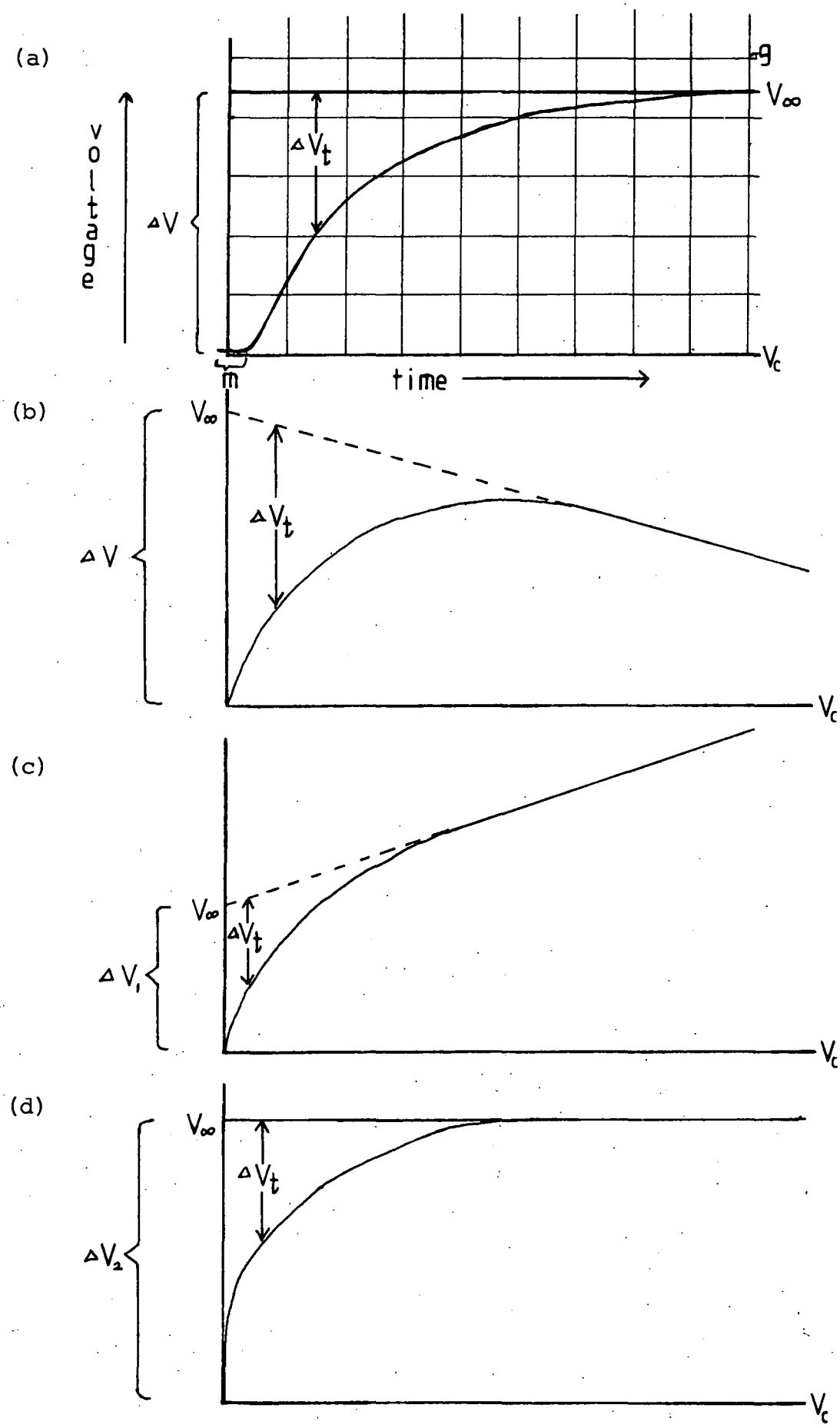
(a)
g
V_∞
ΔV_t
voltage
ΔV
V_c
m
time
(b)
V_∞
ΔV_t
ΔV
V_c
(c)
V_∞
ΔV_t
ΔV_1
V_c
(d)
V_∞
ΔV_t
ΔV_2
V_c

for rate measurements (see above), with a 1 cm path length cell, or using a stopped-flow spectrophotometer with a 2 mm path length cell, at 25°C. In the latter case provided small changes in voltage are measured then equation 2.1 can be used to calculate optical densities from voltages.

equation 2.1 $$O.D. = \log \frac{V_o}{V_o - \Delta V}$$

where V_o = background voltage (usually 5V)

$\Delta V = V_\infty - V_c$

V_c = the voltage in the absence of absorbing species.

V_∞ = the maximum voltage in the presence of the absorbing species.

The value ΔV is measured as shown in Figure 2.1.

2.2.3 Visible Spectra

Visible spectra were recorded on a Pye-Unicam SP-8005 or SP-8100 recording instrument, or measured point by point on the stopped-flow spectrophotometer.

2.2.4 ^{1}H n.m.r. Spectra

^{1}H n.m.r. spectra were measured on a Varian EM 360L instrument operating at 60 MHz, or a Bruker HX 90E instrument operating at 90 Hz and modified for Fourier transform operation and using a deuterium lock. All chemical shifts were measured relative to internal tetramethylsilane and using fully deuterated solvents.

2.2.5 Conductance Measurements

A W.G. Pye and Co. Ltd., Conductance Bridge Cat. No. 11700 was used with a Mullard conductivity cell for all conductivity measurements reported. Dimethyl sulphoxide was used as the solvent for these measurements because it is a good solvating agent. This means there is negligible ion pair formation and therefore the conductance of the solutions give a direct measure of the complex present. By a plot of excess conductance, the conductance of the parent/amine mixture minus the conductance of the parent and amine solutions measured separately, against the stoichiometric amine concentration, the stoichiometry of the n amine: 1 parent can be deduced from the shape of the plot.[129]

2.2.6 pH

The pH of solutions were measured using a Kent EIL 7055 pH meter and a combination electrode. The instrument was calibrated by use of a standard buffer solution of an appropriate pH.

CHAPTER THREE

THE REACTIONS OF 1-(2,2-DIMETHYL-3-HYDROXYPROPOXY)-2,4-DINITRONAPHTHALENE WITH HYDROXIDE IONS

3.1 Introduction

Crampton and Willison have previously reported[130,131] rate and equilibrium data for the formation of the spiro-complex (3.2; R=H) from 1-(3-hydroxypropoxy)-2,4-dinitronaphthal (3.1; R=H) in alkaline media. Kinetic and equilibrium data are presented here for the formation of the spiro-complex (3.2; R=Me) from 1-(2,2-dimethyl-3-hydroxypropoxy)-2,4-dinitro-naphthalene (3.1; R=Me) in alkaline media. Comparison of these two sets of data, together with related measurements on the cyclisation of hydroxy ethers of trinitrobenzene reported by Bernasconi and Gandler,[132] gives information on the effect of gem-dimethyl substitution in the side chain on spiro-complex formation.

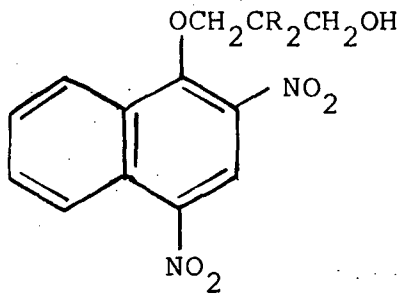

(3.1)

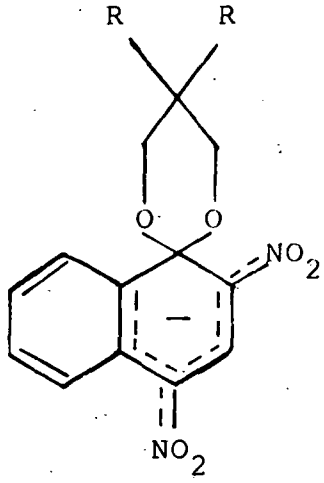

(3.2)

3.2 Experimental

Visible spectra were recorded on a Pye-Unicam SP-8005 spectrophotometer at 28°C.

Kinetic and equilibrium measurements of the first colour forming process were made on a Canterbury SF-3A stopped-flow spectrophotometer at 25°C.

Kinetic measurements for the second colour forming process were made on a Pye-Unicam SP-500 spectrophotometer at 25°C. The second process was followed by an extremely slow unknown colour forming process, thought to be the reaction of some impurity in the parent with base. The optical density for complete conversion and the kinetic data were calculated using the techniques described in Chapter Two.

For all the kinetic measurements the base concentration was always in large excess of the parent concentration so that first order kinetics were observed. All rate coefficients are the mean of five separate determinations. Examples of typical rate measurements are given in Tables 3.1 and 3.2.

^{1}H n.m.r. measurements were made on a Varian EM360L instrument operating at 60MHz and the chemical shifts were measured relative to internal tetramethylsilane.

TABLE 3.1 Typical Results from Rate Measurements

(i) Sodium Hydroxide (0.3$\underline{\underline{M}}$), 1-($HOCH_2CMe_2CH_2O$)-DNN($1 \times 10^{-5}$ $\underline{\underline{M}}$). First process measured at 500nm in water.

(ii) Sodium Hydroxide (0.075$\underline{\underline{M}}$), 1-($HOCH_2CMe_2CH_2O$)-DNN($1 \times 10^{-5}$ $\underline{\underline{M}}$) First process, measured at 500nm in 20/80 (v/v) DMSO-water.

(i)		(ii)	
t/s	ΔV^a	t/s	ΔV^a
0.00	4.1	0.0	2.8
0.05	3.1	0.1	2.2
0.10	2.4	0.2	1.8
0.15	1.9	0.3	1.4
0.20	1.4	0.4	1.2
0.25	1.1	0.5	0.9
0.30	0.9	0.6	0.7
0.40	0.4	0.8	0.5

A plot of $\ln\Delta V$ versus t is linear and yields $k_{obs} = 5.83s^{-1}$

A plot of $\ln\Delta V$ versus t is linear and yields $k_{obs} = 2.23s^{-1}$

a. : $\Delta V = V_\infty - V_t$

TABLE 3.2 Typical Results from Rate Measurements

(i) Sodium Hydroxide (0.075$\underline{M}$), 1-($HOCH_2CMe_2CH_2O$)-DNN (4×10^{-5} $\underline{M}$)

Second process, measured at 435nm in water.

t/s	ΔOD^a
60	0.279
120	0.225
180	0.185
240	0.142
300	0.115
360	0.085
420	0.065
480	0.058
540	0.046
600	0.037
720	0.023
840	0.014
960	0.007

A plot of $\ln\Delta OD$ versus t is linear and yields

$$k_{obs} = 3.7 \times 10^{-3} \text{ l mol}^{-1}\text{s}^{-1}$$

a.: $\Delta OD = OD_\infty - OD_t$

3.3 Results and Discussion

3.3.1 Visible Spectra

In aqueous solution, the reaction between 1-(2,2-dimethyl-3-hydroxypropoxy)-2,4-dinitronaphthalene (4×10^{-5} M) and sodium hydroxide (10^{-2} M) produces an initial orange species immediately on mixing, which is followed by the formation of a yellow species. Visible spectra, in aqueous solution, show that the yellow species has absorption maxima at 390nm and 435nm, identical to the visible spectrum of 2,4-dinitronaphthol (4×10^{-5} M) in water. In 50/50 (v/v) DMSO-water the orange species, with visible maxima at 350nm and 508nm, has a longer lifetime but the eventual product is again 2,4-dinitronaphthol. Spectra are shown in Figure 3.1. The ^{1}H n.m.r. spectra discussed next indicate structure (3.2; R=Me) for the orange species.

3.3.2 ^{1}H n.m.r. Measurements

The ^{1}H n.m.r. spectrum of 1-(2,2-dimethyl-3-hydroxypropoxy)-2,4-dinitronaphthalene in [$^{2}H_6$] DMSO is shown in Figure 3.2(A). The ring protons give bands at δ8.80 (s,H-3), 8.50 (m,H-5 and H-8) and 7.90 (m, H-6 and H-7). Bands are observed in similar positions for other 2,4-dinitronaphthyl ethers.[130,131,133] Bands are observed for the α-CH_2 group at δ4.0(s), the γ-CH_2 group at δ3.4(s) and the methyl groups at δ1.0(s). The hydroxyl proton gives a band at δ4.1(s).

Figure 3.2(B) shows the spectrum of 1-(2,2-dimethyl-3-hydroxypropoxy)-2,4-dinitrohaphthalene in the presence of one

Figure 3.1 Visible spectra of 1-(2,2-dimethyl-3-hydroxypropoxy)-2,4-dinitronaphthalene (4×10^{-5} M) and sodium hydroxide (1×10^{-3} M) in 50/50 (v/v) water-DMSO.

Time increases A to H

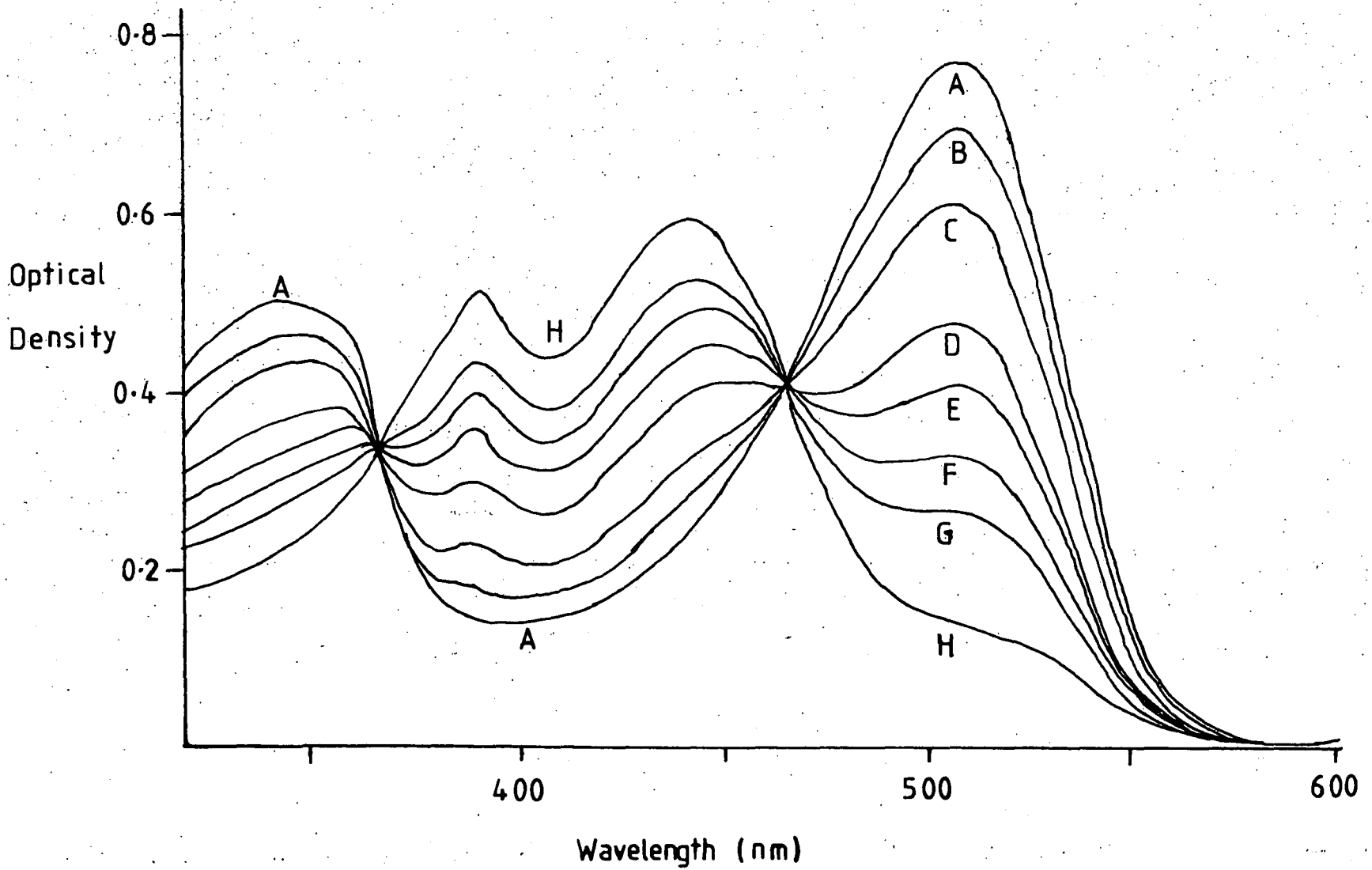

molecular equivalentof sodium deuterioxide. The spectral changes are consistent with the formation of the spiro-adduct (3.2; R=Me). The ring protons now absorb at δ8.86 (s, H-3), 8.63 (dd, H-8), 8.0 (m, H-5) and 7.40 (m, H-6 and H-7). Formation of spiro-adducts of other 2,4-dinitronaphthol systems produce bands close to these positions.[130] The methyl groups are no longer equivalent and give two bands of equal intensity at δ0.98 (s, Me_{trans}) and 1.10 (s, Me_{cis}). The rather simple spectrum of the methylene protons to give bands at δ3.45 and δ3.90 with a geminal coupling constant of 12Hz indicates that, at least the two methylene protons *cis* to the 2-nitro group are equivalent, as are the two methylene protons *trans* to the 2-nitro group. The small bands at δ3.3 and δ0.85 can be attributed to the decomposition of the parent.

This evidence rules out any possibility that the orange intermediate is the σ-adduct produced by hydroxide attack at the 3-position as previously observed[133] in the hydroxy ethers of 2,4,6-trinitrobenzene, or at the 1-position.

3.3.3 Kinetic and Equilibrium Data

In alkaline media the formation of the spiro-adduct is expected[130-132] to involve the rapid equilibrium transfer of the side chain proton followed by a slow intramolecular cyclisation, as shown in Scheme 3.1.

By use of stopped flow spectrophotometry kinetic data for the spiro complex formation, given in Table 3.4, were obtained in water and in 20/80 (v/v) DMSO-water at 25°C. The base concentration was always in large excess over parent concentration so first order kinetics were observed, and measurements made at a wavelength of 500nm.

Figure 3.2 (A) ^{1}H n.m.r. spectrum of 0.2M 1-(2,2-dimethyl-3-hydroxypropoxy)-2,4-dinitronaphthalene in $[^{2}H_{6}]$ DMSO.

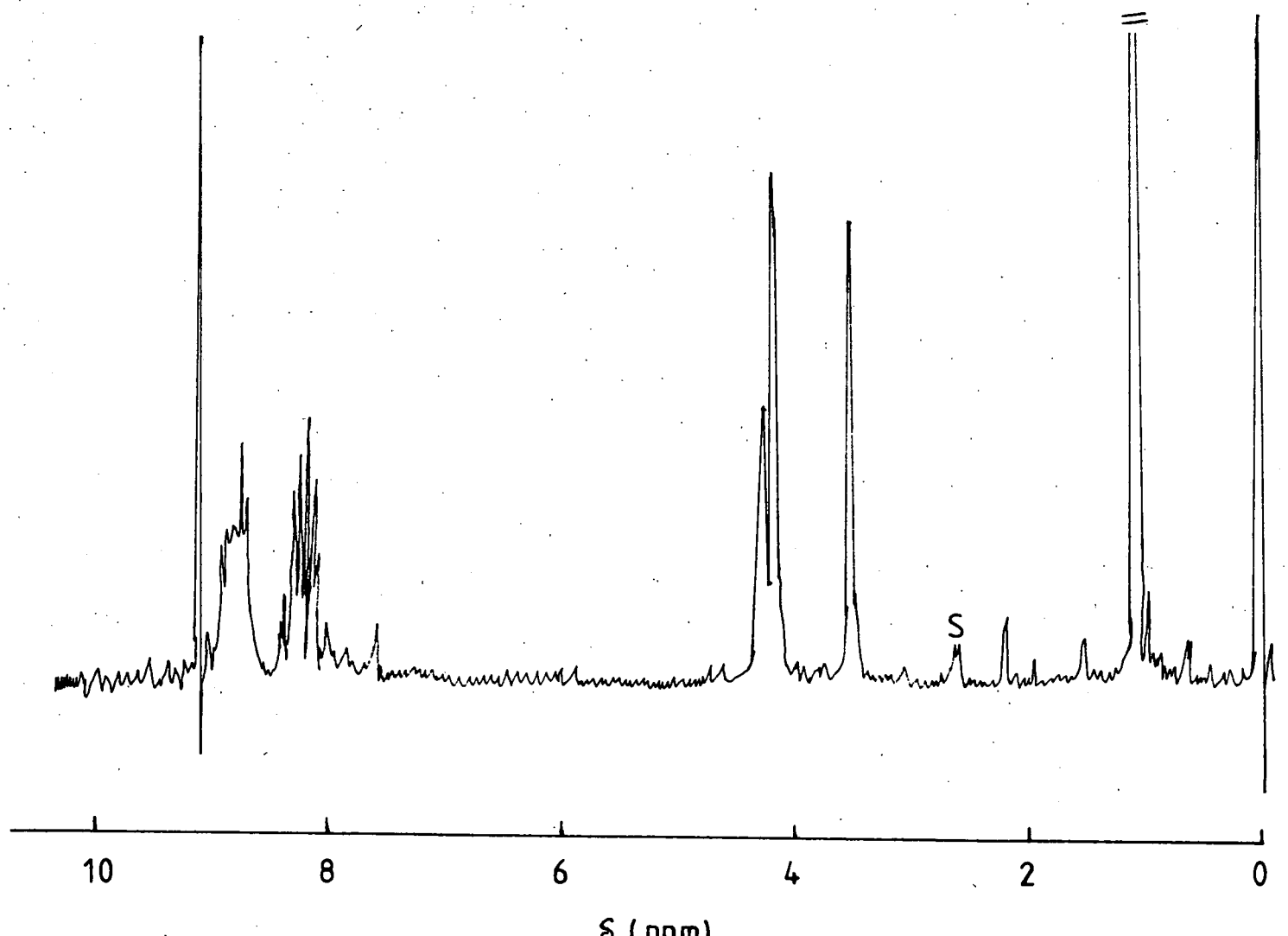

Figure 3.2 (B) Spectrum after the addition of 1 equivalent of base. Bands marked 'S' are due to the solvent

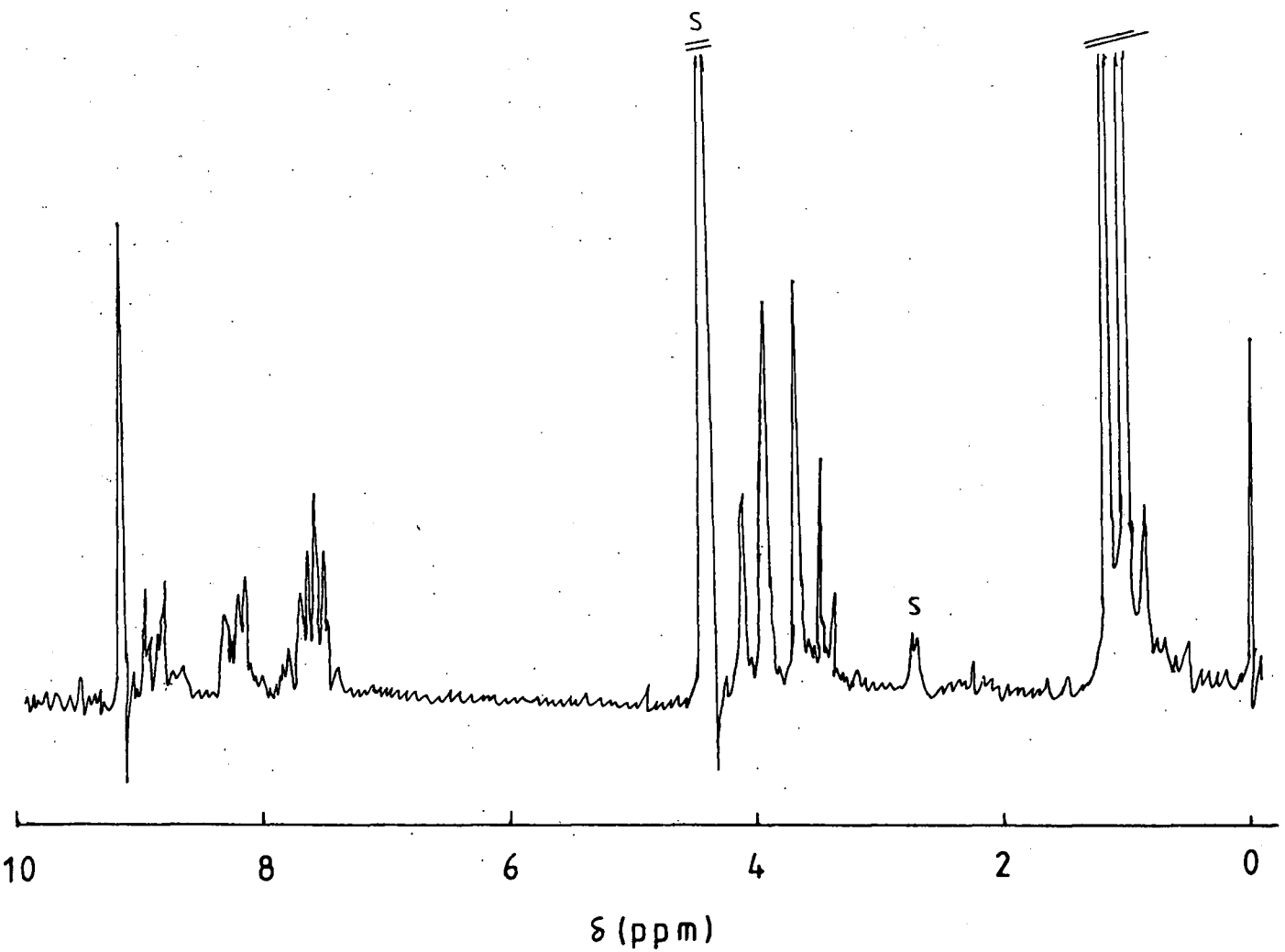

TABLE 3.3 ^{1}H n.m.r. data for 1-(2,2-dimethyl-3-hydroxypropoxy)-2,4-dinitronaphthalene and its spiro-complex formed by reaction with sodium hydroxide

Species	Solvent	δ^{a}(ring)				δ^{a}(side chain)			
		H-8	H-5	H-6 & H-7	H-3	αCH_2	γCH_2	Me_2	OH
1-($HOCH_2CMe_2CH_2O$)-DNN	D_2O	8.5(m)	8.5(m)	7.90(m)	8.80(m)	4.0(s)	3.4(s)	1.0(s)	4.1(s)
(3.2; R=Me)	D_2O	8.63(dd)	8.0(m)	7.40(m)	8.86(s)	3.45[b] & 3.90[b]		0.98 & 1.10	

a. Chemical shifts measured relative to internal TMS.

b. Two protons cis and two protons trans to 2-nitro group. Geminal J = 12 Hz.

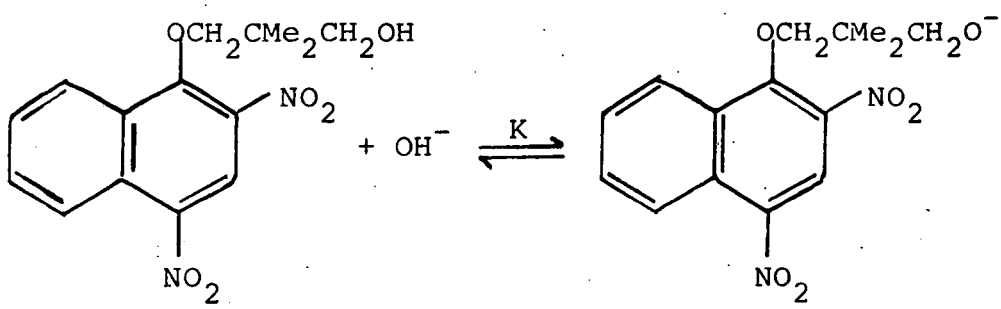

(3.3) (3.4)

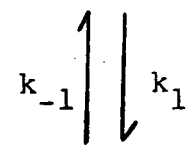

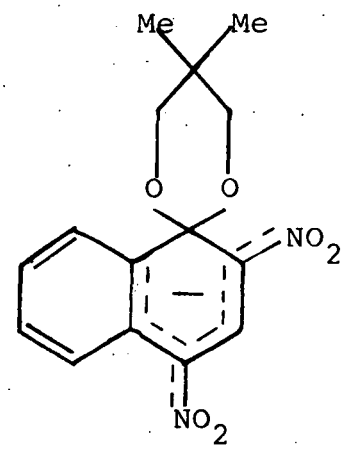

Scheme 3.1

(3.5)

From Scheme 3.1 the rate expression for spiro-complex formation can be derived as equation 3.1.

$$k_{obs} = \frac{k_1 K [OH^-]}{(1+K[OH^-])} + k_{-1} \qquad \text{(equation 3.1)}$$

The overall equilibrium constant for spiro-complex formation, K_c, is defined as equation 3.2.

$$K_c = \frac{KK_1}{(1+K[OH^-])} \qquad \text{(equation 3.2)}$$

However, as the pK_a of 1-(2,2-dimethyl-3-hydroxypropoxy)-2,4-dinitronaphthalene is unlikely[134] to be much lower than 15, it follows that values of K will probably be less than 0.1 1 mol^{-1}. Therefore, the value of the term $1 + K[OH^-]$ in equations 3.1 and 3.2 will be very close to unity for the sodium hydroxide concentrations studied. This assumption, which has been used previously,[129] allows equations 3.1 and 3.2 to be modified to equations 3.3 and 3.4.

$$k_{obs} = K_1K[OH^-] + k_{-1} \qquad \text{(equation 3.3)}$$

$$K_c = KK_1 = \frac{k_1K}{k_{-1}} \qquad \text{(equation 3.4)}$$

The rate data shown in Table 3.4 confirm this assumption as a plot of k_{obs} versus base concentration is linear, as predicted by equation 3.3. In water this plot yields the values k_1K 7 1 $mol^{-1}s^{-1}$ and k_{-1} 3.5 s^{-1}, and in 20:80 DMSO-water k_1K 12 1 $mol^{-1}s^{-1}$ and k_{-1} 1.4 s^{-1}. Using equation 3.4 the rate data gives values for K_c(kin) of 2 1 mol^{-1} in water and K_c(kin) of 8.6 1 mol^{-1} s^{-1} in 20:80 DMSO-water. DMSO would be expected to have a stabilising effect on the complex formation. This explains the increase of the forward rate coefficient and decrease of the reverse rate coefficient, and therefore larger K_c for spiro-complex formation in a DMSO-water mixture.

The slow reaction in water, which produces the yellow species, is the alkaline hydrolysis of the parent to 2,4-dinitronaphthol and is shown in Scheme 3.2. The rate data for this reaction is given in Table 3.5. The rate determining step for the alkaline hydrolysis is hydroxide attack at the 1-position.

TABLE 3.4 Kinetic data for spiro-complex formation from 1-(2,2-dimethyl-3-hydroxypropoxy)-2,4-dinitronaphthalene at 25°C

[NaOH]/M	water		20/80 DMSO-water	
	k_{obs}/s^{-1}	k^{a}_{calc}/s^{-1}	k_{obs}/s^{-1}	k^{b}_{calc}/s^{-1}
0.01			1.59±0.1	1.52
0.025			1.64	1.70
0.035			1.72	1.82
0.05	3.9±0.3	3.8	2.0	2.0
0.075			2.2	2.3
0.10	4.1	4.2	2.7	2.6
0.20	4.9	4.9		
0.30	5.7	5.6		
0.40	6.2	6.3		

a. Calculated using k_1K 7 l mol s^{-1}, k_{-1} 3.5 s^{-1} and equation 3.3.

b. Calculated using k_1K 12 l mol^{-1} s^{-1}, k_{-1} 1.4 s^{-1} and equation 3.3.

Equation 3.5 was the rate expression used to calculate a value for k_2, the second order rate coefficient for base attack, of 0.06 ± 0.1 l mol^{-1}.

$$k_{obs} = \frac{k_2[OH^-]}{1+KK_1[OH^-]} \qquad \text{(equation 3.5)}$$

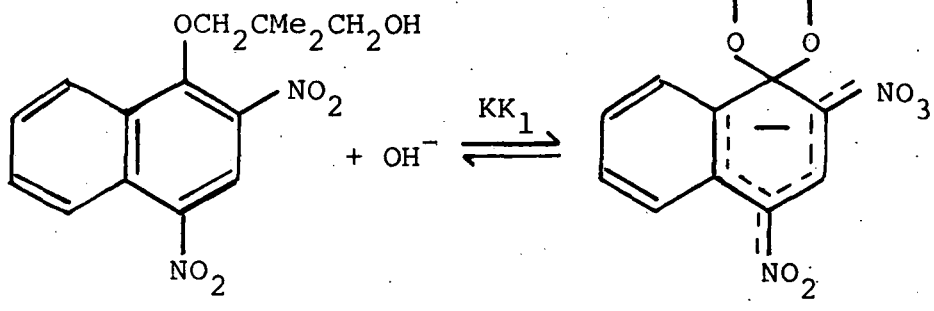

(3.3) (3.5)

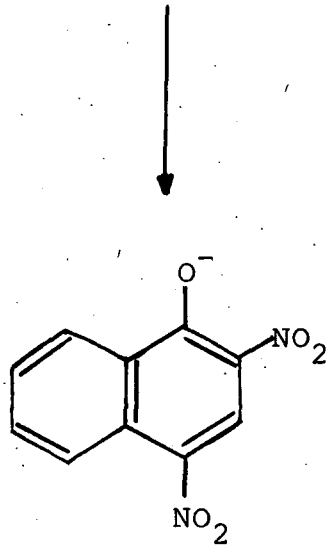

(3.6)

Table 3.5 summarizes the rate and equilibrium data for the cyclisation of the 2,2-dimethyl-3-hydroxypropoxyl ethers of picric acid and 2,4-dinitronaphthol and the 3-hydroxypropoxyl ethers of picric acid and 2,4-dinitronaphthol.

TABLE 3.5 Kinetic data for the formation of 2,4-dinitronaphthol from 1-(2,2-dimethyl-3-hydroxypropoxy)-2,4-dinitronaphthalene in water at 25°C

[NaOH]/M	$10^3 k_{obs}/s^{-1}$	k_2 [a]
0.025	1.4	0.060
0.050	3.0	0.060
0.075	3.7	0.058
0.100	4.5	0.055

a. Calculated using KK_1 2.0 l mol^{-1} and equation 3.5.

Comparison of the data, in Table 3.6, shows that for the 2,4-dinitronaphthyl ethers the value of KK_1 is unchanged and for the picryl ethers the value of KK_1 is halved when there is gem-dimethyl substitution in the side chain.

TABLE 3.6 Effects of gem-dimethyl substitution on spiro-complex formation in water at 25°C

Parent	k_1K l $mol^{-1}s^{-1}$	k_{-1}/s^{-1}	K_1K/ l mol^{-1}
1-($HOCH_2CMe_2CH_2O$)-TNB[a]	4.6	0.4	11.5
1-($HOCH_2CH_2CH_2O$)-TNB[b]	19.7	0.87	22.6
1-($HOCH_2CMe_2CH_2O$)-DNN	7.0	3.5	2.0
1-($HOCH_2CH_2CH_2O$)-DNN[c]	1.7	0.85	2.0

a. Ref. 135, b. Ref. 132, c. Ref. 130.

To explain this we have to consider K and K_1 separately. K is a measure of the acidity of the hydroxyl group. Murto[134] has reported that the pK_a values of propan-1-ol and 2-methylpropan-1-ol in water at 25°C are identical at 16.1, therefore methyl substitution at the β-carbon will have a small effect. Also for alcohols of the type RCH_2OH it has been reported[136,137] that the pK_a values can be calculated using $pK_a = 15.9 - 1.42\sigma^*$. If the value of σ^* for the t-butyl group is used then it is found that 2,2-dimethylpropan-1-ol has a pK_a value of 16.3. Although the pK_a values of the aromatic nitro-compounds compared above will be lower than those of aliphatic alcohols,[130,131] it seems unlikely that gem-dimethyl substitution will have a large effect on their acidities.

K_1 is the equilibrium constant for the internal cyclisation. If gem-dimethyl substitution causes little change to the values of K or KK_1 then it must also have little effect on the values of K_1. This would not be predicted because usually gem-dialkyl substitution into a methylene side chain increases the rate and equilibrium constants for cyclisation reactions. For cyclohexane derivatives two factors are believed[138,139] to favour cyclisation on gem-dialkyl substitution. These are a decrease in unfavourable gauche interactions and a smaller loss in entropy (due to a reduction in the internal rotations in the starting alkyl substituted compound).

For 1-(2,2-dimethyl-3-hydroxypropoxy)-2,4-dinitronaphthalene the latter factor should be operative in the open side chain as gem-dimethyl substitution would be expected to restrict rotation. However to explain why the value of K_1 is little changed for this compound there must be an additional factor to consider.

This is likely to be steric crowding due to the presence of the ortho-nitro group stopping the dioxalan ring from taking up its least strained conformation, and therefore the unfavourable repulsive interactions in the dimethyl compounds cannot be avoided. This explanation also applies to 1-(2,2-dimethyl-3-hydroxypropoxy)-2,4,6-trinitrobenzene.

The second order rate coefficients for the formation of 2,4-dinitronaphthol, from the 2,4-dinitronaphthyl ethers, and picric acid, from the picryl ethers, resulting from nucleophilic attack at the 1-position are compared in Table 3.7.

TABLE 3.7 Rate constants for hydroxide attack at the 1-position of 1-substituted-2,4-dinitronaphthalenes and 1-substituted-2,4,6-trinitrobenzenes in water at 25°C

Parent	k_2/l mol^{-1}s^{-1}
1-($HOCH_2CH_2CH_2O$)-DNN[a]	0.06
1-($HOCH_2CMe_2CH_2O$)-DNN	0.06
1-($HOCH_2CMe_2CH_2O$)-TNB[b]	0.7
1-($HO[CH_2]_6O$)-TNB[b]	0.6
1-(MeO)-TNB[c]	1.4

a. Ref. 130, b. Ref. 135, c. Ref. 140.

It is seen that gem-dimethyl substitution at the β-carbon has little effect. Indeed comparing the trinitrobenzene hydroxy ethers, changing the nature of R in the side chain $-OCH_2R$ group has little effect on the value of k_2. Therefore the effect of changing electron density and steric hindrance at the 1-position by changing R is small. However, the ten-fold increase in the value of k_2 for the trinitrobenzene derivatives compared to the dinitronaphthalene derivates is consistent with

the expected decrease in electron density at the 1-position.

3.4 Derivation of the Rate and Equilibrium Expressions

(a) Formation of the spiro-complex in water.

$$(3.3) + OH^- \underset{\text{fast}}{\overset{K}{\rightleftharpoons}} (3.4) + H_2O$$

$$(3.4) \overset{k_1}{\underset{k_{-1}}{\rightleftharpoons}} (3.5)$$

(i) Calculation of the stoichiometric equilibrium constant, K_c

$$K_c = \frac{[3.5]}{([3.3]+[3.4])[OH^-]} \qquad (1)$$

$$K = \frac{[3.4]}{[3.3][OH^-]} \quad (2) \qquad K_1 = \frac{[3.5]}{[3.4]} \quad (3)$$

Substituting (2) into (1)

$$K_c = \frac{[3.5]}{[3.3][OH^-](1+K[OH^-])} \qquad (4)$$

Combining (2) and (3)

$$KK_1 = \frac{[3.5]}{[3.3][OH^-]} \qquad (5)$$

Substituting (5) into (4)

$$K_c = \frac{KK_1}{1 + K[OH^-]}$$

(ii) Calculation of the rate expression

$$\frac{d[3.5]}{dt} = k_1[3.4] - k_{-1}[3.5] \qquad (6)$$

$$[3.3] + [3.4] + [3.5] = [3.3]_o$$

$$[3.4] = [3.3]_o - [3.3] - [3.5] \qquad (7)$$

Substituting (2) into (7)

$$[3.4] = [3.3]_o - \frac{[3.4]}{K[OH^-]} - [3.5]$$

Re-arranging,

$$[3.4] = \underbrace{\frac{[3.3]_o K[OH^-]}{(1 + K[OH^-])}}_{A} - \frac{3.5\ K[OH^-]}{(1 + K[OH^-])} \qquad (8)$$

Substituting (8) into (6)

$$\frac{d[3.5]}{dt} = k_1 \left(A - \frac{[3.5]K[OH^-]}{(1 + K[OH^-])} \right) - k_{-1}[3.5] \qquad (9)$$

At equilibrium, $\frac{d[3.5]}{dt} = 0.$

$$0 = k_1 \left(A - \frac{[3.5]_e K[OH^-]}{(1 + K[OH^-])} \right) - k_{-1}[3.5]_e \qquad (10)$$

Subtracting (10) from (9)

$$\frac{d[3.5]}{dt} = \frac{k_1 K[OH^-]}{(1+K[OH^-])} ([3.5]_e - [3.5]) + k_{-1}([3.5]_e - [3.5])$$

Re-arranging,

$$\frac{d[3.5]}{dt} \quad \frac{1}{([3.5]_e - [3.5])} = \frac{k_1 K[OH^-]}{(1+K[OH^-])} + k_{-1} \qquad (11)$$

$$\text{Observed rate} = \frac{d\ OD}{dt} = k_{obs}\ (OD_e - OD)$$

Relating the [3.5] to OD.

Only (3.5) absorbs at the wavelength used for rate measurements. Therefore,

$$OD = \varepsilon_{3.5}[3.5] \qquad (12)$$

At equilibrium

$$OD_e = \varepsilon_{3.5}\ [3.5]_e$$

Hence,

$$OD_e - OD = \varepsilon_{3.5}\ ([3.5]_e - [3.5]) \qquad (13)$$

Differentiating (12)

$$\frac{d\ OD}{dt} = \varepsilon_{3.5} \frac{d[3.5]}{dt} \qquad (14)$$

Hence, substituting (14) into (13)

$$\frac{d\ OD}{dt} \cdot \frac{1}{(OD_e - OD)} = \frac{d[3.5]}{dt} \cdot \frac{1}{[3.5]_e - [3.5]}$$

Hence,

$$k_{obs} = \frac{k_1 K [OH^-]}{1 + K[OH^-]} + k_{-1}$$

(b) Nucleophilic attack at the 1-position following spiro-complex formation in water

$$(3.3) + OH^- \underset{}{\overset{KK_1}{\rightleftharpoons}} (3.5) + H_2O$$

$$\downarrow$$

$$(3.6) + ROH$$

$$\frac{d[3.6]}{dt} = k_2 [3.3][OH^-] \qquad (15)$$

At equilibrium

$$\frac{d[3.3]}{dt} + \frac{d[3.5]}{dt} + \frac{d[3.6]}{dt} = 0$$

$$\frac{d[3.6]}{dt} = \frac{-d[3.3]}{dt} - \frac{d[3.5]}{dt} \qquad (16)$$

Differentiating (5)

$$\frac{d[3.3]}{dt} = \frac{d[3.5]}{dt} \cdot \frac{1}{KK_1[OH^-]} \qquad (17)$$

Substituting (17) into (16)

$$\frac{d[3.6]}{dt} = \frac{-d[3.5]}{dt} \left(1 + \frac{1}{KK_1[OH^-]} \right) \qquad (18)$$

Substituting (18) into (15) and re-arranging

$$\frac{-d[3.5]}{dt} \cdot \frac{1}{[3.5]} = \frac{k_2[OH^-]}{(1+KK_1[OH^-])}$$

Relating change of concentration to change of OD. k_2 was measured by following the decay in colour of the spiro-complex (3.5). This was measured at 435nm.

$$OD = \varepsilon_{3.3}[3.3] + \varepsilon_{3.5}[3.5] + \varepsilon_{3.6}[3.6] \qquad (19)$$

Substituting (5) into (19)

$$OD = \frac{\varepsilon_{3.3}[3.5]}{KK_1[OH^-]} + \varepsilon_{3.5}[3.5] + \varepsilon_{3.6}[3.6]$$

$$[3.6]_{stoich} = [3.6] + [3.3] + [3.5]$$

Hence,

$$OD = \varepsilon_{3.6}([3.6]_{stoich} - [3.3] - [3.5]) + \varepsilon_{3.3}\frac{[3.5]}{KK_1[OH^-]} + \varepsilon_{3.5}[3.5]$$

$$= \varepsilon_{3.6}[3.6]_{stoich} - \varepsilon_{3.6}[3.5] - \varepsilon_{3.6}\frac{[3.5]}{1+KK_1[OH^-]} + \varepsilon_{3.3}\frac{[3.5]}{KK_1[OH^-]} + \varepsilon_{3.5}[3.5]$$

$$OD = \varepsilon_{3.6}[3.6]_{stoich} - [3.5]\left(\varepsilon_{3.6} + \frac{\varepsilon_{3.6}}{KK_1[OH^-]}\right) + [3.5]\left(\frac{\varepsilon_{3.3}}{KK_1[OH^-]} + \varepsilon_{3.5}\right)$$

$$OD_\infty = \varepsilon_{3.6}[3.6]_{stoich}$$

Hence,

$$(OD_\infty - OD) = [3.5]\left(\varepsilon_{3.6} + \frac{\varepsilon_{3.6}}{KK_1[OH^-]}\right) - [3.5]\left(\frac{\varepsilon_{3.3}}{KK_1[OH^-]} + \varepsilon_{3.5}\right) \qquad (20)$$

$$\frac{d\ OD}{dt} = \frac{d[3.5]}{dt}\left(\varepsilon_{3.6} + \frac{\varepsilon_{3.5}}{KK_1[OH^-]}\right) - \frac{d[3.5]}{dt}\left(\frac{\varepsilon_{3.3}}{KK_1[OH^-]} + \varepsilon_{3.5}\right) \quad (21)$$

Multiplying the reciprocal of (21) with (20)

$$\frac{-d[3.5]}{dt} \cdot \frac{1}{[3.5]} = \frac{d\ OD}{dt} \cdot \frac{1}{(OD_\infty - OD)}$$

Definition of k_{obs}

$$k_{obs} = \frac{d\ OD}{dt} \cdot \frac{1}{(OD_\infty - OD)}$$

Hence,

$$k_{obs} = \frac{k_2[OH^-]}{1+KK_1[OH^-]}$$

CHAPTER FOUR

THE REACTIONS OF 2,2′,4,4′,6,6′-HEXANITROBIBENZYL WITH ALKOXIDE IONS

4.1 Introduction

The commercially important product 2,2′,4,4′,6,6′-hexanitrostilbene (HNS) can be produced by the dehydrogenation of 2,2′,4,4′,6,6′-hexanitrobibenzyl (HNBB) (4.1) by quinnones in basic media.[68,141] To help understand the mechanism of this reaction a knowledge of the mode or modes of interaction of HNBB and base is important. Reported here are the reversible reaction of HNBB with alkoxide ions.

By analogy with related compounds, such as 2,4,6-trinitrotoluene (TNT) and 2,4,6-trinitrobenzyl chloride (TNBCl),[82] the expected products from the reaction of HNBB with base are the σ-adducts (4.2), where base attack has occurred at the 3-position, and (4.3), where base attack has occurred at the 1-position, and the conjugate base (4.4). However, HNBB has two aromatic rings separated by two methylene groups so that dianionic species may be formed. Two of the possible dianions are (4.5) and (4.6).

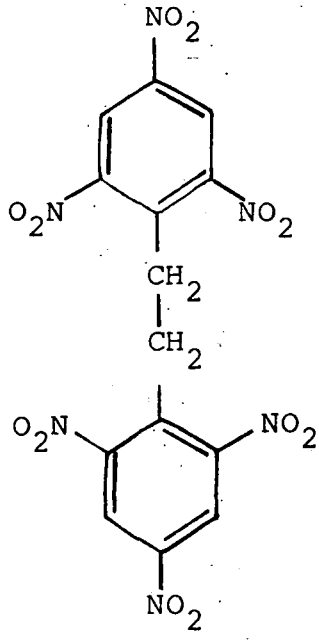

(4.1)

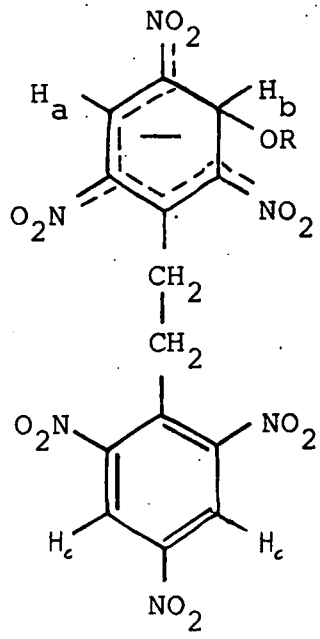

(4.2)

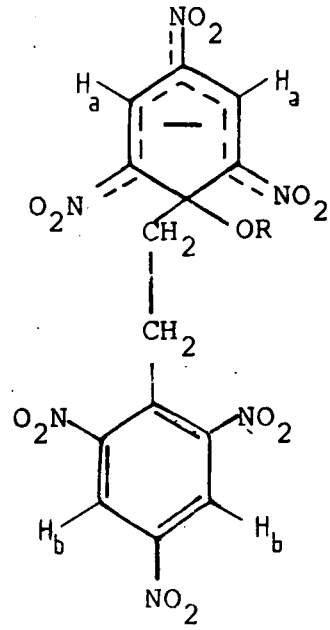

(4.3)

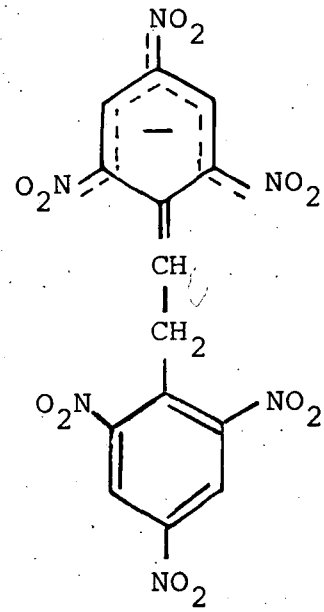

(4.4)

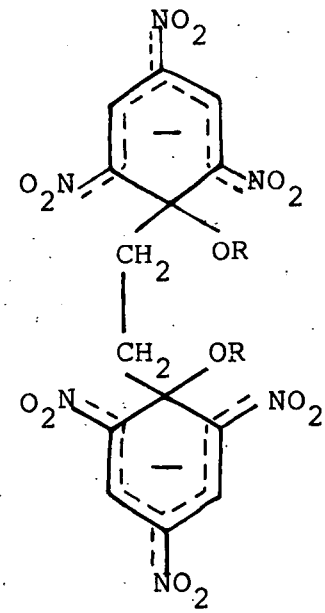

(4.5)

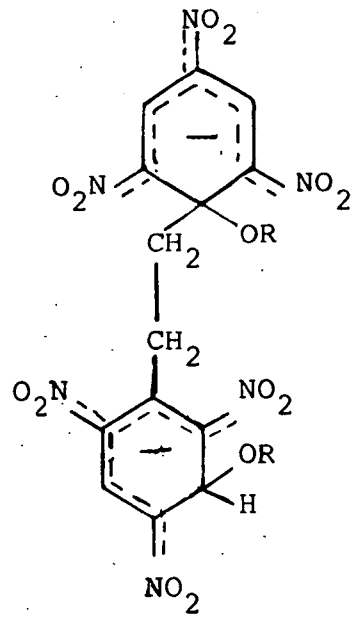

(4.6)

4.2 Experimental

In most cases visible spectra were recorded on a Pye-Unicam SP8005 spectrophotometer at 28°C. However, one spectrum for a short-lived species was constructed from optical density values measured on the stopped-flow spectrophotometer at 25°C.

Kinetic and equilibrium measurements were made on the Canterbury SF-3A stopped-flow spectrophotometer at 25°C. Rates for reactions with one colour forming process, or with two well separated colour forming processes, were calculated using the standard methods described in Chapter Two. All rate measurements are a mean of at least five separate determinations and are precise to ±5%. Optical density measurements were also recorded on a Beckman No.25 spectrophotometer at 25°C.

^{1}H n.m.r. measurements were made with a Varian EM 360L instrument using tetramethylsilane as the internal reference.

TABLE 4.1 Typical results from rate measurements.

(i) HNBB (1×10^{-5} M), Sodium methoxide (0.02M). One process only observed, measured at 480nm in methanol.

(ii) HNBB (1×10^{-5} M), Sodium ethoxide (0.004M) First process, measured at 430nm in ethanol.

(i)		(ii)	
t/s	ΔV	t/ms	ΔV
0.0	3.3	0	4.5
0.1	2.8	10	2.9
0.2	2.3	20	2.1
0.3	1.9	30	1.0
0.4	1.6	40	0.8
0.5	1.4	50	0.4
0.6	1.2	60	0.2
0.8	0.9		

A plot of $\ln\Delta V$ versus t is linear and yields $k_{obs} = 1.56\ s^{-1}$

A plot of $\ln\Delta V$ versus t is linear and yields $k_{obs} = k_{fast} = 47.0\ s^{-1}$

a. $\Delta V = V_\infty - V_t$

4.3 Results and Discussion

4.3.1 ^{1}H n.m.r. Measurements

Figure 4.1 shows the ^{1}H n.m.r. spectrum of HNBB in [$^2H_6$]dimethyl sulphoxide (DMSO). It consists of two singlets at δ3.40 and δ9.10 which are due respectively to the methylene and ring protons. The addition of two molecular equivalents of sodium trideuteriomethoxide in [$^2H_4$] methanol results in the rapid formation of two doublets at δ6.1 and δ8.5, at the expense of the ring proton band. Gradually these bands decreased in intensity with time to be replaced by two singlets at δ8.53 and δ8.6. After six minutes the band at δ8.53 took all the intensity of the ring protons, and the final spectrum, shown in Figure 4.2, which was stable for the next ten minutes, consisted of this band and a singlet of equal intensity at δ2.40. This spectrum is consistent with methoxide attack occurring at the 1- and 1′- positions of HNBB to give the di-adduct (4.5). The shift to high field, relative to the resonance positions of HNBB, of the ring and methylene proton resonances is in agreement with similar shifts in related systems.[25,26] The initial observation of doublets at δ6.1 and δ8.5 indicates that rapid methoxide attack occurs at the unsubstituted 3- and/or 3′-positions.[25,26] When one molecular equivalent of base was added to HNBB initially two doublets at δ6.1 and δ8.5 and a broad band at δ8.9 were observed, and may be attributed to the ring protons of (4.2; R=Me). The band at δ8.9 is due to the ring protons of the unattacked ring and its broadness may indicate that a small amount of electron transfer to give radical anions occurs.[25,26] The band at δ8.6 observed at

Figure 4.1 ^{1}H n.m.r. spectrum of HNBB in [$^{2}H_{6}$] DMSO

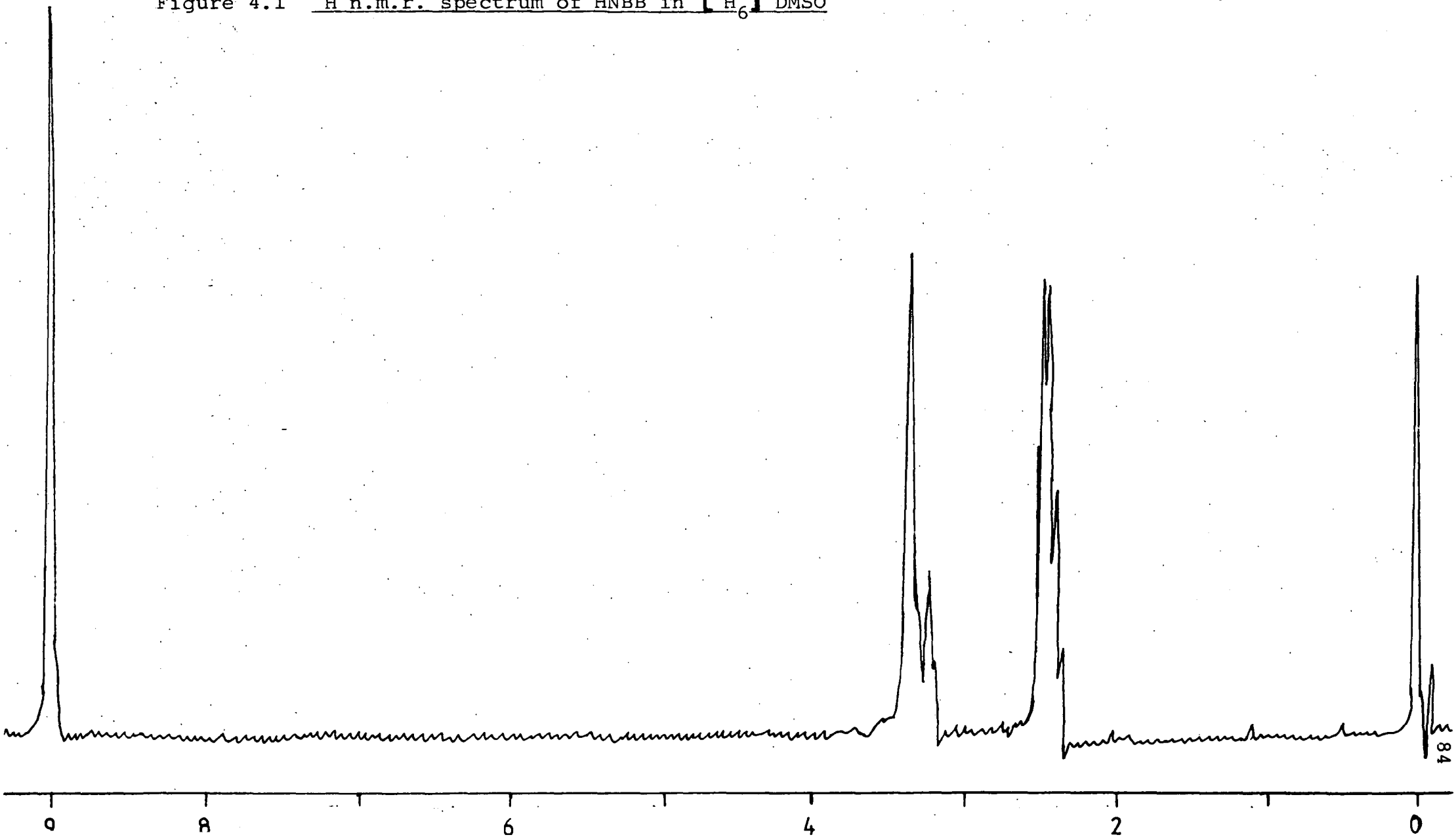

Figure 4.2 Final ^{1}H n.m.r. Spectrum of HNBB with 2 mol.equiv. of $NaOCD_3$ in $[^{2}H_6]$ DMSO.

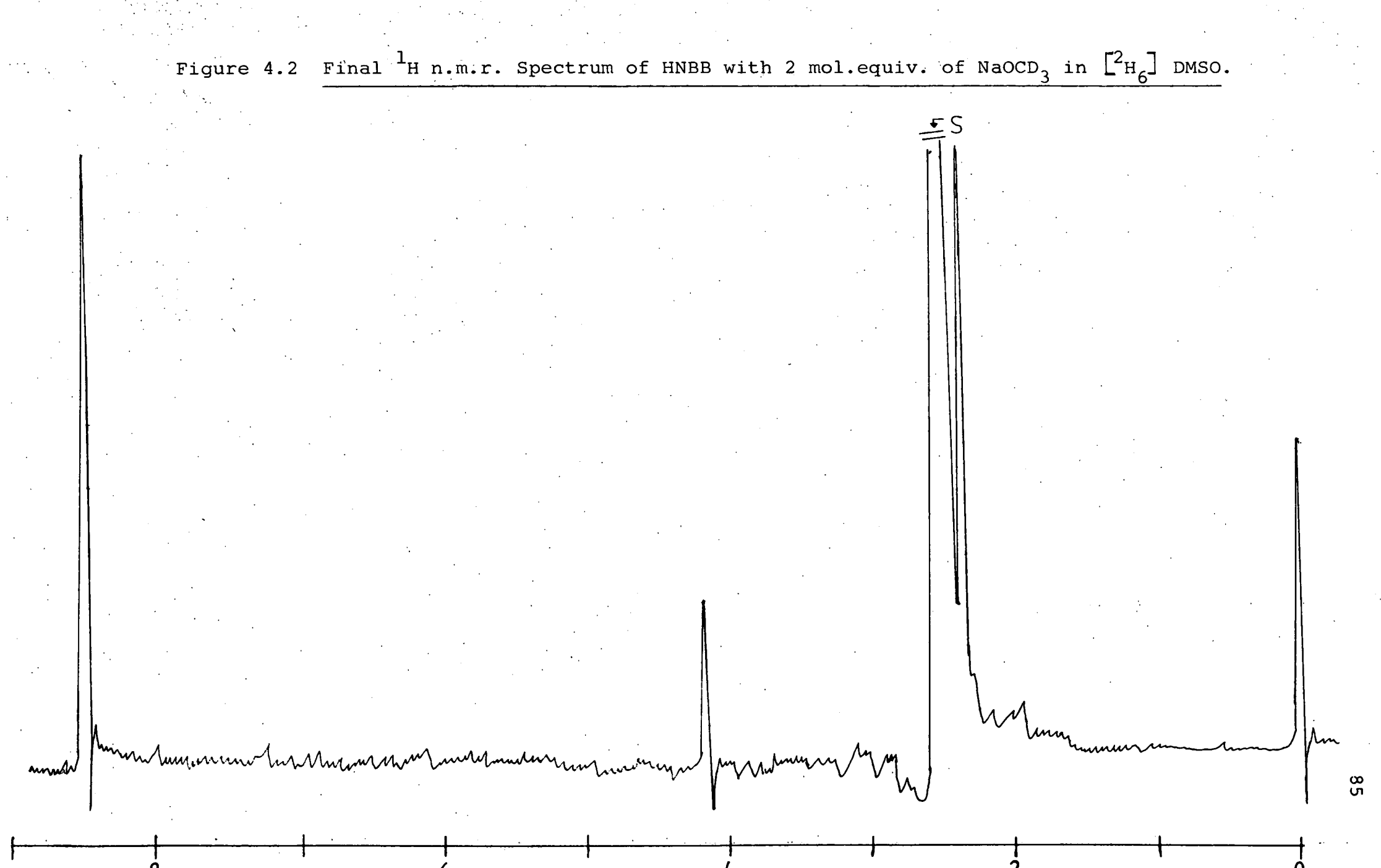

intermediate times in solutions containing two molecular equivalents of base may be due to the ring protons, in the 1-methoxy-substituted ring of the di-adduct (4.6; R=Me) which presumably will be present as transient species. Another possibility is that the band is due to a thermodynamically unfavourable rotational isomer of the di-adduct (4.5; R=Me).

From these measurements it can be concluded that methoxide addition at the 3- or 3′- positions is kinetically favourable, while methoxide addition at the 1- or 1′- positions gives the more thermodynamically favourable adduct.

TABLE 4.2 ^{1}H n.m.r. data for HNBB and its adducts with sodium methoxide in [$^2H_6$] DMSO

Species		δ^a(ring)	δ^a(chain)
HNBB		9.10(s)	3.40(s)
(4.2; Me)	H_b	6.1(d)	Two bands expected.
	H_a	8.5(d)	Too difficult to
	H_c	8.9(s)	measure.
(4.3; Me)	H_a	8.6(s)	Two bands expected.
	H_b	8.9(s)	Too difficult to measure.
(4.5; Me)		8.53(s)	2.40(s)

a. All shifts measured relative to internal TMS.

4.3.2 Reaction with Sodium Methoxide in Methanol

In methanol the visible spectra for the reaction between HNBB and dilute sodium methoxide (<0.2M) show the reversible formation of a red species, absorption maxima at 430nm and 500nm (shoulder), followed after a few minutes by an irreversible decomposition reaction of the substrate. The spectra of the red species is consistent with the formation of a σ-adduct, rather than formation of the conjugate base.[25-28,83]

Stopped-flow spectrophotometry of the system showed that one rapid colour forming reaction was present. Kinetic and equilibrium data were measured for this species and are given in Table 4.3. The best interpretation of the 1-position to give the adduct (4.3; R=Me) is shown in equation 4.1. As the base concentration is in large excess over HNBB concentration equation 4.2 will apply.

$$\text{HNBB} + \text{MeO}^- \underset{k_{-1}}{\overset{k_1}{\rightleftharpoons}} \text{(4.3; R=Me)} \qquad \text{(equation 4.1)}$$

$$k_{obs} = k_1[\text{MeO}^-] + k_{-1} \qquad \text{(equation 4.2)}$$

Values for k_1 of 23 l mol^{-1} s^{-1} and k_{-1} of 1.15 s^{-1} are obtained for a linear plot of k_{obs} versus base concentration. Combination of these values gives a value for K_1 of 20 l mol^{-1} which is in good agreement with that obtained from equilibrium optical density measurements.

There is no evidence, at the base concentrations used, that there is substantial conversion of HNBB into the di-adduct (4.5; R=Me). Only one rate process is observed

TABLE 4.3 Kinetic and equilibrium data for the reaction of HNBB with sodium methoxide in methanol at 25°C

[NaOMe] /M	k_{obs}/s^{-1}	OD(480nm) [a]	K_1 [b] /l mol^{-1}
0.01	1.4±0.1	0.0041	23
0.02	1.6	0.0066	21
0.04	2.1	0.0098	20
0.07	2.8	0.0114	16
0.10	3.4	0.0146	20

a. For 1 x 10^{-5} M HNBB measured with a 2mm cell. A Benesi-Hildebrand plot[76] gives a value of 0.022 for complete conversion, corresponding to a value for ε of 1.1 x 10^4 l mol^{-1}cm^{-1}.

b. Calculated using the expression

$$K_1 = OD(480)/[0.022-OD(480)][NaOMe]$$

---

and the value of the extinction coefficient is too low for the di-adduct (cf ethoxide addition). The di-adduct was observed in the ^{1}H n.m.r. spectra because the presence of DMSO greatly increases the basicity of the medium.[25,26]

The n.m.r. work also indicates that methoxide addition at the 3-position, to give (4.2; R=Me), precedes methoxide addition at the 1-position. However, it is known that the equilibrium constant for methoxide addition at the 3-position of TNT in methanol is 0.07 l mol^{-1}. Therefore, the equilibrium constant for the adduct (4.2; R=Me) would be expsected to be small, hence the failure to observe it.

4.3.3 Reaction with Sodium Ethoxide in Ethanol

Evidence is found for the formation of (4.3; R=Et) preceded by formation of (4.2; R=Et), and for the presence at equilibrium of the di-adduct (4.5; R=Et), in the more basic medium of ethoxide in ethanol.

The visible spectra of HNBB (2×10^{-5}M) with sodium ethoxide (0.001 to 0.2M) were recorded, see Figure 4.3. After two minutes the spectrum observed is typical of σ-adducts with absorption maxima at 432nm and 500nm in dilute base concentration; in more concentrated base the higher energy band was shifted slightly to 438nm. With time absorption maxima were replaced by a band at 380nm with a broad shoulder to longer wavelength. Acidification of the solution containing the first species regenerated HNBB indicating a reversible reaction, while acidification of the solution containing the second species did not, indicating an irreversible reaction.

Optical density values after the completion of σ-adduct formation but before the decomposition had occurred were measured and are presented in Table 4.4. It is found that a Benesi-Hildebrand plot[76] of the reciprocal of optical density versus the reciprocal of base concentration was curved indicating that the reaction is more complicated than simple 1:1 adduct formation. But a short extrapolation of the plot gave an optical density value of 0.666 at 500nm for complete conversion. From this the extinction coefficients for the species formed at the higher base concentrations can be calculated. It is found that the values ε 6.0×10^4 (438nm) and ε 3.33×10^4 l mol^{-1} cm^{-1} (500nm) are approximately double those for adducts of 1:1 stoichiometry.[24] This strongly

Figure 4.3 Visible spectra of HNBB (2×10^{-5} M) and sodium ethoxide in ethanol. (A) [NaOEt] 2×10^{-3} M after 2 minutes; (B) same as A after 30 minutes (indicates irreversible reaction of substrate), (C) [NaOEt] 4×10^{-2} M after 2 minutes

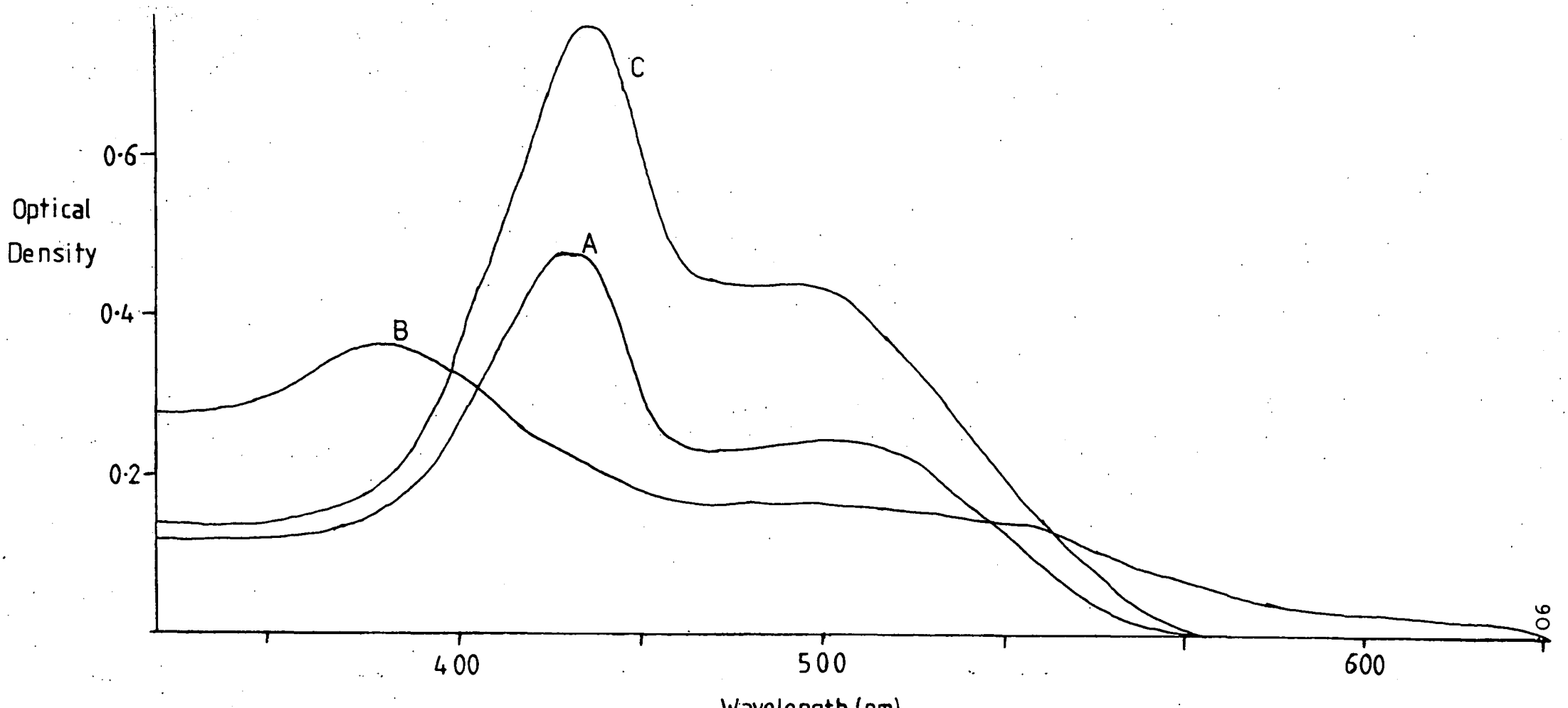

TABLE 4.4 Equilibrium data for the reaction of HNBB (2×10^{-5} M) with sodium ethoxide in ethanol at 25°C.

No.	[NaOEt]/M	OD(500nm)[a] observed	OD(500nm)[b] calculated
1	0.001 01	0.192	0.190
2	0.002 02	0.245	0.253
3	0.004 04	0.297	0.311
4	0.007 06	0.357	0.356
5	0.0099	0.388	0.384
6	0.0199	0.428	0.445
7	0.0398	0.509	0.509
8	0.0597	0.538	0.544
9	0.0796	0.560	0.566
10	0.099	0.582	0.581
11	0.149	0.607	0.604
12	0.198	0.623	0.617

a. In items 1-10 the solutions were made up to constant ionic strength, I=0.1M with sodium perchlorate.

b. Calculated from equations 4.3, 4.4 and 4.5 with values of K_1 1200 l mol^{-1}, K_2 30 l mol^{-1}, ε(4.3; R=Et) 1.67×10^4 l mol^{-1} cm^{-1}, ε(4.5; R=Et) 3.33×10^4 l mol^{-1} cm^{-1}.

suggests that the di-adduct is formed by ethoxide attack on the two picryl rings in more concentrated solution. Presumably from the n.m.r. evidence the most likely strucutre of the di-adduct is (4.5; R=Et) and due to the separation of the picryl rings by two methylene groups, each picryl ring would appear to act independently of the other to produce what could be considered as two 1:1 adducts per molecule, which would create an absorption double that is expected of a 1:1 adduct. The data presented in Table 4.4 can be accommodated by the presence of two equilibria involving ethoxide attack on one (equation 4.3) or two (equation 4.4) rings. The assumption that in items 1-3 there is little di-adduct present allows calculation of an approximate value for K_1, and the assumption that in items 8-12 little HNBB would remain allowing calculation of an approximate value for K_2. Then by iteration

HNBB + EtO^- $\overset{K_1}{\rightleftharpoons}$ (4.3; R=Et) (equation 4.3)

(4.3; R=Et) + EtO^- $\overset{K_2}{\rightleftharpoons}$ (4.5; R=Et) (equation 4.4)

HNBB + (4.3; R=Et) + (4.5; R=Et) = 2×10^5 (equation 4.5)

the values for K_1 of 1200±200 l mol^{-1} and K_2 30±10 l mol^{-1} are obtained which give good agreement between calculated and observed optical densities. The much lower K_2 value indicates that even though the picryl rings are well separated by two methylene groups ethoxide addition on one ring to form the σ-adduct inhibits ethoxide attack on the second ring.

Two, well separated, colour forming processes are observed by stopped-flow spectrophotometry in solutions of low, <0.01M, base concentrations. The faster process is attributed to the formation by ethoxide attack at the 3-position of the σ-adduct (4.2; R=Et) and gives a spectrum with maxima at 430nm and 490nm.

The slower process represents ethoxide attack at the 1-position to form the σ-adduct (4.3; R=Et). The reaction scheme is given by equation 4.6 and since base concentration is in large excess over HNBB concentration it is readily shown by standard

(4.2; R=Et)

HNBB + EtO^- $\underset{k_{-3}}{\overset{k_3}{\rightleftharpoons}}$ (4.3; R=Et) (equation 4.6)

$\overset{k_1}{\underset{k_{-1}}{\rightleftharpoons}}$

methods that equations 4.7 and 4.8 will apply. The data is presented in Table 4.5.

$$k_{fast} = k_3[EtO^-] + k_{-3} \qquad \text{(equation 4.7)}$$

$$k_{slow} = \frac{k_1[EtO^-]}{1+K_3[EtO^-]} + k_{-1} \qquad \text{(equation 4.8)}$$

A linear plot of k_{fast} versus base concentration gave values for k_3 of 4000 l mol^{-1} s^{-1} and k_{-3} of 32 s^{-1}. Combination of these values gives a value for K_3 of 125 l mol^{-1} which gave good agreement with K_3 values calculated from the optical densities at completion of the fast process. Using the value for K_3 of 125 l mol^{-1} a linear plot for k_{slow} versus $[EtO^-]/(1 + K_3[EtO^-])$ is obtained giving values for k_1 of 84 l mol^{-1} s^{-1} and k_{-1} of 0.070 s^{-1}.

TABLE 4.5 Kinetic data for the 1:1 interaction of HNBB (1×10^{-5} M) with sodium ethoxide in ethanol at 25°C

[NaOEt]/ M	k_{fast}/ s^{-1}	OD(430nm)[a]	K_3/ 1 mol^{-1}	k^b_{slow}/ s^{-1}	k^c_{slow}(calc)
0.0010	36.5	0.0039	110	0.14	0.14
0.0015				0.18	0.18
0.0020	41	0.0092	150	0.21	0.20
0.0025				0.23	0.23
0.0040	48	0.0137	130	0.30	0.30
0.0060	52	0.0164	115	0.33	0.36
0.0084	66	0.0209	130		
0.0100	72	0.0218	120		

a. After completion of the fast process. 2mm path length cell. A Benesi-Hildebrand plot gives a value of 0.040 for complete conversion.

b. Calculated from $K_1 = OD(430)/[0.040-OD(430)][NaOEt]$

c. Calculated from equation 4.8 with k_{-1} 0.07 s^{-1}, k_1 84 1 mol^{-1} s^{-1} and K_3 125 1 mol^{-1}.

4.3.4 Comparison with Related Compounds

Table 4.6 allows comparison of the data for the 1:1 adducts of TNT, TNBCl and 1,3,5-trinitrobenzene (TNB) with those for HNBB.

The value of K_1 for ethoxide attack at the 1-positio of HNBB is *ca* 10 times higher than the value of K_3 for attack at the 3-position. TNBCl also shows a thermodynamic preference for attack at the 1-position[82] whereas for TNT only the formation of the 3-alkoxy adduct is observed.[83,142] There are two factors favouring alkoxide addition at the 1-position of HNBB or TNBCl relative to TNT. The first is the inductive electron withdrawing effect of the 2,4,6-trinitrobenzyl or chlorine substituents. The second and probably of more importance is the steric factor. The greater the size of the group at the 1-position, the greater the possibility of relief of steric strain as the group is bent from the ring-plane in the 1-alkoxy adduct.

Although the 1-alkoxy-adduct is thermodynamically preferred, the formation of the 3-alkoxy-adduct, by alkoxide attack at the unsubstituted ring position, is kinetically preferred. A characteristic of the position of addition appears to be the values of the reverse reaction rate coefficients. Thus, values of k_{-1} are at least 100 times lower than values of k_{-3}.

Values of K_3 decrease from TNB to TNBCl to HNBB. This is because adducts formed by addition at the unsubstituted ring position are destabilised by bulky groups at the 1-position A bulky group at the 1-position causes the ortho nitro groups to rotate out of coplanarity with the ring, where nitro groups

TABLE 4.6 Comparison of rate and equilibrium data for HNBB with those for related compounds

	k_3/l mol^{-1}s^{-1}	k_{-3}/s^{-1}	K_3/l mol^{-1}	k_1/l mol^{-1}s^{-1}	k_{-1}/s^{-1}	K_1/l mol^{-1}
HNBB-methoxide				23	1.15	20
TNBCl-methoxide[82]			<20	770	2.2	350
TNT-methoxide[83]	280	3000	0.07			
*TNB-methoxide[78]	7300	330	20			
HNBB-ethoxide	4000	32	125	84	0.07	1200
TNBCl-ethoxide[82]	10000	14	700	7000	<1	>10000
*TNB-ethoxide[78]	40000	20	2000			

* Refers to addition at an unsubstituted position.

display their maximum electron withdrawing ability.

The data for HNBB provides no evidence for the formation of the conjugate base (4.4) by deprotonation of the substrate. This was expected as a major reaction for TNBCl or TNT with alkoxide ions as the removal of a side chain proton to form the conjugate base.[82] As these proton transfer reactions are slow, it would be expected the deprotonation of HNBB by alkoxide ions would also be slow. Therefore it is likely the fairly rapid irreversible decomposition reaction of HNBB, mentioned earlier, occurs before there is any appreciable formation of (4.4) in alcoholic solutions of base. Later, evidence of an anionic species produced when HNBB is deprotonated by amine bases will be given.

4.4 Derivation of the Rate Expressions

(i) Formation of the 3-alkoxy-adduct in alcohol.

$$(\underline{4.1}) \quad + \quad RO^- \quad \underset{k_{-3}}{\overset{k_3}{\rightleftharpoons}} \quad (\underline{4.2})$$

As $[RO^-] \gg [4.1]$

$$k_{obs} = k_f + k_r \qquad (\underline{1})$$

where k_f is the first order rate coefficient for the forward reaction and k_r is the first order coefficient for the reverse reaction.

$$k_f = k_3[RO^-] \qquad (\underline{2})$$

$$k_r = k_{-3} \qquad (\underline{3})$$

Substituting (2) and (3) into (1)

$$k_{obs} = k_3[RO^-] + k_{-3}$$

(ii) Formation of the 1-alkoxy-adduct in alcohol.

$$(\underline{4.1}) \quad + \quad RO^- \quad \underset{k_{-3}}{\overset{k_3}{\rightleftharpoons}} \quad (\underline{4.2}) \quad \underset{k_{-1}}{\overset{k_1}{\rightleftharpoons}} \quad (\underline{4.3})$$

$$K_3 = \frac{[4.2]}{[4.1][RO^-]} \qquad (\underline{4})$$

$$[4.1] + [4.2] + [4.3] = [4.1]_o \qquad (\underline{5})$$

Substituting (4) into (5).

$$[4.3] + [4.1](1+K_3[RO^-]) = [4.1]_o$$

Re-arranging,

$$[4.1] = A - \frac{[4.3]}{1 + K_3[RO^-]} \qquad (6)$$

where $A = \frac{[4.1]_o}{1 + K_3[RO^-]}$

$$\frac{d[4.3]}{dt} = k_1[4.1][RO^-] - k_{-1}[4.3] \qquad (7)$$

Substituting (6) into (7)

$$\frac{d[4.3]}{dt} = k_1[RO^-]\left(A - \frac{[4.3]}{1+K_3[RO^-]}\right) - k_{-1}[4.3] \qquad (8)$$

At equilibrium, $\frac{d[4.3]}{dt} = 0.$

$$0 = k_1[RO^-]\left(A - \frac{[4.3]_e}{1+K_3[RO^-]}\right) - k_{-1}[4.3]_e \qquad (9)$$

Subtracting (9) from (8)

$$\frac{d[4.3]}{dt} = \frac{k_1[RO^-]}{1+K_3[RO^-]}([4.3]_e - [4.3]) + k_{-1}([4.3]_e - [4.3])$$

Re-arranging,

$$\frac{d[4.3]}{dt} \cdot \frac{1}{([4.3]_e - [4.3])} = \frac{k_1[RO^-]}{1+K_3[RO^-]} + k_{-1} \qquad (10)$$

In the reaction there are 3 species present, (4.1), (4.2) and (4.3). At the wavelength the reaction is studied (4.1) does not absorb.

Hence,

$$OD = \varepsilon_{4.3}[4.3] + \varepsilon_{4.2}[4.2] \qquad (11)$$

Substituting (4) into (11), then (6)

$$OD = \varepsilon_{4.2}\left(A - \frac{[4.3][RO^-]K_3}{1+K_3[RO^-]}\right) + \varepsilon_{4.3}[4.3]$$

Re-arranging,

$$OD = [4.3]\left(\varepsilon_{4.3} - \frac{\varepsilon_{4.2} K_3 [RO^-]}{1+K_3[RO^-]} \right) + \varepsilon_{4.2} \cdot A \qquad (12)$$

At equilibrium,

$$OD_e = [4.3]_e \left(\varepsilon_{4.3} - \frac{\varepsilon_{4.2} K_3 [RO^-]}{1+K_3[RO^-]} \right) + \varepsilon_{4.2} \cdot A \qquad (13)$$

Differentiating (12)

$$\frac{dOD}{dt} = \frac{d[4.3]}{dt} \left(\varepsilon_{4.3} - \frac{\varepsilon_{4.2} K_3 [RO^-]}{1+K_3[RO^-]} \right) \qquad (14)$$

Combining (12), (13) and (14).

$$\frac{dOD}{dt} \cdot \frac{1}{OD_e - OD} = \frac{d[4.3]}{dt} \cdot \frac{1}{([4.3]_e - [4.3])}$$

Hence, as the definition of k_{obs} is

$$k_{obs} = \frac{dOD}{dt} \cdot \frac{1}{(OD_e - OD)}$$

it has been shown

$$k_{obs} = \frac{k_1 [RO^-]}{1+K_3[RO^-]} + k_{-1}$$

CHAPTER FIVE

THE REACTIONS OF 2,2′,4,4′,6,6′-HEXANITROSTILBENE WITH ALKOXIDE IONS

5.1 Introduction

An important commercial method for producing the thermally stable explosive 2,2′,4,4′,6,6′-hexanitrostilbene (HNS) (5.1),[4,143] involves the reaction of 2,4,6-trinitrotoluene (TNT) with aqueous sodium hypochlorite in mixed solvents.[2] Intense colours are observed during this reaction. If the species producing these colours can be identified it may be of help in determining the reaction mechanism. Therefore the colour forming reactions of HNS with alkoxides have been investigated and are reported in this chapter.

As for 2,2′,4,4′,6,6′-hexanitrobibenzyl (HNBB), reported in the previous chapter, and previous studies of TNT derivatives with bases,[25-28,82] likely products of the 1:1 interaction of HNS with bases are the σ-adducts (5.2) and (5.3) with alkoxide attack at the 3- or 1-positions respectively. The 1:2 interaction of HNS with base is likely to produce the di-adduct (5.5). For HNS there is the additional possibility of base attack, or proton abstraction, at the olefinic bond.[144,145] Fyfe[146] has shown base addition at the β-carbon atom of the double bond occurs in α-cyano-4-nitro-4′-X-stilbenes.

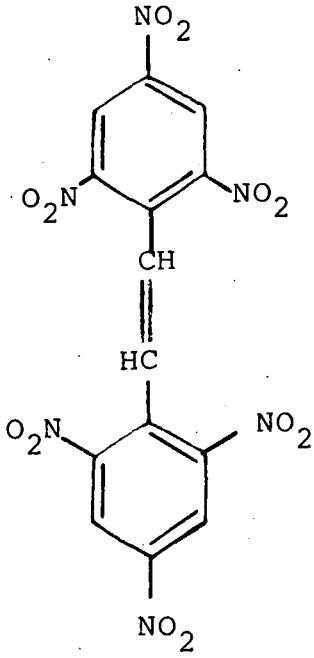

(5.1)

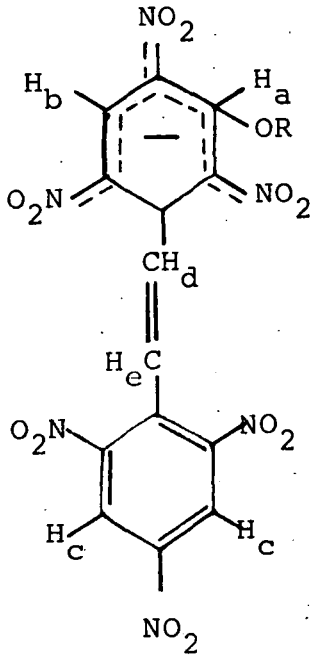

(5.2)

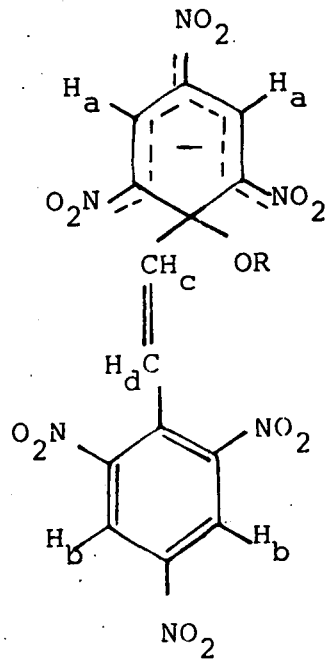

(5.3)

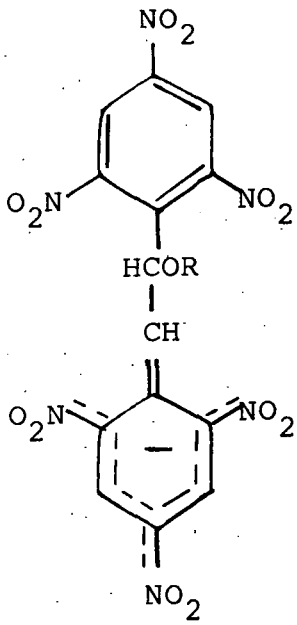

(5.4)

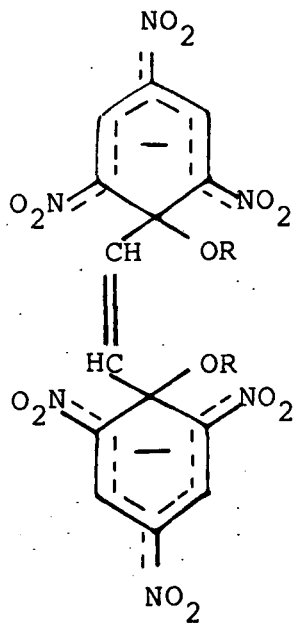

(5.5)

5.2 Experimental

Visible spectral measurements were made using a Pye-Unicam SP 500, Pye-Unicam SP 8005, Beckman No.25 or Hi-Tech SF-3L stopped-flow spectrophotometer. All rate measurements were made using a Hi-Tech SF-3L stopped-flow spectrophotometer at 25°C under first order conditions. Rate coefficients are the mean of at least five separate determinations and are precise to ±5%.

^{1}H n.m.r. measurements were made with either a Varian EM 360L instrument or with a Bruker HX 90E instrument modified for Fourier transform operation using a deuterium lock. Chemical shifts were measured relative to internal tetramethylsilane.

TABLE 5.1 Typical results from rate measurements

(i) HNS (2×10^{-5} M), sodium methoxide (0.007M).
Medium process, measured at 470nm in methanol.

(ii) HNS (1×10^{-5} M), sodium ethoxide (2×10^{-3} M).
Fast process, measured at 480nm in ethanol.

(i)		(ii)	
t/s	ΔV^a	t/ms	ΔV^a
0.0	3.4	10	4.8
0.1	2.9	15	3.6
0.2	2.4	20	2.7
0.3	2.0	25	2.0
0.4	1.7	30	1.4
0.5	1.4	35	1.0
0.6	1.2	40	0.7
0.8	0.9		

A plot of $\ln\Delta V$ versus t is linear and yields $k_{med} = 1.74\ s^{-1}$

A plot of $\ln\Delta V$ versus t is linear and yields $k_{fast} = 61.3\ s^{-1}$

a. $\Delta V = V_\infty - V_t$

TABLE 5.2 Typical results from rate measurements

(i) HNS (2×10^{-5} M), sodium methoxide (1.6×10^{-4} M). Slow process, measured at 470nm in methanol.

(i)

t/s	ΔOD^a
0	0.497
300	0.468
600	0.438
1200	0.378
1800	0.324
2400	0.277
3000	0.232
3600	0.194
4200	0.160

a. $\Delta OD = OD_\infty - OD_t$

5.3 Results and Discussion

5.3.1 ^{1}H n.m.r. Measurements

Figure 5.1 shows the ^{1}H n.m.r. spectrum of 0.02M HNS in 80:20 (v/v) $[^2H_6]$ DMSO-$[^2H_4]$ methanol. Two singlets with the expected intensity ratio 2:1 are observed at δ9.10 and δ7.12, due to the ring and olefinic protons respectively. (N.B. HNS is the trans isomer). When one molecular equivalent of sodium trideuteriomethoxide reacts with HNS evidence for (5.3; R=Me) is obtained, (see Figure 5.2). The singlets at δ8.9 and δ8.65 are attributed to the ring protons while the olefinic protons give an AB quartet at δ6.45 and δ6.8 with a value for J, the coupling constant, of 17 Hz being typical of trans-orientation.[147] Transient bands were also observed at δ9.00, 8.5 and 6.2 which are attributed[25,145] to the ring protons of (5.2; R=Me). As for HNBB, in the previous chapter, the 3-alkoxy-adduct is kinetically favoured while the 1-alkoxy-adduct is the thermodynamically more stable product. Figure 5.3 is the spectrum produced when two molecular equivalents of sodium trideuteriomethoxide is mixed with HNS. The singlets at δ8.53 and 6.05 are attributed to the ring and olefinic protons respectively of the symmetrical di-adduct (5.5; R=Me). Similar spectra were also obtained in a 50:50 (v/v) $[^2H_6]$ DMSO-$[^2H_4]$ methanol solvent system and typical double absorption spectra, λ_{max} *ca* 430nm and 480nm, of a σ-adduct were recorded in these solutions.

Visible spectra of HNS in the presence of sodium methoxide in methanol indicate a different species is formed with a maximum at 470nm. However, due to the insolubility

FIGURE 5.1 ^{1}H n.m.r. spectrum of HNS in 80:20 (v/v) $[^{2}H_{6}]$ DMSO-$[^{2}H_{4}]$ methanol

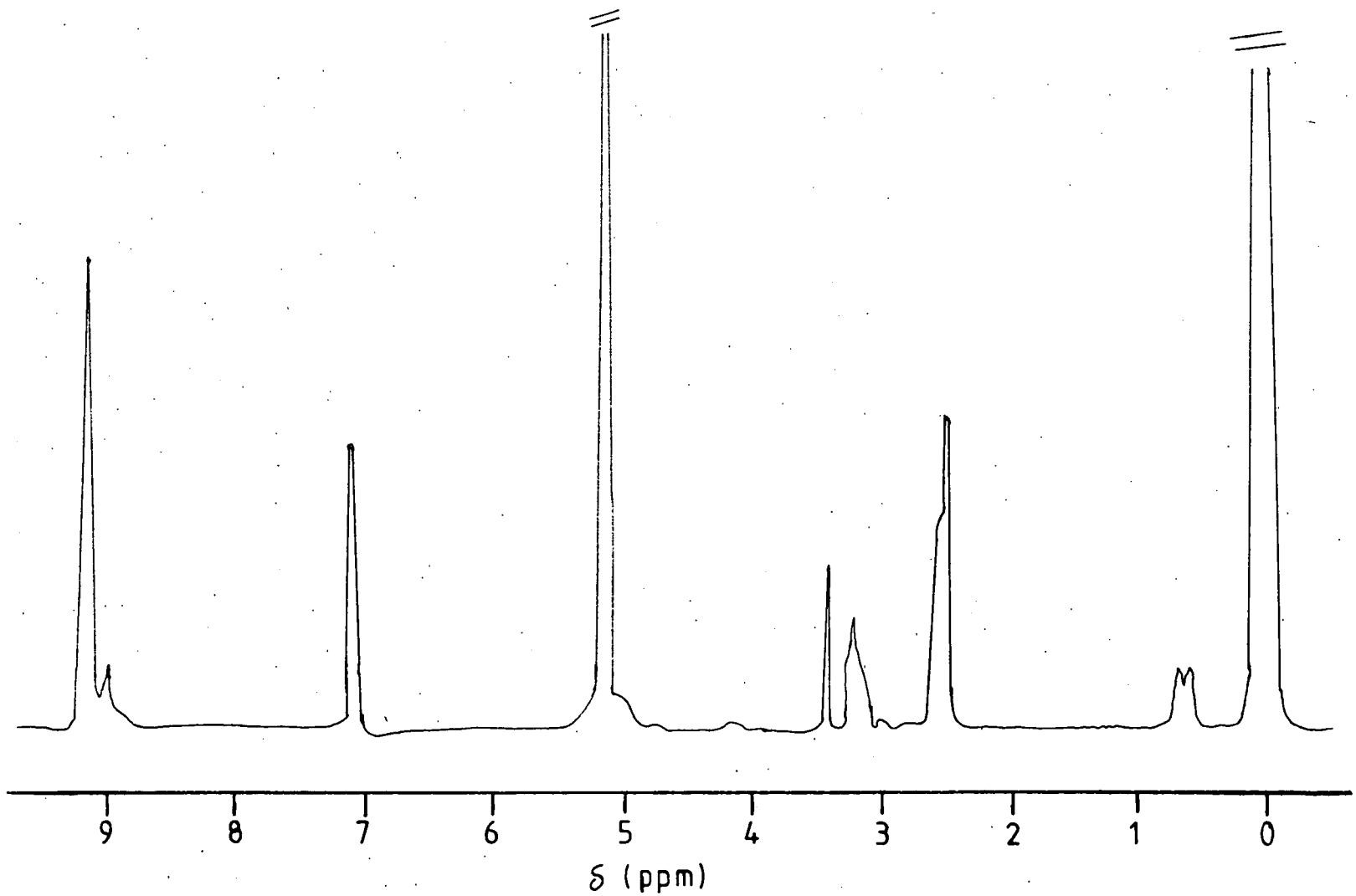

FIGURE 5.2 ^{1}H n.m.r. spectrum of HNS with 1 equivalent of $NaOCD_3$ in 80:20 (v/v) $[^{2}H_6]$ DMSO-$[^{2}H_4]$ methanol

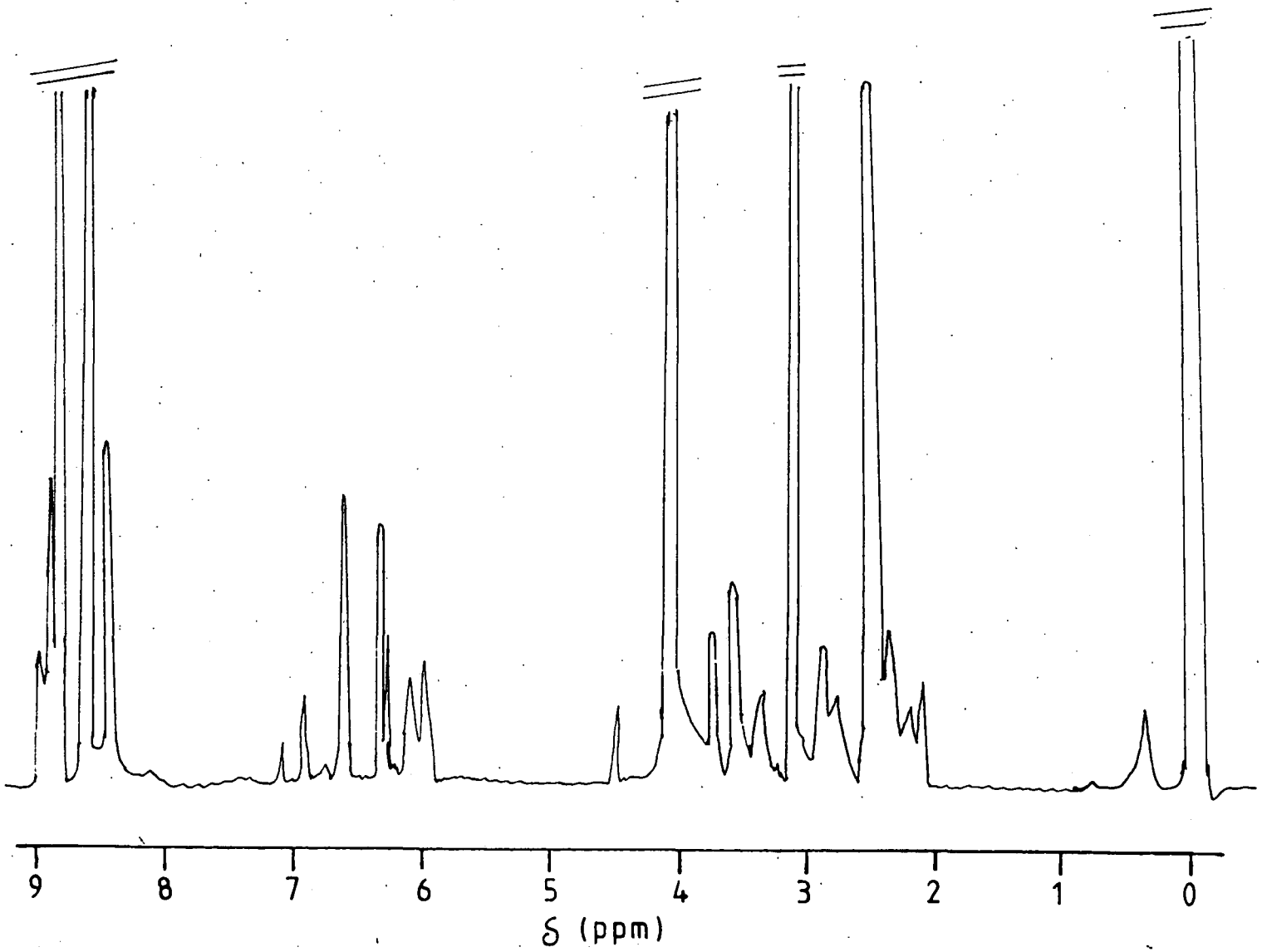

FIGURE 5.3 ^{1}H n.m.r. spectrum of HNS with 2 equivalents of $NaOCD_3$ in 80:20 (v/v) $[^{2}H_6]$ DMSO-$[^{2}H_4]$ methanol.

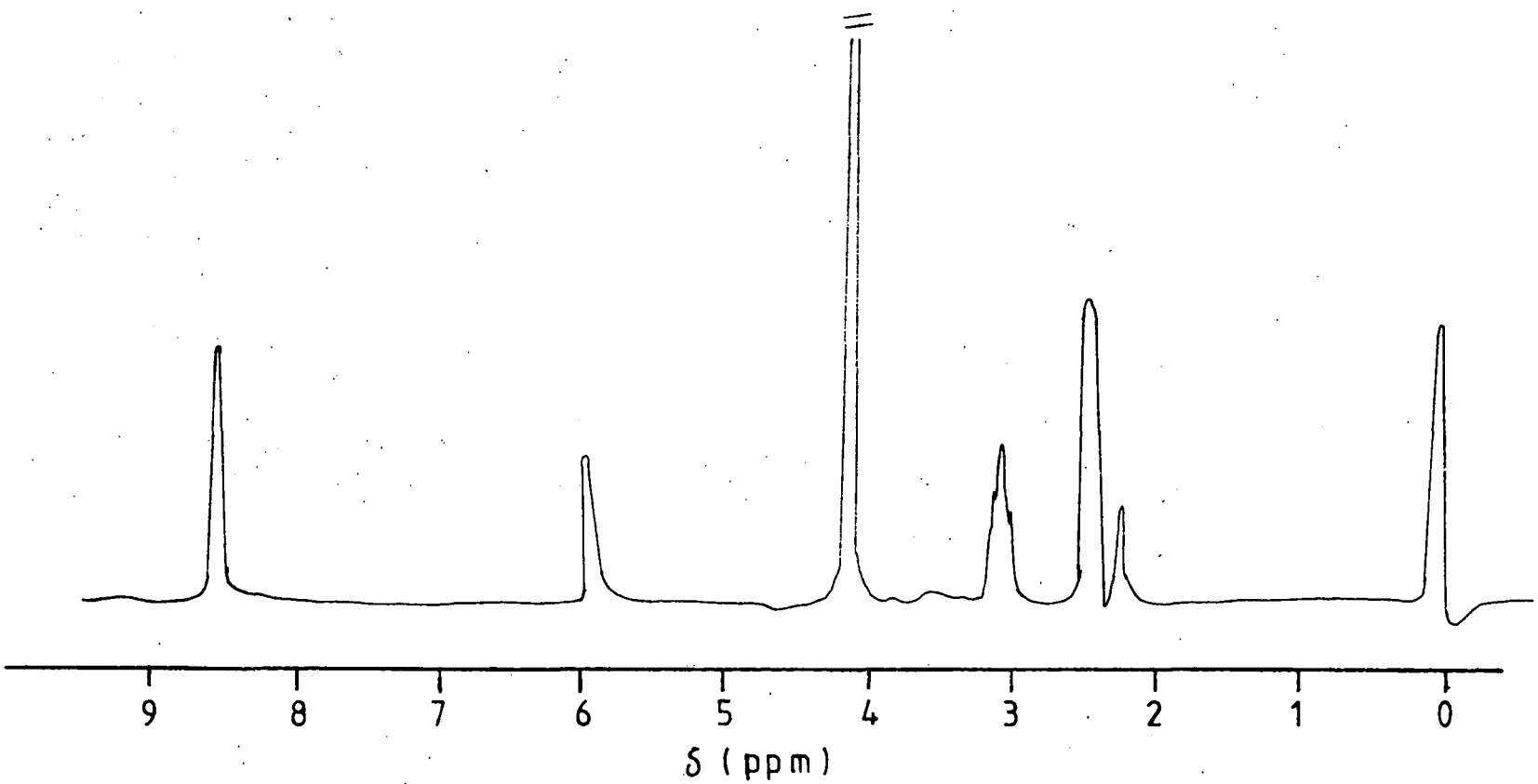

of HNS in methanol, and in 80:20 (v/v) methanol-DMSO, no clear ^1H n.m.r. spectra could be obtained in these media.

5.3.2 Reactions with Sodium Methoxide in Methanol

Three reversible processes can be observed for the 1:1 reaction of HNS with methoxide ions in methanol. The first process is too fast to measure by stopped-flow spectrophotometry, while the second colour forming process, giving an orange species with absorption maxima at 420nm and 480nm, is also fast but can be measured by stopped-flow spectrophotometry. These processes are taken to be the formation of (5.2; R=Me), by alkoxide attack at the 3-position, and the formation of (5.3; R=Me), by alkoxide attack at the 1-position, respectively. The third process is very much slower and can be measured by conventional spectroscopy. It gives a yellow species with absorption maxima at 470nm (ε 3.0 x 10^4 l mol^{-1} cm^{-1}) as shown in Figure 5.4. As stated previously n.m.r. measurements in methanol have not allowed the structure of the final product to be determined. However it seems highly probable that this species has the structure (5.4; R=Me). The visible spectrum is quite unlike that of σ-adducts formed by base attack at the aromatic ring-positions which show two maxima in the visible region.

The kinetic and equilibrium data presented in Table 5.4 are best analysed according to Scheme 5.1. All measurements were made with methoxide concentration buffered[148] or with methoxide concentration in large excess of the substrate concentration. The three colour forming processes were well separated and designated k_{fast}, k_{med} and k_{slow}.

TABLE 5.3 Chemical shifts for HNS and its adducts in 80:20 [$^2H_6$] DMSO-[$^2H_4$] methanol

Species		δ^a(ring)	δ^a(olefin)
HNS		9.10(s)	7.12(s)
(5.2; R=Me)	H_a	6.2(s)	Impossible
	H_b	8.53(s)	to determine
	H_c	9.00(s)	
(5.3: R=Me)	H_a	8.65(s)	AB quartet[b]
	H_b	8.9(s)	6.45, 6.8[c]
(5.5; R=Me)		8.53(s)	6.05(s)

a. δ values measured relative to internal TMS.

b. AB quartet defined in reference 147.

c. J = 17 Hz.

FIGURE 5.4 Visible spectra of HNS (2×10^{-5} M) and sodium methoxide 0.04M in methanol after A, 1 minute; B, 3 minutes; C, 20 minutes. These spectra show the conversion of (5.3; R=Me) to another species, probably (5.4; R=Me)

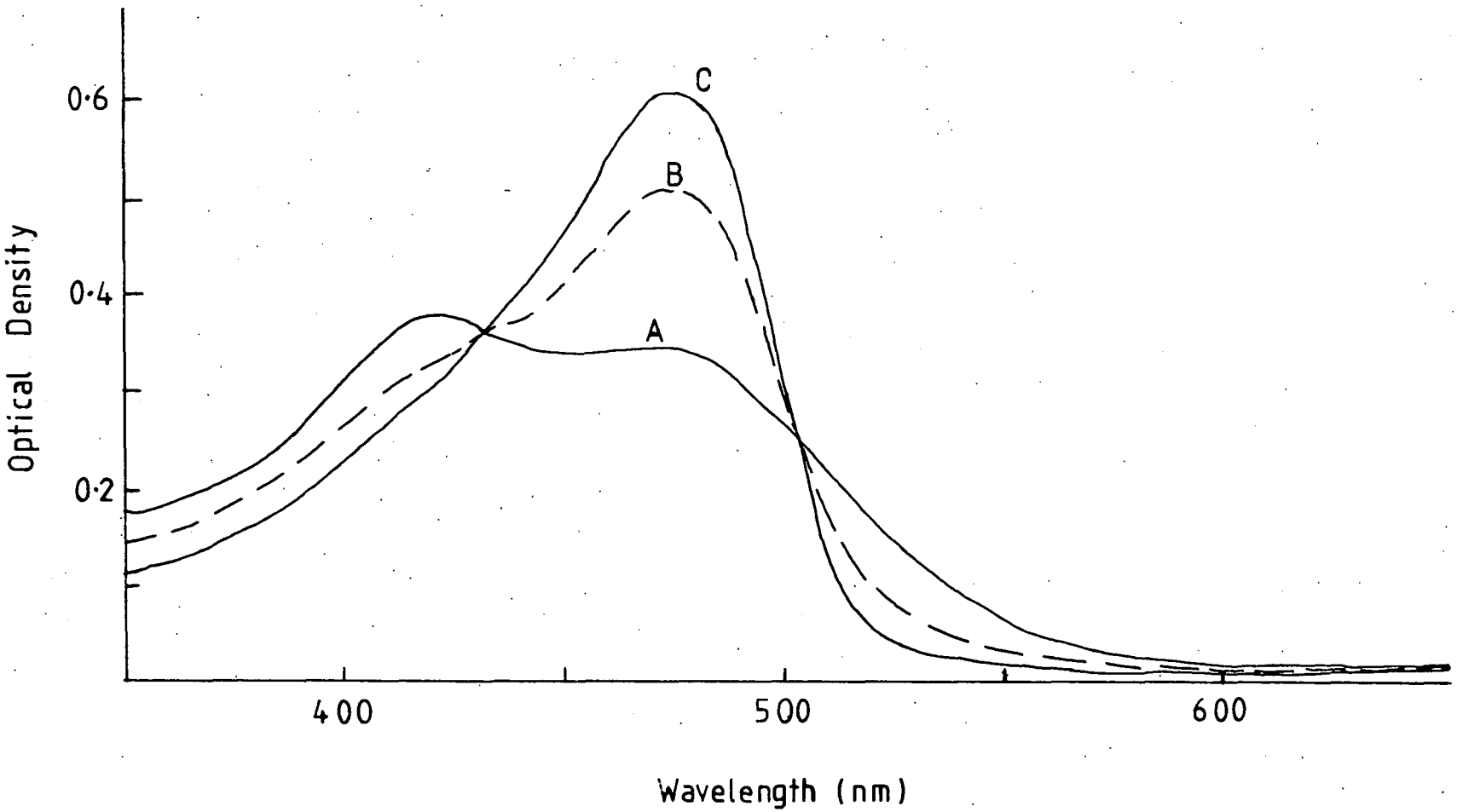

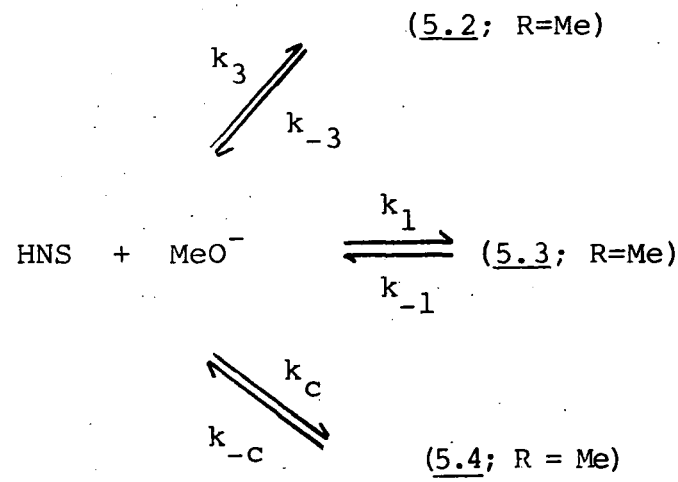

Scheme 5.1

By standard methods[75] it can be shown that equations 5.1, 5.2 and 5.3 apply.

$$k_{fast} = k_3[MeO^-] + k_{-3} \qquad \text{(equation 5.1)}$$

$$k_{med} = \frac{k_1[MeO^-]}{1+K_3[MeO^-]} + k_{-1} \qquad \text{(equation 5.2)}$$

$$k_{slow} = \frac{k_c[MeO^-]}{1+K_1[MeO^-]+K_3[MeO^-]} + k_{-c} \qquad \text{(equation 5.3)}$$

The kinetic data for methoxide attack on HNS is given in Table 5.4. Using equation 5.2 the k_{med} data is best fitted by the values K_3 10 l mol^{-1}, k_1 145 l mol^{-1} s^{-1} and k_{-1} 0.75 s^{-1}. Combination of these latter values gives a value for K_1 of 200±10 l mol^{-1}. Equation 5.3 is used for the k_{slow} data. Here the data is best fitted by using the known values for K_3 of 10 l mol^{-1} and K_1 of 200 l mol^{-1} with values for k_c of 1.45±0.05 l mol^{-1} s^{-1} and of k_{-c} (2±2) x 10^{-5} s^{-1}. The high uncertainty of k_{-c} makes the value of K_c ($=k_c/k_{-c}$) imprecise and therefore it is preferred to quote a value that $K_c \geq 10^5$ l mol The large conversion to the third species, at very low base concentrations, is shown by the optical density measurements for

TABLE 5.4 Kinetic results for reaction of HNS with methoxide ions in methanol at 25°C

$10^5[MeO^-]$/M	Conditions	k_{med}/s^{-1}	k_{calc} [d]	$10^4 k_{slow}/s^{-1}$	$10^4 k_{calc}$ [e]	OD(470nm) [f]
3.2	a			0.63±0.03	0.66	0.48
6.9	a			1.25	1.20	0.55
16	a			2.5	2.45	0.57
23	b			3.3	3.4	
31	b			4.3	4.4	0.57
48	b			6.3	6.5	0.56
100	c	0.88±0.08	0.89	12.3	12.2	0.56
200	c			20	20	
400	c	1.19	1.30	32	32	
500	c	1.43	1.44			
600	c			43	39	
700	c	1.72	1.70			
800	c			45	44	
1000	c	2.10	2.07	49	47	
2000	c			55	56	
4000	c	4.50	4.90			
7000	c	6.9	6.7			
10000	c	8.1	8.0			

a. 4-Bromophenol-4-bromophenoxide buffers.

b. Phenol-phenoxide buffers prepared according to ref. 148.

c. Sodium methoxide in methanol.

d. Calculated from equation 5.2 with k_1 145 $\ell\,mol^{-1}s^{-1}$.

k_{-1} 0.75 s^{-1} and K_3 10 l mol^{-1}

e. Calculated from equation 5.3 with k_c 1.45 $\ell\,mol^{-1}s^{-1}$

k_{-c} 2 x 10^{-5} s^{-1}, K_1 200 l mol^{-1} and K_3 10 l mol^{-1}.

f. At the completion of the slow reactions with 2 x 10^{-5} M HNS.

the completed third process. This confirms that the value of K_c will be high, in agreement with the kinetic measurements.

5.3.3 Reaction with Sodium Ethoxide in Ethanol

The visible spectra in ethanol of HNS (2×10^{-5}M) and sodium ethoxide (0.004 - 0.2M) recorded after one minute showed the double absorption maxima characteristic of a σ-adduct.[25,26] In dilute ethoxide solutions the maxima were at 425 and 490nm, while in more concentrated solutions they shifted to 435 and 480nm. These bands slowly faded with time to be replaced by a new band at 474nm. Using the data in Table 5.5 a Benesi-Hildebrand plot[75] of the reciprocal of optical density, measured after σ-adduct formation was complete but before decomposition had occurred, versus the reciprocal of base concentration, was curved indicating the presence of more than one equilibrium. A short extrapolation of this plot gave an optical density for complete conversion at 480nm of 0.543. From this the extinction coefficients for the high base concentration species are calculated to be $\varepsilon 4.6 \times 10^4$ (435nm) and 2.7×10^4 l mol^{-1} cm^{-1} (480nm). These are approximately double the extinction coefficients expected for adducts of 1:1 stoichiometry.[25-28] As found for the reaction of HNBB with ethoxide ions, this suggests the formation of the di-adduct by ethoxide attack on both aromatic rings. From ^{1}H n.m.r. measurements the di-adduct is most likely to have the structure (5.5; R=Et). The fact that 1:2 adduct occurs even in fairly dilute ethoxide solutions reflects the greater basicity of an ethoxide in ethanol medium compared to methoxide in methanol.

The data in Table 5.5 is analysed according to

TABLE 5.5 Equilibrium optical densities for the reaction of HNS (2×10^{-5} M) with sodium ethoxide in ethanol at 25°C

No.	[NaOEt][a]/M	OD(480nm) observed	OD(480nm)[b] calculated
1	0.000 42	0.175	0.175
2	0.000 63	0.194	0.202
3	0.000 84	0.218	0.219
4	0.001 04	0.236	0.232
5	0.002 10	0.260	0.269
6	0.004 18	0.301	0.304
7	0.006 25	0.320	0.326
8	0.008 30	0.340	0.344
9	0.0106	0.362	0.360
10	0.0212	0.415	0.409
11	0.0424	0.452	0.455
12	0.0636	0.478	0.478
13	0.0848	0.489	0.491
14	0.106	0.501	0.500
15	0.212	0.523	0.520

a. In items 1 - 13 the solutions were made up to constant Ionic strength, I=0.1M, with sodium perchlorate.

b. Calculated with values of K_1 4000 l mol^{-1} s^{-1}, K_2 50 l mol^{-1}, ε(5.3; R=Et) 1.36×10^4 l mol^{-1} cm^{-1}, ε (5.5; R=Et) 2.72×10^4 l mol^{-1} cm^{-1}.

Scheme 5.2. The following assumptions were made. First, that the extinction coefficient of (5.3; R=Et) at 480nm is exactly half of the measured extinction coefficient for (5.5; R=Et)

$$\text{HNS} + \text{EtO}^- \overset{k_1}{\rightleftharpoons} (5.3;\ \text{R=Et})$$

$$(5.3;\ \text{R=Et}) + \text{EtO}^- \overset{k_2}{\rightleftharpoons} (5.5;\ \text{R=Et})$$

Scheme 5.2

Second, that for items 1-4 (low base concentration) little of the 1:2 adduct will be present allowing an approximate value for K_1 to be calculated, and for items 10-15 (high base concentration) little free HNS will remain in solution so allowing an approximate value for K_2 to be calculated. Then by iteration values for K_1 4000 l mol^{-1} and K_2 50 l mol^{-1} were found to give a good fit between calculated and observed optical densities. The value of K_2 is an eighth of the value of K_1 which indicates that alkoxide addition on one picryl ring inhibits alkoxide attack on the other picryl ring, despite the two picryl rings being separated by two carbon atoms.

At base concentrations lower than 0.005M the 1:1 interactions of HNS and ethoxide ions are dominant. When studied using stopped-flow spectrophotometry two well separated colour forming reactions were observed. The first process is attributed to the formation of the 3-alkoxy-adduct (5.2; R=Et) and the second process to the formation of the 1-alkoxy-adduct (5.3; R=Et). The data for these reactions are given in Table 5.6 Using equation 5.4 a plot of k_{fast} versus ethoxide concentration is linear giving the values for k_3 of 1.2×10^4 l mol^{-1} s^{-1} and k_{-3} of 25 s^{-1}. Combination of these values gives a value for K_3 ($=k_3/k_{-3}$) of 480 l mol^{-1}. This value of K_3 and use of

TABLE 5.6 Kinetic results for formation of the 1:1 adducts from HNS (1×10^{-5} M) and sodium ethoxide in ethanol at 25°C

[NaOEt]/M	k_{fast}/s^{-1}	k_{slow}/s^{-1}	k_{slow}(calc)[a]
0.0006	30±3	0.210±0.02	0.21
0.0008	32	0.245	0.24
0.0010	37	0.28	0.28
0.0015	48	0.34	0.33
0.0020	51	0.40	0.38
0.0030	62	0.43	0.43
0.0040	72	0.45	0.47

a. Calculated using equation 5.2 with k_1 300 l mol^{-1} s^{-1} k_{-1} 0.075 s^{-1} and K_3 480 l mol^{-1}.

equation 5.5 enables calculation for k_1 of 300 l mol^{-1} s^{-1} and k_{-1} of 0.075 s^{-1}.

$$k_{fast} = k_3[EtO^-] + k_{-3} \qquad \text{(equation 5.4)}$$

$$k_{slow} = \frac{k_1[EtO^-]}{1+K_3[EtO^-]} + k_{-1} \qquad \text{(equation 5.5)}$$

5.3.4 Comparison with Related Compounds

The kinetic and equilibrium data relating to alkoxide additions to the aromatic rings of the compounds HNS, HNBB, trinitrobenzyl chloride (TNBCl), TNT and 1,3,5-trinitrobenzene (TNB) is collected in Table 5.7. The results are in accord with the generally higher basicity of ethoxide solutions compared to methoxide solutions. It is known[137] that the unsaturated side chain CH=CHPic is more electron withdrawing than its saturated analogue CH_2CH_2Pic, but less electron withdrawing than CH_2Cl. This is reflected by the values of the equilibrium constants as those of HNS fall between those of HNBB and TNBCl.

HNS, like HNBB and TNBCl, forms a kinetically favoured 3-alkoxy-adduct which is less thermodynamically stable than the 1-alkoxy-adduct. For TNT only the 3-alkoxy-adduct is formed.[83] Presumably the major reason for no 1-alkoxy-adduct of TNT in its substituent in the picryl ring is electron releasing whilst in the picryl rings of HNS, HNBB and TNBCl there are electron withdrawing substituents.

In the formation of alkoxy-adducts two factors are important. These are the steric hindrance and the electron

TABLE 5.7 Comparison of kinetic and equilibrium data for HNS with those for related compounds

	k_3/l mol^{-1}s^{-1}	k_{-3}/s^{-1}	K_3/l mol^{-1}	k_1/l mol^{-1}s^{-1}	k_{-1}/s^{-1}	K_1/l mol^{-1}
HNS - methoxide			10	145	0.75	200
HNBB - methoxide[a]				23	1.15	20
TNBCl - methoxide[b]			<20	770	2.2	350
TNT - methoxide[c]	280	3000	0.07			
TNB - methoxide	7300	300	20			
HNS - ethoxide	12000	25	480	300	0.075	4000
HNBB - ethoxide[a]	4000	32	125	84	0.07	1200
TNBCl - ethoxide[b]	10000	14	700	7000	<1	>1000
TNB - ethoxide	40000	20	2000			

a. From Chapter Four

b. Ref. 82

c. Ref. 83

d. Ref. 75 (refers to addition at the unsubstituted position)

withdrawing ability of the substituent at the 1-position on the picryl ring. The 1-alkoxy-adduct is the more thermodynamically stable because the carbon atom, at which alkoxide attack occurs, becomes sp^3 hybridised and the bulky substituent becomes perpendicular to the ring. This enables the ortho nitro groups, previously twisted out of the ring plane by the bulky substituent, to rotate and become planar to the ring. Here the ortho nitro groups exert their maximum electron withdrawing ability and hence increase their ability to stabilise the 1-alkoxy-adduct. However, in the 3-alkoxy-adduct the ortho nitro group will remain slightly twisted out of the ring plane and therefore unable to exert their maximum electron withdrawing ability to stabilise the adduct.

The third reversible interaction of HNS with alkoxide ions has been to produce a species with high thermodynamic stability. E.s.r. measurements[149] on the reaction between HNS and alkoxides show that $< 0.1\%$ of the substrate produces radicals. Therefore the most likely structure for the third species is (5.4) produced by alkoxide attack at the olefinic bond of HNS. Equation 5.3 predicts that as the stability of the ring adduct increases the rate of production of (5.4) decreases. This is why the species (5.4) is more readily formed in methanolic methoxide solutions. In the more basic media of ethoxide in ethanol, or methoxide in methanol-DMSO, the rate of production of (5.4) will be slow and in competition with the irreversible decomposition of the substrate.

5.4 Derivation of the Rate Expressions

(i) For alkoxide additions on the aromatic ring.

The rate expressions

$$k_{fast} = k_3[RO^-] + k_{-3}$$

$$k_{med} = \frac{k_1[RO^-]}{1+K_3[RO^-]} + k_{-1}$$

are derived in an analogous manner to the same expressions in Chapter Four.

(ii) For alkoxide addition at the olefinic bond.

$$(5.1) + RO^- \underset{k_{-1}}{\overset{k_1}{\rightleftharpoons}} (5.3) \qquad (5.3) \underset{k_{-3}}{\overset{k_3}{\rightleftharpoons}} (5.2)$$

$$(5.3) \underset{k_{-c}}{\overset{k_c}{\rightleftharpoons}} (5.4)$$

The rate of formation of (5.2) and (5.3) is very fast compared to the rate of formation of (5.4) and $[RO^-]$ is in large excess of [5.1].

Therefore,

$$\frac{d[5.4]}{dt} = k_c[5.1][RO^-] - k_{-c}[5.4] \qquad (1)$$

$$K_3 = \frac{[5.2]}{[5.1][RO^-]} \qquad (2) \qquad K_1 = \frac{[5.3]}{[5.1][RO^-]} \qquad (3)$$

$$[5.1] + [5.2] + [5.3] + [5.4] = [5.1]_o \qquad (4)$$

Substituting (2) and (3) into (4).

$$[5.1] + K_3[5.1][RO^-] + K_1[5.1][RO^-] + [5.4] = [5.1]_o$$

Re-arranging,

$$[5.1] = A - \frac{[5.4]}{1+K_1[RO^-]+K_3[RO^-]} \qquad (5)$$

where $A = \frac{[5.4]_o}{1+K_1[RO^-]+K_3[RO^-]}$

Substituting (5) into (1)

$$\frac{d[5.4]}{dt} = k_c[RO^-]\left(A - \frac{[5.4]}{1+K_1[RO^-]+K_3[RO^-]}\right) - k_{-c}[5.4] \qquad (6)$$

At equilibrium, $\frac{d[5.4]}{dt} = 0$

$$0 = k_c[RO^-]\left(A - \frac{[5.4]_e}{1+K_1[RO^-]+K_3[RO^-]}\right) - k_{-c}[5.4]_e \qquad (7)$$

Subtracting (7) from (6)

$$\frac{d[5.4]}{dt} = \frac{k_c[RO^-]}{1+K_1[RO^-]+K_3[RO^-]}([5.4]_e-[5.4]) + k_{-c}([5.4]_e-[5.4])$$

Re-arranging,

$$\frac{d[5.4]}{dt} \cdot \frac{1}{[5.4]_e-[5.4]} = \frac{k_c[RO^-]}{1+K_1[RO^-]+K_3[RO^-]} + k_{-c}$$

$$k_{obs} = \frac{dOD}{dt} \cdot \frac{1}{(OD_e-OD)} \text{ by definition.}$$

Therefore it is necessary to relate the change in optical density to the change in the [5.4].

Of the species present only (5.1) does not absorb at the wavelength at which the reaction was studied.

$$OD = \varepsilon_{5.2}[5.2] + \varepsilon_{5.3}[5.3] + \varepsilon_{5.4}[5.4] \quad (8)$$

Substituting (2) and (3) into (8)

$$OD = \varepsilon_{5.2}K_3[5.1][RO^-] + \varepsilon_{5.3}K_1[5.1][RO^-] + \varepsilon_{5.4}[5.4] \quad (9)$$

Substituting (5) into (9)

$$OD = \left(\varepsilon_{5.2}K_3[RO^-] + \varepsilon_{5.3}K_1[RO^-]\right)\left(A - \frac{[5.4]}{1+K_1[RO^-]+K_3[RO^-]}\right) + \varepsilon_{5.4}[5.4].$$

Re-arranging,

$$OD = B - \left(\frac{\varepsilon_{5.2}K_3[RO^-]+\varepsilon_{5.3}K_1[RO^-]}{1+K_1[RO^-]+K_3[RO^-]}\right)[5.4] + \varepsilon_{5.4}[5.4]$$

where $B = A(\varepsilon_{5.2}K_3[RO^-] + \varepsilon_{5.3}K_1[RO^-])$

Re-arranging again,

$$OD = B - (C - \varepsilon_{5.4})[5.4] \quad (10)$$

where $C = \dfrac{\varepsilon_{5.2}K_3[RO^-] + \varepsilon_{5.3}K_1[RO^-]}{1+K_1[RO^-] + K_3[RO^-]}$

At equilibrium

$$OD_e = B - (C - \varepsilon_{5.4})[5.4]_e \quad (11)$$

Differentiating (10)

$$\frac{dOD}{dt} = \frac{d[5.4]}{dt}(C - \varepsilon_{5.4}) \quad (12)$$

Combining (10), (11) and (12)

$$\frac{d\,OD}{dt} \cdot \frac{1}{(OD_e - OD)} = \frac{d[5.4]}{dt} \cdot \frac{1}{([5.4]_e - [5.4])}$$

Hence

$$k_{obs} = \frac{k_c[RO^-]}{1+K_1[RO^-]+K_3[RO^-]} + k_{-c}$$

CHAPTER SIX

THE REACTIONS OF 2,4,6-TRINITROBENZYL CHLORIDE WITH ALIPHATIC AMINES IN DIMETHYL SULPHOXIDE

6.1 Introduction

Recent work[150] has shown that nitrogen bases can be used to produce 2,2´,4,4´,6,6´-hexanitrostilbene (HNS) from 2,4,6-trinitrobenzyl chloride (TNBCl).

Previous work[92] has reported two types of process, σ-adduct formation and side-chain deprotonation, for the reaction of TNBCl with amines in DMSO. Kinetic and equilibrium data for the latter process and equilibrium data for the former process are available.[92] Reported here are kinetic and equilibrium data for the formation of σ-adducts by the reactions of TNBCl with four different amines in DMSO. Comparison of this data, with that for the σ-adduct forming reactions between 1,3,5-trinitrobenzene (TNB) and amines in DMSO,[78,151-154] allows the examination of the steric and electronic effects of the $-CH_2Cl$ group on σ-adduct formation.

Visible spectroscopic measurements have shown[92] that σ-adducts formed between TNBCl and amines in DMSO give maxima at 450nm-452nm and 510nm-550nm, and the conjugate base gives maxima at 373nm, 490nm and 600nm. The data is best interpreted by Scheme 6.1. σ-adduct formation, whether by amine attack at the substituted or unsubstituted position, involves a zwitterionic intermediate. Proton transfer from this intermediate is shown, presumably for steric reasons, not to be diffusion controlled. All three processes are observed for primary amines but amine attack at the substituted position to form the 1-amido-adduct is not observed for secondary amines. Here, the 1-amido-adduct is presumably disfavoured because of extreme steric congestion that would result if it was formed.

Evidence has been reported[86] that substituted ammonium ions, present for kinetic measurements, can be stabilised by association with chloride ions, $R'\overset{+}{R}NH_2 \ldots Cl^-$. The measurements reported in this work have been made in the presence of substituted ammonium perchlorate or substituted ammonium chloride salts and the results found to support the above assertion.

6.2 Experimental

Visible spectra were recorded on a Pye-Unicam SP 8005 spectrophotometer.

Kinetic and equilibrium measurements were made at 25°C using a Hi-tech SF-3L spectrophotometer or Pye-Unicam SP 8100 recording spectrophotometer. All solutions of reagents were freshly prepared before use. The rate coefficients measured on the stopped-flow spectrophotometer are the mean of at least five separate determinations and are precise to ±5%, while the rate coefficients measured on the conventional recording spectrophotometer are the mean of duplicate runs.

A Kent EIL 7055 pH meter was used to check the acidity of the ammonium salts. Solutions were adjusted so as to contain less than 0.1% of free amine or acid.

^1H n.m.r. measurements have already been reported in previous work[92] and repetition was felt to be unnecessary.

Scheme 6.1

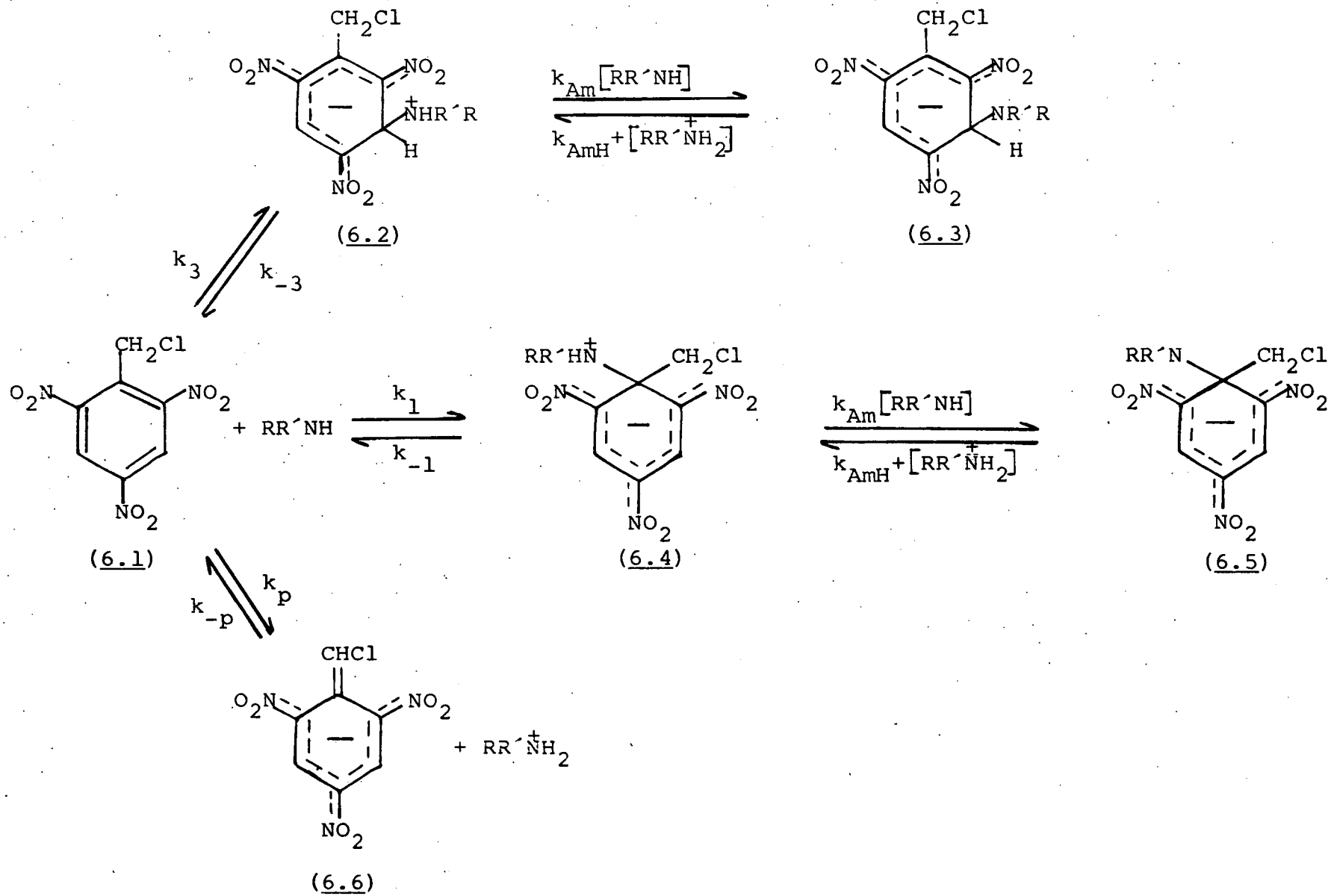
CH2Cl
O2N
NO2
NHR´R
H
NO2
(6.2)
kAm[RR´NH]
kAmH+[RR´NH2]
NR´R
(6.3)
k3
k-3
(6.1)
+ RR´NH
k1
k-1
RR´HN
(6.4)
RR´N
(6.5)
kp
k-p
CHCl
(6.6)
+ RR´NH2

TABLE 6.1 Typical results from rate measurements

(i) TNBCl (5×10^{-6} M), benzylamine (0.03M). First process, measured at 450nm, in DMSO.

(ii) TNBCl (1×10^{-5} M), piperidine (0.03M). Only process, measured at 450nm, in DMSO containing piperidinium chloride (0.1M).

(i)		(ii)	
t/ms	ΔV^a	t/ms	ΔV^a
0	5.0	0	4.2
10	4.1	5	3.6
20	3.2	10	3.1
30	2.6	15	2.5
40	2.0	20	2.1
60	1.3	30	1.5
80	0.8	40	1.1
A plot of $\ln\Delta V$ versus t is linear and yields $k_{obs} = 22.8\ s^{-1}$		A plot of $\ln\Delta V$ versus t is linear and yields $k_{obs} = 34.3\ s^{-1}$	

a. $\Delta V = V_\infty - V_t$

TABLE 6.2

Typical results from rate measurements.

(i) TNBCl (5×10^{-6} M), n-butylamine (0.004M). Second process, measured at 450nm, in DMSO containing n-butylammonium perchlorate (0.1M).

(ii) TNBCl (5×10^{-6} M), n-butylamine (0.004M). Second process, measured at 450nm, in DMSO containing n-butylammonium chloride (0.1M).

(i)		(ii)	
t/s	ΔV^a	t/s	ΔV^a
0.00	3.30	0.00	3.4
0.05	2.90	0.05	3.0
0.10	2.40	0.10	2.6
0.15	2.10	0.15	2.3
0.20	1.85	0.20	2.0
0.25	1.70	0.25	1.8
0.30	1.40	0.30	1.6
0.40	1.00	0.40	1.2

A plot of $\ln\Delta V$ versus t is linear and yields $k_{obs} = 2.9\ s^{-1}$

A plot of $\ln\Delta V$ versus t is linear and yields $k_{obs} = 2.6\ s^{-1}$

a. $\Delta V = V_\infty - V_t$

6.3 Kinetic Analysis

The rate equations used in this chapter will be given in this section along with the explanation of any assumption that is used. However, the complete derivation of the rate expressions will be given in Section 6.7.1.

All rate measurements were made with the amine concentration in large excess over the parent concentration and consequently all the colour forming reactions measured were first order. When reactions between TNBCl and amines were studied in DMSO containing no added amine salt; sufficient excess of amine was used so that at equilibrium there was >95% conversion of TNBCl to amido-adduct. For reactions with buffers (amine plus amine salt) the buffer components were in large excess of the TNBCl concentration.

$$\ln \frac{OD_\infty}{OD_\infty - OD} = k_{obs} \cdot t \qquad \text{(equation 6.1)}$$

Equation 6.1 applies under these conditions.[152] Amine attack at the unsubstituted 3-position gives the expression equation 6.2.[152] Here the zwitterionic form (6.2) is assumed to be a steady-state intermediate.

$$k_{obs} = \frac{k_3 k_{Am} [Am]^2 + k_{-3} k_{AmH^+} [AmH^+]}{k_{-3} + k_{Am}[Am]} \qquad \text{(equation 6.2)}$$

$$k_{obs} = \frac{k_3 k_{Am} [Am]^2}{k_{-3} + k_{Am}[Am]} \qquad \text{(equation 6.3)}$$

$$k_{obs} = k_3 [Am] \qquad \text{(equation 6.4)}$$

$$\frac{[Am]}{k_{obs}} = \frac{1}{k_3 k_{Am} [Am]} + \frac{1}{k_3} \qquad \text{(equation 6.5)}$$

If the reactions are studied with no added amine salt then the concentration of amine salt is very small and equation

6.3 applies. By assuming $k_{Am}[Am] >> k_{-3}$ equation 6.3 becomes equation 6.4 or inversion of equation 6.3 gives equation 6.5

Two well separated rate processes are observed for the reactions of TNBCl with primary amines. The first is rapid amine attack at the unsubstituted 3-position of TNBCl, followed by a slower amines attack at the substituted 1-position. For amine attack at the 1-position the rate expression can be expressed as equation 6.6, that is the sum of the forward and reverse reaction coefficients. It can be shown using standard methods[75] that, allowing for prior attack at the 3-position, the general rate expression is given by equation 6.7. If there is no added amine salt present in solution then, the k_r term is negligible, and in some cases equation 6.8 can be found to be useful. The terms $(OD)_3$ and $(OD_\infty)_3$ are the optical

$$k_{obs} = k_f + k_r \qquad \text{(equation 6.6)}$$

$$k_{obs} = \frac{k_1 k_{Am}[Am]^2}{(k_{-1}+k_{Am}[Am])\left(1+K_{c,3}\frac{[Am]^2}{[AmH^+]}\right)} + \frac{k_{-1}k_{AmH^+}[AmH^+]}{k_{-1}+k_{Am}[Am]} \qquad \text{(equation 6.}$$

$$k_{obs} = \frac{k_1 k_{Am}[Am]^2}{(k_{-1}+k_{Am}[Am])\,1+\left(\frac{(OD)_3}{(OD_\infty)_3-(OD)_3}\right)} \qquad \text{(equation 6.8)}$$

$$k_{obs} = \frac{k_1[Am]^2}{\left(\frac{k_{-1}}{k_{Am}}+[Am]\right)\left(1+\frac{(OD)_3}{(OD_\infty)_3-(OD)_3}\right)} + \frac{\frac{k_{-1}k_{AmH^+}}{k_{Am}}[AmH^+]}{\left(\frac{k_{-1}}{k_{Am}}+[Am]\right)} \qquad \text{(equation 6.}$$

density at completion of the faster process forming the 3-adduct and the optical density for complete conversion to the 3-adduct respectively. Equation 6.8 will also be used in the re-arranged form of equation 6.9.

Equation 6.10 has been given in previous work[92] for the removal of a side chain proton by amine.

$$k_{obs} = \frac{k_p[Am]}{1+K_{c,1}\frac{[Am]^2}{[AmH^+]}} + k_{-p}[AmH^+] \qquad \text{(equation 6.10)}$$

6.4 Equilibrium Constants

Because σ-adduct formation between TNBCl and amines involves two steps, linked by the zwitterionic intermediate, it is usual to refer to the overall equilibrium constant. For example, $K_{c,3}$ is the overall equilibrium constant for conversion of TNBCl to the 3-amido-adduct, and is defined by equation 6.11. In addition, $K_{c,3}$ is normally defined in two other ways. Equation 6.12 relates $K_{c,3}$ with K_3, the equilibrium constant for the formation of the zwitterionic intermediate, and to the acid dissociation constants of the zwitterion K_a^z, and protonated amine, $K_a^{AmH^+}$; while equation 6.13 relates $K_{c,3}$ to the rate coefficients associated with formation of the 3-amido-adduct. The overall equilibrium constant for the 1-amido-adduct, $K_{c,1}$, can be defined by exactly analogous expressions.

$$k_{obs} = \frac{[6.3][AmH^+]}{[6.1][Am]^2} \qquad \text{(equation 6.11)}$$

$$k_{obs} = K_3 \cdot \frac{K_a^z}{K_a^{AmH^+}} \qquad \text{(equation 6.12)}$$

$$k_{c,3} = \frac{k_3 \cdot k_{Am}}{k_{-3} \cdot k_{AmH^+}} \qquad \text{(equation 6.13)}$$

6.5 Results

Four amines, n-butylamine, benzylamine, pyrrolidine and piperidine have been used to study the reactions of TNBCl with amines in DMSO. The kinetic and equilibrium data will now be reported and because each amine reacts in slightly different ways with TNBCl the data for each amine will be given separate treatment.

6.5.1 Reaction with n-butylamine

As reported previously[92] three processes were observed. Two fast σ-adduct forming reactions followed by a slower proton transfer reaction. The data are interpreted according to Scheme 6.1. The data for the formation of the 3-amido-adduct are given in Table 6.3. At the base concentrations used $k_{Am}[Am] >> k_{-3}$ so equation 6.4 applies and yields a value for k_3 of 3000 l mol^{-1} s^{-1}. When the n-butylamine concentration is 0.004M if a lower limit of $k_{Am}[Am]/k_{-3}$ of 4 is set then it can be calculated that the ratio $k_{Am}/k_{-3} > 1000$, and also $K_3 k_{Am} > 3 \times 10^6$ l^2 mol^{-2} s^{-1}. For attack at the 1-positior the rate data is interpreted by equation 6.8 with values for k_1 of 700 l mol^{-1} s^{-1} and k_{Am}/k_{-1} of 2000 l mol^{-1}.

The data obtained in the presence of 0.1M n-butylammonium chloride are in Table 6.4. The rate of amine attack at the 3-position was too fast to measure with the available techniques, but using the optical densities measured at the completion of this fast process a value for $K_{c,3}$ of 73±4 l mol^{-1} has been obtained. Due to the complete conversion of TNBCl to the 1-amido-adduct even at low base concentrations, the measurements was restricted. A value for $K_{c,1}$ of 23,000±500 l mol^{-1} has been calculated and this compares with a $K_{c,1}$ value

TABLE 6.3 Kinetic and equilibrium data for the reaction of TNBCl (5×10^{-6} M) and n-butylamine in DMSO at 25°C

[n-butylamine]/M	k_{fast}/s^{-1}	$k_3^a/l\ mol^{-1}s^{-1}$	$(OD)_3^b$	k_{slow}/s^{-1}	k_{calc}^c	$(OD)_1^d$
0.0004			0.0026	0.10	0.11	0.024
0.0005			0.0057	0.13	0.13	0.024
0.0006			0.0045	0.19	0.18	0.025
0.0008			0.0067	0.23	0.23	0.026
0.0010			0.0087	0.27	0.27	0.027
0.0020			0.0164	0.27	0.25	0.027
0.0040	10.6	2660	0.0200			0.027
0.0060	20.0	3330	0.0210			0.027
0.0080	24.2	3020	0.0210			0.027
0.0100	33.6	3360	0.0210			0.027

a. Calculated using equation 6.4.

b. Optical density at completion of fastest reaction; measured at 450nm.

c. Calculated from equation 6.8 with k_1 700 l mol^{-1} and k_{Am}/k_{-1} 2000 l mol^{-1}.

d. Optical density at completion of slower reaction forming 1-adduct; measured at 450nm.

TABLE 6.4 Kinetic and equilibrium data for reaction of TNBCl with n-butylamine in DMSO containing n-butylammonium perchlorate (0.1M) at 25°C

[n-butylamine]/M	$(OD)_3$ [a]	$K_{c,3}$/l mol^{-1}	$(OD)_1$ [b]	$K_{c,1}$/l mol^{-1}	k_{obs}/s^{-1}	k_{calc}/s^{-1}
0.001			0.0039	23,000	2.2	2.2
0.002			0.0100	23,000	2.2	2.1
0.004			0.0173	29,000	2.9	2.9
0.006			0.0205	-	3.9	3.9
0.008			0.0209	-	4.9	4.9
0.010			0.0209	-	6.0	6.1
0.020	0.0045	76	0.021	-	10.3	9.9
0.030	0.0074	70	0.021	-	12.1	11.5
0.040	0.0106	77	0.021	-	12.0	11.7
0.050	0.0123	71	0.021	-	10.7	11.1
0.060	0.0137	69	0.021	-	10.5	10.5

a. Optical density at completion of reaction giving 3-adduct; measured at 450nm. A Benesi-Hildebrand type plot[76] gives a value for $(OD_\infty)_3$ of 0.0192.

b. Optical density at completion of reaction giving 1-adduct; measured at 450nm.

c. Calculated from equation 6.7 with k_1 630 l mol^{-1} s^{-1}, $K_{c,3}$ 73 l mol^{-1}, k_{Am}/k_{-1} 2000 l mol^{-1} and k_{AmH^+} 55 l mol^{-1} s^{-1}.

of 20,000 l mol^{-1} previously reported.[92] With increasing base concentration the rate coefficients for the 1-adduct pass through a maximum and the data are interpreted according to equation 6.7. At n-butylamine concentrations >0.01M the condition $k_{Am}[Am] >> k_{-1}$ will apply and the k_r term will be negligible thus allowing the calculation of a value for k_1 of 630 l mol^{-1} s^{-1}. Hence, the ratio $k_{-1}k_{AmH^+}/k_{Am}$ $(=k_1/k_{c,1})$ is calculated to be 0.0274 s^{-1}. Finally, using the fact that little of the 3-amido-adduct will be initially present at low (<0.008M) amine concentrations, and the previously calculated values of k_1 and $k_{-1}k_{AmH^+}/k_{Am}$, equation 6.9 can be used to calculate k_{Am}/k_{-1}. The value obtained for k_{Am}/k_{-1} is 2000±500 l mol^{-1}. Using these calculated parameters equation 6.7 fits the data over the whole concentration range.

Table 6.5 contains the data obtained in the presence of 0.1M n-butylammonium chloride, which show differences from those obtained with the perchlorate salt. Calculation from the optical density measurements for completion of the first process gives a value for $K_{c,3}$ of 150±20 l mol^{-1}. Again $K_{c,1}$ cannot be calculated with great accuracy from the optical density measurements but like $K_{c,3}$ it is considerably larger than the overall equilibrium constants obtained with the perchlorate salt. A value for k_1 of 630 l mol^{-1} s^{-1} is obtained from the data at higher concentrations and, assuming k_{Am}/k_{-1} will remain at 2,000 l mol^{-1}, a value for k_{AmH^+} of 32 l mol^{-1} is obtained. Combination of the kinetic parameters allows $K_{c,1}(=k_1k_{Am}/k_{-1}.k_{AmH^+})$ to be calculated as 40000 l mol^{-1}.

TABLE 6.5 Kinetic and equilibrium data for reaction of TNBCl with n-butylamine in DMSO containing n-butylammonium chloride (0.1M) at 25°C

$[n\text{-}BuNH_2]$	$(OD)_3$ [a]	$K_{c,3}$/l mol^{-1}	$(OD)_1$ [b]	$K_{c,1}$/l mol^{-1}	k_{obs}/s^{-1}	k^{c}_{calc}/s^{-1}
0.001			0.0056	37,000	1.49	1.50
0.002			0.0132	42,000	1.66	1.64
0.004			0.0175	31,000	2.6	2.55
0.006			0.0188	24,000	3.8	3.6
0.008			0.020		4.8	4.6
0.010			0.021		5.8	5.5
0.015	0.0057	160	0.021		7.8	7.2
0.020	0.0083	160	0.021		8.9	7.9
0.030	0.0128	170	0.021		8.3	8.4
0.040	0.0143	130	0.021		8.2	7.5

a. Optical density at completion of reaction giving 3-adduct. A Bensei-Hildebrand type plot[76] gives a value for $(OD_\infty)_3$ of 0.021.

b. Optical density at completion of reaction giving 1-adduct.

c. Calculated from equation 6.7 with k_1 630 l mol^{-1} s^{-1}, $K_{c,3}$ 150 l mol^{-1}, k_{Am}/k_{-1} 2000 l mol^{-1}, and k_{AmH^+} 32 l mol^{-1} s^{-1}.

6.5.2 Reaction with benzylamine

Two σ-adduct formation reactions are observed. With no added amine salt in solution rate data for amine attack at the 3-position has been obtained and are presented in Table 6.6. The proton transfer step is found to be partially rate limiting and the data therefore best interpreted with the use of equation 6.5. A plot of $[Am]/k_{obs}$ versus $1/[Am]$ is linear and yields a value for K_3k_{Am} of 1.4×10^5 l^2 mol^{-2} s^{-1} from the slope and for k_3 of 1000 l mol^{-1} s^{-1} from

TABLE 6.6 Kinetic data for the fast reaction of TNBCl with benzylamine in DMSO at 25°C, yielding the 3-adduct

[Benzylamine]/M	k_{fast}/s^{-1}	k^a_{calc}/s^{-1}	$(OD)_3^b$
0.010	5.9	5.9	0.025
0.015	9.6	10.1	0.028
0.020	14.9	14.8	0.026
0.030	23.0	24	0.029
0.040	33.1	34	0.028
0.060	53.3	54	0.028

a. Calculated from equation 6.5 with k_3 1000 l mol^{-1} s^{-1}, K_3k_{Am} 1.4×10^5 l^2 mol^{-2} s^{-1}.

b. Measured at 450 nm.

---

the intercept. Data for solutions containing 0.1M benzylammonium perchlorate are in Table 6.7. The optical density measurements at completion of the first process allow a value for $K_{c,3}$ of 5 l mol^{-1} to be calculated. The optical density measurements at completion of the second process give a value of $K_{c,1}$ of 1000 l mol^{-1}. This $K_{c,1}$ value is considerably

TABLE 6.7 Kinetic and equilibrium data for the reaction of TNBCl with benzylamine in DMSO containing benzylammonium perchlorate (0.1M) at 25°C

[Benzylamine]/M	$(OD)_3$ [a]	$K_{c,3}$/l mol^{-1}	$(OD)_1$	$K_{c,1}$/l mol^{-1}	k_{obs}/s^{-1}	k_{calc} [b]/s^{-1}
0.005			0.0051	1000	2.9	2.9
0.0075			0.0088	940	2.8	2.9
0.01			0.0119	880	3.1	3.1
0.02			0.0200	910	4.2	4.6
0.04			0.0241	1070	7.6	8.0
0.06			0.0250		11.9	11.1
0.08	0.0070	7.7	0.0250		13.2	13.4
0.10	0.0079	6.0	0.0259		15.2	14.7
0.15	0.0106	4.5	0.0255		16.1	15.8
0.20	0.0146	5.6	0.0259			

a. Optical density at completion of reaction giving 3-adduct; measured at 450nm. A Benesi-Hildebrand plot[76] gives value for $(OD_\infty)_3$ of 0.021.

b. Calculated from equation 6.7 with k_1 230 l mol^{-1} s^{-1}, $K_{c,3}$ 5 l mol^{-1}, k_{Am}/k_{-1} 200 l mol^{-1} and k_{AmH^+} 46 l mol^{-1} s^{-1}.

larger than has been previously[92] calculated. However it is believed that the new $K_{c,1}$ value of 1000 l mol^{-1} is more reliable. Sufficient kinetic data is available to calculate the kinetic parameters of the second process in an analogous way to those calculated for the reaction with n-butylamine and its perchlorate. The calculated values are k_1 230 l mol^{-1} s^{-1}, for the ratio $k_{-1}k_{AmH^+}/k_{Am}$ 0.23 s^{-1} and for the ratio k_{Am}/k_{-1} 200 l mol^{-1}. Combining these results gives a value for k_{AmH^+} of 46 l mol^{-1} s^{-1}. Use of these rate coefficients and equation 6.7 gives calculated values in good agreement with the observed values.

Table 6.8 contains the data measured with 0.1M benzylammonium chloride. The values of k_1 and the ratio k_{Am}/k_{-1} are unchanged within experimental error. Significant differences are found in the calculated values for $K_{c,3}$ 10 l mol^{-} $K_{c,1}$ 2000 l mol^{-1}, the ratio $k_{-1}k_{AmH^+}/k_{Am}$ 0.125 s^{-1} and k_{AmH^+} 25 l mol^{-1} s^{-1}.

The rate coefficients for the third process giving the conjugate base has been measured, at 620nm, with a conventional spectrophotometer, in solutions containing 0.1M benzylammonium perchlorate. Equation 6.10, using a value for $K_{c,1}$ of 2000 l mol^{-1}, is used to interpret the results in Table 6.9. Values for k_p of 3.4 l mol^{-1} s^{-1} and k_{-p} of 0.024 l mol^{-1} s^{-1} are calculated.

6.5.3 Reaction with piperidine

Two reversible colour forming processes are observed for the reaction of TNBCl with piperidine. The fast process is the formation of the σ-adduct by amine addition at the 3-position; the assignment of the position will be justified later.

TABLE 6.8 Kinetic and equilibrium data for the reaction of TNBCl with benzylamine in DMSO containing benzylammonium chloride (0.1M) at 25°C

[Benzylamine]/M	$(OD)_3$	$K_{c,3}$[a]/l mol^{-1}	$(OD)_1$	$K_{c,1}$[b]/l mol^{-1}	k_{obs}/s^{-1}	k_{calc}[c]
0.0025			0.0031	2200	1.9	1.9
0.005			0.0084	2000	1.8	1.9
0.0075			0.0123	1800	2.0	2.1
0.01			0.0175	2300	2.5	2.5
0.02			0.0223	2000	4.1	4.0
0.04			0.0241		7.5	7.9
0.06	0.0059	12	0.0246		10.4	10.2
0.07	0.0072	11	0.0246			
0.08	0.0088	12	0.025		12.0	11.6
0.09	0.0092	10	0.024			
0.10	0.0101	10	0.025		12.8	12.0
0.15	0.0132	9	0.025			

a. Calculated from equation 6.11 using a value for $(OD_\infty)_3$ of 0.020; measured at 450nm.

b. Calculated using a value for $(OD_\infty)_1$ of 0.025; measured at 450nm.

c. Calculated from equation 6.7 with k_1 250 l mol^{-1} s^{-1}; $K_{c,3}$ 10 l mol^{-1}, k_{-1} k_{AmH^+}/k_{Am} 0.125 k_{Am}/k_{-1} 200 l mol^{-1}.

TABLE 6.9 Rate data for the deprotonation of TNBCl by benzylamine in DMSO containing 0.1M benzylammonium chloride

[Benzylamine]/M	k_{obs}/s^{-1}	k^{a}_{calc}/s^{-1}
0.001	0.0054	0.0057
0.002	0.0075	0.0087
0.004	0.0114	0.0125
0.006	0.0144	0.0140
0.008	0.0153	0.0143
0.01	0.0131	0.0138
0.02	0.0108	0.0100
0.04	0.0065	0.0065

a. Calculated from equation 6.10 with values of k_p 3.4 l $mol^{-1}s^{-1}$, k_{-p} 0.024 l mol^{-1} s^{-1} and $K_{c,1}$ 2000 l mol^{-1}.

The slow process is removal of a side chain proton to form the conjugate base.

In solutions containing 0.1M piperidinium perchlorate a plot of k_{obs} versus $[Am]^2$, data in Table 6.10, for the fast process is linear. This indicates that $k_{-3} >> k_{Am}[Am]$ and therefore equation 6.2 applies. Values for K_3k_{Am} of 2.6×10^4 l mol^{-2} s^{-1} and for k_{AmH^+} of 280 l mol^{-1} s^{-1} are obtained from the slope and intercept of the plot respectively. The value for $K_{c,3}$ of 93 l mol^{-1} is calculated from K_3k_{Am}/k_{AmH^+}. The absence of curvature in the plot allows an upper limit for the ratio k_{Am}/k_{-3} of 2 to be calculated.

TABLE 6.10 Kinetic data for the reaction of TNBCl with piperidine in DMSO containing 0.1M piperidinium perchlorate

[piperidine]/M	k_{obs}/s^{-1}	k^{a}_{calc}/s^{-1}
0.01	30	31
0.015	36	34
0.02	41	39
0.03	50	50
0.04	69	69
0.05	94	93

a. Calculated from equation 6.2 with K_3k_{Am} 2.6×10^4 l^2 mol^{-2} s^{-1}, k_{AmH}+ 280 l mol^{-1} s^{-1}, $k_{Am}[Am] << k_{-3}$.

In the presence of 0.1M piperidinium chloride $K_{c,3}$ is calculated as 200 l mol^{-1} from the kinetic data, and as 220±30 l mol^{-1} from the equilibrium data. This is very good agreement. All the data is given in Table 6.11.

6.5.4 Reaction with pyrrolidine

Two reversible colour forming reactions, attributed to the formation of the 3-adduct and to transfer of a side chain proton, were observed. By use of tetraethylammonium perchlorate as a neutral electrolyte all measurements were made at constant ionic strength.

TABLE 6.11 Kinetic and equilibrium data for reaction of TNBCl with piperidine in DMSO containing 0.1M piperidinium chloride at 25°C

[piperidine]/M	k_{obs}/s^{-1}	k_{calc} [b]	$(OD)_3$	$K_{c,3}$ [b]/l mol^{-1}
0.01	14.4	14.4	0.0079	258
0.02	21.6	21.6	0.0177	213
0.03	34.7	33.5	0.0246	197
0.04	51.0	50.5	0.0306	242
0.05	69	72	0.0325	217
0.06	102	99	0.0343	226

a. Calculated from equation 6.2 with K_3k_{Am} 2.4 x 10^4 l^2 mol^{-2} s^{-1}, k_{AmH^+} 120 l mol^{-1} s^{-1} and $k_{-3} >> k_{Am}[Am]$.

b. Calculated from $(OD)_3$ values using a value of 0.0385 for complete conversion to 3-adduct; measured at 450nm.

Data for the σ-adduct forming reaction at the 3-position in the absence of added pyrrolidinium salts is given in Table 6.12. Equation 6.5 allows the calculation for K_3k_{Am} of (5.8±0.5) x 10^5 l^2 mol^{-2} s^{-1} and k_3 of (1.7±1) x 10^4 l $mol^{-1}s$ from this data. Combining these values gives the ratio k_{Am}/k_{-3} of 34 l mol^{-1}.

TABLE 6.12 Kinetic data for the reaction of TNBCl with pyrrolidine in DMSO containing 0.1M tetraethylammonium perchlorate at 25°C

[pyrrolidine]/l^{-1}mol	k_{obs}/s^{-1}	k^a_{calc}/s^{-1}
0.002	2.2	2.2
0.004	7.7	8.2
0.006	18	17.3
0.008	28.7	29.2
0.010	43.6	43.3

a. Calculated from equation 6.5 with K_3k_{Am} 5.8 x 10^5 l^2 mol^{-2} s^{-1} and k_3 1.7 x 10^4 l $mol^{-1}s^{-1}$.

The data in Table 6.13 is again for the formation of the 3-adduct but here constant concentrations of pyrrolidinium perchlorate are present. By extrapolating this data to zero amine concentration a value for k_{AmH^+} of 2400±100 l mol^{-1} s^{-1} is obtained. The calculation for $K_{c,3}$ of 240 l mol^{-1} from the kinetic parameters are in good agreement with that obtained from equilibrium optical densities.

TABLE 6.13 Kinetic and equilibrium data for reaction of TNBCl with pyrrolidine in the presence of pyrrolidinium perchlorate at 25°C

[Pyrrolidine]/M	[Pyrrolidinium perchlorate]/M	k_{obs}/s^{-1}	k_{calc}[b]$/s^{-1}$	OD_3[c]	$K_{c,3}$[d]/l mol^{-1}
0.001	0.01	24	24		
0.002	0.01	26	25		
0.004	0.01	28	29	0.0134	260
0.006	0.01	36	37	0.0219	260
0.007	0.01	41	42	0.0246	250
0.008	0.01	48	48	0.0269	230
0.009	0.01	56	55	0.0297	240
0.010	0.01	64	61	0.0325	260
0.012	0.01	81	77	0.0348	240
0.004	0.02	53	51	0.0095	330
0.006	0.02	60	58	0.0134	240
0.008	0.02	69	67	0.0205	260
0.015	0.02	125	120	0.0337	260

a. I = 0.1M with tetraethylammonium perchlorate.

b. Calculated from equation 6.2 with K_3k_{Am} 5.8×10^5 l^2 mol^{-2} s^{-1}, k_{AmH^+} 2400 l $mol^{-1}s^{-1}$ (and k_{Am}/k_{-3} 34 l mol^{-1}

c. Measured at 450nm at completion of rapid forming reaction.

d. Calculated using a value for $(OD_\infty)_3$ of 0.045.

TABLE 6.14 Kinetic and equilibrium data for the reaction of TNBCl with pyrrolidine perchlorate in the presence of pyrrolidine at 25°C

[Pyrrolidine]/M	[Pyrrolidine perchlorate][a]/M	k_{obs}/s^{-1}	k_{calc}[b]$/s^{-1}$	$(OD)_3$[c]	$K_{c,3}$/l mol^{-1}
0.006	0	18	17	0.043	
0.006	0.001	19	19	0.038	210
0.006	0.002	21	21	0.034	210
0.006	0.004	25	25	0.029	230
0.006	0.006	30	29	0.025	230
0.006	0.008	32	33	0.023	250
0.006	0.010	36	37	0.021	260
0.010	0	43	43		
0.010	0.001	44	45		
0.010	0.002	47	47		
0.010	0.004	51	50		
0.010	0.006	52	54		
0.010	0.008	57	57		
0.010	0.010	62	61		

a. I = 0.1M with tetraethylammonium perchlorate.

b. Calculated from equation 6.2 with $K_3 k_{Am}$ 5.8×10^5 i^2 mol^{-2} s^{-1}, k_{AmH^+} 2400 l mol^{-1} and (k_{Am}/k_{-3} 34 l mol^{-1}.

c. Measured at 450nm at completion of rapid colour forming reaction.

Further rate data were obtained for the formation of the 3-adduct by varying the concentration of amine perchlorate at constant amine concentration. These data are given in Table 6.14 and are in good agreement with the parameters obtained previously.

Table 6.15 contains the data for the slower reaction involving deprotonation of the substrate. The data are interpreted according to equation 6.10 using the previously determined value for $K_{c,3}$ of 240 l mol^{-1}. The plot of k_{obs} versus $[Am]/(1 + K_{c,3}[Am]^2/[AmH^+])$ is linear the slope giving a value for k_p of 143 l mol^{-1} s^{-1}, whilst the intercept, equal to $k_{-p}[AmH^+]$, is indistinguishable from zero.

TABLE 6.15 Rate data for the deprotonation of TNBCl by pyrrolidine in DMSO containing 0.1M pyrrolidinium perchlorate at 25°C

[Pyrrolidine]/M	k_{obs}/s^{-1}	k^a_{calc}/s^{-1}
0.001	0.14	0.14
0.002	0.27	0.28
0.003	0.39	0.42
0.004	0.55	0.55
0.005	0.66	0.67
0.006	0.83	0.79
0.008	1.12	0.99

a. Calculated using equation 6.10 with k_p 143 l mol^{-1} s^{-1} and $K_{c,3}$ 240 l mol^{-1}.

6.6 Discussion of Data

6.6.1 The effects of chloride ions

Table 6.16 compares rate and equilibrium data for reactions involving n-butylammonium, benzylammonium and piperidinium salts, where total salt concentration has been maintained at 0.1M. It is shown that $K_{c,3}$, the overall equilibrium constant for formation of the 3-adduct, and $K_{c,1}$, the overall equilibrium constant for the formation of the 1-adduct, are larger in the presence of chloride ions than in the presence of perchlorate ions. Similar effects of chloride ions have been observed by Buncel and Eggiman[86] for the reactions of 1,3,5-trinitrobenzene (TNB) with aniline in the presence of DABCO, and by Crampton and Greenhalgh[151] for the reaction of TNB with piperidine. This effect of chloride ions on $K_{c,3}$ and $K_{c,1}$ is attributed to the association of Cl^- with the substituted ions ($RR'NH_2^+ \ldots Cl^-$). It is assumed that the perchlorate ions with much more dispersed charge will not interact strongly with the substituted ammonium ions. Scheme 6.2 is a modification of Scheme 6.1 which allows the effect of chloride ions on the reaction of TNBCl with amines.

$$TNBCl + 2RR'NH + Cl^- \underset{}{\overset{K_{c,3}}{\rightleftharpoons}} (TNBCl.NRR')^- + RR'\overset{+}{N}H_2 + Cl^-$$

$$\Big\Vert\, K_{Cl^-}$$

$$RR'NH_2^+ \ldots Cl^-$$

Scheme 6.2

$(K_{c,3})_{Cl^-}$ is defined as the overall equilibrium constant for σ-adduct formation at the 3-position. It is related to $K_{c,3}$ and K_{Cl^-}, the equilibrium constant for the association of ammonium ions with chloride ions by equation 6.14. The same reasoning and an analogous equation for the

$$(K_{c,3})_{Cl^-} = K_{c,3}\,(1 + K_{Cl^-}[Cl^-]) \qquad \text{(equation 6.14)}$$

formation of the 1-adduct applies. From the measurements it is found that the effect of 0.1M chloride ions approximately doubles the values of the equilibrium constants, and this gives a value *ca* 10 l mol^{-1} for the association constants, K_{Cl^-}, for each of the substituted ammonium ions used.

Comparison of the rate data in Table 6.16 show that while k_1, the ratio k_{Am}/k_{-1} and K_3k_{Am} are, within experimental error, unchanged by the presence of 0.1M chloride ions, the values of k_{AmH^+} reduced by a factor *ca* 2. These observations are compatible with association of the substituted ammonium ions with chloride ions resulting in lower rates of protonation of the anionic σ-adducts.

6.6.2 Attack at the unsubstituted ring position

Because association effects are unimportant for perchlorate salts the rate and equilibrium data measured in their presence will be used for subsequent discussion. Table 6.17 allows the data for amine attack at the 3-position, the unsubstituted ring position, of TNBCl to be compared with the data for amine attack at the unsubstituted ring position of TNB.[151,152] The data in the first five rows has been directly measured or calculated from measured values. The data in the last two rows has been calculated assuming the ratio of acidities $K_a^Z/K_a^{AmH^+}$ has a value of 500, which is independent of the nature of the amine and of the substrate. It is known[155,1] that the trinitrocyclohexadienate group, although negatively charged, is electron withdrawing relative to hydrogen, and this explains why the ratio $K_a^Z/K_a^{AmH^+}$ is greater than unity. Also

TABLE 6.16 Effects of chloride ions on equilibrium and rate data at 25°C

	$K_{c,3}$[a] ($l\ mol^{-1}$)	$K_{c,1}$[a] ($l\ mol^{-1}$)	k_1 ($l\ mol^{-1}s^{-1}$)	k_{Am}/k_{-1} ($l\ mol^{-1}$)	k_{AmH^+} ($l\ mol^{-1}s^{-1}$)	K_3k_{Am} ($l^2\ mol^{-2}s^{-1}$)	k_{AmH^+}[b] ($l\ mol^{-1}s^{-1}$)
n-Butylammonium perchlorate	73	23000	630	2000	55		
n-Butylammonium chloride	150	40000	630	2000	32		
Benzylammonium perchlorate	5	1000	230	200	46		
Benzylammonium chloride	10	2000	250	200	25		
Piperidinium perchlorate						2.6×10^4	280
Piperidinium chloride						2.4×10^4	120

a. In the presence of chloride ions these data are re-defined as $(K_{c,3})_{Cl^-}$ or $(K_{c,1})_{Cl^-}$.

b. Attack at 3-position.

TABLE 6.17 Comparison of kinetic and equilibrium parameters for reaction at unsubstituted ring positions of TNBCl and TNB

		Benzylamine[a]	n-Butylamine[a]	Pyrrolidine[b]	Piperidine[b]
$k_3/\ell\ mol^{-1}s^{-1}$	TNBCl	1000	3000	1.7×10^4	$>1.3 \times 10^4$
	TNB	13000	45000	7.5×10^5	$> 2 \times 10^5$
$K_3k_{Am}/\ell^2 mol^{-2}s^{-1}$	TNBCl	1.4×10^5	$>3.0 \times 10^6$	5.8×10^5	2.6×10^4
	TNB	1.6×10^6	5.5×10^7	1.0×10^7	6×10^5
$k_{Am}/k_{-3}(\ell\ mol^{-1})$	TNBCl	140	>1000	34	< 2
	TNB	120	1200	14	<10
$K_{c,3}/\ell\ mol^{-1}$	TNBCl	5	73	240	93
	TNB	105	1000	3500	2140
$k_{AmH^+}/\ell\ mol^{-1}s^{-1}$	TNBCl[c]	3×10^4	$>4 \times 10^4$	2400	280
	TNB	1.5×10^4	6×10^4	3000	280
$k_{Am}^d/\ell\ mol^{-1}s^{-1}$	TNBCl	1.5×10^7	$>2 \times 10^7$	1.2×10^6	1.4×10^5
	TNB	7.5×10^6	3×10^7	1.5×10^6	1.4×10^5
k_{-3}^d/s^{-1}	TNBCl	1×10^5	2×10^4	3.5×10^4	$> 7 \times 10^4$
	TNB	6×10^4	2.3×10^4	1×10^5	$>4.7 \times 10^4$

a. Data for reaction with TNB from reference 152.

b. Data for reaction with TNB from reference 151.

c. For the benzylamine and butylamine cases this is calculated as $K_3k_{Am}/K_{c,3}$.

d. These data are based on the assumption that $K_a^Z/k_a^{AmH^+}$ has the value 500.

for the reactions of TNB a value of 500 for this ratio has been justified previously,[152,153] and it is unlikely that this ratio would change for TNBCl. The 3-adduct is fourteen to twenty-three times more stable, depending upon the amine, for TNB compared with TNBCl. This is similar to the observation that 3-alkoxy adducts formed from TNT are found to be less stable than those formed from TNB.[82] The electron withdrawing ability of a $-CH_2Cl$ group might be expected to increase the stability of the 3-adducts formed from TNBCl relative to TNB. However, a bulky group at the 1-position causes the ortho nitro groups to rotate out of the ring plane, where they cannot exert their maximum electron withdrawing ability, thereby reducing the adducts stability. It can be seen in Table 6.17 that almost entirely all the decrease in stability of the TNBCl adducts results from a decrease in k_3, the rate coefficient for amine attack on the substrate.

Values of $K_{c,3}$ decrease in the order pyrrolidine > piperidine > n-butylamine > benzylamine and largely reflect the basicity order of the amines.[157,158] The reactivity order of the amines, k_3 values, parallels that obtained for S_NAr substitution of 1-chloro-2,4-dinitrobenzene in ethanol.[159] The rate coefficient, k_{Am}, for proton transfer from the zwitterion to amine is not diffusion controlled. The reduction in value of k_{Am} has been attributed previously [152,153] to steric hindrance, in that the reaction site is crowded and cannot easily be approached by bases larger than hydroxide ion. The increased steric hindrance is reflected by the decrease in the value of k_{Am} in the series primary amine > pyrrolidine > piperidine. Also it is observed that the values k_{Am} and k_{AmH^+}

the rate coefficient for proton transfer from substituted ammonium ions to anionic adducts, are, for a given amine, almost identical for TNBCl and TNB. These results indicate that the steric situation at the reaction site is similar in both cases as attack occurs at the unsubstituted position between two nitro groups. They also provide strong evidence that the adduct forming reaction occurs at the 3-position, and not at the 1-position, with pyrrolidine and piperidine because of the similarity in the values of k_{Am} and k_{AmH^+}.

6.6.3 Attack at the substituted position

Only the primary amines studied formed amido adducts by attack at the 1-position. At this position the CH_2Cl group is substituted in the ring and its electronic effects determine the stability of the 1-adduct. The data is presented in Table 6.18.

Values of k_1 are *ca* five times smaller than corresponding values of k_3. Values of $K_{c,1}$ are respectively three hundred and two hundred times larger than $K_{c,3}$ for benzylamine and n-butylamine respectively. Formation of the 1-adduct relieves steric strain at the 1-position caused by interaction between the bulky CH_2Cl group and the ortho nitro groups. In the σ-adduct the CH_2Cl group is perpendicular to the ring allowing the ortho nitro groups to rotate to be co-planar with the ring, where they exert their maximum electron withdrawing power. The electron withdrawing character of the CH_2Cl group attached to the carbon where nucleophilic attack occurs is probably an additional stabilising factor. F-strain[160] (steric hindrance to the approach of the reagent) probably accounts for amine attack at the 3-position being faster than at the 1-positio

TABLE 6.18 Summary of kinetic and equilibrium data for formation of 1-adducts in DMSO containing 0.1M substituted ammonium perchlorate salts at 25°C

	n-butylamine	Benzylamine
k_1/l mol^{-1}s^{-1}	630	230
k_{Am}/k_{-1}/l mol^{-1}	2000	200
$K_{c,1}$/l mol^{-1}	23000	1000
k_{AmH^+}/l mol^{-1}s^{-1}	55	46
k_{Am}^a/l mol^{-1}s^{-1}	2.7 x 10^4	2.3 x 10^4
k_{-1}^a/s^{-1}	13	110

a. These values are calculated using $K_a^Z/K_a^{AmH^+} = 500$. It is assumed that the presence of the CH_2Cl group will not greatly effect the electron-withdrawing capability of the cyclohexadienate ring.

The values of the rate coefficients, k_{Am} and k_{AmH^+}, relating to the proton transfer steps are reduced by factors of *ca* 10^3 when reaction occurs at the 1-position. The presence of the CH_2Cl group at the reaction site causes an additional unfavourable steric effect which results in these reactions.

The cyclic secondary amines do not form 1-amido adducts under the conditions in which they were studied. This failure can be explained by the fact that due to the bulk of the CH_2Cl group and the piperidine molecule the adduct formed would be thermodynamically unfavourable due to a sterically crowded environment. It has been reported recently[103,161] that cyclic secondary amines, particularly piperidine, have large steric

requirements. This is supported by the observation[162] that the bulky sulphite ion will only attack at unsubstituted positions in the TNBCl ring. More evidence[163] is supplied from studies of alkoxy adducts. It is found that 1,1-dialkoxy adducts become less favoured relative to their 1,3-isomers as the steric bulk of the alkoxy groups increase. There is also a kinetic explanation for the non-observance of the 1-adduct with cyclic amines. The 1-adduct may have greater thermodynamic stability than the 3-isomers but the rate of their formation is very slow that the transfer of the side-chain proton to form the conjugate base takes precedence.

6.7 Derivation of Equations

6.7.1 Rate expressions

(i) σ-adduct formation in solutions containing added amine salt.

For the formation of the 3-adduct the following scheme applies.

$$(\underline{6.1}) + 2Am \underset{k_{-3}}{\overset{k_3}{\rightleftharpoons}} (\underline{6.2}) + Am \underset{k_{AmH^+}}{\overset{k_{Am}}{\rightleftharpoons}} (\underline{6.3}) + AmH^+$$

$$\frac{d[6.3]}{dt} = k_{Am}[Am][6.2] - k_{AmH^+}[AmH^+][6.3] \qquad (\underline{1})$$

An assumption is made in the above scheme that any contribution of the solvent in the deprotonation step of (6.2) or the protonation step of (6.3) is small or zero.

$$\frac{d[6.2]}{dt} = k_3[6.1][Am] + k_{AmH^+}[AmH^+][6.3] - k_{-3}[6.2] - k_{Am}[Am][6.2]$$

If (6.2), the zwitterion, is treated as a steady-state intermediate[78,153,154] then $\frac{d[6.2]}{dt} = 0$.

$$\therefore \quad [6.2] = \frac{k_3[6.1][Am] + k_{AmH^+}[AmH^+][6.3]}{k_{-3} + k_{Am}[Am]} \qquad (\underline{2})$$

Substituting (2) into (1)

$$\frac{d[6.3]}{dt} = k_{Am}[Am]\,(k_3[6.1][Am] + k_{AmH^+}[AmH^+][6.3]) - k_{AmH^+}[AmH^+][6.3]$$

Multiplying $k_{AmH^+}[AmH^+][6.3]$ by $\frac{k_{-3} + k_{Am}[Am]}{k_{-3} + k_{Am}[Am]}$

and re-arranging,

$$\frac{d[6.3]}{dt} = \frac{k_3 k_{Am}[Am]^2[6.1] - k_{-3}k_{AmH^+}[AmH^+][6.3]}{k_{-3} + k_{Am}[Am]} \qquad (\underline{3})$$

$$[6.1]_o = [6.1] + [6.2] + [6.3]$$

$[6.2] \sim 0$ as (6.2) is treated as a steady-state intermediate.

$$\therefore [6.1] = [6.1]_o + [6.3] \qquad (4)$$

where o denotes initial concentration.

Substituting (4) into (3)

$$\frac{d[6.3]}{dt} = \frac{k_3 k_{Am}[Am]^2[6.1]_o - k_3 k_{Am}[Am]^2[6.3] - k_{-3}k_{AmH^+}[AmH^+][6.3]}{k_{-3} + k_{Am}[Am]} \qquad (5)$$

At equilibrium $\frac{d[6.3]}{dt} = 0$

$$0 = \frac{k_3 k_{Am}[Am]^2[6.1]_o - k_3 k_{Am}[Am]^2[6.3]_e - k_{-3}k_{AmH^+}[AmH^+][6.3]_e}{k_{-3} + k_{Am}[Am]} \qquad (6)$$

where e denotes concentration at equilibrium.

Subtracting (6) from (5)

$$\frac{d[6.3]}{dt} = \left(\frac{k_3 k_{Am}[Am]^2 + k_{-3}k_{AmH^+}[AmH^+]}{k_{-3} + k_{Am}[Am]}\right)([6.3]_e - [6.3]) \qquad (7)$$

Relating [6.3] to OD

The parent, (6.1) does not absorb at the wavelength where the reaction is studied. As (6.2) is a steady-state intermediate its concentration is very small so if it does absorb at the wavelength where the reaction is studied its contribution is negligible. Therefore the only absorbing species is (6.3)

$$OD = \varepsilon_{6.3}[6.3] \qquad (8)$$

At equilibrium,

$$OD_e = \varepsilon_{6.3}[6.3]_e \qquad (9)$$

$$OD_e - OD = \varepsilon_{6.3} ([6.3]_e - [6.3]) \qquad (10)$$

Differentiating (8)

$$\frac{d\ OD}{dt} = \varepsilon_{6.3} \frac{d[6.3]}{dt}$$

Hence,

$$\frac{d\ OD}{dt} \cdot \frac{1}{OD_e - OD} = \frac{d[6.3]}{dt} \cdot \frac{1}{([6.3]_e - [6.3])} \qquad (11)$$

k_{obs} is defined thus,

$$k_{obs} = \frac{d\ OD}{dt} \cdot \frac{1}{(OD_e - OD)} \qquad (12)$$

Therefore combining (11), (12) and (7)

$$k_{obs} = \frac{k_3 k_{Am} [Am]^2 + k_{-3} k_{AmH^+} [AmH^+]}{k_{-3} + k_{Am}[Am]}$$

For the formation of the 1-adduct the following scheme applies

$$(6.1) + 2Am \underset{}{\overset{k_{c,3}}{\rightleftharpoons}} (6.3) + AmH^+$$

$$\overset{k_1}{\underset{k_{-1}}{\rightleftharpoons}} (6.4) + Am \overset{k_{Am}}{\underset{k_{AmH^+}}{\rightleftharpoons}} (6.5) + AmH^+$$

Formation of the 3-adduct (6.3) is rapid compared to the formation of the 1-adduct (6.5).

(3) is the rate equation for the formation of the 3-adduct. (13) is derived in an analogous way for the formation of the 1-adduct.

$$\frac{d[6.5]}{dt} = \frac{k_1 k_{Am} [Am]^2 [6.1] - k_{-1} k_{AmH^+} [AmH^+] [6.5]}{k_{-1} + k_{Am}[Am]} \qquad (13)$$

$$[6.1]_o = [6.1] + [6.3] + [6.5] \qquad (14)$$

The overall equilibrium constant for formation of the 3-adduct is defined as follows;

$$K_{c,3} = \frac{[6.3][AmH^+]}{[6.1][Am]^2}$$

$$\therefore \quad [6.1]_o = [6.1] + K_{c,3}\frac{[Am]^2[6.1]}{[AmH^+]} + [6.5]$$

Re-arranging,

$$[6.1] = \frac{[6.1]_o - [6.5]}{1 + K_{c,3}\frac{[Am]^2}{[AmH^+]}} \qquad (15)$$

Substituting (14) into (13)

$$\frac{d[6.5]}{dt} = \frac{k_1 k_{Am}[Am]^2[6.1]_o - k_1 k_{Am}[Am]^2[6.5]}{(k_{-1}+k_{Am}[Am])\left(1+K_{c,3}\frac{[Am]^2}{[AmH^+]}\right)} - \frac{k_{-1}k_{AmH^+}[AmH^+][6.5]}{k_{-1}+k_{Am}[Am]} \qquad (16)$$

At equilibrium $\frac{d[6.5]}{dt} = 0.$

$$0 = \frac{k_1 k_{Am}[Am]^2[6.1]_o - k_1 k_{Am}[Am]^2[6.5]_e}{(k_{-1}+k_{Am}[Am])\left(1+K_{c,3}\frac{[Am]^2}{[AmH^+]}\right)} - \frac{k_{-1}k_{AmH^+}[AmH^+][6.5]_e}{k_{-1}+k_{Am}[Am]} \qquad (17)$$

Subtracting (17) from (16)

$$\frac{d[6.5]}{dt} = \left(\frac{k_1 k_{Am}[Am]^2}{(k_{-1}+k_{Am}\,Am)\left(1+K_{c,3}\frac{[Am]^2}{[AmH^+]}\right)} - \frac{k_{-1}k_{AmH^+}[AmH^+]}{k_{-1}+k_{Am}[Am]}\right)([6.5]_e - [6.5$$

(18)

By definition,

$$k_{obs} = \frac{d\,OD}{dt} \cdot \frac{1}{(OD_e - OD)} \qquad (19)$$

Relating [6.5] to OD.

In the reaction the absorbing species are (6.3) and (6.5).

$$OD = \varepsilon_{6.3}[6.3] + \varepsilon_{6.5}[6.5] \qquad (20)$$

Substituting (14) into (20), then (15)

$$OD = \varepsilon_{6.5}[6.5] + \varepsilon_{6.3}\left(K_{c,3}\frac{[Am]^2}{[AmH^+]}\left(\frac{[6.1]_o - [6.5]}{1+K_{c,3}\frac{[Am]^2}{[AmH^+]}}\right)\right) \qquad (21)$$

Re-arranging,

$$OD = [6.5].\ A + B \qquad (22)$$

$$\text{where } A = \varepsilon_{6.5} - \frac{\varepsilon_{6.3}K_{c,3}[Am]^2}{[AmH^+]+K_{c,3}[Am]^2}$$

$$\text{and } B = \frac{\varepsilon_{6.3}[6.1]_o K_{c,3}[Am]^2}{[AmH^+]+K_{c,3}[Am]^2}$$

$$OD_e = [6.5]_e.\ A + B \qquad (23)$$

Differentiating (22)

$$\frac{d\ OD}{dt} = \frac{d[6.5]}{dt} \cdot A \qquad (24)$$

Combining (22), (23) and (24),

$$\frac{d\ OD}{dt} \cdot \frac{1}{(OD_e - OD)} = \frac{d[6.5]}{dt} \cdot \frac{1}{([6.5]_e - [6.5])} \qquad (25)$$

Combining (18), (19) and (25)

$$k_{obs} = \frac{k_1 k_{Am}[Am]^2}{(k_{-1}+k_{Am}[Am])\left[1+K_{c,3}\frac{[Am]^2}{[AmH^+]}\right]} + \frac{k_{-1}k_{AmH^+}[AmH^+]}{k_{-1}+k_{Am}[Am]}$$

(ii) σ-adduct formation in solutions containing no added amine salt.

This is the scheme for the overall σ-adduct formation.

$$P + 2Am \underset{k_r}{\overset{k_f}{\rightleftharpoons}} A + AmH^+$$

As all experimental measurements were made with [Am] in large excess over [P] the rate expression is given by (26).

$$\text{rate} = \frac{d[A]}{dt} = k_f^1[P] - k_r^2[A]^2 \qquad (26)$$

where k_f^1 = first-order forward rate constant

and k_r^2 = second-order reverse rate constant.

(26) can be integrated by standard methods[75] to give (27)

$$\ln \left\{ \frac{[P]_o[A]_e + [A]_e([P]_o - [A]_e)}{[P]_o([A]_e - [A])} \right\} = \frac{(2[P]_o - [A]_e)}{[A]_e} k_f^1 t \qquad (27)$$

where o denotes initial concentration

and e denotes concentration at equilibrium.

If the reaction ≥ 95% complete, then $[P]_e \sim [P]_o$ giving (28).

$$\ln \frac{[A]_e}{[A]_e - [A]} = k_f^1 t \qquad (28)$$

This equation is in the form of a first-order rate equation so that $k_f^1 t = k_{obs}$.

For the formation of the 3-adduct it has been shown above that

$$k_{obs} = \frac{k_3 k_{Am}[Am]^2 + k_{-3}k_{AmH^+}[AmH^+]}{k_{-3} + k_{Am}[Am]}$$

With no added amine salt $[AmH^+] \sim 0$

$$\therefore \quad k_{obs} = (k_f^1)_3 t = \frac{k_3 k_{Am}[Am]^2}{k_{-3} + k_{Am}[Am]}$$

For formation of the 1-adduct it has been shown above that

$$k_{obs} = \frac{k_1 k_{Am}[Am]^2}{(k_{-1}+k_{Am}[Am])\left(1+K_{c,3}\frac{[Am]^2}{[AmH^+]}\right)} + \frac{k_{-1}k_{AmH^+}[AmH^+]}{k_{-1}+k_{Am}[Am]} \qquad (29)$$

$K_{c,3}$ can be defined thus,

$$K_{c,3} = \frac{(OD)_3}{(OD_\infty)_3-(OD)_3} \cdot \frac{[AmH^+]}{[Am]^2}$$

Re-arranging,

$$K_{c,3}\frac{[Am]^2}{[AmH^+]} = \frac{(OD)_3}{(OD_\infty)_3-(OD)_3} \qquad (30)$$

Substituting (30) into (29), and with no added amine salt $[AmH^+] \sim 0$.

$$k_{obs} = (k_f^1)_1 t = \frac{k_1 k_{Am}[Am]^2}{\left(1+\frac{OD_3}{(OD_\infty)_3-OD_3}\right)\left(k_{-1}+k_{Am}[Am]\right)}$$

(iii) Deprotonation of the substrate to form the conjugate base.

$$(6.3) + AmH^+$$

$$(6.1) + 2\,Am \underset{}{\overset{K_{c,3}}{\rightleftharpoons}} (6.5) + AmH^+ \qquad (K_{c,1})$$

$$\overset{k_p}{\underset{k_{-p}}{\rightleftharpoons}} (6.6) + AmH^+ + Am$$

$$\frac{d[6.6]}{dt} = k_p[6.1][Am] - k_{-p}[6.6][AmH^+] \qquad (31)$$

$$[6.1]_o = [6.1] + [6.3] + [6.5] + [6.6] \qquad (32)$$

where ô denotes initial concentration.

The σ-adduct formation reactions are fast in comparison to the deprotonation reaction.

$$K_{c,1} = \frac{[6.5][AmH^+]}{[6.1][Am]^2} \qquad K_{c,3} = \frac{[6.3][AmH^+]}{[6.1][Am]^2}$$

$$\therefore \quad [6.1]_o = [6.1] + K_{c,3}\frac{[Am]^2}{[AmH^+]} + K_{c,1}\frac{[Am]^2}{[AmH^+]}\ [6.1] + [6.6]$$

$$[6.1] = [6.1]_o - \frac{[6.6]}{1+K_{c,1}\frac{[Am]^2}{[AmH^+]} + K_{c,3}\frac{[Am]^2}{[AmH^+]}} \qquad (33)$$

Substituting (33) into (31)

$$\frac{d[6.6]}{dt} = \frac{k_p[6.1]_o[Am] - k_p[6.6][Am]}{1+K_{c,1}\frac{[Am]^2}{[AmH^+]} + K_{c,3}\frac{[Am]^2}{[AmH^+]}} - k_{-p}[6.6][AmH^+] \qquad (34)$$

At equilibrium $\frac{d[6.6]}{dt} = 0$

$$0 = \frac{k_p[6.1]_o[Am] - k_p[6.6]_e[Am]}{1 + K_{c,1}\frac{[Am]^2}{[AmH^+]} + K_{c,3}\frac{[Am]^2}{[AmH^+]}} - k_{-p}[6.6]_e[AmH^+] \qquad (35)$$

Subtracting (35) from (34)

$$\frac{d[6.6]}{dt} = \frac{k_p[Am]}{1 + K_{c,1}\frac{[Am]^2}{[AmH^+]} + K_{c,3}\frac{[Am]^2}{[AmH^+]}}([6.6]_e - [6.6])$$

$$+ k_{-p}[AmH^+]([6.6]_e - [6.6])$$

By definition

$$k_{obs} = \frac{d\ OD}{dt} \cdot \frac{1}{OD_e - OD} \qquad (37)$$

The usual method shown above for σ-adduct formation can be used to relate OD to $[6.6]$.

Therefore,

$$\frac{d\ OD}{dt} \cdot \frac{1}{OD_e - OD} = \frac{d[6.6]}{dt} \cdot \frac{1}{([6.6]_e - [6.6])} \qquad (38)$$

Combining (36), (37) and (38)

$$k_{obs} = \frac{k_p [Am]}{1+K_{c,1} \frac{[Am]^2}{[AmH^+]} + K_{c,3} \frac{[Am]^2}{[AmH^+]}} - k_{-p} [AmH^+]$$

If $1 + K_{c,1} \frac{[Am]^2}{[AmH^+]} >> K_{c,3} \frac{[Am]^2}{[AmH^+]}$ then

$$k_{obs} = \frac{k_p [Am]}{1+K_{c,1} \frac{[Am]^2}{[AmH^+]}} + k_{-p} [AmH^+]$$

If $1 >> K_{c,1} \frac{[Am]^2}{[AmH^+]} + K_{c,3} \frac{[Am]^2}{[AmH^+]}$ then

$$k_{obs} = k_p [Am] + k_{-p} [AmH^+]$$

6.7.2 Equilibrium constants

(i) Defining K_c

$$(6.1) + 2Am \underset{k_{-x}}{\overset{k_x}{\rightleftharpoons}} Z + Am \underset{k_{AmH^+}}{\overset{k_{Am}}{\rightleftharpoons}} A + AmH^+$$

(v_f over the forward path, v_r under the reverse path)

where Z = Zwitterion

A = Adduct

x = 1 or 3 depending on whether 1-adduct or 3-adduct is formed.

For the equilibrium shown above the overall equilibrium constant $K_{c,x}$ is defined by

$$K_{c,x} = \frac{[A][AmH^+]}{[6.1][Am]^2}$$

At equilibrium $v_f = v_r$

$$\therefore \quad k_x k_{Am} [6.1] [Am]^2 = k_{-x} k_{AmH^+} [A] [AmH^+]$$

Hence,

$$K_{c,3} = \frac{k_x}{k_{-x}} \cdot \frac{k_{Am}}{k_{AmH^+}}$$

K_a^Z, the acid dissociation constant of Z is defined from $Z \rightleftharpoons A + H^+$ and $K_a^{AmH^+}$, the acid dissociation constant of the protonated amine $[AmH^+]$ is defined from

$AmH^+ \rightleftharpoons Am + H^+$

$$\therefore \quad K_{c,x} = \frac{k_x}{k_{-x}} \cdot \frac{K_a^Z}{K_a^{AmH^+}}$$

Relating $(K_{c,3})_{Cl^-}$ to $K_{c,3}$

$$\underline{(6.1)} + 2Am + Cl^- \underset{}{\overset{K_{c,3}}{\rightleftharpoons}} \underline{(6.3)} + AmH^+ + Cl^-$$

$$AmH^+ \cdots\cdots Cl^- \quad (K_{Cl^-})$$

$$(K_{c,3})_{Cl^-} = \frac{[6.3]([AmH^+] + [AmH^+ \cdots Cl^-])}{[6.1][Am]^2} \qquad (39)$$

$$K_{Cl^-} = \frac{[AmH^+ \cdots Cl^-]}{[AmH^+][Cl^-]} \qquad (40)$$

Substituting (40) into (39).

$$(K_{c,3})_{Cl^-} = \frac{[6.3]([AmH^+] + K_{Cl^-}[AmH^+][Cl^-])}{[6.1][Am]^2}$$

Re-arranging,

$$(K_{c,3})_{Cl} = \frac{[6.3][AmH^+]}{[6.1][Am]^2} \quad (1 + K_{Cl^-}[Cl^-]) \qquad (41)$$

$$K_{c,3} = \frac{[6.3][AmH^+]}{[6.1][Am]^2} \qquad (42)$$

Substituting (42) into (41)

$$(K_{c,3})_{Cl^-} = K_{c,3}\ (1 + K_{Cl^-}[Cl^-])$$

$(K_{c,1})_{Cl^-}$ can be related to $K_{c,1}$ in an analogous way.

CHAPTER SEVEN

THE REACTIONS OF 2,2´,4,4´,6,6´-HEXANITROBIBENZYL WITH ALIPHATIC AMINES IN DIMETHYL SULPHOXIDE

7.1 Introduction

It has been discovered[11] that the addition of amines to the Shipp-Kaplan reaction[2] increases the yield of the commercially important explosive 2,2′,4,4′,6,6′-hexanitrostilbene (HNS). It has also been found[12] that the reaction between amines and 2,2′,4,4′,6,6′-hexanitrobibenzyl (HNBB) can be used to produce HNS in high yields. Therefore it was of interest to study the reactions of amines with HNBB. In this chapter the reactions between HNBB and n-butylamine, benzylamine, piperidine, pyrrolidine and 1,4-diazabicyclo-[2,2,2]octane (DABCO) in dimethyl sulphoxide (DMSO) are reported.

If HNBB is considered as a picryl (Pic) ring with a Ch_2Ch_2Pic substituent then reactions between HNBB and amines can be predicted from the reactions of TNBCl, a picryl ring with a CH_2Cl substituent, with amines, which were reported in the previous chapter. Figure 7.1 shows possible 1:1 σ-adducts formed by amine attack at the 3-position (7.3) or the 1-position (7.5), formed *via* their respective zwitterionic intermediates (7.2) and (7.3). However, as for the reactions between HNBB and alkoxide ions, after the initial formation of the 1:1 σ-adducts there is a further possibility of attack on the second ring, at the 1′- or 3′-position, to form 1:2 σ-adducts such as (7.6) and (7.7) shown in Figure 7.2. It might be expected that deprotonation of the substrate would produce the conjugate base (7.8). However the evidence to be presented shows that transfer of side-chain protons leads preferentially to the dianion (7.9).

Figure 7.2

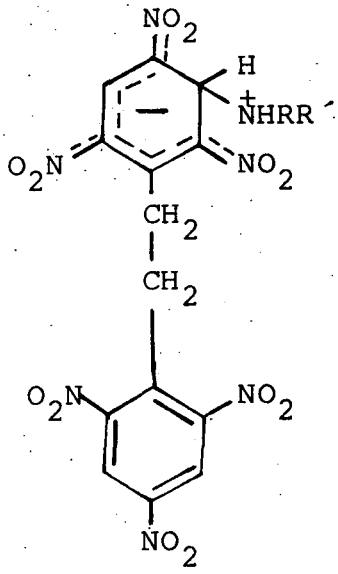

(7.2)

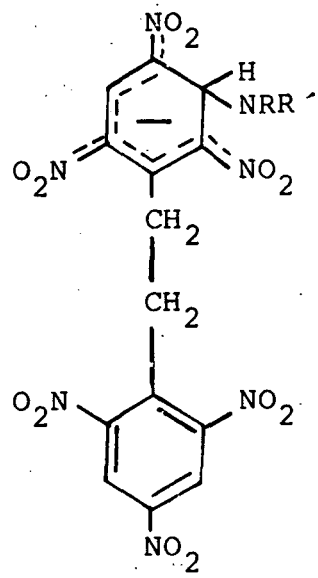

(7.3)

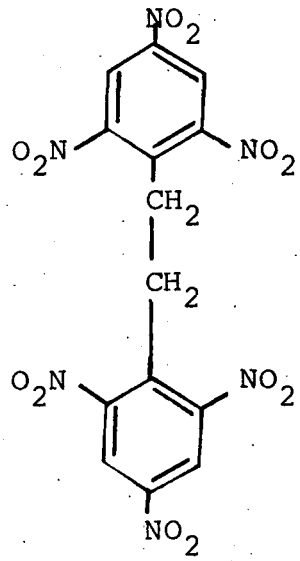

(7.1)

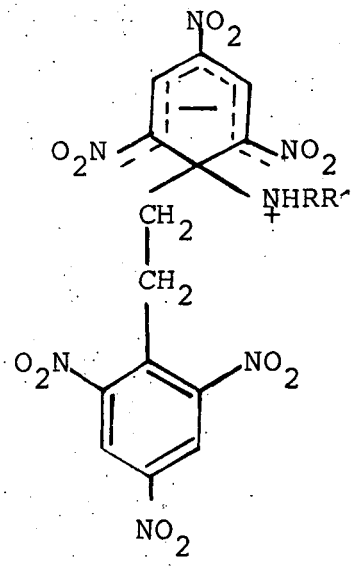

(7.4)

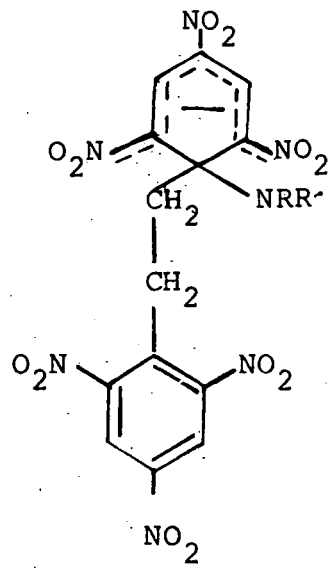

(7.5)

Measurements were made in the presence of substituted ammonium perchlorate or chloride salts. Again the results reported here provide evidence[86] for the stabilisation of the substituted ammonium ions by association with chloride ions, $RR'\overset{+}{N}H_2....Cl^-$.

Figure 7.2

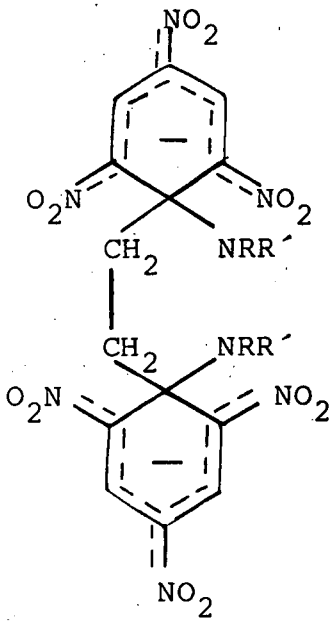

(7.6)

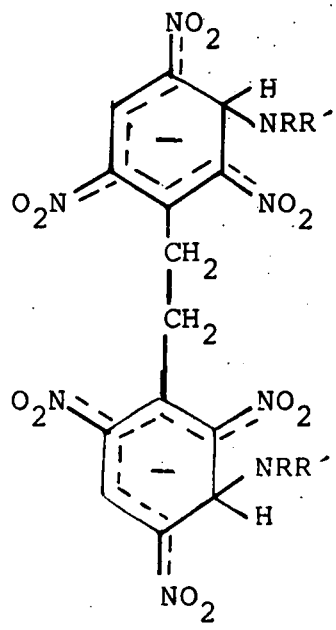

(7.7)

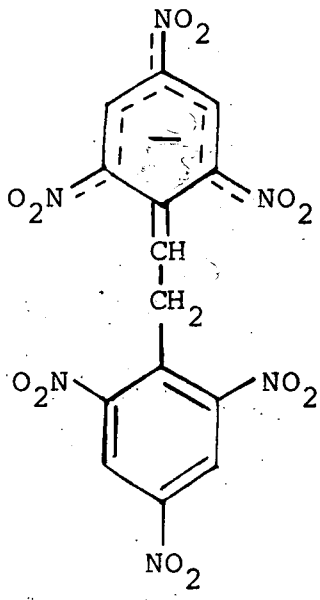

(7.8)

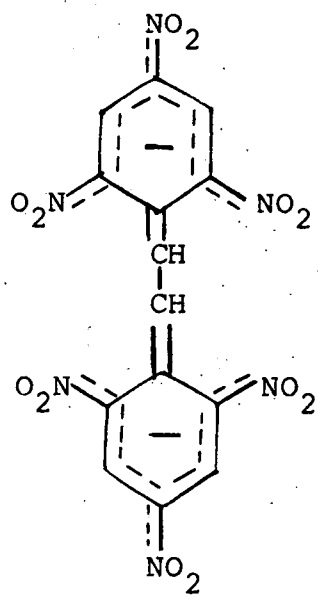

(7.9)

7.2 Experimental

Visible spectra were recorded on a Pye-Unicam SP 8005 spectrophotometer, using either a 10mm pathlength cell or an adjustable (usually 0.02mm) pathlength microcell.

Rapid rate measurements were made using a Hi-Tech SF-3L stopped-flow spectrophotometer at 25°C. The rate coefficients are the mean of at least five separate determinations and are precise to ±5%. Slow rate measurements were made using a SP 8100 recording spectrophotometer at 25°C. Here, the rate coefficients are the mean of duplicate runs. Both spectrophotometers were used to measure optical densities. In all cases freshly prepared solutions of reagents were used and measurements were made with amine concentration in large excess of substrate concentration.

A Kent EIL 7055 pH meter was used to check that the substituted ammonium salts contained less than 1% free amine or acid.

Conductance measurements were made on a W.G. Pye and Company Limited conductance bridge Cat.No. 11700 using a Mullard conductivity cell in DMSO.

^{1}H n.m.r. measurements were made on a Varian EM 360L instrument operating at 60MHz and the chemical shifts were measured relative to internal tetramethylsilane.

TABLE 7.1 Typical results from rate measurements.

(i) HNBB (5×10^{-6} M), DABCO (0.08M).

Only process; measured at 600nm in DMSO.

(ii) HNBB (1×10^{-5} M), piperidine (0.02M).

Only process; measured at 450nm in DMSO containing 0.1M piperidinium chloride.

(i)		(ii)	
t/s	ΔV^a	t/ms	ΔV^a
0	3.7	0	4.3
2.5	3.0	10	3.5
5	2.4	20	2.8
7.5	2.0	30	2.1
10	1.5	40	1.8
12.5	1.3	50	1.4
15	1.1	60	1.1
20	0.7	80	0.6

A plot of ln ΔV versus to is linear and yields $k_{obs} = 0.082\ s^{-1}$

A plot of ln ΔV versus t is linear and yields $k_{obs} = 22.88\ s^{-1}$.

a. $\Delta V = V_\infty - V_t$

TABLE 7.2 Typical results from rate measurements

(i) HNBB (5×10^{-6} M), n-butylamine (0.01M)

First process; measured at 460nm in DMSO.

(ii) HNBB (1×10^{-5} M), benzylamine (0.06M).

Only process, measured at 460nm in DMSO containing 0.1M benzylammonium perchlorate.

(i)		(ii)	
t/ms	ΔV^a	t/ms	ΔV^a
0	3.0	0	5.4
10	2.4	50	4.2
20	2.0	100	3.3
30	1.7	150	2.6
40	1.4	200	2.0
50	1.2	250	1.6
60	1.0	300	1.2
80	0.7		

A plot of ln ΔV versus t is linear and yields $k_{obs} = 17.8\ s^{-1}$

A plot of ln ΔV versus t is linear and yields $k_{obs} = 4.90\ s^{-1}$

a. $\Delta V = V_\infty - V_t$

TABLE 7.3 Typical results from rate measurements

(i) HNBB (2×10^{-5} M), pyrrolidine (0.01M). Only process; measured at 450nm in DMSO.

(ii) HNBB (5×10^{-6} M), piperidine (0.1M). Deprotonation process; measured at 640nm in DMSO containing 0.1M piperidinium perchlorate.

(i)		(ii)	
t/ms	ΔV^a	t/s	ΔV^a
0	3.4	0	6.0
10	2.9	5	4.9
20	2.4	10	4.0
30	2.1	15	3.2
40	1.65	20	2.7
60	1.2	25	2.2
80	0.8	30	1.8
		35	1.4
		40	1.0

A plot of ln ΔV versus t yields a value of $k_{obs} = 18.25\ s^{-1}$.

A plot of ln ΔV versus t yields a value of $k_{obs} = 0.0415\ s^{-1}$.

a. $\Delta V = V_\infty - V_t$

7.3 Results

7.3.1 Reactions with DABCO

DABCO is a tertiary amine and is known to react with trinitrotoluene (TNT) and trinotrobenzyl chloride (TNBCl) to form the conjugate base without preliminary formation of the σ-adduct. (Tertiary amines cannot form σ-adducts). The reaction of HNBB with DABCO produces a deep blue species in an irreversible reaction which decays to give a brown coloured species. Visible spectra of HNBB (2×10^{-5} M) and DABCO (0.01-0.1M) in DMSO show that the blue species has maxima at 620nm (ε 4.2×10^4 l mol^{-1} cm^{-1}) and 380nm (ε 1.3×10^4 l mol^{-1} cm^{-1}). An example of such spectra is shown in Figure 7.3. In solutions containing 0.01M DABCO the formation of the blue species is complete after *ca* six minutes and then decays slowly. In solutions containing 0.1M DABCO the formation of the blue species is complete after *ca* six seconds before it decays slowly. In DMSO solutions containing 0.1M DABCO perchlorate, (*N.B.* at the pH of the solutions used in this work only one nitrogen atom per DABCO molecule is protonated to give the mono perchlorate salt), the rate of formation and decay of the blue species is increased.

Absorption maxima at 373nm (ε 8×10^3 l mol^{-1} cm^{-1}), 490nm (1.5×10^4 l mol^{-1} cm^{-1}) and 600nm (8×10^3 l mol^{-1} cm^{-1}) for the conjugate base of TNBCl and at 377nm (9×10^3 l mol^{-1} cm^{-1}) 530nm (1.5×10^4 l mol^{-1} cm^{-1}) and 640 (9×10^3 l mol^{-1} cm^{-1}) for the conjugate base of TNT have been reported.[83,93,94,117,118,164] The visible spectra of the blue species formed from HNBB bears little similarity with the above spectra and the blue species has extinction coefficients which are approximately twice as

FIGURE 7.3 Visible spectrum of HNBB (2×10^{-5}M) and DABCO (0.2M) in DMSO

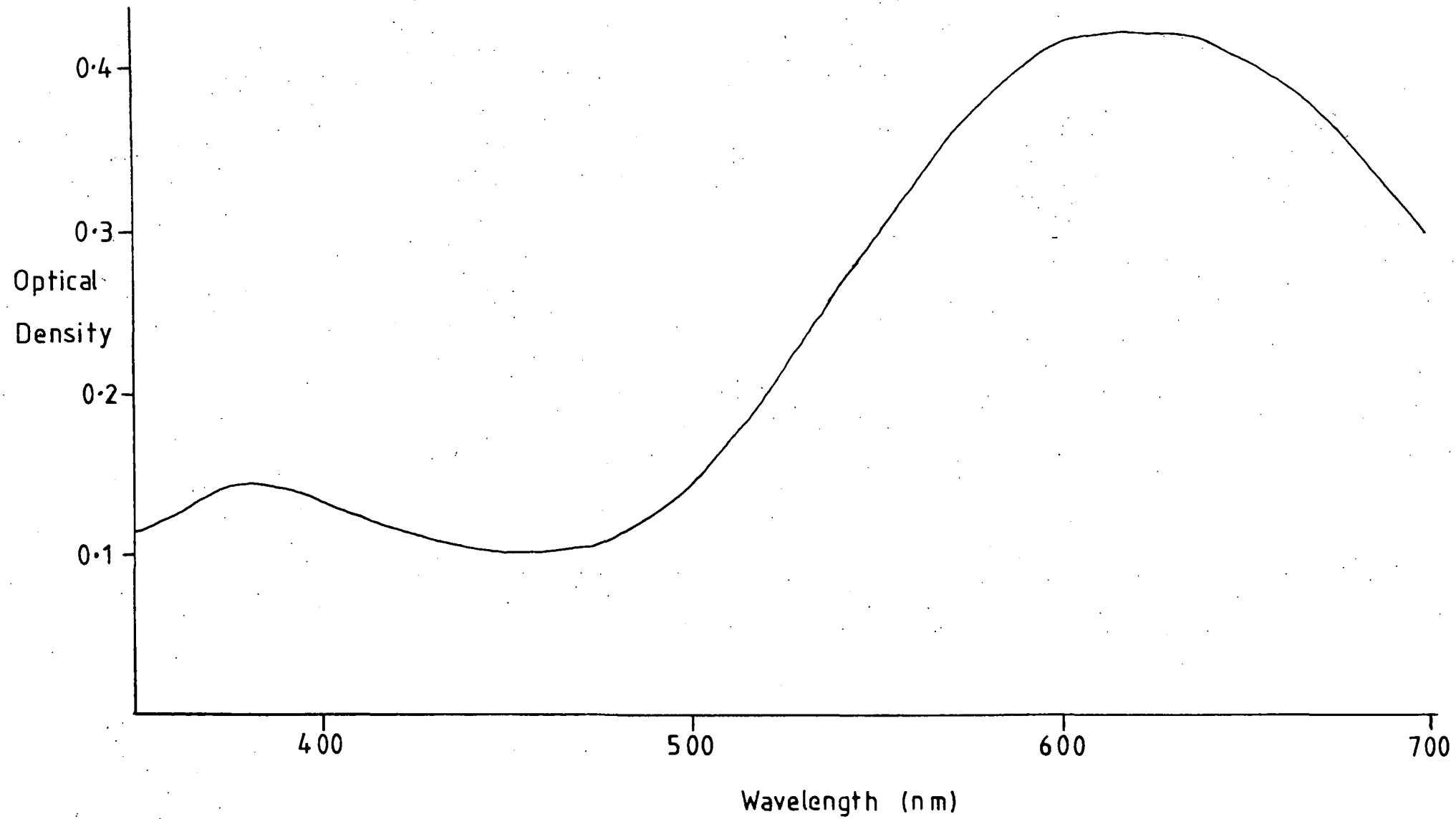

large. These differences suggest that both aromatic rings of HNBB are involved in charge delocalisation, which in turn would be explained if the blue species is the dianion (7.9). Strong evidence for the blue species being the dianion, formed by removal of two chain protons from HNBB, is given by ^{1}H n.m.r. measurements, (which will be reported below), and by conductance measurements. The conductance measurements, reported in Table 7.4, show that the blue species is formed by the reaction of two amine molecules per HNBB molecule. Visible spectra, recorded with a microcell when the equilibrium had been reached after about two minutes, were identical to those of the blue species formed in more dilute solutions. The curvature observed for the plot in Figure 7.4 indicates that the overall equilibrium constant for dianion formation, $K_{p,c}$, is not infinitely high, and allows the calculation (at I = 0.12M) of a very approximate value for $K_{p,c}$, defined by equation 7.4, of *ca* 200. Polarography measurements[165] have also shown that HNS accepts two electrons per molecule in one step to give the dianion.

The possibility that the blue species is a radical also had to be considered, although from previous work[7] it is known that tri-nitroaromatic compounds show a preference for forming anions rather than radicals. E.s.r. measurements[149] indicate that no radicals are present when the blue species is formed. Further evidence that supports this conclusion is that the formation of the blue species proceeds to completion even in the presence of free radical inhibitors such as di-tert-butyl nitroxide or oxygen.

Acidification of the blue species by aqueous HCl produces a solid which, after purification and solution in [$^{2}H_{6}$] DMSO,

TABLE 7.4 Conductance measurements for the reaction between HNBB (0.04M) and DABCO in DMSO.

[DABCO]/M	10^3 Excess Conductance[a]/mho[b]
0.01	0.885
0.02	1.67
0.03	2.41
0.04	3.23
0.05	3.76
0.06	4.42
0.07	4.90
0.08	5.35
0.09	5.64
0.10	5.78
0.12	5.91
0.16	6.01
0.25	6.04

a. A plot of Excess Conductance versus [DABCO] is shown in Figure 7.4. This gives for the ratio HNBB:DABCO a value of 1:1.875.

b. mho = ohm^{-1}.

FIGURE 7.4 A plot of Excess Conductance versus [DABCO] for the data given in Table 7.4

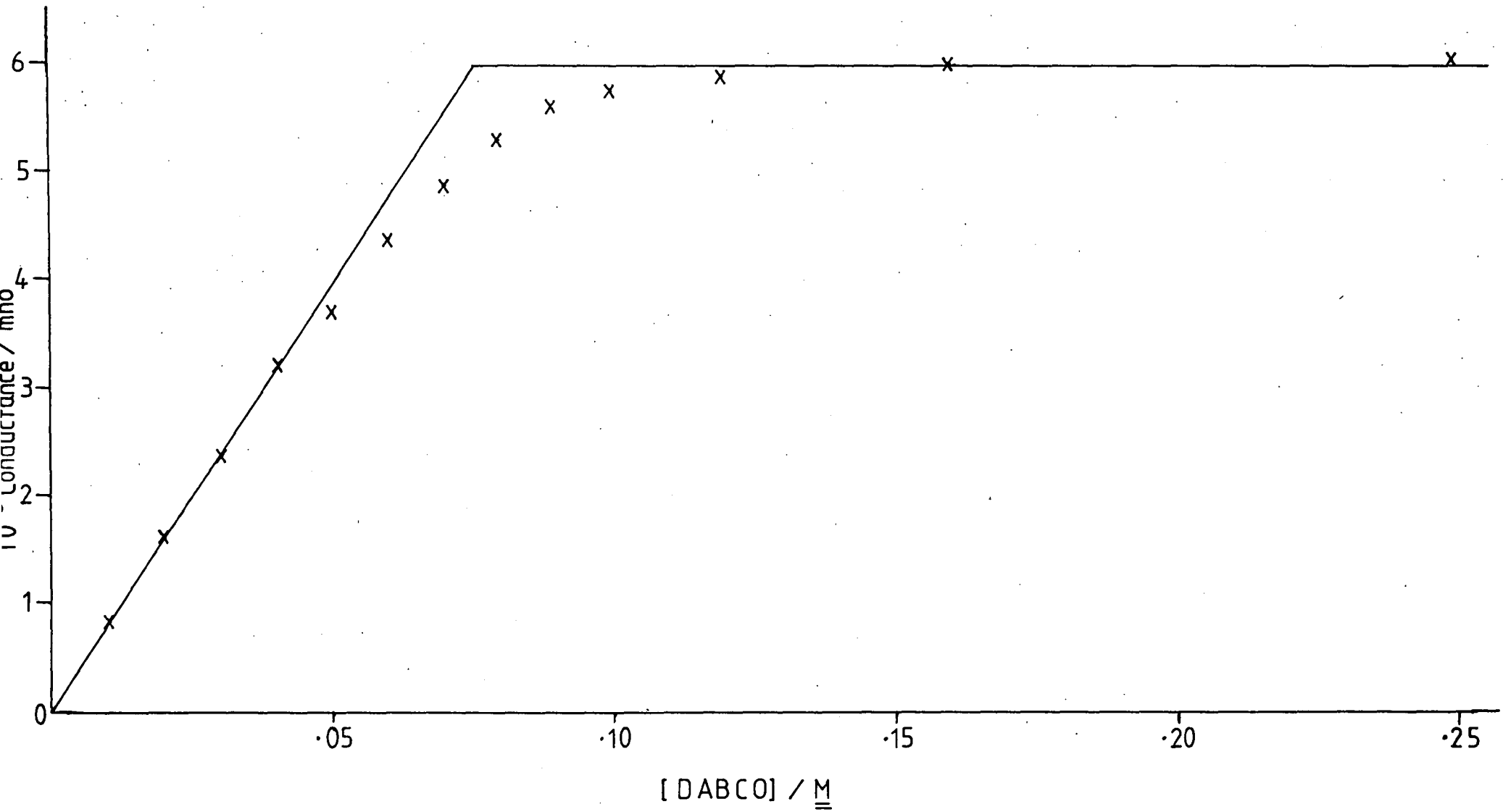

gave a spectrum identical to that of HNS. Bands were observed in the approximate ratio of 2:1 for ring protons (δ9.10) to olefinic protons (δ7.13). A broad band was also observed at δ5.10 presumably due to water present in the damp sample.

The formation of the dianion presumably occurs *via* the monoanion. If the monoanion were present in relatively large concentrations it would be expected that it would react as a carbanion. However the blue species has not been observed[165] to react with ketones to form any products by nucleophilic attack at the carbonyl bond. Also if the monoanion is present in relatively large concentrations there is the possibility of deuterium exchange. The ^{1}H n.m.r. spectrum in $[^{2}H_{6}]$DMSO was recorded of the solid that came down on adding deuterium oxide to the blue species. The major bands observed were at δ9.17, 9.10, 7.13 and 3.33. The bands at δ9.17 and δ7.13 are approximately in the ratio of 2:1 and are assigned to the ring protons and olefinic protons of HNS respectively. The bands at δ9.10 and δ3.33 are approximately in the ratio of 1:1 and are assigned to the ring protons and chain protons of HNBB respectively. The slight difference in chemical shifts reported here with those reported in earlier chapters is assumed to be caused by the n.m.r. spectrometer. No deuterium incorporation was observed in either HNS or HNBB.

All ^{1}H n.m.r. measurements for the reaction of HNBB (0.10M) with DABCO were made in $[^{2}H_{6}]$DMSO. The spectrum of HNBB showed bands at δ9.10 (ring protons) and δ3.37 (chain protons), which are within experimental error of the spectrum of HNBB reported in Chapter Four. The spectrum of DABCO in $[^{2}H_{6}]$DMSO produces one large singlet at δ2.6. The spectrum

recorded one minute after the addition of five molecular equivalents of DABCO to HNBB shows two sharp bands at δ8.20 and δ6.10. With time the δ8.20 band moved downfield eventually reaching a position of δ9.10, while the δ6.10 band moved upfield stopping at δ5.80. The final spectrum, taken after thirty minutes, shows major bands at δ9.10, 7.5, 7.10 and 5.80, with a few smaller bands in the δ8.9-8.35 region. The band at δ8.20 is attributed to the ring protons of the dianion which is in rapid equilibrium, on the n.m.r. timescale, with HNS. This band therefore moves downfield to δ9.10 where it is known the ring protons of HNS resonate. Also the band at δ7.10 can be attributed to the olefinic protons of HNS. Earlier it was shown the product of the reaction between HNBB and DABCO is HNS. The bands at δ7.50 and those between δ8.9 and δ8.35 are attributed to one or more species produced by some unknown reaction or reactions. Ninety seconds after the addition of half a molecular equivalent of DABCO the band at δ9.10 (ring protons) collapses to form a broad band; a broad band at δ8.57 appears, attributed to the ring protons of the dianion; and a pronounced curvature in the baseline at about δ6.2 is observed, probably attributable to the proton on the nitrogen atom of the conjugate acid of DABCO. After eight minutes the band at δ8.57 has moved downfield to δ9.13 and over the next five minutes sharpens. As this band moves downfield a band at δ7.53 appears and increases in intensity for the next six minutes; as do the bands in the δ8.68-8.43 region. After about twelve minutes a band at δ7.17 appears and grows in intensity with time. The final spectrum after thirty-six minutes shows bands at δ9.13, attributable to the ring protons of HNS and unreacted HNBB; at δ7.17, attributable to the olefinic protons of HNS; at δ7.5 and several

small bands between δ8.68 and δ8.43, attributed to some species produced by an unknown reaction. A slight curvature of the base line *ca* δ5.8 is also noticeable presumably due to the protonated DABCO proton. A band at δ3.40 was also observable which may be due to the chain protons of HNBB, although the appearance of several bands with chemical shifts in this region, due to some unknown species, does not make this assignment certain. Spectra in the presence of one molecular equivalent and two molecular equivalents of DABCO produce similar bands for the dianion as those given for half and five molecular equivalents.

The kinetic data for the formation of the dianion has been interpreted using Scheme 7.1. Here the rate limiting step is the removal of a proton from the $-CH_2CH_2-$ link between the

$$(\underline{7.1}) + R'RNH \underset{k_{-p}}{\overset{k_p}{\rightleftharpoons}} (\underline{7.8}) + R'R\overset{+}{N}H_2$$

$$(\underline{7.8}) + R'RNH \underset{k_{-2p}}{\overset{k_{2p}}{\rightleftharpoons}} (\underline{7.9}) + R'R\overset{+}{N}H_2$$

Scheme 7.1

picryl rings to form the monoanion. This is followed rapidly by the loss of a second proton to form the dianion, which is in rapid equilibrium with the monoanion. The rate expression derived from Scheme 7.1 is equation 7.1. If $k_{2p}[Am] >> k_{-p}[AmH^+]$ then equation 7.1 reduces to equation 7.2. When there is no added amine salt present in solution then equation 7.2 becomes equation 7.3 as $[AmH^+] \sim 0$.

$$k_{obs} = \frac{k_{2p}k_{p}[Am]^2 + k_{-p}k_{-2p}[AmH^+]^2}{k_{2p}[Am] + k_{-p}[AmH^+]} \qquad \text{(equation 7.1)}$$

$$k_{obs} = k_{p}[Am] + \frac{k_{-p}[AmH^+]^2}{k_{2p}[Am]^2} \qquad \text{(equation 7.2)}$$

Equation 7.3 only applies if there is >95% conversion of HNBB to dianion.

$$k_{obs} = k_{p}[Am] \qquad \text{(equation 7.3)}$$

Equation 7.3 allows a value for k_p of 1.05±0.05 l mol^{-1} s^{-1} to be calculated from the data in Table 7.5, for the reaction of HNBB with DABCO in DMSO with no added amine salt present.

TABLE 7.5 Kinetic data for the reaction between HNBB (2.5×10^{-6} M) and DABCO in DMSO at 25°C

[DABCO]/M	10^2 k_{obs}/s^{-1}	k_p/l mol^{-1} s^{-1}	OD_{600}[b]
0.01	1.1	1.1	0.0195
0.02	2.1	1.05	0.0195
0.04	4.2	1.05	0.0200
0.06	6.4	1.07	0.0200
0.08	8.2	1.03	0.0200
0.10	10.0	1.00	0.0195

a. $k_p = k_{obs}/[Am]$

b. Optical densities show the reaction has gone to completion at the concentrations studied. The cell pathlength was 2mm.

Data for this reaction in DMSO containing 0.1M DABCO perchlorate and 0.2M DABCO perchlorate are given in Table 7.6.

For these data equation 7.2 applies and plots of $k_{obs}[Am]$ versus $[Am]^2$ give values for k_p of 1.1±0.05 l mol^{-1} s^{-1} and k_{-p}/K_{2p} of (1±0.2) x 10^{-2} l mol^{-1} s^{-1}. The overall equilibrium constant $K_{p,c}$ (= $k_p K_{2p}/k_{-p}$) is defined in equation 7.4. Combination of the rate coefficients

$$K_{p,c} = K_p . K_{2p} = \frac{[7.9][AmH^+]^2}{[7.1][Am]^2} \qquad \text{(equation 7.4)}$$

give a value for $K_{p,c}$ of 110. This value is in agreement with the approximate $K_{p,c}$ value of 200 calculated from the conductance measurements.

It has been found[165] that the presence of oxygen increases the yields of HNS produced from HNBB in the presence of base. Therefore using de-gassed DMSO, preparing the reagents under nitrogen, and by an ingenious modification to the stopped-flow spectrophotometer to allow the kinetics to be measured under nitrogen, a study of the reaction of HNBB with DABCO in DMSO containing 0.1M perchlorate was made. The data are incorporated in Table 7.6. Within experimental error the rate coefficients, found by using equation 7.3, remained the same as those for the reaction studied under air, i.e. k_p 1.1 l mol^{-1} s^{-1}, k_{-2p}/K_{2p} 0.01 l mol^{-1} s^{-1}. However, as DMSO contains oxygen atoms there exists the possibility that these oxygen atoms might participate in enhancing the reaction yield (and perhaps changing the reaction mechanism) instead of dissolved oxygen. To test this possibility the kinetics of the reaction were measured in de-gassed acetonitrile under nitrogen. These data are given in Table 7.7. The value for k_p of 1.1 l mol^{-1} s^{-1} was calculated using equation 7.3 and is, within experimental error, identical to those k_p values measured in DMSO.

TABLE 7.6 Kinetic and equilibrium data for the reaction between HNBB (5×10^{-6} M) and DABCO in DMSO containing DABCO perchlorate at 25°C

[DABCO perchlorate]/M	[DABCO]/M	k_{obs}/s^{-1}	k^{a}_{calc}/s^{-1}
0.01	0.01	0.026	0.021
0.01	0.02	0.028	0.027
0.01	0.04	0.044	0.047
0.01	0.06	0.063	0.068
0.01	0.08	0.076	0.089
0.01	0.10	0.111	0.111
0.02	0.02	0.042	0.042
0.02	0.04	0.063	0.054
0.02	0.06	0.079	0.073
0.02	0.08	0.093	0.093
0.02	0.10	0.118	0.114
0.01[b]	0.01	0.024	0.021
0.01[b]	0.02	0.024	0.027
0.01[b]	0.04	0.044	0.047
0.01[b]	0.06	0.067	0.068
0.01[b]	0.08	0.090	0.089
0.01[b]	0.10	0.111	0.111

a. Calculated using k_p 1.1 l mol^{-1} s^{-1}, k_{-p}/K_{2p} 0.01 l mol^{-1} s^{-1} and equation 7.2.

b. These data were measured under nitrogen.

TABLE 7.7 Kinetic data for the reaction of HNBB (2.5×10^{-6} M) with DABCO in acetonitrile, at 25°C, under nitrogen

[DABCO]/M	$10^2 k_{obs}/s^{-1}$	k_p^a/l mol^{-1}s^{-1}	OD_{600}^b
0.01	1.3		0.0141
0.02	2.5		0.0173
0.04	4.4	1.1	0.0182
0.06	6.6	1.1	0.200
0.08	8.5	1.1	0.200
0.10	10.3	1.0	0.200

a. $k_p = k_{obs}/[Am]$. Only for those concentrations where there is >90% conversion of HNBB to dianion.

b. Measured using a 2mm pathlength cell.

Due to the insolubility of DABCO perchlorate in acetonitrile no rate measurements could be made in acetonitrile containing 0.1M DABCO perchlorate. Comparison of the optical density values for formation of the dianion in acetonitrile with those for formation of the dianion in DMSO show complete conversion to the dianion occurs at lower DABCO concentrations in DMSO than in acetonitrile. This indicates $K_{p,c}$ is slightly smaller in acetonitrile than in DMSO which by inference because the k_p values are identical suggests k_{-p}/K_{2p} is smaller in acetonitrile than DMSO.

7.3.2 Reaction with piperidine

The visible spectra of HNBB (either 1×10^{-5} M or 2×10^{-5} M) with piperidine (0.005 - 0.1M) in DMSO showed that initially a red species, with maxima at 450nm and 516nm, was

formed and this was converted, indicated by good isobestic points, into a blue species with absorption maxima at 620nm (large and broad) and 378nm (small). Figure 7.5 shows an example of these spectra. When piperidine concentration <0.005 M only the blue species is observed. These spectra are interpreted as σ-adduct formation followed by the formation of the dianion. In the presence of 0.1M piperidinium chloride only the spectrum due to the blue species was recorded with the absorption maxima at slightly higher wavelength; 630-640nm (large and broad) and 380nm (small). This time, however, the blue species converts, indicated by reasonably good isobestic points, into another red species with maxima at 444nm and 520nm. This final spectrum suggests that another σ-adduct has been formed. It is believed that amines react with HNBB to produce HNS, and therefore the final σ-adduct probably results from some interaction of HNS with piperidine. The spectra of HNS and piperidine will be reported in Chapter Eight. Although they have similar maxima (λ_{max} 450nm and 520-530nm) to those of the second species they are not identical.

Conductance measurements, (measured when the equilibrium was reached after *ca* two minutes), given in Table 7.8, have shown the stoichiometry of the reaction to form the blue species is 1:2 HNBB: piperidine, therefore indicating that the blue species is the dianion (7.9). As with DABCO it is seen in Figure 7.6 that a plot of excess conductance versus piperidine concentration, for the data in Table 7.8, is curved indicating that the overall equilibrium constant for dianion formation, $K_{p,c}$, is not infinitely high. Again using equation 7.4 and at I = 0.12M a very approximate value for $K_{p,c}$ of 1000 l mol^{-1} can be calculated for the deprotonation of HNBB by piperidine.

FIGURE 7.5 The visible spectrum of 1×10^{-5} M HNBB with 0.1 M piperidine in DMSO after (A) 1 minute; (B) 5 minutes; (C) 11 minutes.

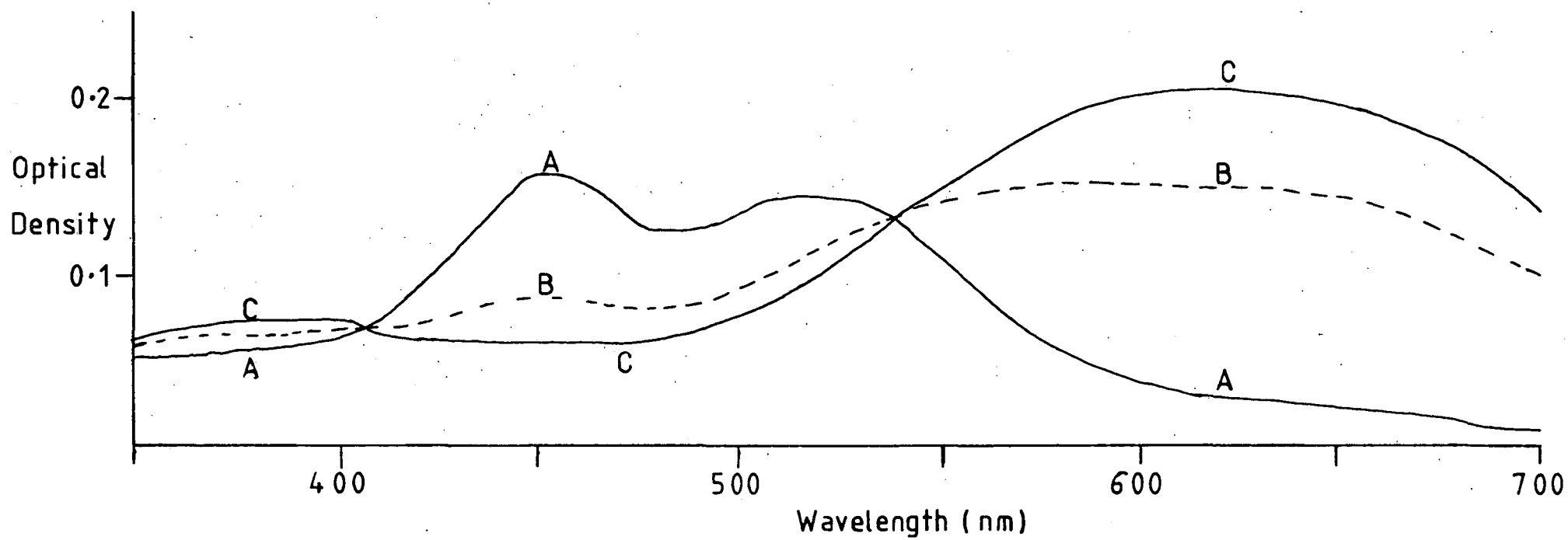

TABLE 7.8 Conductance measurements for the reaction of HNBB (0.04M) with piperidine in DMSO

[piperidine]/M	10^3 Excess Conductance[a]/mho[b]
0.01	0.92
0.02	1.77
0.03	2.61
0.04	3.53
0.05	4.09
0.06	4.88
0.07	5.54
0.08	6.23
0.09	6.39
0.10	6.59
0.12	6.66
0.16	6.69
0.20	6.68
0.25	6.78

a. A plot of Excess Conductance versus [piperidine] is shown in Figure 7.6. This gives for the ratio HNBB : piperidine a value of 1:1.875.

b. mho = ohm^{-1}.

Figure 7.6 A plot of Excess Conductance versus [piperidine] for the data in Table 7.8

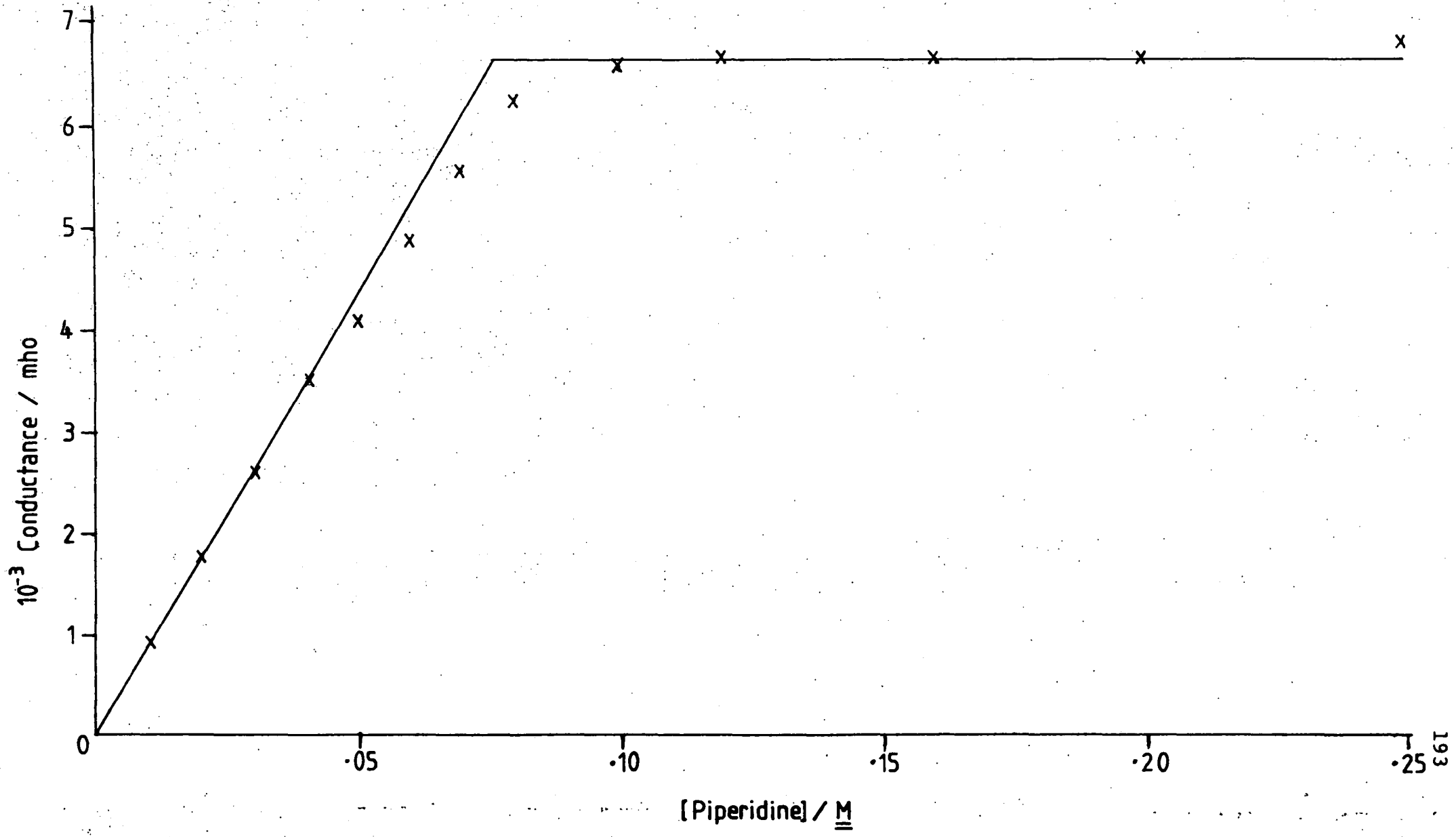

^{1}H n.m.r. measurements made in [$^2H_6$]DMSO confirm the formation of the dianion. Spectra for the addition of one, two, five and ten molecular equivalents of piperidine to HNS dissolved in [$^2H_6$]DMSO were recorded. Once again the band attributable to the ring protons appears at δ8.2. Another band also appeared at δ6.7(2), or δ5.10(5), or δ6.10(10); its slightly different position depending on the molecular equivalents of piperidine, indicated by the bracketed numbers, used. This band may be the result of the nitrogen proton of the piperidinium ion rapidly exchanging with the chain protons of the dianion. Bands attributable to HNS at δ9.2 and δ7.2 were only observed after *ca* thirty-six minutes in solutions containing one molecular equivalent of piperidine. In the other solutions the band at δ8.2 just decayed slowly with time. The formation of the σ-adduct expected before the formation of the dianion, as indicated by the visible spectra, was not observed. At the concentrations used for ^{1}H n.m.r. studies it is probable that the σ-adduct is formed and converts to the dianion very rapidly; too rapidly for its observation by the ^{1}H n.m.r. technique used.

Study of the reaction of HNBB with piperidine in DMSO on the stopped-flow spectrophotometer showed two colour forming processes at 450nm. The first process is interpreted as σ-adduct formation at the 3-position. Evidence that it is the 3-adduct rather than the 1-adduct will be given later.

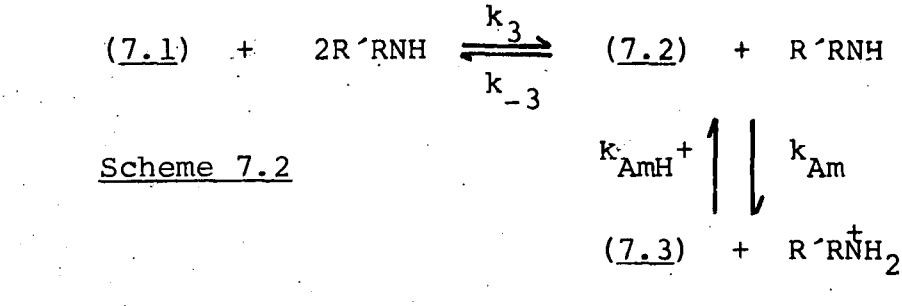

Scheme 7.2

The general rate expression for σ-adduct formation at the 3-position, derived from Scheme 7.2, is equation 7.5. If there is no added piperidinium salt then $[AmH^+]$ is very small (approximately zero) and provided conversion of HNBB to the adduct >95% then equation 7.6 applies.

$$k_{obs} = \frac{k_3 k_{Am} [Am]^2 + k_{-3} k_{AmH^+} [AmH^+]}{k_{-3} + k_{Am} [Am]} \qquad \text{(equation 7.5)}$$

$$k_{obs} = \frac{k_3 k_{Am} [Am]^2}{k_{-3} + k_{Am} [Am]} \qquad \text{(equation 7.6)}$$

As a plot of k_{obs}^{fast} versus piperidine concentration squared, for the data in Table 7.9, is found to be linear then the condition $k_{-3} >> k_{Am}[Am]$ must apply, indicating proton transfer is rate limiting, and equation 7.6 becomes equation 7.7. From the slope of the plot a value for $K_3 k_{Am}$ of

$$k_{obs} = K_3 k_{Am} [Am]^2 \qquad \text{(equation 7.7)}$$

$(1.1 \pm 0.05) \times 10^4$ l^2 mol^{-1} s^{-1} is calculated. The second process observed for piperidinium concentrations >0.01M is believed to be due to the formation of the 1:2 adduct. No rate coefficients can be calculated from k_{obs}^{slow} as the process has not gone to complete conversion at the piperidine concentrations used. However, rough calculations show the reaction appears to second order with respect to amine concentration. Attempts to calculate the equilibrium constants $K_{C,3}$, the overall equilibrium constant for 3-adduct formation, and $K_{D,3}$, overall equilibrium constant for 3-, 3'-adduct formation, from optical density measurements failed due to the rapid decay of the σ-adduct

The reaction of HNBB with piperidine has been studied in DMSO containing 0.1M piperidinium perchlorate, data in Table 7.10, and 0.1M piperidinium chloride, data in Table 7.11. In these

TABLE 7.9 Kinetic data for the reactions of HNBB (5×10^{-6} M) with piperidine in DMSO at 25°C

[piperidine]/M	k_{obs}^{fast}/s^{-1}	k_{calc}^{a}	OD_{fast}^{b}	k_{obs}^{slow}/s^{-1}	OD_{slow}^{b}
0.006	0.38±0.2	0.40	0.0218		
0.008	0.62	0.70	0.0228		
0.01	0.94	1.10	0.0223		
0.02	4.7	4.4	0.0205		0.0250
0.04	19	18	0.0205		0.0297
0.06	41	40	0.0205		0.0306
0.08	70	70	0.0209		0.0334
0.10			0.0227	5.6	0.0343
0.15			0.0214	11.6	0.0353
0.20			0.0214	19.1	0.0372

a. Calculated using K_3k_{Am} 1.1×10^4 l^2 mol^{-2} s^{-1} and equation 7.7.

b. Measured at 450nm using a 2mm pathlength cell.

TABLE 7.10 Kinetic and equilibrium data for the reaction of HNBB (2×10^{-5} M) with piperidine in DMSO containing 0.1 M piperidinium perchlorate at 25°C

[piperidine]/M	k_{obs}/s^{-1}	k^{a}_{calc}/s^{-1}	OD[b](450nm)	$K^{c}_{c,3}$/l mol^{-1}
0.01	42±2	43	0.0044	56
0.02	45	46	0.0086	29
0.03	54	52	0.0177	30
0.04	62	60	0.0273	30
0.05	78	70	0.0343	28
0.06	85	82	0.0429	29

a. Calculated using K_3k_{Am} 1.1×10^4 l^2 mol^{-2} s^{-1}, k_{AmH^+} 410 l mol^{-1} s^{-1} and equation 7.8.

b. Measured using a 2mm pathlength cell.

TABLE 7.11 Kinetic and equilibrium data for the reaction of HNBB (1×10^{-5} M) with piperidine in DMSO containing 0.1 M piperidinium chloride at 25°C

[piperidine]/M	k_{obs}/s^{-1}	k^{a}_{calc}/s^{-1}	OD(450nm)[b]	$K^{c}_{c,3}$/l mol^{-1}
0.01	19±1	20	0.0024	64
0.02	24	23	0.0084	63
0.03	30	29	0.0155	68
0.04	35	37	0.0223	69
0.05	46	47	0.0250	59
0.06	57	59	0.0273	56

a. Calculated using K_3k_{Am} 1.1×10^4 l^2 mol^{-2} s^{-1}, k_{AmH^+} 190 l mol^{-1} s^{-1} and equation 7.8.

b. Calculated using an optical density value for complete conversion of 0.042.

solutions containing piperidinium salts only one colour forming process was observed for the reaction measured at 450nm. If, once again, $k_{-3} >> k_{Am}[Am]$ then equation 7.5 is modified to equation 7.8. A plot of k_{obs} versus $[Am]^2$

$$k_{obs} = K_3 k_{Am}[Am]^2 + k_{AmH^+}[AmH^+] \qquad \text{(equation 7.8)}$$

gives values for $K_3 k_{Am}$ and k_{AmH^+} from the slope and intercept respectively. For the data measured in the presence of perchlorate salt values for $K_3 k_{Am}$ of (1.1±0.1) x 10^4 l^2 mol^{-2} s^{-1} and for k_{AmH^+} of 410±20 l mol^{-1} s^{-1} are obtained. Equation 7.9 defines the overall equilibrium constant $K_{c,3}$. This allows

$$K_{c,3} = \frac{k_3 k_{Am}}{k_{-3} k_{AmH^+}} = \frac{[7.3][AmH^+]}{[7.1][Am]^2} \qquad \text{(equation 7.9)}$$

a value to be calculated for $K_{c,3}$ of 32 l mol^{-1} from the kinetic data which is in good agreement with that calculated from optical density measurements. For the data in the presence of chloride salt values for $K_3 k_{Am}$ of (1.1±0.1) x 10^4 l^2 mol^{-2} s^{-1} and k_{AmH^+} of 190±10 l mol^{-1} are obtained. These rate coefficient give a value for $K_{c,3}$ of 58 l mol^{-1} which is also in good agreement with the $K_{c,3}$ value calculated from optical density measurements.

Data for the deprotonation of HNBB by piperidine to form the dianion in DMSO containing 0.1M piperidinium chloride are given in Table 7.12. As for the deprotonation of HNBB by DABCO Scheme 7.1 applies, but unlike DABCO the deprotonation of HNBB by piperidine is preceded by rapid σ-adduct formation. Again assuming $k_{2p}[Am] >> k_{-p}[AmH^+]$ and taking into account the σ-adduct formation equation 7.2 is modified to become equation 7.10. Equation 7.10 fits the data reasonably well up to a

TABLE 7.12 Rate data for the deprotonation of HNBB by piperidine to form the dianion (7.9) in DMSO containing 0.1M piperidinium chloride at 25°C

[piperidine]/M	$10^2 k_{obs}/s^{-1}$	$10^2 k^a_{calc}$	$10^2 k^b_{calc}$	OD[c](640nm)
0.005	0.97	0.90	0.90	0.035
0.01	1.75	1.70	1.71	0.035
0.02	2.72	2.92	2.98	0.037
0.04	3.98	3.70	4.02	0.037
0.06	4.08	3.50	4.14	0.038
0.08	3.99	3.06	4.06	0.036
0.10	4.24	2.65	4.01	0.037
0.15	4.43	1.92	4.16	0.037
0.20	4.68	1.49	4.61	0.037

a. Calculated from equation 7.10 with k_p 1.8 l mol^{-1} s^{-1}, k_{-p}/K_{2p} 0 l mol^{-1} s^{-1} and $K_{c,3}$ 58 l mol^{-1}.

b. Calculated from equation 7.11 with k_p 1.8 l mol^{-1} s^{-1}, k'_p 0.16 l mol^{-1} s^{-1}, k_{-p}/K_{2p} 0 l mol^{-1} s^{-1} and $K_{c,3}$ 58 l mol^{-1}.

c. Measured using a 2mm pathlength cell and 5 x 10^{-6}M HNBB.

piperidine concentration of 0.04M, using values for k_p of 1.8 l mol^{-1} s^{-1} and k_{-p}/K_{2p} 0 1 mol^{-1} s^{-1}, but then the observed rate constants become progressively larger than the calculated rate constants. If there is an additional reaction pathway involving formation of the dianion *via* proton transfer from the σ-adduct (7.3; R´RN = $C_5H_{10}N$) to give (7.10; R´RN = $C_5H_{10}N$), (see Figure 7.7), then the data can be well fitted by equation 7.11 and the values k_p 1.8 l mol^{-1} s^{-1}, k_{-p}/K_{2p} 0 1 mol^{-1} s^{-1} and k_p' 0.16 l mol^{-1} s^{-1}. k_p' is the rate coefficient for proton transfer from the σ-adduct (7.3; R´RN = $C_5H_{10}N$) to give (7.10; R´RN = $C_5H_{10}N$).

$$k_{obs} = \frac{k_p[Am]}{1+K_{c,3}[Am]^2/[AmH^+]} + \frac{k_{-p}[AmH^+]^2}{K_{2p}[Am]} \qquad \text{(equation 7.10)}$$

$$k_{obs} = \frac{k_p[Am]}{1+K_{c,3}[Am]^2/[AmH^+]} + \frac{k_{-p}[AmH^+]^2}{K_{2p}[Am]} + \frac{k_p'K_{c,3}[Am]^3}{[AmH^+]+K_{c,3}[Am]^2} \text{(equation 7}$$

Scheme 7.3 represents the final interpretation of the data. The equilibria $K_{x,c}$ and $k_{y,c}$ will be explained in the discussion section below as they represent alternative pathways of (7.10) converting into the dianion (7.9).

From conductance measurements a very approximate value for $K_{p,c}$ of 1000 was calculated. Combining this $K_{p,c}$ value and k_p 1.8 l mol^{-1} allows k_{-p}/K_{2p} (= $k_p/K_{p,c}$) as *ca* 1.8 x 10^{-3} to be estimated. This low value is in agreement with the small value of k_{-p}/K_{2p} required by the kinetic data.

Figure 7.7

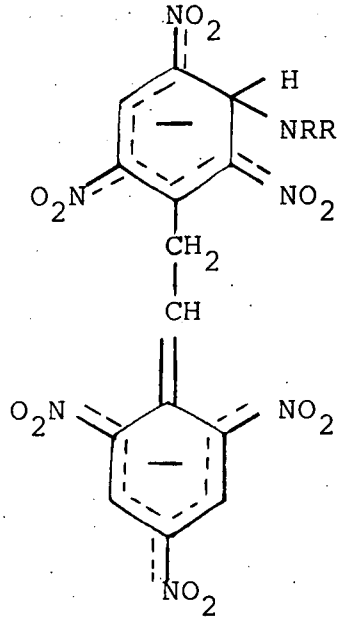

(7.10)

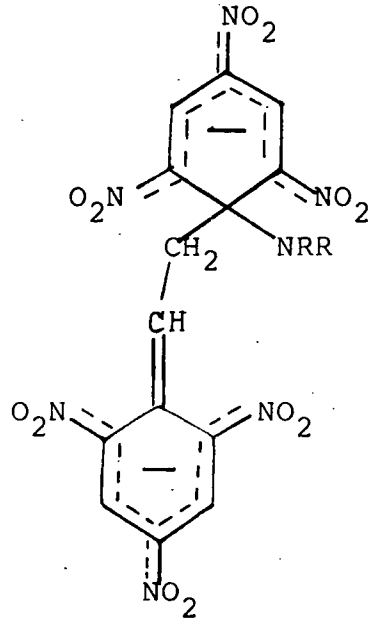

(7.11)

Scheme 7.3

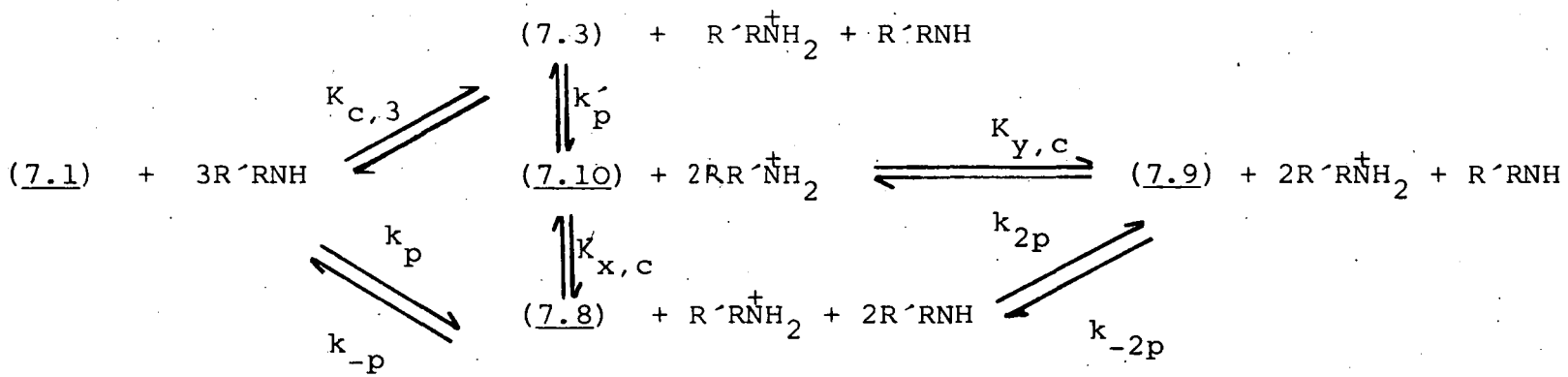
(7.3) + R´RNH2+ + R´RNH
(7.1) + 3R´RNH
Kc,3
k´p
(7.10) + 2R´RNH2+
Ky,c
(7.9) + 2R´RNH2+ + R´RNH
kp
k-p
K´x,c
k2p
k-2p
(7.8) + R´RNH2+ + 2R´RNH

7.3.3 Reaction with pyrrolidine

Pyrrolidine, being a secondary amine, reacts in an analogous way to piperidine with HNBB. The visible spectra of HNBB (2×10^{-5} M) with pyrrolidine (0.001 - 0.5M) therefore are similar; an initial red species being formed, with absorption maxima at 450nm (ε 2.1×10^{-4} l mol^{-1} cm^{-1}) and 530nm at pyrrolidine concentrations 0.1M, followed by the formation of a blue species with maxima at 380 and 630nm. The red species has the spectrum expected for a 1:1 σ-adduct while that of the blue species is expected for a dianion. At high pyrrolidine concentrations the maxima moved to 455 and 520nm and the extinction efficient at 455nm of 4×10^{4} l mol^{-1} cm^{-1} indicates formation of a 1:2 σ-adduct, possibly with the structure (7.7). Even at these higher pyrrolidine concentrations the σ-adduct formation is followed by the formation of the dianion.

Study of the reaction between HNBB and pyrrolidine in DMSO containing 0.1M neutral tetraethylammonium perchlorate salt by stopped-flow spectrophotometry shows two separate colour forming processes. The first process was measured kinetically and is attributed to amine attack at the 3-position; data in Table 7.13. Again this statement will be justified below. Only optical density measurements of the second process were made due to experimental difficulties. It is assumed these measurements are produced by the 1:2 adduct.

The data in Table 7.13 are best interpreted using equation 7.6 but in the more convenient form of equation 7.12. Previously in Chapter Six and for a related system[151] the ratio k_{Am}/k_{-3} has been observed to have a higher value for reaction

TABLE 7.13 Kinetic and equilibrium data for the reaction of HNBB (1×10^{-5} M) with pyrrolidine in DMSO containing 0.1 M tetramethylammonium perchlorate at 25°C

[Pyrrolidine]/M	k_{obs}/s^{-1}	k^{a}_{calc}/s^{-1}	OD^{b}_{fast}	OD^{b}_{slow}
0.008	15.5	15.1	0.0419	0.0516
0.009	18.3	18.5	0.0410	0.0535
0.010	21.2	22	0.0419	0.0545
0.015	43	43	0.0391	0.0575
0.020	70	69	0.0419	0.0645

a. Calculated using K_3k_{Am} 3.1×10^5 $l^2 mol^{-2} s^{-1}$, k_{Am}/k_{-3} 40 l mol^{-1} and equation 7.12.

b. Measured with a 2mm pathlength cell at 450nm.

---

with pyrrolidine than with piperidine. Therefore, the limit $k_{-3} >> k_{Am}[Am]$ which leads to equation 7.7 for the reaction with piperidine does not apply for the reaction with pyrrolidine. The reciprocal of the slope

$$\frac{[Am]}{k_{obs}} = \frac{1}{K_3k_{Am}[Am]} + \frac{1}{k_3} \qquad \text{(equation 7.12)}$$

for a plot of $[Am]/k_{obs}$ versus $1/[Am]$ yields a value for K_3k_{Am} of $(3.1 \pm 0.3) \times 10^5$ l^2 mol^{-2} s^{-1} and a value for k_3 of 7750 ± 1000 l mol^{-1} s^{-1} can be calculated from the reciprocal of the intercept. Combination of these values gives k_{Am}/k_{-3} 40 l mol^{-1}.

In Table 7.14 data for the reaction of HNBB with pyrrolidine in DMSO containing pyrrolidinium perchlorate. Here pyrrolidine

TABLE 7.14 Kinetic and equilibrium data for σ-adduct formation from HNBB (2×10^{-5} M) and pyrrolidine in DMSO at 25°C

[pyrrolidine]/M	[pyrrolidine perchlorate][a]/M	k_{obs}/s^{-1}	k^{b}_{calc}/s^{-1}	OD[c]	$K^{d}_{c,3}$/l mol^{-1}
0.004	0.01			0.009	75
0.006	0.01	39	40	0.017	70
0.008	0.01	45	45	0.027	74
0.010	0.01	50	50	0.032	62
0.012	0.01	57	57	0.043	73
0.015	0.01	67	68	0.053	76
0.01	0	21	22	0.084	-
0.01	0.001	23	25	0.071	55
0.01	0.002	27	28	0.066	73
0.01	0.004	32	33	0.056	80
0.01	0.007	41	41	0.044	77
0.01	0.010	50	50	0.034	68
0.01	0.020	75	78	0.022	71

a. Solutions made up to constant ionic strength, I = 0.1 M, with tetraethylammonium perchlorate.

b. Calculated from equation 7.13 with K_3k_{Am} 3.1×10^5 l^2 mol^{-2} s^{-1}, k_{Am}/k_{-3} 40 l mol^{-1} and k_{AmH^+} 3900 l mol^{-1} s^{-1}.

c. Measured at completion of the fast colour forming reaction at 450nm with a 2mm pathlength cell.

d. Calculated from $OD.[AmH^+]/(0.084-OD)[Am]^2$.

concentrations were limited so that only the first process, formation of the 3-adduct, was observed. The data are best fitted using equation 7.13 with the values K_3k_{Am} 3.1 x 10^5 l^2 mol^{-2} s^{-1}, k_{AmH+} 3900 l $mol^{-1}s^{-1}$ and k_{Am}/k_{-3} 40 l mol^{-1}.

$$k_{obs} = \frac{K_3k_{Am}[Am]^2 + k_{AmH^+}[AmH^+]}{1 + k_{Am}[Am]/k_{-3}} \qquad \text{(equation 7.13)}$$

A value for $K_{c,3}$ of 79 l mol^{-1} using equation 7.9 is calculated which is in good agreement with that obtained from the optical densities.

Data for formation of the blue dianion are in Table 7.15. With pyrrolidine concentration <0.08M a good fit is obtained using equation 7.10 with values for k_p of 5.5 l mol^{-1} s^{-1} and k_{-p}/K_{2p} of 0.007 l $mol^{-1}s^{-1}$. Combination of these quantities gives a value for $K_{p,c}$ (= k_pK_{2p}/k_{-p}), the overall equilibrium constant for formation of the dianion, of 800. As observed in the similar reaction with piperidine, the rate data at higher amine concentrations require the use of equation 7.11 which includes a term involving k'_p, (k'_p 0.4 l mol^{-1} s^{-1}). Hence, with pyrrolidine there is also evidence for the formation of the dianion by a pathway initially involving proton transfer to amine from the adduct (7.3; R'RN = C_4H_8N), as shown in Scheme 7.3.

TABLE 7.15 Rate data for formation of the blue dianion from HNBB and pyrrolidine in DMSO containing 0.1M pyrrolidinium perchlorate at 25°C

[pyrrolidine]/M	$10^2 k_{obs}/s^{-1}$	$10^2 k^a_{calc}/s^{-1}$	$10^2 k^b_{calc}/s^{-1}$	OD[c](640nm)
0.005	4.0	4.1	4.1	0.024
0.008	4.6	5.1	5.1	0.032
0.01	6.1	5.8	5.8	0.032
0.02	8.5	8.7	9.0	0.036
0.04	10.2	10.2	11.0	0.038
0.06	9.2	9.1	10.8	0.039
0.08	10.7	7.7	10.3	0.033
0.10	10.0	6.6	10.1	0.037
0.15	11.5	4.7	10.3	0.036
0.20	11.7	3.5	11.3	0.036

a. Calculated from equation 7.10 with k_p 5.5 l mol^{-1} s^{-1}, k_{-p}/K_{2p} 0.007 l mol^{-1} s^{-1} and $K_{c,3}$ 75 l mol^{-1}.

b. Calculated from equation 7.11 with k_p 5.5 l mol^{-1} s^{-1}, k_{-p}/K_{2p} 0.007 l mol^{-1} s^{-1}, k_p' 0.4 l mol^{-1} s^{-1} and $K_{c,3}$ 75 l mol^{-1}.

c. For 5×10^{-6}M HNBB measured with a 2mm pathlength cell.

7.3.4 Reaction with n-butylamine

The reaction of HNBB with n-butylamine in DMSO provides evidence for all the processes shown in Scheme 7.4. Visible spectra recorded with a conventional spectrophotometer showed maxima at 460nm and 520-530nm typical of 1:1 σ-adducts. Conversion into the dianion was slow even in solutions containing n-butylammonium salts. The blue dianion converts even more slowly (good isobestic points) into a second red species. This species is observed in DMSO containing 0.1M n-butylammonium chloride and 0.1M n-butylamine and has maxima at 456nm and 510nm. These maxima are similar to those produced when HNS reacts with n-butylamine (spectra reported in next chapter). It is believed HNBB is converted to HNS by amines although it has only been shown for the reaction of HNBB with DABCO. Therefore this second species may be the σ-adduct formed between HNS, or some derivative of HNS, with n-butylamine.

A ^{1}H n.m.r. spectrum, recorded about one minute after mixing in [$^{2}H_6$]DMSO, showed bands of equal intensity at δ8.38 and δ2.33 attributed respectively to the ring and methylene protons of the 1-, 1′-di-adduct (7.6; R′RN = $CH_2CH_2CH_2CH_2NH$). Then conversion to the dianion followed with a band at δ8.2, as observed previously for DABCO and piperidine.

The σ-adducts were sufficiently stable to allow calculation of $K_{C,1}$ and $K_{D,1}$ from the optical density data, which are defined in equations 7.14 and 7.15 respectively, and with an extinction coefficient for complete formation of the di-adduct at 460nm of *ca* 6 x 10^4 l mol^{-1} cm^{-1}. Optical density measurements have been measured in DMSO containing 0.1M n-butylammonium perchlorate, data reported in Table 7.16; 0.02M n-butylammonium

Scheme 7.4

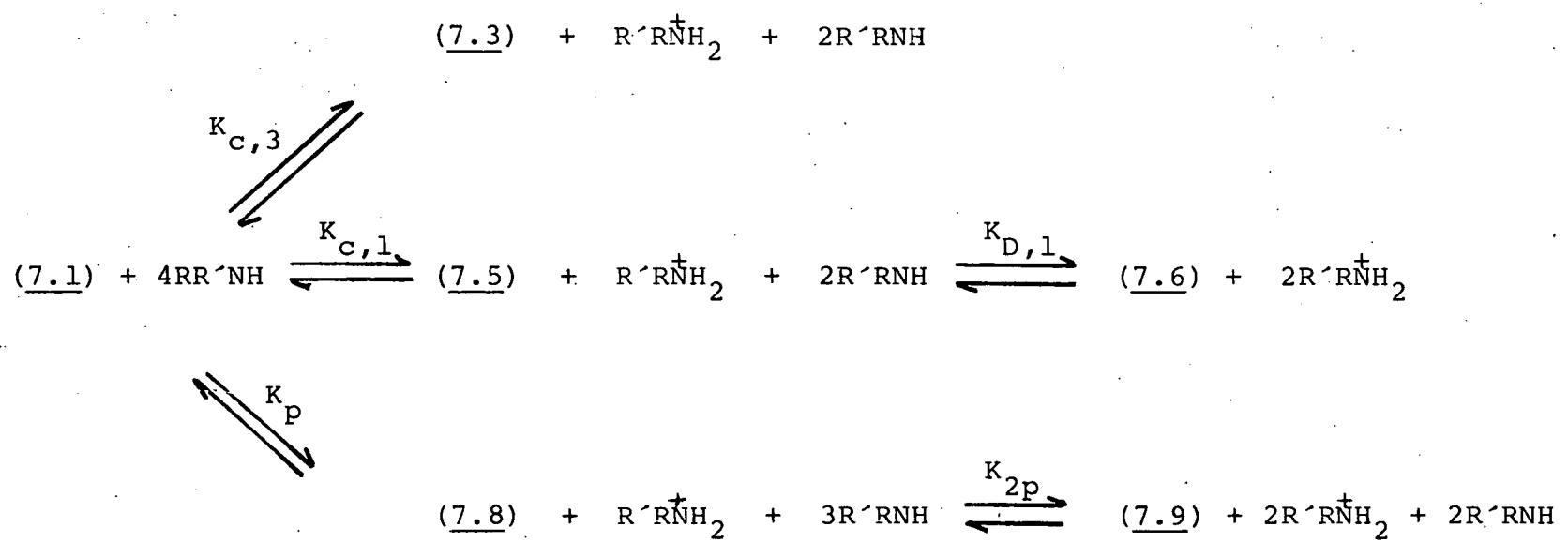
(7.3) + R´RNH2+ + 2R´RNH
Kc,3
(7.1) + 4RR´NH
Kc,1
(7.5) + R´RNH2+ + 2R´RNH
KD,1
(7.6) + 2R´RNH2+
Kp
(7.8) + R´RNH2+ + 3R´RNH
K2p
(7.9) + 2R´RNH2+ + 2R´RNH

chloride and 0.08$\underline{M}$ tetraethylammonium perchlorate (Ionic strength I = 0.1$\underline{M}$), data reported in Table 7.17; 0.1$\underline{M}$n-butylammonium chloride, data reported in Table 7.18. The values of the equilibrium constants

$$K_{c,1} = \frac{[7.3][AmH^+]}{[7.1][Am]^2} \qquad \text{(equation 7.14)}$$

$$K_{D,1} = \frac{[7.6][AmH^+]}{[7.1][Am]^2} \qquad \text{(equation 7.15)}$$

are calculated to be: in DMSO containing 0.1$\underline{M}$ n-butylammonium perchlorate $K_{c,1}$ 1150 l mol^{-1}, $K_{D,1}$ 17 l mol^{-1}; in DMSO containing 0.02$\underline{M}$ n-butylammonium chloride (I = 0.1$\underline{M}$ made up using tetraethylammonium perchlorate) $K_{c,1}$ 1500 l mol^{-1}, $K_{D,1}$ 18 l mol^{-1}; in DMSO containing 0.1$\underline{M}$ n-butylammonium chloride $K_{c,1}$ 2400 l mol^{-1}, $K_{D,1}$ 20 l mol^{-1}. As found in related work[86,151] and the previous chapter specific effects due to the chloride ions are present.

Kinetic measurements were limited to low n-butylamine concentrations where only the adducts of 1:1 stoichiometry were present. Two rapid well separated processes were observed when the reaction of HNBB and n-butylamine was examined by stopped-flow spectrophotometry. These processes are taken to be the formation of the 3-adduct, (7.3; R´RN = $CH_3CH_2CH_2CH_2NH$) followed by formation of the 1-adduct, (7.5; R´RN = $CH_3CH_2CH_2CH_2N$ The rate data in Table 7.19 for the faster process were obtained in solutions without added n-butylammonium salt. Scheme 7.2 represents the faster process and equation 7.6 is the relevant rate expression. However, the data in Table 7.19 corresponds:

$$k_{obs} = k_3[Am] \qquad \text{(equation 7.16)}$$

to equation 7.16, a limiting form of equation 7.6 when

TABLE 7.16 Equilibrium data for σ-adduct formation from HNBB (2×10^{-5} M) and n-butylamine in DMSO containing 0.1 M n-butylammonium perchlorate at 25°C

[n-butylamine]/M	OD(460nm)	OD(calc)
0.00097	0.010	0.007
0.00192	0.026	0.024
0.00395	0.100	0.090
0.00590	0.164	0.172
0.00799	0.263	0.248
0.00980	0.334	0.323
0.0194	0.515	0.519
0.0381	0.628	0.680
0.0594	0.813	0.806
0.0792	0.891	0.901
0.0990	0.954	0.964
0.198	1.13	1.11
0.396	1.16	1.17
0.594	1.17	1.18
1.16	1.19	1.19

a. Calculated with values of $K_{c,1}$ 1150 l mol^{-1}, $K_{D,1}$ 17 l mol^{-1} and with optical densities for complete conversion to the 1:1 adduct of 0.595 and to the 1:2 adduct of 1.19.

TABLE 7.17 Equilibrium data for σ-adduct formation from HNBB (2×10^{-5} M) and n-butylamine in DMSO containing 0.02 M n-butylammonium chloride and 0.08 M tetraethylammonium perchlorate at 25°C

[n-butylamine]/M	OD(460nm)	OD[a](Calc)
0.00373	0.429	0.419
0.00595	0.540	0.541
0.00791	0.618	0.602
0.00987	0.667	0.652
0.0147	0.768	0.752
0.0196	0.841	0.835
0.0291	0.960	0.959
0.0384	1.01	1.03
0.0598	1.12	1.12
0.0797	1.15	1.15
0.0997	1.16	1.17
0.199	1.20	1.19
0.399	1.18	1.20
0.598	1.20	1.20

a. Calculated with values of $K_{c,1}$ 1500 l mol^{-1}, $K_{D,1}$ 18 l mol^{-1} and with optical densities for complete conversion to the 1:1 adduct of 0.60 and to the 1:2 adduct of 1.20.

TABLE 7.18 Equilibrium data for σ-adduct formation from HNBB (2×10^{-5} M) and n-butylamine in DMSO containing 0.1 M n-butylammonium at 25°C

[n-butylamine]/M	OD(460nm)	OD[a](calc)
0.00098	0.018	0.013
0.00193	0.055	0.048
0.00393	0.158	0.158
0.00595	0.265	0.269
0.00791	0.340	0.354
0.00986	0.418	0.416
0.0147	0.510	0.510
0.0195	0.560	0.564
0.0290	0.635	0.636
0.0383	0.686	0.696
0.0598	0.837	0.816
0.0797	0.930	0.930
0.0996	1.00	0.965
0.199	1.08	1.10
0.398	1.14	1.14
0.598	1.14	1.15
0.797	1.16	1.16

a. Calculated with values of $K_{c,1}$ 2400 l mol^{-1}, $K_{D,1}$ 20 l mol^{-1} and with optical densities for complete conversion to the 1:1 adduct of 0.58 and to the 1:2 adduct of 1.16.

TABLE 7.19 Rate data for formation of the 3-adduct (7.3; R′RN = $CH_3CH_2CH_2CH_2NH$) from HNBB(5×10^{-6} M) and n-butylamine in DMSO at 25°C

[n-butylamine]/M	k_{obs}/s^{-1}	k_3^a/l $mol^{-1}s^{-1}$	OD(460nm)
0.1	17.4	1740	0.019
0.015	27	1800	0.019
0.02	31	1550	0.019
0.025	37	1480	0.020
0.03	69	1720	0.020

a. $k_3 = k_{obs}/[Am]$

$k_{Am}[Am] >> k_{-3}$. Using equation 7.16 a value for k_3 of 1700± 200 l $mol^{-1}s^{-1}$.

In the presence of n-butylammonium salts the formation of the 3-adduct is too fast for measurement by stopped-flow spectrophotometry but optical density measurements are possible. The formation of the 1-adduct is shown in Scheme 7. 5. Treatment of (7.4), the zwitterionic intermediate, as a steady-state intermediate leads to the kinetic expression of equation 7.17.

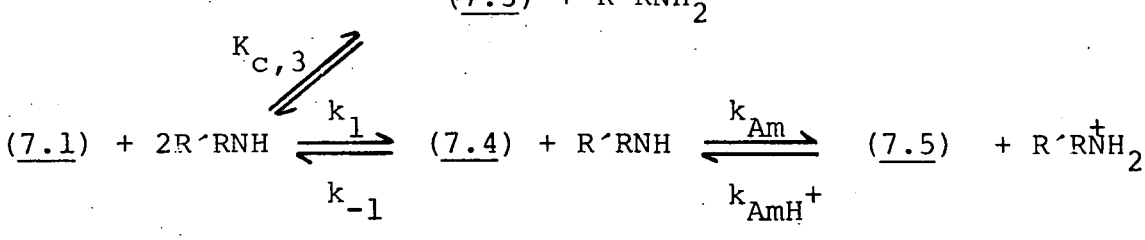

Scheme 7.5

If $k_{Am}[Am] >> k_{-1}$ this reduces to equation 7.18.

$$k_{obs} = \frac{k_1 k_{Am}[Am]^2}{(k_{-1}+k_{Am}[Am])(1+K_{c,3}[Am]^2/[AmH^+])} + \frac{k_{-1}k_{AmH^+}[AmH^+]}{k_{-1}+k_{Am}[Am]}$$

(equation 7.17)

$$k_{obs} = \frac{k_1[Am]}{1+K_{c,3}[Am]^2/[AmH^+]} + \frac{k_{-1}k_{AmH^+}[AmH^+]}{k_{Am}[Am]}$$

(equation 7.18)

The kinetic and equilibrium data reported in Table 7.20 were measured in DMSO containing 0.1M n-butylammonium perchlorate From the optical density for the formation of the 3-adduct a value for $K_{c,3}$ of 25±5 l mol^{-1} is calculated. Using this quantity in equation 7.18 the following values of k_1 150 l mol^{-1} s^{-1} and $k_{-1}k_{AmH^+}/k_{Am}$ 0.14 s^{-1} fit the kinetic data. Combination of the rate coefficients give a value for $K_{c,1}$ of 1100 l mol^{-1}, which is in good agreement with that obtained from the optical density measurements in Table 7.16. The data given here require that $k_{Am}/k_{-1} >> 5000$ l mol^{-1}.

The same procedure is followed for the data reported in Table 7.21 measured in DMSO containing 0.02M n-butylammonium chloride and 0.08M tetraethylammonium perchlorate. Here values for $K_{c,3}$ 31±5 l mol^{-1}, k_1 150 l mol^{-1} s^{-1} and $k_{-1}k_{AmH^+}/k_{Am}$ 0.10 s^{-1} fit the data f amine concentrations ≤ 0.4M. $K_{c,1}$ calculated from the rate coefficients gives a value of 1500 l mol^{-1}, which is in good agreement with that obtained from optical density measurements in Table 7.17. The poor agreement between measured and calculated values for amine concentrations > 0.04M may be due to appreciable formation of the 1',1'-adduct at these concentrations. For the reaction in DMSO containing 0.1M n-butylammonium chloride equation 7.18 is again used to fit the data; data given in Table 7.22. However, this data does not include optical density measurements for the formation of the 3-adduct. It has been

TABLE 7.20 Kinetic and equilibrium data for σ-adduct formation from HNBB (1×10^{-5} M) and n-butylamine in DMSO containing 0.1 M n-butylammonium perchlorate at 25°C

[n-butylamine]/M	OD[a](460nm)	$K^{b}_{c,3}$/l mol^{-1}	k_{obs}/s^{-1}	k^{c}_{calc}	OD[d](460nm)
0.002			6.7	7.3	0.0024
0.004			4.2	4.1	0.0071
0.006			3.2	3.2	0.0146
0.008			3.0	3.0	0.0205
0.010			2.9	2.9	0.0255
0.015			3.1	3.1	0.0353
0.020	0.0042	29	3.5	3.4	0.0414
0.030	0.0081	28			0.0526
0.040	0.0110	23	4.8	4.7	0.0575
0.060	0.0173	21			0.0716
0.080	0.0232	22			0.0800

a. At completion of the rapid colour forming reaction. The value for complete conversion to 3-adduct is 0.040 as determined in a solution containing no added n-butylammonium perchlorate.

b. Calculated using $OD(460)[AmH^+]/[0.040-OD(460)][Am]^2$.

c. Calculated from equation 7.18 with k_1 150 l mol^{-1} s^{-1}, $k_{-1}k_{AmH^+}/k_{Am}$ 0.14 s^{-1} and $K_{c,3}$ 25 l mol^{-1}.

d. At completion of the slower colour forming reaction giving the l-adduct.

TABLE 7.21 Kinetic and equilibrium data for σ-adduct formation from HNBB (5×10^{-6} M) and n-butylamine in DMSO containing 0.2 M n-butylammonium chloride and 0.08 M tetraethylammonium perchlorate at 25°C

[n-butylamine]/M	OD[a](460nm)	$K^{b}_{c,3}$/l mol^{-1}	k_{obs}/s^{-1}	k^{c}_{calc}	OD[d](460nm)
0.002			1.39	1.30	0.0040
0.003			1.06	1.11	0.0092
0.005			1.08	1.12	0.0155
0.0075			1.27	1.30	0.0205
0.01	0.0026	27	1.48	1.50	0.0237
0.015	0.0067	29	1.75	1.80	0.0297
0.02	0.0088	33	1.79	1.95	0.0343
0.04	0.0159	33	1.98	1.77	0.0458
0.07	0.0186	22	2.60	1.25	0.0535
0.10	0.0214	-	3.07	0.93	0.0565

a. At completion of the rapid colour forming reaction. A value for complete conversion to the 3-adduct is 0.022 as determined in solution containing no added n-butylammonium perchlorate.

b. Calculated using $OD(460)[AmH^+]/[0.022-OD(460)][Am]^2$.

c. Calculated from equation 7.18 with k_1 150 l mol^{-1} s^{-1}, $k_{-1}k_{AmH^+}/k_{Am}$ 0.10 s^{-1} and $K_{c,3}$ 31 l mol^{-1}.

d. At completion of the slower colour forming process, giving the 1-adduct.

TABLE 7.22 Kinetic data for σ-adduct formation from HNBB (1×10^{-5} M) and n-butylamine in DMSO containing 0.1 M n-butylammonium chloride at 25°C

[n-butylamine]/M	k_{obs}/s^{-1}	k^{a}_{calc}/s^{-1}
0.002	3.1	3.3
0.003	2.5	2.5
0.005	2.1	2.0
0.0075	2.0	1.9
0.010	2.1	2.0
0.015	2.5	2.4
0.020	3.0	2.8
0.040	3.5	3.5

a. Calculated from equation 7.18 with k_1 150 l mol^{-1} s^{-1}, k_{-1} k_{AmH^+}/k_{Am} 0.06 s^{-1} and $K_{c,3}$ 50 l mol^{-1}.

---

shown previously in Chapter Six and elsewhere[151] that equilibrium constants of 1:1 adducts measured in solutions containing substituted ammonium chloride ions are double those measured in solutions containing substituted ammonium perchlorate ions. This allows a value for $K_{c,3}$ of 50 l mol^{-1} to be estimated, (i.e. twice the value of $K_{c,3}$ measured in solutions containing n-butylammonium perchlorate). Using the values $K_{c,3}$ 50 l mol^{-1}, k_1 150 l mol^{-1} s^{-1} and $k_{-1}k_{AmH^+}/k_{Am}$ 0.06 s^{-1} with equation 7.18 the data in Table 7.22 are well fitted. Again using the rate coefficients a value for $K_{c,1}$ of 2500 l mol^{-1} is calculated, in good agreement with the $K_{c,1}$ value calculated from the optical density measurements in Table 7.18.

Rate data for formation of the dianion are reported in Table 7.23 and were measured at 640nm using a conventional spectrophotometer. The dianion is formed as shown in Scheme 7.1. From this scheme equation 7.19 is obtained if it is assumed $k_{2p}[Am] >> k_{-p}[AmH^+]$ and the prior formation of the 1-adduct is taken into account. Equation 7.19 corresponds

$$k_{obs} = \frac{k_p[Am]}{1+K_{c,3}[Am]^2/[AmH^+]} + \frac{k_{-p}[AmH^+]^2}{K_{2p}[Am]} \qquad \text{(equation 7.19)}$$

well with the data for n-butylamine concentrations $\leq$ 0.1M. However, equation 7.19 only allows for the parent to react with the amine to give the dianion. If in addition there is a pathway for deprotonation of the σ-adduct then equation 7.20 would be predicted to fit the data. The most probable σ-adduct to transfer a proton would be (7.5; $R'RN=CH_3CH_2CH_2CH_2NH$) to give (7.11;$R'RN=CH_3CH_2CH_2CH_2NH$) shown in Figure 7.7. Scheme 7.6 depicts the processes involved in the formation of the dianion. The equilibria designated $K_{x,c}$ and $K_{y,c}$ will be explained below in the discussion section. They are the two possible pathways for (7.11) to convert into the dianion. The values obtained are k_p 0.8 l $mol^{-1}s^{-1}$ k_{-p}/K_{2p} 1 x 10^{-4} l mol^{-1}

$$k_{obs} = \frac{k_p[Am]+k'_pK_{c,1}[Am]^3/[AmH^+]}{1 + K_{c,1}[Am]^2/[AmH^+]} + \frac{k_{-p}[AmH^+]^2}{K_{2p}[Am]} \qquad \text{(equation 7.2}$$

s^{-1} and k'_p 0.03 l mol^{-1} s^{-1}. Combination of the former two quantities gives a value for $K_{p,c}$ (K_p. K_{2p}) of 8000.

TABLE 7.23 Rate data for formation of the blue dianion from HNBB (2×10^{-5} M) and n-butylamine in DMSO containing (0.1M) n-butylammonium chloride at 25°C

[n-butylamine]/M	$10^3 k^a_{obs}/s^{-1}$	$10^3 k^b_{calc}/s^{-1}$	$10^3 k^c_{calc}/s^{-1}$
0.001	1.9	1.8	1.8
0.002	2.0	2.0	2.0
0.003	2.4	2.3	2.3
0.004	2.6	2.6	2.6
0.006	2.7	2.7	2.8
0.008	2.9	2.6	2.7
0.010	2.9	2.4	2.6
0.015	2.2	1.8	2.3
0.020	2.0	1.4	2.1
0.040	2.0	0.8	2.0

a. Measured at 640nm with a conventional spectrophotometer.

b. Calculated from equation 7.19 with k_p 0.8 l mol^{-1} s^{-1}, k_{-p}/K_{2p} (1×10^{-4} l mol^{-1} s^{-1}) and $K_{c,1}$ 2500 l mol^{-1}.

c. Calculated from equation 7.20 with k_p 0.8 l mol^{-1} s^{-1}, k_{-p}/k_{2p} 1×10^{-4} l mol^{-1} s^{-1}, k'_p 0.03 l mol^{-1} s^{-1} and $K_{c,1}$ 2500 l mol^{-1}.

Scheme 7.6

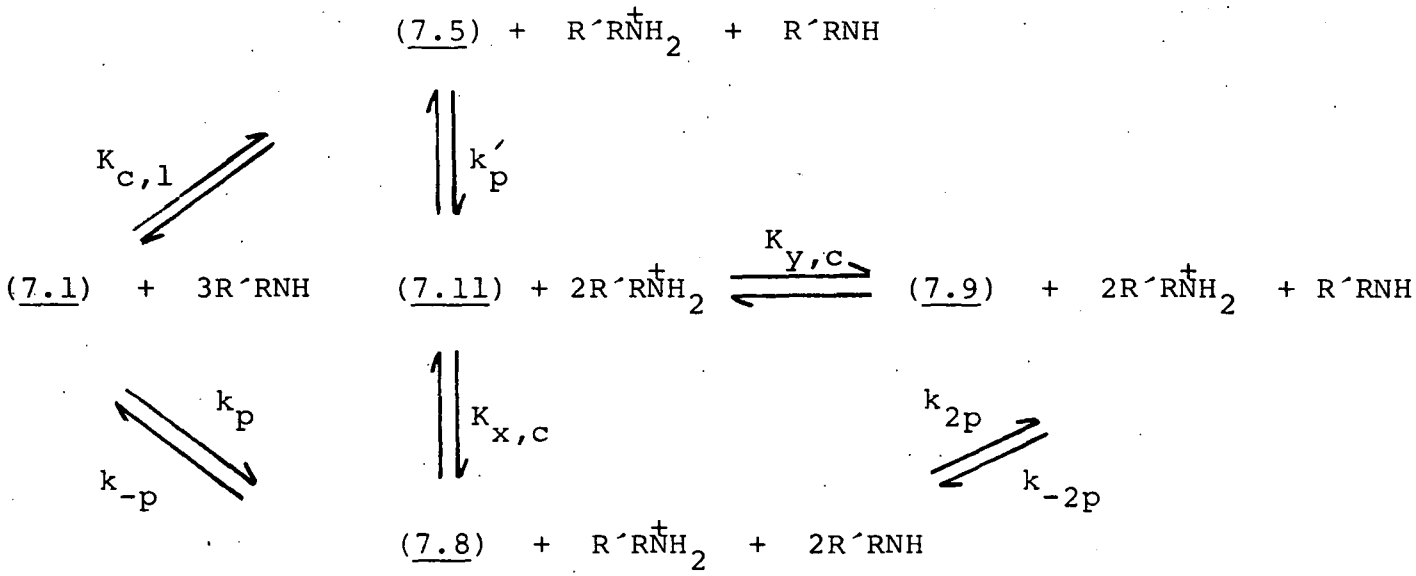
(7.5) + R´RNH$_2^+$ + R´RNH
$K_{c,1}$
k'_p
(7.1) + 3R´RNH
(7.11) + 2R´RNH$_2^+$
$K_{y,c}$
(7.9) + 2R´RNH$_2^+$ + R´RNH
k_p
k_{-p}
$K_{x,c}$
k_{2p}
k_{-2p}
(7.8) + R´RNH$_2^+$ + 2R´RNH

7.3.5 Reaction with benzylamine

Benzylamine reacts with HNBB in the same way as n-butylamine. Visible spectra of HNBB (1×10^{-5}M) with benzylamine (0.001 - 0.1M) in DMSO show a red species with two maxima typical of a 1:1 σ-adduct. At a benzylamine concentration of 0.001M the maxima are at 454nm and 530-540nm, and with increasing benzylamine concentrations shift towards each other until at a benzylamine concentration of 0.1M the maxima are at 462nm and 520nm. In solutions containing added benzylammonium salts the red species is converted, indicated by good isobestic points, into a blue species giving the expected maxima for the dianion at 620nm (broad) and at 380nm (small). Once again conversion of the blue dianion to a second red species is observed; maxima at 460nm and 520-530nm are typical of 1:1 σ-adduct formation. Again the maxima are at similar wavelengths to those observed for σ-adduct formation between HNS and benzylamine (see Chapter Eight). This suggests that HNBB produces HNS from its reaction with benzylamine which then reacts with the excess benzylamine present.

Conductance measurements on solutions of HNBB and benzylamine in DMSO have been made. These measurements are reported in Table 7.24. It took about one hour (at low benzylamine concentration) to twenty minutes (at high benzylamine concentration) for the equilibrium to be reached. This indicates that the stability of the σ-adduct is high, and therefore allows a greater possibility for a side reaction, *e.g.* decomposition reactions of the substrate, which could lead to the conductance measurements here having larger errors than the conductance measurements reported earlier in this chapter.

TABLE 7.24 Conductance measurements for the reaction of HNBB (0.04M) and benzylamine in DMSO.

[Benzylamine]/M	10^3 Excess Conductance[a]/mho[b]
0.01	0.86
0.02	1.62
0.03	2.37
0.04	3.12
0.05	3.60
0.06	4.22
0.07	4.71
0.08	5.10
0.09	5.26
0.10	5.47
0.12	5.56
0.16	5.68
0.20	5.76[f]
0.25	5.77

a. A plot of Excess Conductance versus benzylamine concentration is shown in Figure 7.8. This gives the ratio HNBB: amine a value of 1:1.875.

However, dianion formation is still indicated by two amine molecules reacting per HNBB molecule to produce the blue species. The conductance data are shown plotted against benzylamine concentration in Figure 7.8 and there is curvature in the plot indicating the equilibrium constant $K_{p,c}$ is not infinitely high. A calculation (at I = 0.13M) using equation 7.4 produces an approximate value for $K_{p,c}$ of *ca* 200. A more accurate value for $K_{p,c}$ will be given with the kinetic data for dianion formation.

Figure 7.8 A plot of excess conductance versus [benzylamine] for the data given in Table 7.24

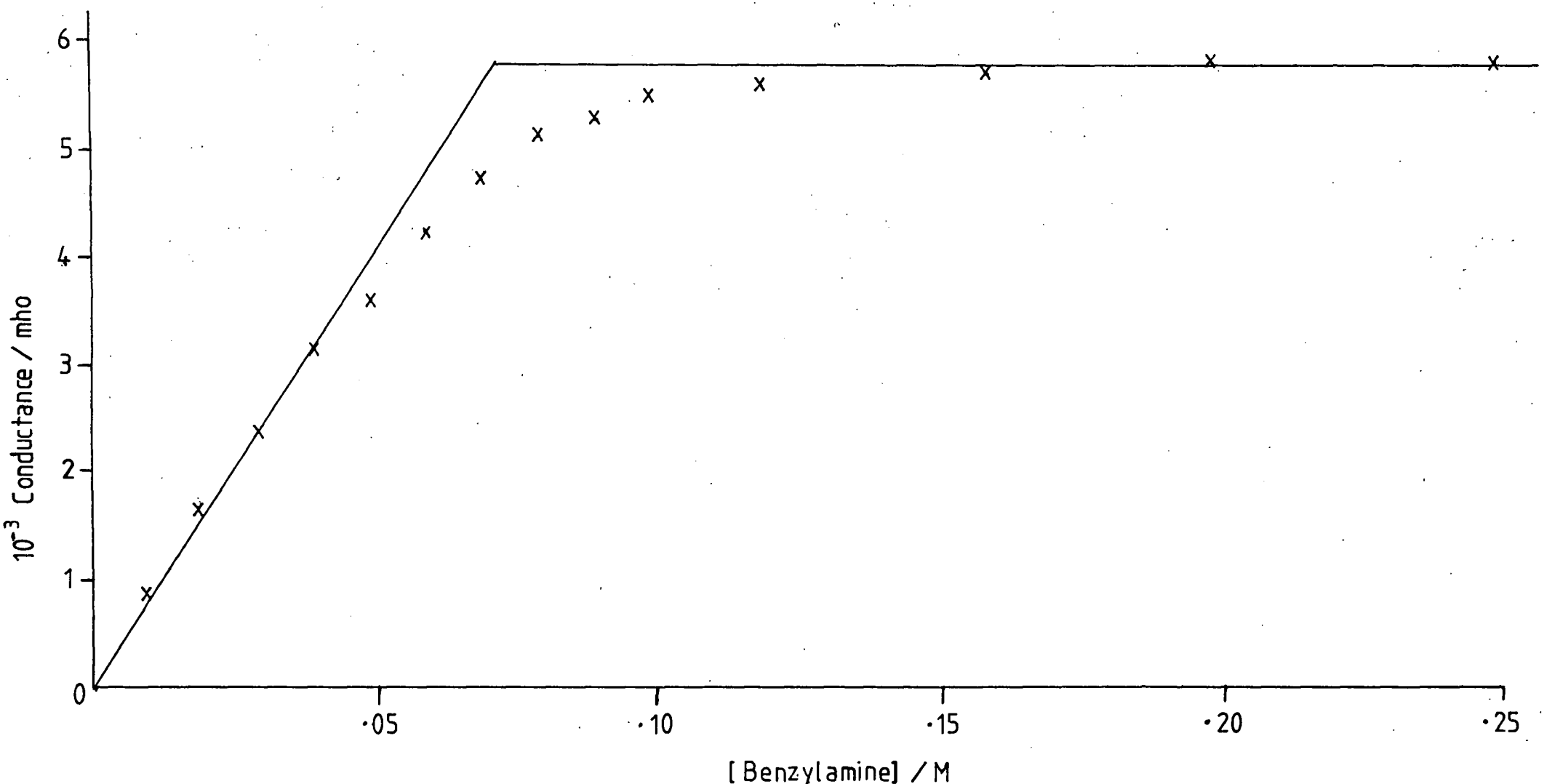

Optical density data, presented in Table 7.25, were measured at the completion of the σ-adduct forming reactions in the presence of 0.1M n-butylammonium chloride. Values for $K_{c,1}$ 140 l mol^{-1} and $K_{D,1}$ of 1.1 l mol^{-1} were obtained by fitting the data to equations 7.14 and 7.15.

TABLE 7.25 Equilibrium data for σ-adduct formation from HNBB (2×10^{-5}M) and benzylamine in DMSO containing 0.1M benzylammonium chloride at 25°C.

[benzylamine]/M	OD(460nm)	OD[a](calc)
0.00196	0.006	0.003
0.00399	0.017	0.013
0.00597	0.029	0.027
0.00795	0.051	0.046
0.00992	0.066	0.068
0.0148	0.137	0.134
0.0196	0.182	0.200
0.0292	0.303	0.314
0.0385	0.372	0.393
0.0607	0.491	0.498
0.0890	0.549	0.551
0.101	0.595	0.589
0.202	0.720	0.737
0.404	0.920	0.934
0.606	1.06	1.02
0.809	1.08	1.07

a. Calculated with values of $K_{c,1}$ 140 l mol^{-1}; $K_{D,1}$ 1.1 l mol^{-1} and with optical densities for complete conversion to the 1:1 adduct of 0.57 and to the 1:2 adduct of 1.14.

Kinetic studies were again limited to the formation of adducts of 1:1 stoichiometry. In DMSO containing no added benzylammonium salt a value for k_3 of 550 l $mol^{-1}s^{-1}$ was obtained using equation 7.16 for the data in Table 7.26. Data obtained in the presence of 0.1M benzylammonium perchlorate are in Table 7.27. From the optical density measurements for completion of the faster process, formation of the 3-adduct, a value for $K_{c,3}$ of 1.25 l mol^{-1} was calculated. The kinetic data for the slower process were interpreted using Scheme 7.5 and equation 7.18. Values of k_1 60 l mol^{-1} s^{-1} and k_{-1} k_{AmH^+}/k_{Am} 0.8 s^{-1} were calculated, which combined gives $K_{c,1}$ 75 l mol^{-1}. The same procedures were used for the data in Table 7.28, obtained in the presence of 0.1M benzylammonium chloride. Here values of k_1 60 l mol^{-1} s^{-1}, $k_{-1}k_{AmH^+}/k_{Am}$ 0.4 s^{-1}, $K_{c,3}$ 2.2 l mol^{-1} and $K_{c,1}$ 150 l mol^{-1} were calculated.

TABLE 7.26 Rate data for formation of the 3-adduct from HNBB (5×10^{-6}M) and benzylamine in DMSO at 25°C

[benzylamine]/M	k_{obs}/s^{-1}	k_3^a/l $mol^{-1}s^{-1}$	OD(460nm)
0.04	20.4	510	0.017
0.06	32	540	0.021
0.07	37	530	0.021
0.08	42	530	0.022
0.09	51	570	0.022
0.10	57	570	0.021

a. $k_3 = k_{obs}/[Am]$

TABLE 7.27 Kinetic and equilibrium data for σ-adduct formation from HNBB (1×10^{-5} M) and benzylamine in DMSO containing 0.1M benzylammonium perchlorate at 25°C

[benzylamine]/M	OD[a](460nm)	$K^{b}_{c,3}$/l mol^{-1}	k_{obs}/s^{-1}	k^{c}_{calc}	OD[d](460nm)
0.006			13.6	13.7	0.0011
0.008			10.5	10.5	0.0026
0.010			8.8	8.6	0.0031
0.020			5.9	5.2	0.0102
0.040			4.9	4.4	0.0236
0.060			5.0	4.9	0.0306
0.080			5.5	5.5	0.0372
0.100			6.2	6.1	0.0400
0.150			7.4	7.5	0.0477
0.200	0.012	1.25	8.1	8.4	0.0545
0.300	0.019	1.25			
0.400	0.024	1.25			
0.600	0.030	1.40			

a. At completion of the rapid colour forming reaction. A value for complete conversion to the 3-adduct is 0.36.

b. Calculated using $OD(460)[AmH^{+}]/[0.036-OD(460)][Am]^{2}$.

c. Calculated from equation 7.18 with k_1 60 l mol^{-1} s^{-1}, $K_{c,3}$ 1.25 l mol^{-1} and $k_{-1}k_{AmH^{+}}/k_{Am}$ 0.8 s^{-1}.

d. At completion of the slower colour forming reaction.

TABLE 7.28 Kinetic and rate equilibrium for σ-adduct formation from HNBB (1×10^{-5} M) and benzylamine in DMSO containing 0.1 M benzylammonium chloride at 25°C

[benzylamine]/M	OD[a](460nm)	$K^{b}_{c,3}$/l mol^{-1}	k_{obs}/s^{-1}	k^{c}_{calc}/s^{-1}	OD[d](460nm)
0.006			6.8	7.0	0.0026
0.008			5.5	5.5	0.0040
0.010			4.6	4.6	0.0053
0.020			3.3	3.2	0.0159
0.040			3.4	3.4	0.0311
0.060			4.0	3.9	0.0389
0.080			4.6	4.7	0.0429
0.100	0.0083	2.4	5.2	5.3	0.0458
0.200	0.021	2.5			
0.300	0.028	2.2			
0.400	0.031	1.8			
0.600	0.037	2.1			

a. At completion of the rapid colour forming reaction. A value for complete conversion to 3-adduct is 0.042.

b. Calculated from $OD(460)[AmH^+]/[0.042-OD(460)][Am]^2$.

c. Calculated from equation 7.18 with k_1 60 l mol^{-1} s^{-1}, $K_{c,3}$ 2.2 l mol^{-1} and $k_{-1}k_{AmH^+}/k_{Am}$ 0.4 s^{-1}.

d. At completion of the slower reaction.

The data for formation of the dianion by deprotonation of HNBB are given in Table 7.29. The values are in accord with equation 7.20 with values of k_p 0.24 l mol^{-1} s^{-1}, k_p' 0.007 l mol^{-1} s^{-1}, k_{-p}/K_{2p} 0.002 l mol^{-1} s^{-1} and $K_{c,1}$ 150 l mol^{-1}. A value for $K_{p,c}$ (= k_p K_{2p}/k_{-p}) of 120 is calculated.

TABLE 7.29 Rate data for formation of the blue dianion from HNBB (2×10^{-5}M) and benzylamine in DMSO containing 0.1M benzylammonium chloride at 25°C

[benzylamine]/M	10^3 k^a_{obs}/s^{-1}	10^3 k^b_{calc}/s^{-1}	10^3 $^ck_{calc}/s^{-1}$
0.005	4.7	5.2	5.2
0.0075	4.2	4.3	4.3
0.010	4.0	4.1	4.1
0.020	4.1	4.1	4.1
0.040	3.3	3.5	3.5
0.060	2.9	3.0	2.9
0.080	2.7	2.2	2.6
0.100	2.6	1.8	2.4
0.200	2.4	1.0	2.3

a. Measured at 620nm with a conventional spectrophotometer.

b. Calculated using equation 7.19 with k_p 0.24 l mol^{-1} s^{-1}, k_{-p}/K_{2p} 0.002 l mol^{-1} s^{-1} and $K_{c,1}$ 150 l mol^{-1}.

c. Calculated using equation 7.20 with k_p 0.24 l mol^{-1} s^{-1}, k_{-p}/K_{2p} 0.002 l mol^{-1} s^{-1}, k_p' 0.007 l mol^{-1} s^{-1} and $K_{c,1}$ 150 l mol^{-1}.

TABLE 7.30 ^1H n.m.r. data for HNBB with amines in [$^2H_6$]DMSO

Species	δ(ring)	δ(methylene)
HNBB	9.10	7.13
(7.9)	8.2	*ca* 7.00
(7.6; RR'N=$CH_3CH_2CH_2CH_2NH$)	8.38	2.33

7.4 Discussion

The results reported in this chapter relate to an ionic strength of 0.1M. It has been found that the equilibrium constants $K_{c,3}$ and $K_{c,1}$ measured in solutions containing 0.1M substituted ammonium chloride are about twice as large as those measured in solutions containing 0.1M substituted ammonium perchlorate. This has been observed for related compounds in the literature[151,166] and in Chapter Six. The explanation of this effect has been attributed to a stabilising association between the substituted ammonium ions and chloride ions, which are observed to reduce k_{AmH}^{+} by a factor of *ca* two. In the subsequent discussion for σ-adduct formation only the data obtained in the presence of perchlorate salts will be used.

7.4.1 Attack at the unsubstituted position

The kinetic and equilibrium data for formation of the 3-amido-adducts of TNBCl and 1,3,5-trinitrobenzene (TNB) are compared in Table 7.31 with the equivalent data obtained for HNBB. The data for HNBB have not been statistically adjusted.

Along the series TNB, TNBCl, HNBB, the values for $K_{c,3}$ fall for a given amine. Amine attack at the unsubstituted position of TNBCl and HNBB would be expected to be encouraged compared to attack on TNB as the CH_2Cl and CH_2CH_2Pic substituents are electron withdrawing compared to hydrogen, (see Chapter Four) However, the lowering in values of $K_{c,3}$ would suggest that the steric effect, due to bulky substituents at the 1-position, is dominant. Depending on the amine $K_{c,3}$ values for TNB amido-adducts are 40 to 80 times larger than $K_{c,3}$ values for TNBCl,

TABLE 7.31 Comparison of kinetic and equilibrium data for reaction at unsubstituted positions of HNBB, TNBCl[a] and TNB.[b]

		Benzylamine	n-Butylamine	Pyrrolidine	Piperidine
k_3 /l mol^{-1}s^{-1}	HNBB	550	1700	8000	> 5000
	TNBCl	1000	3000	17000	> 13000
	TNB	13000	45000	750000	>200000
$K_{c,3}$ /l mol^{-1}	HNBB	25	25	79	26
	TNBCl	55	73	240	93
	TNB	105	1000	3500	2140
K_3k_{Am} /l^{2}mol^{-2}s^{-1}	HNBB			3.1×10^5	1.1×10^4
	TNBCl			5.8×10^5	2.6×10^5
	TNB			1.0×10^5	6×10^5
k_{Am}/k_{-3} (l mol^{-1})	HNBB			40	< 2
	TNBCl			34	< 2
	TNB			14	<10
k_{AmH^+}/ 1 mol^{-1}s^{-1}	HNBB			3900	420
	TNBCl			2400	280
	TNB			3000	280
$\frac{k_{-3}k_{AmH^+}}{k_{Am}}$ /s^{-1}	HNBB	450	70	100	>200
	TNBCl	200	41	70	>140
	TNB	125	75	210	> 90

a. Data for TNBCl from Chapter Six.

b. Data for TNB from references 151, 152.

which are 3 to 4 times larger than $K_{c,3}$ values for HNBB. The steric effect is due to the bulky substituent at the 1-position forcing the ortho nitro-groups out of the ring-plane where they exert their maximum electron withdrawing ability. The larger $K_{c,3}$ value for TNBCl than for HNBB may derive from a larger steric effect of the CH_2CH_2Pic substituent relative to the CH_2Cl substituent, and/or a larger inductive withdrawing effect of the CH_2Cl substituent relative to the CH_2CH_2Pic substituent. The values of k_3, the rate coefficient for amine attack at the 3-position, similarly fall in the order TNB > TNBCl > HNBB and largely account for variations in values of $K_{c,3}$. The basicity order of the amines[157-159] is reflected, for a given nitro-compound, by the order in which the $K_{c,3}$ and k_3 values fall, *ie* pyrrolidine > piperidine > n-butylamine > benzylamine.

The rate coefficient for proton transfer from a substituted ammonium ion to an anionic adduct, k_{AmH^+}, (see Scheme 7.2) was measured for the reactions with piperidine and pyrrolidine. The values are similar to those for the corresponding reactions involving TNBCl to TNB and are considered typical for the reaction at unsubstituted ring-positions in trinitro-aromatic substrates. When reaction occurs at a substituted ring position it is known (see Chapter Six) that steric effects cause large reductions in the rate coefficients for proton transfer.

Earlier the assumption was made that piperidine and pyrrolidine form the 3-adduct with HNBB by attack at an unsubstituted ring position. This assumption has been justified by the comparison of the HNBB data with that of the TNB and the TNBCl data.

7.4.2 Attack at the 1- and 1′-positions

The data collected in Table 7.32 is for the formation of the 1-amido-adduct of HNBB with primary amines. Comparison of $K_{c,1}$ with $K_{c,3}$ for benzylamine ($K_{c,1}/K_{c,3}$=60) and n-butylamine ($K_{c,1}/K_{c,3}$=46) show that the 1-adduct is thermodynamically preferred. This is attributed mainly to the steric relief found in the 1-adduct, due to the CH_2CH_2Pic substituent rotating out of the ring plane. This allows the ortho nitro-groups to achieve co-planarity with the ring. An additional effect is the electron withdrawing effect of the CH_2CH_2Pic substituent. Steric hindrance for attack of the amine at the 1-position (F-strain)[160] probably accounts for k_1 values being lower than the corresponding k_3 values. Comparison of the final rows in Tables 7.31 and 7.32 allow the relative values of k_{-1} and k_{-3} to be estimated. It is expected that the acidity of the zwitterionic intermediate relative to that of corresponding substituted ammonium ion, measured by k_{am}/k_{AmH^+}, will not vary greatly with the position of attack.[151] Thus comparison of the data for benzylamine and for n-butylamine gives ratios of k_{-3}/k_{-1} of *ca* 500, indicating slower expulsion of amine from the 1-position than from the 3-position.

TABLE 7.32 Comparison of kinetic and equilibrium data for reaction at the 1-position of HNBB and TNBCl[a]

		Benzylamine	n-Butylamine
$K_{c,1}$ (l mol^{-1})	HNBB	75	1150
	TNBCl	1000	23000
$K_{D,1}$ (l mol^{-1})	HNBB	0.6	17
K_1 (l mol^{-1} s^{-1})	HNBB	60	150
	TNBCl	230	630
$k_{-1}k_{AmH^+}/k_{Am}$ (s^{-1})	HNBB	0.8	0.14
	TNBCl	0.23	0.028

a. Data from Chapter Six.

HNBB and secondary amines are not observed to form 1-adducts. This was also found for TNBCl and secondary amines in Chapter Six. The reason for the non-formation of the 1-adduct is presumably for steric reasons.[103,161] If the 1-adduct was formed the bulky secondary amine attached at the 1-position already containing a bulky substituent, and adjacent to ortho nitro-groups, would cause a sterically crowded environment. The 1-adduct therefore, would be kinetically and/or thermodynamically unfavourable.

The values of $K_{D,1}$ for conversion of the 1:1 σ-adduct to the 1:2 σ-adduct are lower than the $K_{C,1}$ values by factors of 120 for benzylamine and 70 for n-butylamine. A factor of 40 for the corresponding reaction with ethoxide ions in ethanol was obtained in Chapter Four. Statistical correction of these factors reduces them by half, but the conclusion that formation of the 1-adduct inhibits formation of the 1-, 1′-diadduct, even though the two picryl rings are separated by two methylene groups, remains.

7.4.3 Formation of the dianion by proton transfer from the methylene groups

Conductance measurements have shown the blue species is the dianion, formed by the transfer of two protons from HNBB to amine. ^{1}H n.m.r. measurements have shown it to have the structure (7.9). The kinetic studies have been interpreted using Scheme 7.1. Here, the formation of the monoanion (7.8) is found to be the rate determining step followed by rapid conversion to the dianion (7.9). Appreciable build-up of monoanion was not observed. These results imply that the monoanion has greater acidity than HNBB. Why should this be so?

The ready formation of dianions from 2,2′-biindenyl and 9,9′-bifluorenyl hydrocarbons has been rationalised[167] by coulombic stabilisation of the anions by simultaneous interaction with two metal cations. However, in the systems studied ion-association between alkylammonium cations and the dianion in DMSO are unlikely, as shown by the conductance measurements. The low stability of (7.8) relative to that of (7.9) can be rationalised in terms of two possible factors. The first is the steric strain in (7.8) due to the close proximity of the CH_2Pic group and an ortho nitro-group which may be partially removed during the formation of (7.9) by ionisation of one of the CH_2Pic hydrogens. The second factor is electronic; there is the possibility of the negative charge being delocalised over the whole molecule in (7.9). Another electronic factor which should be considered is the electronic effects in HNBB compared to those in the monoanion. In HNBB the CH_2 protons are activated by a picryl ring and a picryl ring through a CH_2 group, whereas in the monoanion they are activated by a picryl ring and a $C_6H_2(NO_2)_3^-$ group coupled through a double bond. The $C_6H_2(NO_2)_3^-$ group is known[156,168] to be electron withdrawing relative to hydrogen despite being negatively charged. It is therefore a possibility that the electronic influence of the $C_6H_2(NO_2)_3^-$ group *via* a double bond might be greater than that of the picryl ring *via* a methylene group.

Summarised in Table 7.33 are the values of k_p, the rate coefficient for proton transfer. k_p decreases with respect to amine in the order pyrrolidine > piperidine > n-butylamine, DABCO > benzylamine and is similar to that observed for σ-adduct formation. Values are between 14 and 23 times smaller than those for the reaction of TNBCl with the corresponding amines.

TABLE 7.33 Summary of rate data for transfer of methylene protons

		Benzylamine	n-Butylamine	Pyrrolidine	Piperidine	DABCO
k_p/l mol^{-1} s^{-1}	HNBB	0.24	0.8	5.5	1.8	1.1
	TNBCl	3.4[a]	17[b]	140[a]	42[b]	16.4[b]
k'_p/l mol^{-1} s^{-1}	HNBB	0.007	0.003	0.4	0.16	

a. Data from Chapter Six.

b. Data from reference 92.

The formation of the dianion can also be produced *via* the deprotonation of σ-adducts. With n-butylamine and benzylamine k_p' represents proton transfer of a methylene proton from the 1-adduct (7.5) and the ratios of k_p/k_p' have the values of 11 and 14 respectively.

Schemes 7.3 and 7.6 show how the formation of the dianion has been interpreted for the deprotonation of HNBB by secondary and primary amines respectively. Subsequent discussion will concentrate on the deprotonation of the dianion using secondary amines, but an analogous discussion can be applied to the same process using primary amines.

The data for formation of the dianion (7.9) shows that deprotonation of the σ-adduct (7.3) to give (7.10) is rate-limiting. The species (7.10) then has two possible pathways to form the dianion. These are designated in Scheme 7.3 as the equilibria $K_{x,c}$ and $K_{y,c}$. Schemes 7.7 and 7.8 show how these pathways may proceed in more detail. The equilibrium constant $K_{x,c}$ is the overall equilibrium constant for the route from (7.10) to (7.8) *via* (7.12) in Scheme 7.7. This pathway is expulsion of the amine molecule from (7.10) *via* the zwitterionic intermediate (7.12) to produce the monoanion, which then rapidly loses a proton to give the dianion (not shown in Scheme 7.7). The equilibrium constant $K_{y,c}$ is the overall equilibrium constant for the route which goes clockwise from (7.10) to (7.9) in Scheme 7.8. This pathway is the deprotonation of (7.10) to form the trianion (7.13), which then expels an amine molecule *via* the zwitterionic intermediate (7.14) to produce the dianion (7.9) The data, however, provides no information as to the possible timing of these processes.

Scheme 7.7

Interpretation of the equilibrium $K_{x,c}$ shown in Scheme 7.3

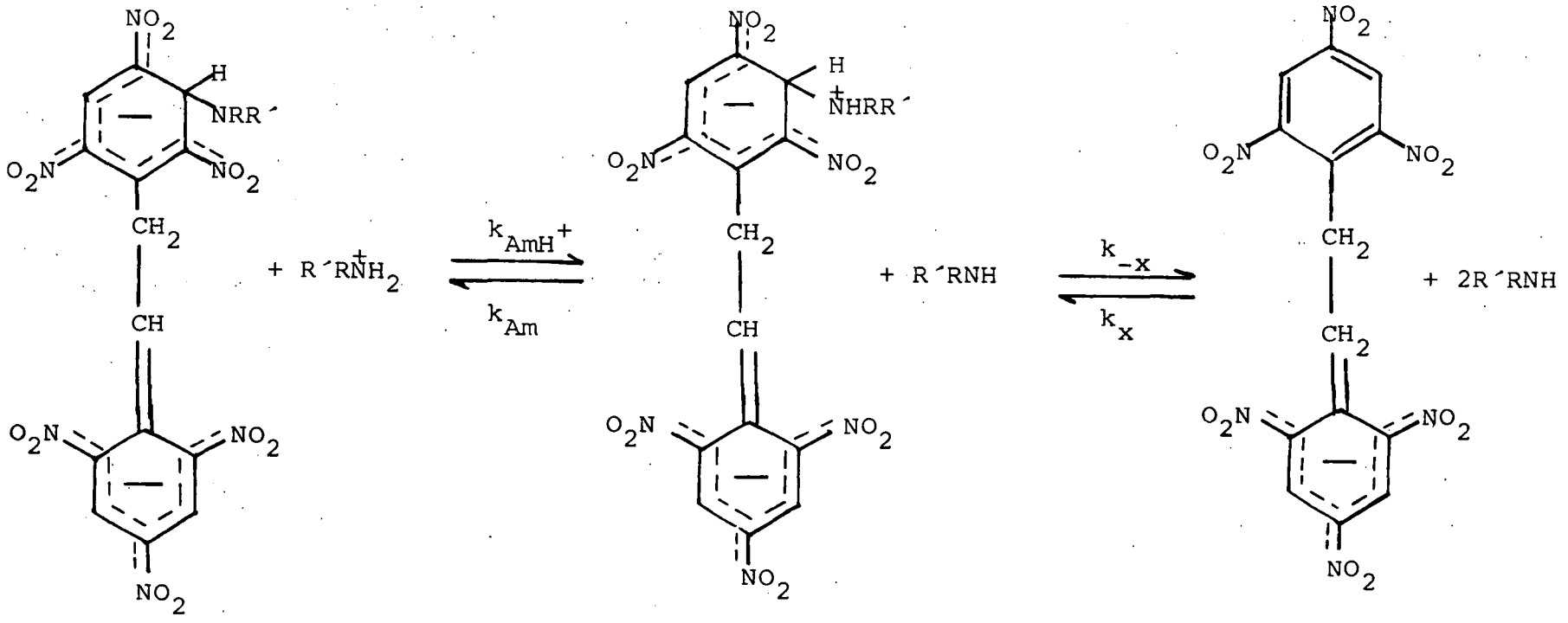

(7.10) (7.12) (7.8)

Scheme 7.8

Interpretation of the equilibrium $K_{y,c}$ shown in Scheme 7.3

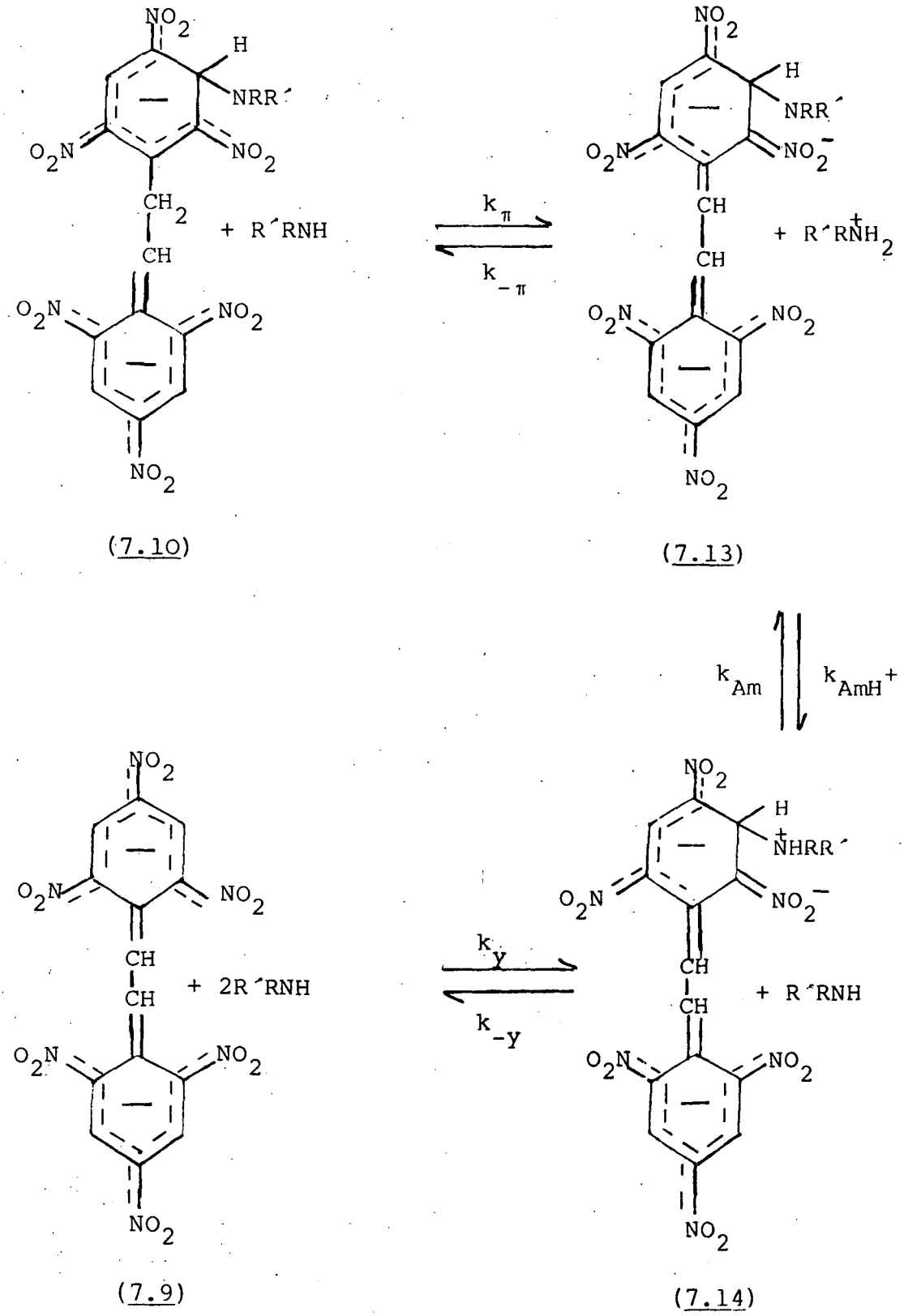

7.5 Derivation of the Rate Expressions

The rate expressions for the formation of the 1- and 3-amido-adducts from HNBB are derived in an analogous way to those amido-adducts formed from TNBCl in the previous chapter. The only new rate expressions used in this chapter were for the formation of the dianion (7.9).

(i) Formation of the dianion by a tertiary amine, *i.e.* no prior σ-adduct formation, from the substrate only.

$$(7.1) + Am \underset{k_{-p}}{\overset{k_p}{\rightleftharpoons}} (7.8) + AmH^+$$

$$(7.8) + Am \underset{k_{-2p}}{\overset{k_{2p}}{\rightleftharpoons}} (7.9) + AmH^+$$

$$\frac{d[7.9]}{dt} = k_{2p}[7.8][Am] - k_{-2p}[7.9][AmH^+] \qquad (1)$$

$$\frac{d[7.8]}{dt} = k_p[7.1][Am] + k_{-2p}[7.9][AmH^+] - k_{2p}[7.8][Am] - k_{-p}[7.8][AmH$$

Treating (7.8) as a steady-state intermediate, $\frac{d[7.8]}{dt} = 0$.

$$\therefore \quad [7.8] = \frac{k_p[7.1][Am] + k_{-2p}[7.9][AmH^+]}{k_{2p}[Am] + k_{-p}[AmH^+]} \qquad (2)$$

Substituting (2) into (1)

$$\frac{d[7.9]}{dt} = k_{2p}[Am]\left(\frac{k_p[7.1][Am] + k_{-2p}[7.9][AmH^+]}{k_{2p}[Am] + k_{-p}[AmH^+]}\right) - k_{-2p}[7.9][AmH^+] \qquad (3)$$

$k_{-2p}[7.9][AmH^+]$ is multiplied by 1.

i.e. $k_{-2p}[7.9][AmH^+] \times \frac{k_{2p}[Am] + k_{-p}[AmH^+]}{k_{2p}[Am] + k_{-p}[AmH^+]}$

$$= \frac{k_{-p}k_{-2p}[7.9][AmH^+]^2 + k_{-2p}k_{2p}[7.9][Am][AmH^+]}{k_{2p}[Am] + k_{-p}[AmH^+]}$$

Re-inserting into (7.3)

$$\frac{d[7.9]}{dt} = \frac{k_{2p}k_p[Am]\ [7.1]^2 - k_{-p}k_{-2p}[7.9][AmH^+]^2}{k_{2p}[Am] + k_{-p}[AmH^+]} \qquad (7.4)$$

$$[7.1]_o = [7.1] + [7.9] + [7.8]$$

As (7.8) is a steady-state intermediate $[7.8] \sim 0$.

$$[7.1] = [7.1]_o - [7.9] \qquad (7.5)$$

Substituting (7.5) into (7.4)

$$\frac{d[7.9]}{dt} = \frac{A - k_{2p}k_p[Am]^2[7.9] - k_{-p}k_{-2p}[7.9][AmH^+]^2}{k_{2p}[Am] + k_{-p}[AmH^+]} \qquad (7.6)$$

where $A = k_{2p}k_p[Am]^2[7.1]_o$

At equilibrium $\frac{d[7.9]}{dt} = 0$.

$$0 = \frac{A - k_{2p}k_p[Am]^2[7.9]_e - k_{-p}k_{-2p}[7.9]_e[AmH^+]^2}{k_{2p}[Am] + k_{-p}[AmH^+]} \qquad (7.7)$$

Subtracting (7.7) from (7.6)

$$\frac{d[7.9]}{dt} = \frac{k_{2p}k_p[Am]^2 + k_{-p}k_{-2p}[AmH^+]^2}{k_{2p}[Am] + k_{-p}[AmH^+]} \quad ([7.9]_e - [7.9])$$

In previous chapters it has been shown that for a single absorbing species present in solution, in this case (7.9), the concentration of that species is related to the optical density by the following equation;

$$\frac{d\ OD}{dt} \cdot \frac{1}{OD_e - OD} = \frac{d[7.9]}{dt} \cdot \frac{1}{[7.9]_e - [7.9]}$$

By definition,

$$k_{obs} = \frac{d\ OD}{dt} \cdot \frac{1}{OD_e - OD}$$

Therefore,

$$k_{obs} = \frac{k_{2p}k_p[Am]^2 + k_{-p}k_{-2p}[AmH^+]^2}{k_{2p}[Am] + k_{-p}[AmH^+]}$$

(ii) Formation of the dianion by a secondary amine, *i.e.* prior formation of the 3-amido-adduct, from the substrate only.

$$(\underline{7.1}) + 2Am \underset{k_{-p}}{\overset{k_p}{\rightleftharpoons}} (\underline{7.8}) + Am \underset{k_{-2p}}{\overset{k_{2p}}{\rightleftharpoons}} (\underline{7.9}) + AmH^+$$

$$(\underline{7.1}) + 2Am \overset{K_{c,3}}{\rightleftharpoons} (\underline{7.3}) + AmH^+$$

As the formation of the 3-adduct is rapid compared to the formation of the dianion, then equation (4) can be derived as shown above,

$$\frac{d[7.9]}{dt} = \frac{k_{2p}k_p[Am][7.1] - k_{-p}k_{-2p}[7.9][AmH^+]}{k_{2p}[Am] + k_{-p}[AmH^+]} \qquad (\underline{4})$$

$$[7.1]_o = [7.1] + [7.3] + [7.9] \qquad (\underline{8})$$

$$K_{c,3} = \frac{[7.3][AmH^+]}{[7.1][Am]^2}$$

$$[7.3] = \frac{K_{c,3}[7.1][Am]^2}{[AmH^+]} \qquad (\underline{9})$$

Substituting (9) into (8) and re-arranging,

$$[7.1] = \frac{[7.1]_o - [7.1]}{1+K_{c,3}[Am]^2/[AmH^+]} \qquad (\underline{10})$$

Substituting (10) into (4)

$$\frac{d[7.9]}{dt} = \frac{B - k_{2p}k_p[Am]^2[7.9]}{(1+K_{c,3}[Am]^2/[AmH^+])(k_{2p}[Am]+k_{-p}[AmH^+])} - \frac{k_{-p}k_{-2p}[AmH^+]^2[7.9]}{k_{-p}[AmH^+]+k_{2p}[Am]} \qquad (\underline{11})$$

where $B = k_{2p}k_p[Am]^2[7.1_o]$.

At equilibrium, $\frac{d[7.9]}{dt} = 0$.

$$0 = \frac{B - k_{2p}k_p[Am]^2[7.9]_e}{(1+K_{c,3}[Am]^2/[AmH^+])(k_{2p}[Am]+k_{-p}[AmH^+])} + \frac{k_{-p}k_{-2p}[AmH^+]^2[7.9]}{k_{2p}[Am] + k_{-p}[AmH^+]}$$

(12)

Subtracting (12) from (11)

$$\frac{d[7.9]}{dt} = \frac{k_{2p}k_p[Am]^2 + k_{-p}k_{-2p}[AmH^+](1+K_{c,3}[Am]^2/[AmH^+])}{(1+K_{c,3}[Am]^2/[AmH^+])(k_{2p}[Am] + k_{-p}[AmH^+])}([7.9]_e-[7$$

(7.9) is the principal absorbing species at the wavelength at which the reaction was studied, though (7.3) may absorb slightly as well. It has been shown in Chapter Six that in such cases [7.9] is related to OD by the following equation.

$$\frac{d[7.9]}{dt} \cdot \frac{1}{[7.9]_e-[7.9]} = \frac{d\ OD}{dt} \cdot \frac{1}{OD_e-OD}$$

By definition,

$$k_{obs} = \frac{d\ OD}{dt} \cdot \frac{1}{OD_e-OD}$$

Therefore,

$$k_{obs} = \frac{k_{2p}k_p[Am]^2}{(1+K_{c,3}[Am]^2/[AmH^+])(k_{2p}[Am]+k_{-p}[AmH^+])} + \frac{k_{-p}k_{-2p}[AmH^+]^2}{k_{2p}[Am]+k_{-p}[AmH^+]}$$

(iii) Formation of the dianion by a secondary amine from the substrate and from deprotonation of the 3-adduct.

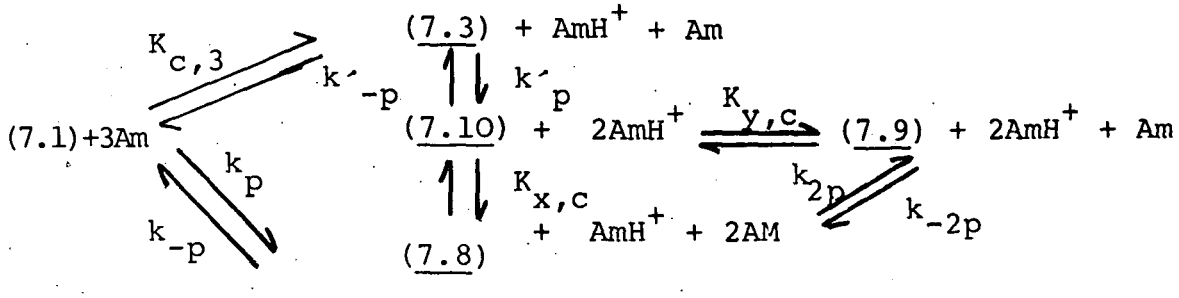

In the following derivation $k'_p >> k'_{-p}$ will be assumed so that term incorporating k'_{-p} is unnecessary.

$$\frac{d[7.9]}{dt} = k_{2p}[7.8][Am] - k_{-2p}[7.9][AmH^+] + k'_p[7.3][Am] \qquad (13)$$

Treating (7.8) as a steady-state intermediate as shown above and substituting equations (2) and (9) into (13)

$$\frac{d[7.9]}{dt} = k_{2p}[Am]\left(\frac{k_p[7.1][Am]+k_{-2p}[7.9][AmH^+]}{k_{2p}[Am] + k_{-p}[AmH^+]}\right)$$

$$- k_{-2p}[AmH^+][7.9] + k'_pK_{c,3}[Am]^3[7.1]/[AmH^+] \qquad (14)$$

As before (see derivation of equation (4)) the first two terms of (14) can be combined.

$$\frac{d[7.9]}{dt} = \frac{k_{2p}k_p[Am]^2[7.1] - k_{-p}k_{-2p}[7.9][AmH^+]^2}{k_{2p}[Am] + k_{-p}[AmH^+]}$$

$$+ k'_pK_{c,3}[7.1][Am]^3/[AmH^+] \qquad (15)$$

$$[7.1]_o = [7.1] + [7.3] + [7.9] + [7.10]$$

$K_{x,c}$ and $K_{y,c}$ are very rapid, $\therefore$ $[7.10] \sim 0$.

Therefore,

$$[7.1]_o = [7.1] + [7.3] + [7.9]$$

which is equation (8)

As before,

$$[7.1] = \frac{[7.1]_o - [7.9]}{1+K_{c,3}[Am]^2/[AmH^+]} \qquad (10)$$

Substituting (10) into (15)

$$\frac{d[7.9]}{dt} = \frac{B - k_p k_{2p}[Am]^2[7.9]}{(1+K_{c,3}[Am]^2/[AmH^+])(k_{2p}[Am] + k_{-p}[AmH^+])}$$

$$- \frac{k_{-p}k_{-2p}[AmH^+]^2[7.9]}{k_{2p}[Am] + k_{-p}[AmH^+]}$$

$$+ \frac{k'_p K_{c,3}[Am]^3([7.1]_o - [7.9])}{[AmH^+] + K_{c,3}[Am]^2} \qquad (16)$$

At equilibrium, $\frac{d[7.9]}{dt} = 0$.

$$0 = \frac{B - k_{2p}k_p[Am]^2[7.9]_e}{(1+K_{c,3}[Am]^2/[AmH^+])(k_{2p}[Am]+k_{-p}[AmH^+])} - \frac{k_{-p}k_{-2p}[AmH^+]^2[7.9]_e}{k_{2p}[Am] + k_{-p}[AmH^+]}$$

$$+ \frac{k'_p K_{c,3}[Am]^3([7.1]_o - [7.9]_e)}{[AmH^+] + K_{c,3}[Am]^2} \qquad (17)$$

Subtracting (17) from (16)

$$\frac{d[7.9]}{dt} \cdot \frac{1}{[7.9]_e - [7.9]} = \frac{k_p k_{2p}[Am]^2}{(1+K_{c,3}[Am]^2/[AmH^+])(k_{2p}[Am]+k_{-p}[AmH^+])}$$

$$+ \frac{k_{-p}k_{-2p}[AmH^+]^2}{k_{2p}[Am]+k_{-p}[AmH^+]} + \frac{k'_p K_3[Am]^3}{[AmH^+]+K_{c,3}[Am]^2}$$

Using the principles outlined in previous chapters [7.9] can be related to OD by the following equation.

$$\frac{d[7.9]}{dt} \cdot \frac{1}{[7.9]_e - [7.9]} = \frac{d\ OD}{dt} \cdot \frac{1}{OD_e - OD}$$

By definition,

$$k_{obs} = \frac{d\ OD}{dt} \cdot \frac{1}{OD_e - OD}$$

Therefore,

$$k_{obs} = \frac{k_p k_{2p}[Am]^2}{(1+K_{c,3}[Am]^2/[AmH^+])(k_{2p}[Am]+k_{-p}[AmH^+])}$$

$$+ \frac{k_{-p}k_{-2p}[AmH^+]^2}{k_{2p}[Am]+k_{-p}[AmH^+]} + \frac{k'_p K_{c,3}[Am]^3}{[AmH^+]+K_{c,3}[Am]^2}$$

If $k_{2p}[Am] >> k_{-p}[AmH^+]$

$$k_{obs} = \frac{k_p[Am]}{1+K_{c,3}[Am]^2/[AmH^+]} + \frac{k_{-p}[AmH^+]}{K_{2p}[Am]} + \frac{k'_p K_{c,3}[Am]^3}{[AmH^+]+K_{c,3}[Am]^2}$$

(iv) Formation of the dianion by primary amines, *i.e.* prior formation of the 1-adduct, from the substrate and from deprotonation of the 1-adduct.

Analogous procedures to those described above for the secondary amines can be used to show

$$k_{obs} = \frac{k_p k_{2p}[Am]^2}{(1+K_{c,3}[Am]^2/[AmH^+])(k_{2p}[Am]+k_{-p}[AmH^+])}$$

$$+ \frac{k_{-p}k_{-2p}[AmH^+]^2}{k_{2p}[Am]+k_{-p}[AmH^+]} + \frac{k'_p K_{c,1}[Am]^3}{[AmH^+] + K_{c,3}[Am]^2}$$

CHAPTER EIGHT

THE REACTIONS OF 2,2',4,4',6,6',-HEXANITROSTILBENE WITH ALIPHATIC AMINES IN DIMETHYL SULPHOXIDE

8.1 Introduction

Another preparation of 2,2′,4,4′,6,6′-hexanitrostilbene (HNS) is using the 'Hungarian Method'.[169] This method employs a copper sulphate/pyridine catalyst with base to produce HNS in high yields from 2,2′,4,4′,6,6′-hexanitrobibenzyl (HNBB) or 2,4,6-trinitrotoluene (TNT) in various solvents. The use of amine bases in the preparation of HNS was mentioned in Chapter Seven. Therefore, there is an interest to study the interactions of HNS with amines.

The interactions of 2,4,6-trinitrobenzyl chloride (TNBCl) and HNBB with amines have been reported in previous chapters. Using this knowledge the interactions of HNS with amines in DMSO can be predicted. The formation of σ-adducts, *via* zwitterionic intermediates, would be expected as shown in Scheme 8.1. Depending on the amine used addition may occur at either the 3- or 1-position. Proton transfer from zwitterion to amine may be rate-limiting. Because HNS has two activated rings formation of the 1:1 σ-adduct may be followed by amine attack on the second ring to form a di-anionic species. This di-anionic species may be formed by amine addition at the 1- and 1′-, 3- and 3′-, or 1- and 3′- positions. Unlike HNBB it is improbable that deprotonation of HNS will occur to produce the conjugate base of HNS. However, amine addition at the olefinic bond may occur, once again *via* a zwitterionic intermediate. The major reaction pathways possible are summarised in Scheme 8.2. (The structures of the species (8.1), (8.2), etc. are given in Figure 8.1). This scheme, for compactness, has not included free amine molecules, ammonium ions or zwitterionic intermediates.

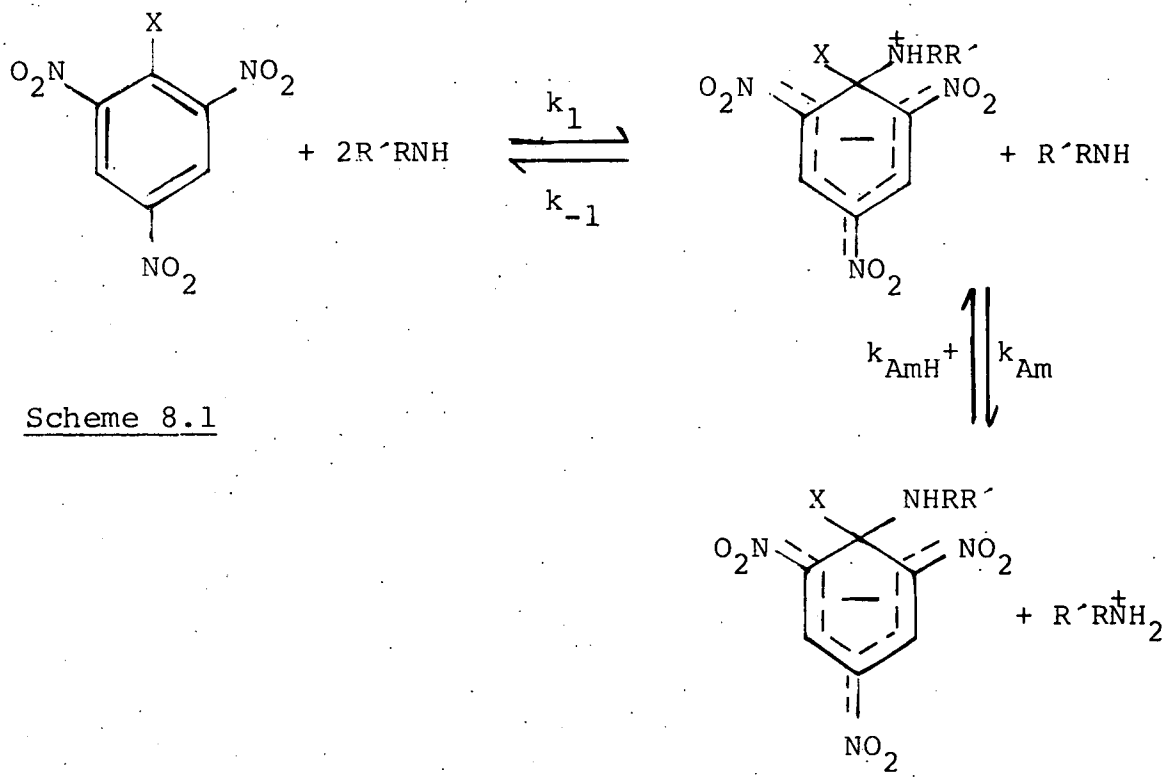

Scheme 8.1

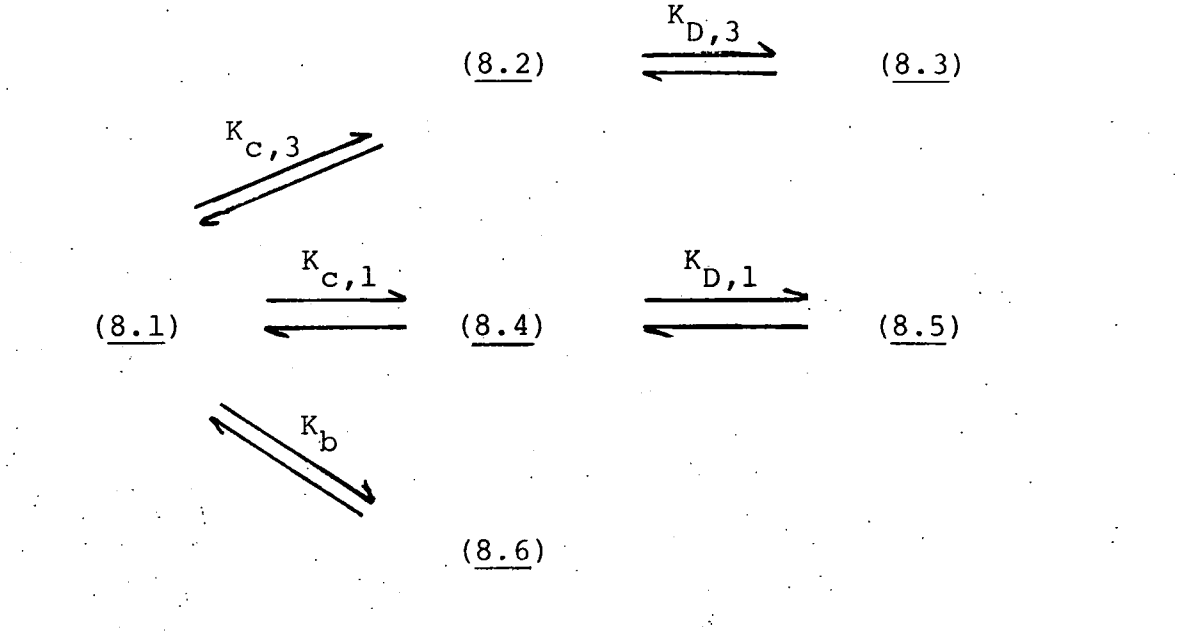

Scheme 8.2

Figure 8.1

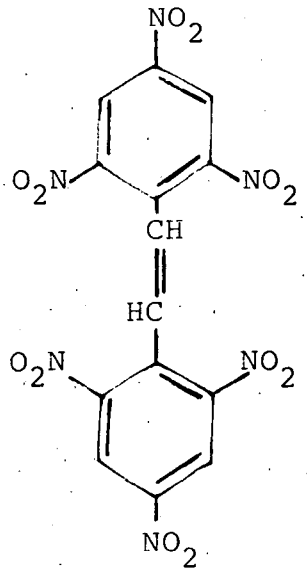

(8.1)

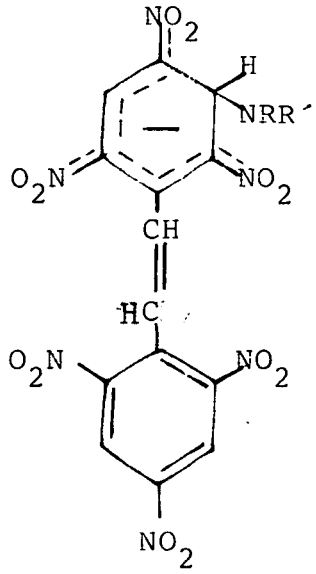

(8.2)

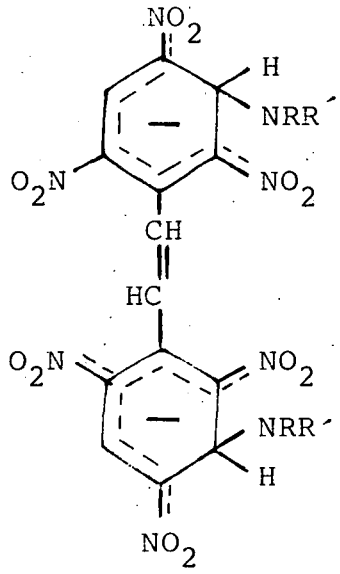

(8.3)

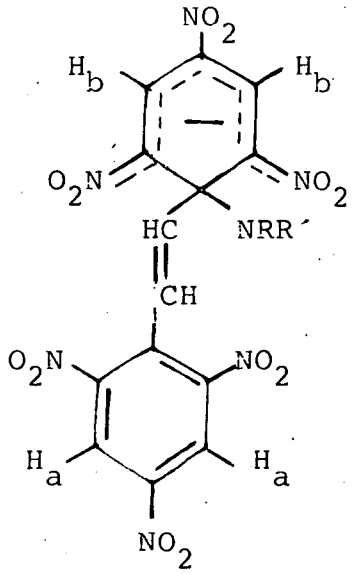

(8.4)

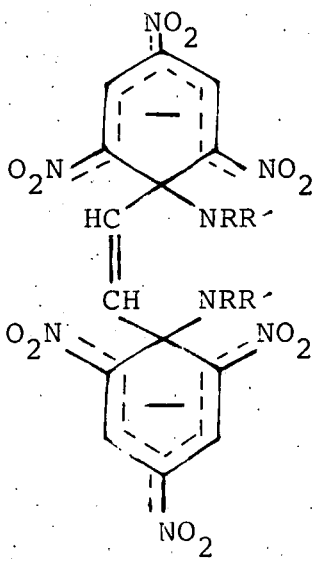

(8.5)

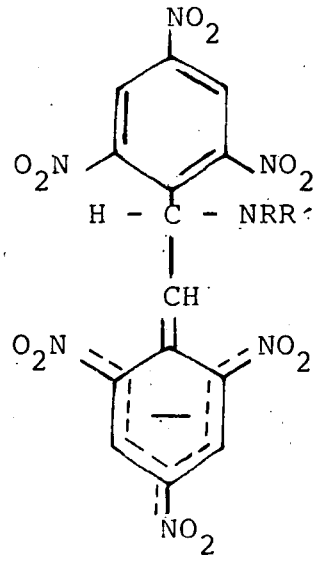

(8.6)

8.2 Experimental

All visible spectra were measured on a SP 8005 spectrophotometer.

Kinetic and equilibrium measurements were made on a Hi-Tech SF-3L stopped-flow spectrophotometer or a Pye-Unicam SP 8100 conventional spectrophotometer at 25°C. First order kinetics were always observed because base concentration was kept in large excess of parent concentration. For reactions of HNS with amines in the absence of added salts a sufficient excess of amine was used to ensure >95% conversion to product at equilibrium. For reactions with buffers (amines plus amine salt the buffer components were in large excess of HNS concentration. The observed rate coefficients are a mean of at least five separate determinations, when measured using the stopped-flow spectrophotometer, and at least two separate determinations when measured using a conventional spectrophotometer. Examples of typical rate measurements are given in Tables 8.1 and 8.2.

^{1}H n.m.r. measurements were made with a Varian EM 360L instrument operating at 60MHz using tetramethylsilane as the internal reference.

A Kent EIL 7055 pH meter was used to check the acidity of the ammonium salts. Solutions were adjusted so as to contain less than 0.1% of free amine or acid.

TABLE 8.1 Typical results from rate measurements.

(i) HNS (1×10^{-5} M), piperidine (0.1M).
Formation of 3-adduct measured at 450nm in DMSO containing 0.1M piperidinium chloride.

(ii) HNS (4×10^{-5} M), pyrrolidine (0.002M).
Formation of (8.6; R´RN = C_4H_8N), measured at 510nm in DMSO containing 0.1M pyrrolidinium perchlorate

(i)		(ii)	
t/ms	ΔV[a]	t/s	ΔOD[b]
0	3.00	0	0.531
10	2.60	100	0.440
20	2.20	200	0.384
30	1.80	300	0.341
40	1.50	400	0.307
60	1.15	600	0.251
80	0.80	800	0.208
		1000	0.174

A plot of $\ln\Delta V$ versus t is linear and yields $k_{obs} = 16.4\ s^{-1}$

A plot of $\ln\Delta OD$ versus t is linear and yields $k_{obs} = 1.17 \times 10^{-3}\ s^{-1}$

a. $\Delta V = V_\infty - V_t$

b. ΔOD calculated using the Guggenheim method.

TABLE 8.2 Typical results from rate measurements

(i) HNS (1×10^{-5} M), n-butylamine (0.06M). Formation of 1-adduct, measured at 455nm in DMSO containing 0.1M n-butylammonium perchlorate.

(ii) HNS (1×10^{-5} M), benzylamine (0.008M). Formation of 3-adduct, measured at 450nm in DMSO containing 0.1M benzylammonium chloride.

(i)		(ii)	
t/ms	ΔV^a	t/ms	ΔV^a
20	4.0	0	4.1
30	3.6	25	3.5
40	3.3	50	2.9
60	2.6	75	2.4
80	2.0	100	2.0
100	1.6	150	1.5
120	1.2	200	1.0
A plot of $\ln\Delta V$ versus t is linear and yields $k_{obs} = 11.50\ s^{-1}$		A plot of $\ln\Delta V$ versus t is linear and yields $k_{obs} = 7.05\ s^{-1}$.	

a. $\Delta V = V_\infty - V_t$

8.3 Results

8.3.1 ^{1}H n.m.r. measurements

The reactions between HNS and 1,4-diazabicyclo-[2,2,2]octane (DABCO), piperidine and n-butylamine in [$^{2}H_{6}$] DMSO have been studied by ^{1}H n.m.r. spectroscopy.

The ^{1}H n.m.r. spectrum of HNS (0.02M) in [$^{2}H_{6}$] DMSO shows two bands with an intensity ratio of 2:1 at δ9.13 (ring protons) and δ7.15 (olefinic protons) respectively. Within the accuracy of the instrument used this spectrum is identical to that of HNS in fully deuteriated 80:20 (v/v) DMSO-methanol, where bands were measured at δ9.10 and δ7.12, which was reported in Chapter Five.

Addition of one molecular equivalent of DABCO to HNS in [$^{2}H_{6}$] DMSO immediately resulted in a collapsing and broadening of the band at δ9.13 and the disappearance of the band at δ7.15. The broadening of the low field band suggests an electron transfer reaction to produce radicals is involved. Also, on mixing a blue colour was observed. With time the band at δ9.13 sharpened and after seven minutes the band at δ7.15 re-appeared and increased in intensity with time. After twelve minutes a spectrum was recorded with bands at δ9.13 and δ 7.15 with an intensity ratio of 2:1. This spectrum remained unchanged for a further eighteen minutes when measurements were stopped. However the final spectrum indicated that only half the number of protons were present in each band compared to the first spectrum.

Spectra of the reaction of HNS with half and one molecular equivalent of piperidine in [$^{2}H_{6}$] DMSO are similar to

that of HNS with DABCO. That is the band at δ7.15 disappears immediately the solutions are mixed and returns after about ten minutes; while the band at δ9.13 collapses and broadens. Again the solution is a blue colour. Both bands return to their original sharpness and the chemical shifts are those of 2:1 (ring protons:olefinic protons) but are perhaps not as intense. With two molecular equivalents of piperidine the same initial spectra are observed. However the band at δ7.15 does not re-appear and the broadened, less intense, band at δ9.13 continues to disappear. After sixteen minutes neither of these bands are observed. The first spectrum recorded after mixing HNS with ten molecular equivalents of piperidine shows neither the δ7.15 or the δ9.13 bands.

These spectra are difficult to interpret due to the lack of new bands expected for the products. The blue colour and broadening of the bands suggests an electron transfer process, possibly the formation of the dianion by transfer of two electrons to HNS. The disappearance of the bands on additic of two or more molecular equivalents indicates that at least two piperidine molecules are needed per molecule of HNS to complete this unknown reaction.

^{1}H n.m.r. spectra for the reaction of HNS with two molecular equivalents of n-butylamine show three bands, of equal intensity, at δ9.00, 8.50 (ring protons) and 6.63 (olefinic protons). In Figure 8.2 one of these spectra is shown. These spectra are consistent with the formation of (8.4; R´RN = $CH_3CH_2CH_2CH_2NH$) except the olefinic protons would be expected to give an AB quartet.[147] An AB quartet was observed for the olefinic protons for the formation of (8.4;R´RN = CD_3)

and reported in Chapter Five. The chemical shift of δ6.63 is approximately in the centre of where the chemical shift values of an AB quartet would be expected. Perhaps the equivalence of these olefinic protons is due to rapid proton exchange with the butylammonium cations present in solution. After about an hour all the bands had decayed. With five molecular equivalents of base bands at δ8.37 and δ6.60 are observed which are never very intense and decay rapidly. These bands may be attributable to (8.5; R´RN = $CH_3CH_2CH_2CH_2NH$).

The ^1H n.m.r. spectral evidence is generally poor and therefore inconclusive. σ-Adduct formation between HNS and piperidine was not observed by ^1H n.m.r. but kinetic evidence for σ-adduct formation will be given below. There is both ^1H n.m.r. and kinetic evidence (again given below) for σ-adduct formation between HNS and n-butylamine. The lack of ^1H n.m.r. evidence for σ-adduct formation between HNS and piperidine will be shown later from the kinetic and equilibrium studies to be due to its low thermodynamic stability compared with the thermodynamic stability of the σ-adduct formed between HNS and n-butylamine.

8.3.2 Reaction with DABCO

DABCO being a tertiary amine would not be expected to form σ-adducts by reaction with HNS. The reaction of HNS (2×10^{-5} M) with DABCO (0.1-1M) produces a blue species followed by a brown species. Visible spectra of these solutions show the blue species has maxima at 620nm and 480nm and slowly (within about thirty minutes after mixing) converts into a brown species with maxima at 486nm and 380nm.

FIGURE 8.2 ^{1}H n.m.r. spectrum of HNS (0.02M) and 2 molecular equivalents of n-butylamine in [$^{2}H_{6}$] DMSO

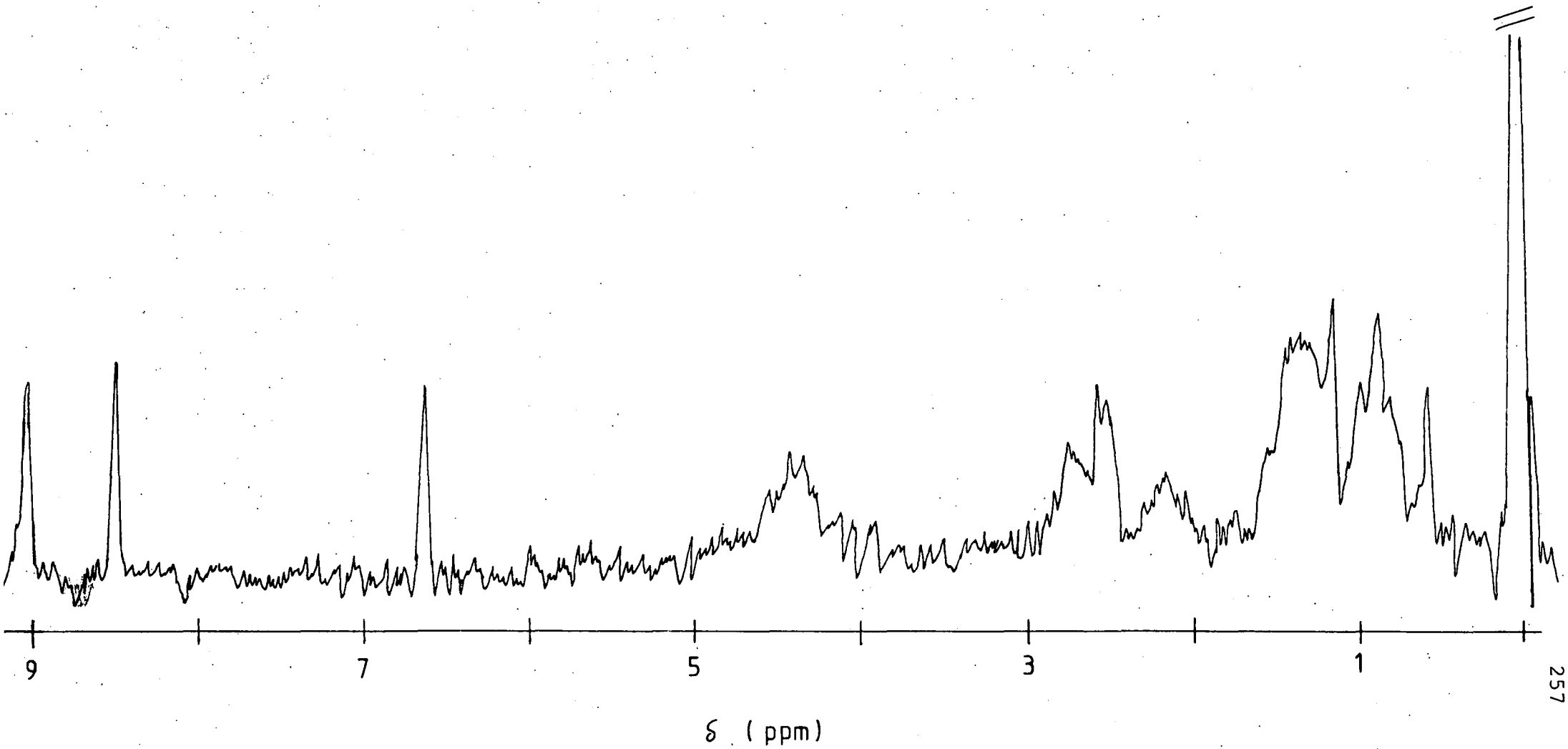

TABLE 8.3 Tabulation ^{1}H n.m.r. data for HNS and its adducts with n-butylamine in [$^{2}H_6$] DMSO

Species		δ^a(ring)	δ^a(olefinic bond)
HNS		9.13(s)	7.15(s)
(8.4; $R'RN=CH_3CH_2CH_2CH_2NH$)	H_a	8.5(s)	6.63(s)[b]
	H_b	9.0(s)	
(8.5; $R'RN=CH_3CH_2CH_2CH_2NH$)		8.37(s)	6.60(s)

a. All shifts measured relative to internal TMS.

b. Expected[147] to be a quartet as observed for analogous adduct of HNS with methoxide ions; see Chapter Five.

The spectrum of the blue species indicates that some of the second (brown) species is already present by the time it is recorded. The shape and size of the spectrum of the blue species, as well as its colour, suggest the formation of the dianion of HNS (8.7) by addition of two electrons. DABCO would not be expected to remove two olefinic protons from HNS to form the dianionic conjugate base of HNS. Therefore if the dianion (8.7) is produced it would be identical to the dianion of HNBB produced by removal of two chain protons. The

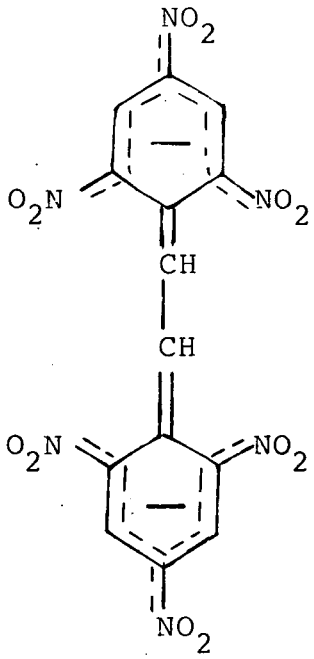

(8.7)

brown species is unknown but could be a Janowsky type complex by the attack of the dianion of HNS (8.7) on a neutral HNS molecule. It is known from e.s.r. measurements[149] of HNS (1×10^{-5} M) with DABCO (0.1 M) in DMSO that a free radical species *ca* 0.1% of the original HNS concentration, appears as the brown colouration appears.[149] Spin-spin splitting values of $a_{(N)}$ 4.7 gauss and $a_{(H)}$ 1.8 gauss were measured. This shows the radical

is unusual as a value of $a_{(N)}$ *ca* 12 gauss for the nitrogen atoms in the nitro groups of HNS would have been expected.[170] At present the radical species had not been identified, but its low concentration suggests its production may only be a minor process, and its formation may not be responsible for the brown colouration observed.

8.3.3 Reaction with piperidine

Visible spectra of HNS (1×10^{-5} M) and piperidine (0.001 - 0.1 M) in DMSO were recorded. A red species with maxima at 450nm and 520-530nm is produced first, and slowly decays to be replaced by a species with a large broad maximum at about 640nm. Study of the reaction at 450nm on the stopped-flow spectrophotometer shows one fast colour forming process at low piperidine concentrations while at high piperidine concentrations the fast process is followed by a slower colour forming process. Only the fast process was measured and this is assumed to be σ-adduct formation by amine attack at the 3-position to form (8.2; R´RN = $C_5H_{10}N$). Evidence to justify this assumption will be given later. The following slower reaction at high piperidine concentrations may be formation of (8.3; R´RN = $C_5H_{10}N$)

The kinetic and equilibrium data for the σ-adduct formation reaction between HNS and piperidine in DMSO is given in Table 8.4. Using Scheme 8.3 the general kinetic expression, given by equation 8.1, can be derived.

$$k_{obs} = \frac{k_3 k_{Am}[Am]^2 + k_{-3}k_{AmH^+}[AmH^+]}{k_{-3} + k_{Am}[Am]} \qquad \text{(equation 8.1)}$$

When there is no added amine salt present and conversion to the σ-adduct is ≥95% then equation 8.1 reduces to equation 8.2

$$k_{obs} = \frac{k_3 k_{Am}[Am]^2}{k_{-3} + k_{Am}[Am]} \qquad \text{(equation 8.2)}$$

The data in Table 8.4 is best interpreted using equation 8.3 which is obtained from equation 8.2 if $k_{-3} >> k_{Am}[Am]$ is assumed. A value of $K_3 k_{Am}(4\pm0.4) \times 10^4\ l^2\ mol^{-2}\ s^{-1}$ is obtained.

$$k_{obs} = K_3 k_{Am}[Am]^2 \qquad \text{(equation 8.3)}$$

TABLE 8.4 Kinetic data for the reaction of HNS (1×10^{-5} M) with piperidine in DMSO at 25°C

[Piperidine]/M	k_{obs}/s^{-1}	k^a_{calc}/s^{-1}	OD[b] (fast)	OD[c] (slow)
0.004	0.74	0.64	0.0334	
0.006	1.7	1.4	0.0343	
0.008	2.8	2.6	0.0343	
0.01	3.8	4.0	0.0343	0.0353
0.02	17	16	0.0334	0.0410
0.03	33	36	0.0343	0.0429
0.04	51	55	0.0343	0.0458

a. Calculated using $K_3 k_{Am}$ $4 \times 10^4\ l^2\ mol^{-2}\ s^{-1}$.

b. Measured at 450nm at completion of the 3-adduct formation. A 2mm pathlength cell was used.

c. Measured at 450nm at the completion of the second colour forming process.

Rate and equilibrium measurements for the σ-adduct formation reaction between HNS and piperidine in DMSO containing 0.1M piperidinium perchlorate, data in Table 8.5, or 0.1M piperidinium chloride, data in Table 8.6, have been made using stopped-flow spectrophotometry. At the concentrations studied

Scheme 8.3

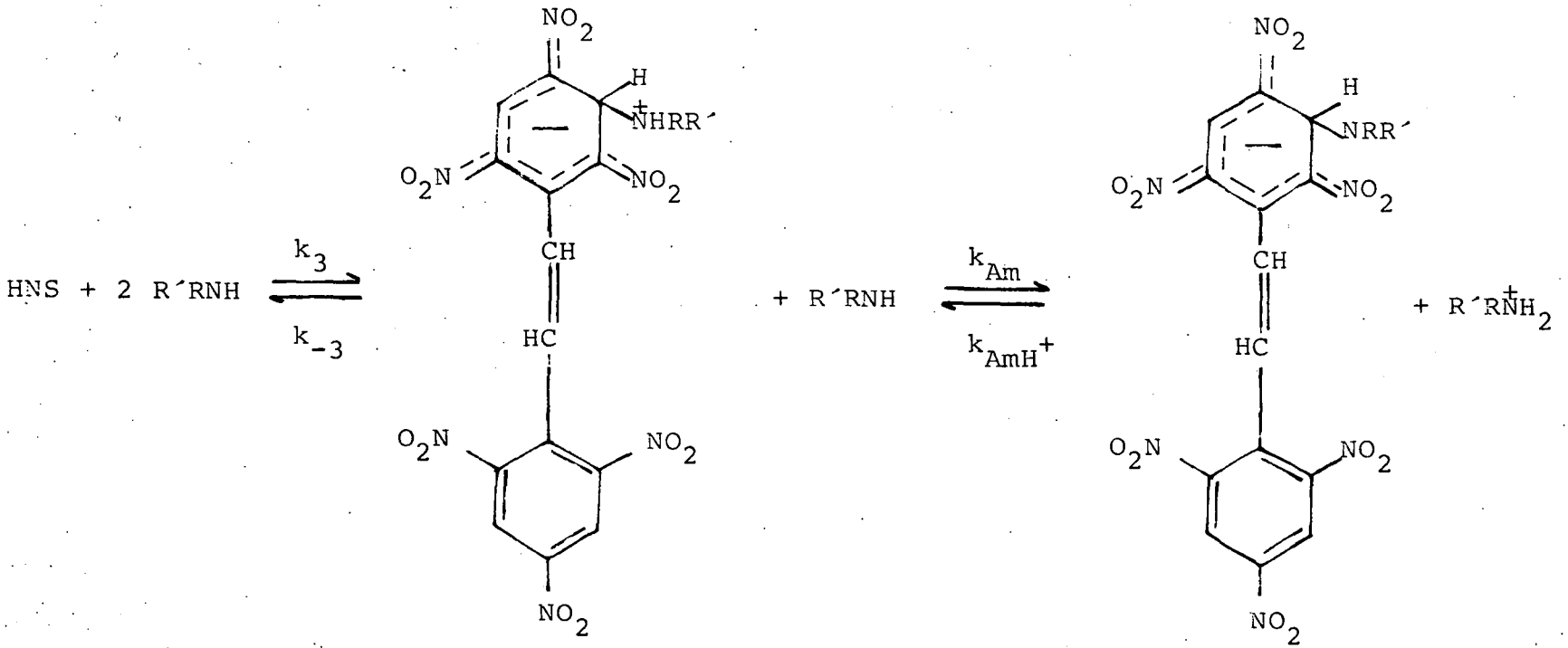
HNS + 2 R´RNH
k3
k-3
NO2
H
NHRR´
O2N
NO2
CH
HC
O2N
NO2
NO2
(8.2.Z)
+ R´RNH
kAm
kAmH+
NO2
H
NRR´
O2N
NO2
CH
HC
O2N
NO2
NO2
+ R´RNH2
(8.2)

TABLE 8.5 Kinetic and equilibrium data for the reaction of HNS (1×10^{-5} M) with piperidine in DMSO containing 0.1 M piperidinium perchlorate at 25°C

[Piperidine]/M	k_{obs}/s^{-1}	k^{a}_{calc}/s^{-1}	OD(450nm)	$K^{b}_{c,3}$/l mol^{-1}
0.01	31±1	31	0.0060	168
0.015	33	36	0.0100	140
0.02	43	43	0.0148	138
0.025	52	52	0.0191	135
0.03	60	63	0.0241	152
0.04	86	91	0.0287	138

a. Calculated using K_3k_{Am} 4×10^4 l^2 mol^{-2} s^{-1}, k_{AmH}+ 270 l mol^{-1} s^{-1} and equation 8.4.

b. Calculated using an optical density for complete conversion to 3-adduct of 0.0417 and equation 8.6.

TABLE 8.6 Kinetic and equilibrium data for the reaction between HNS (1×10^{-5} M) and piperidine in DMSO containing 0.1 M piperidinium chloride at 25°C

[Piperidine]/M	k_{obs}/s^{-1}	k^{a}_{calc}/s^{-1}	OD^{b}(450nm)	$K^{c}_{c,3}$/l mol^{-1}
0.0075	14	14	0.0057	324
0.01	16	16	0.0089	317
0.015	20	20	0.0141	274
0.02	25	27	0.0218	359
0.03	44	45	0.0269	296
0.04	64	71	0.0306	298

a. Calculated using K_3k_{Am} 3.7×10^4 l^2 mol^{-2} s^{-1}, k_{AmH}+ 120 l mol^{-1} s^{-1} and equation 8.4.

b. Measured using a 2mm pathlength cell.

c. Calculated using an optical density for complete conversion to 3-adduct of 0.0370 and equation 8.6.

only one colour forming process was observed. Both sets of data are best interpreted using equation 8.4, which is a modified form of equation 8.1 noting the assumption that $k_{-3} >> k_{Am}[Am]$.

$$k_{obs} = K_3 k_{Am}[Am]^2 + k_{AmH}{}^+[AmH^+] \qquad \text{(equation 8.4}$$

In 0.1M piperidinium perchlorate solution a plot of k_{obs} versus $[Am]^2$ is linear and gives values for $K_3 k_{Am}$ of 4×10^4 l^2 mol^{-2} s^{-1} and for $k_{AmH}{}^+$ of 270 l mol^{-1} s^{-1}. Combination of these values gives a value for $K_{c,3}$ (defined in equation 8.5) of 148 l mol^{-1}. This value is in good agreement with the $K_{c,3}$

$$K_{c,3} = \frac{k_3 . k_{Am}}{k_{-3} . k_{AmH}{}^+} \qquad \text{(equation 8.5)}$$

value calculated from the optical density measurements using equation 8.6. In 0.1M piperidinium chloride solution equation 8.4 again fitted the data to give a value for $K_3 k_{Am}$ of

$$K_{c,3} = \frac{[8.2]\ [AmH^+]}{[8.1]\ [Am]^2} \qquad \text{(equation 8.6)}$$

3.7×10^4 l^2 mol^{-2} s^{-1} and for $k_{AmH}{}^+$ of 120 l mol^{-1} s^{-1}. Using equation 8.5 gives a value for $K_{c,3}$ of 310 l mol^{-1} which is in reasonable agreement with the $K_{c,3}$ value calculated from the optical density values.

8.3.4 Reaction with pyrrolidine

Mixing solutions in DMSO of HNS (2×10^{-5}M) and pyrrolidine (0.001-0.1M) results in the rapid formation of a red species whose visible spectra, λ_{max} 450nm and 520-530nm, is typical of σ-adducts.[92] There is a slow subsequent reaction giving rise to an increase in absorption at 630-640nm.

Spectra recorded in the presence of a 0.1M pyrrolidinium perchlorate indicate the slow formation of a species with λ_{max} *ca* 510nm. This is thought to be the adduct (8.6; R´RN = C_4H_8N) formed by amine addition to the olefinic bond. The analogous reaction of HNS with methanolic methoxide has been described in Chapter Five. When [pyrrolidine]<0.05M little of the σ-adduct formed by attack on the aromatic ring is observed but at higher amine concentrations the visible spectra show fast formation of (8.2; R´RN = C_4H_8N) followed by conversion to (8.6).

Kinetic data for the rapid reaction giving (8.6; R´RN = C_4H_8N) were obtained by stopped-flow spectrophotometry in solutions containing pyrrolidine in DMSO with and without added tetraethylammonium perchlorate (to maintain constant ionic strength). They are presented in Table 8.7. A very much slower colour forming reaction was also observed and optical densities at the completion of the reaction are also given. The data in Table 8.7 are interpreted using Scheme 8.3 and equation 8.7 (a modification of equation 8.2). Values for K_3k_{Am}

$$k_{obs} = \frac{K_3k_{Am}[Am]^2}{1 + \frac{k_{Am}}{k_{-3}}[Am]} \qquad \text{(equation 8.7)}$$

7.5×10^5 l^2 mol^{-2} s^{-1} and for k_{Am}/k_{-3} of 21 l mol^{-1} give calculated rate coefficients which best fit the data. They are intermediate between the observed rate coefficients measured in DMSO and in DMSO containing 0.1M tetramethylammonium perchlorate. The value of k_{Am}/k_{-3} is the parameter most subject to error.

Further rate and equilibrium measurements have been made on the fast process. Table 8.8 contains data measured in DMSO containing 0.006M pyrrolidine with varying pyrrolidinium

TABLE 8.7 Kinetic and equilibrium data for the reaction of HNS (1×10^{-5} M) and pyrrolidine in DMSO at 25°C

[Pyrrolidine]/M	k^a_{obs}/s^{-1}	k^b_{calc}/s^{-1}	k^c_{obs}/s^{-1}	OD^d_{fast} (450nm)	OD^e_{slow} (450r
0.004	10.1	11.1	11.5	0.042	0.044
0.005		17.0	18.6	0.042	0.044
0.006	23.5	24.0	27	0.042	0.045
0.008	35	41	46	0.042	0.048
0.010	55	62	60	0.042	0.050

a. These measurements were made in DMSO.

b. Calculated using K_3k_{Am} 7.5×10^5 l^2 mol^{-2} s^{-1}, k_{Am}/k_{-3} 21 l mol^{-1} and equation 8.7.

c. These measurements were made in DMSO, containing 0.1M tetraethylammonium perchlorate.

d. Measured at completion of the fast process.

e. Measured at completion of the second process.

TABLE 8.8 Kinetic and equilibrium data for the reaction of HNS (1×10^{-5} M) with pyrrolidine (0.006M) in DMSO containing pyrrolidinium perchlorate at 25°C

[Pyrrolidine perchlorate]/M	k^a_{obs}/s^{-1}	k^b_{calc}	OD^c (450nm)	$K^d_{c,3}/l\ mol^{-1}$
0	24	24	0.0419	
0.002	27	28	0.0343	252
0.004	31	31	0.0311	320
0.007	37	37	0.0241	263
0.01	43	43	0.0218	301
0.02	59	61	0.0155	326

a. Ionic strength = 0.1M by using tetraethylammonium perchlorate

b. Calculated using K_3k_{Am} 7.5×10^5 l^2 mol^{-2} s^{-1}, k_{Am}/k_{-3} 21 l mol^{-1}, k_{AmH^+} 2100 l mol^{-1} s^{-1} and equation 8.8.

c. Measured at completion of the first process.

d. Calculated using $K_{c,3} = OD(450)[AmH^+]/[0.0419-OD(450)][Am]^2$.

perchlorate concentrations. They are interpreted using equation 8.8 which is a modified form of equation 8.2. Using the previous values for K_3k_{Am} of 7.5×10^5 l^2 mol^{-2} s^{-1} and for k_{Am}/k_{-3} of 21 l mol^{-1} a value for $k_{AmH}+$ of 2100 l mol^{-1} s^{-1} can be calculated. The data given in Table 8.9 were measured

$$k_{obs} = \frac{K_3k_{Am}[Am]^2 + k_{AmH}+[AmH^+]}{k + \frac{k_{Am}}{k_{-3}}[Am]} \qquad \text{(equation 8.8)}$$

in DMSO solutions containing 0.01 M or 0.02 M pyrrolidinium perchlorate They are again best fitted using equation 8.8 with values for K_3k_{Am} of (7.5±0.3) x 10^5 l^2 mol^{-2} s^{-1}, for k_{Am}/k_{-3} of 21±6 l mol^{-1} and for $k_{AmH}+$ of 2100±100 l mol^{-1} s^{-1}. The overall equilibrium constant $K_{c,3}$, defined by equation 8.5, is calculated as 360 l mol^{-1}, which is in agreement with a value for $K_{c,3}$ calculated from the optical density data.

A conventional spectrophotometer was used at a wavelength of 510nm to measure a very slow colour forming process, which followed the rapid colour forming process measured on the stopped-flow spectrophotometer. This reaction is interpreted as amine attack on the olefinic bond of HNS as shown in Scheme 8.4. The rate expression allowing for preliminary formation of the 3-adduct is given by equation 8.9. However by assuming $k_{Am}[Am] >> k_{-b}$ equation 8.9 reduces to equation 8.10. The value of $k_{-b}k_{AmH}+[AmH^+]/k_{Am}[Am]$ is expected to be small (the equivalent term for methoxide attack on the olefinic bond of HNS in methanol was shown to be very small in Chapter Five) so that equation 8.10 can be modified into equation 8.11. For the data given in

$$k_{obs} = \frac{k_bk_{Am}[Am]^2}{(k_{-b}+k_{Am}[Am])(1+K_{c,3}[Am]^2/[AmH+])} + \frac{k_{-b}k_{AmH}+[AmH^+]}{k_{-b}+k_{Am}[Am]} \qquad \text{(equation 8.9}$$

$$K_{c,1} = \frac{[8.4]\ [AmH^+]}{[HNS]\ [Am]^2}$$ (equation 8.12

$$K_{D,1} = \frac{[8.5]\ [AmH^+]}{[8.4]\ [Am]^2}$$ (equation 8.13

$$[HNS]_o = [HNS] + [8.4] + [8.5]$$ (equation 8.14

line can be extrapolated to give a value for the optical density of complete conversion to the di-adduct of 0.0926. Because a curved line is extrapolated this value is subject to large error. It is assumed the optical density of complete conversion to the mono-adduct is 0.0463, *i.e.* half that of the di-adduct. Using these values and equations 8.12, 8.13 and 8.14 values for $K_{c,1}$ of 4500 l mol^{-1} and for $K_{D,1}$ of 65 l mol^{-1} fit the data in Table 8.11.

Kinetic measurements were limited to low n-butylamine concentrations where only σ-adducts of 1:1 stoichiometry were observed. Two fast processes were observed which are taken to be amine attack at the 3-position to give (8.2; R´RN = $CH_3CH_2CH_2CH_2NH$) followed by amine attack at the 1-position to give (8.4; R´RN = $CH_3CH_2CH_2CH_2NH$). The general rate expression derived from Scheme 8.3 for formation of the 3-adduct is given by equation 8.1.

The rate data for the faster process, obtained in solutions without added n-butylammonium ions, is given in Table 8.12. The data fits equation 8.15 which is derived from equation 8.1 when $k_{Am}[Am] >> k_{-3}$ and $[AmH^+]$ is extremely small. A value for k_3 of 5300±300 l mol^{-1} s^{-1} is calculated.

$$k_{obs} = k_3[Am]$$ (equation 8.15

TABLE 8.12 Rate measurements for formation of (8.2; R´RN = $CH_3CH_2CH_2CH_2NH$) from HNS (5×10^{-6}M) and n-butylamine in DMSO at 25°C

[n-butylamine]/M	k_{obs}/s^{-1}	k_3^a/l $mol^{-1}s^{-1}$	OD[b](460nm)
0.005	26.3	5250	0.0182
0.006	30.3	5050	0.0186
0.008	43.3	5400	0.0186
0.010	54.8	5500	0.0195
0.012	64.1	5350	0.0186

a. $k_3 = k_{obs}/[Am]$

b. Measured at completion of the first process. Indicates conversion to 3-adduct >95%.

In solutions containing 0.1M n-butylammonium perchlorate the formation of the 3-adduct is too rapid for rate measurements but at higher amine concentrations a value for $K_{c,3}$ of 146±5 l mol^{-1} can be calculated from the equilibrium optical densities. These data along with rate measurements for the formation of the 1-adduct are given in Table 8.13. The scheme for σ-adduct formation by amine addition at the 1-position is given in Scheme 8.6, from which the general rate expression, given by equation 8.16, is derived. This includes a term which allows for preliminary formation of the 3-adduct. The data in Table 8.13 best fits equation 8.17, which is a modified form of equation 8.16.

$$k_{obs} = \frac{k_1 k_{Am}[Am]^2}{(k_{-1}+k_{Am}[Am])(1+K_{c,3}[Am]^2/[AmH^+])} + \frac{k_{-1}k_{AmH^+}[AmH^+]}{k_{-1}+k_{Am}[Am]} \quad \text{(equation 8}$$

Scheme 8.6

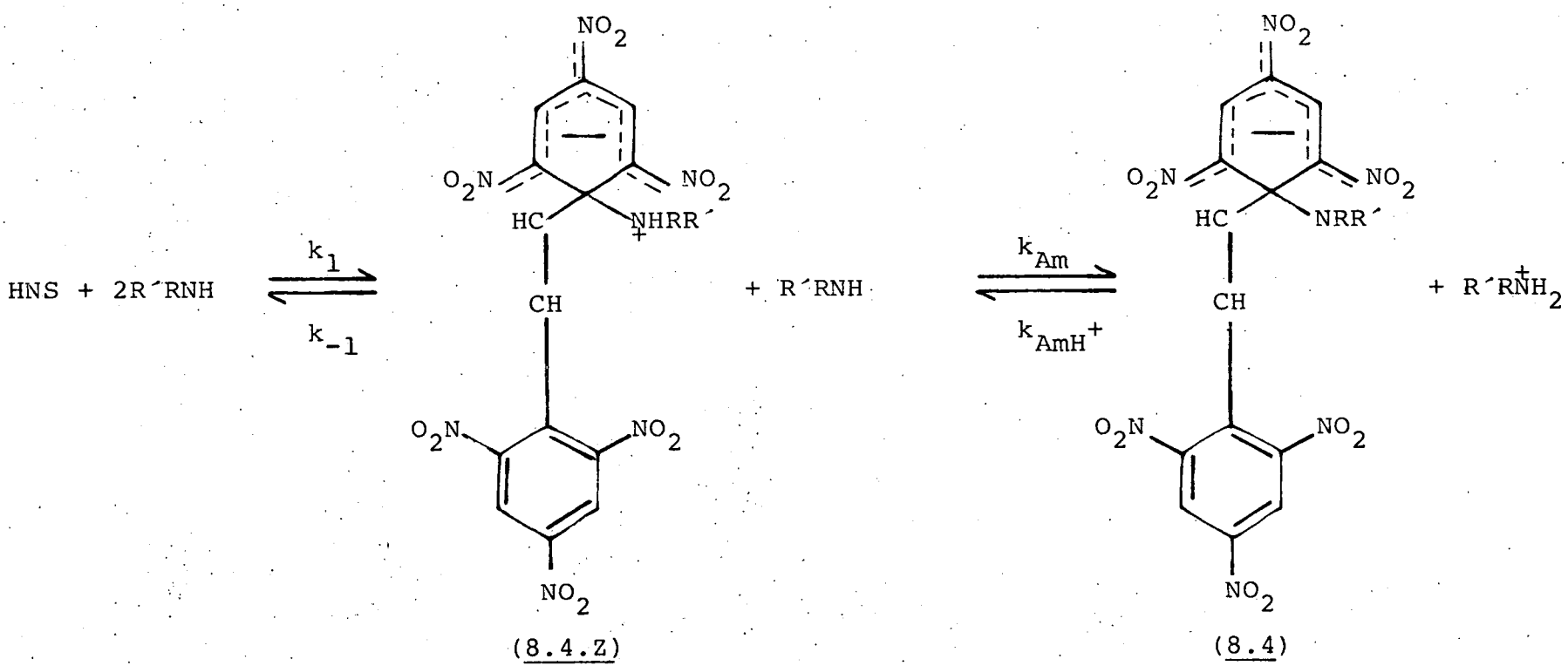

(8.4.Z) (8.4)

TABLE 8.13 Kinetic and equilibrium data for the σ-adduct forming reactions of HNS (1×10^{-5} M) with n-butylamine in DMSO containing 0.1 M n-butylammonium perchlorate at 25°C

[n-butylamine]/M	OD_3^a(455nm)	$K_{c,3}^b$/l mol^{-1}	k_{obs}/s^{-1}	k_{calc}^c/s^{-1}
0.001			13.2	12.9
0.002			9.3	8.9
0.004			7.1	7.2
0.006			7.3	7.4
0.008			7.9	8.0
0.010			8.6	8.8
0.015	0.0092	149	10.2	10.4
0.020			11.8	11.3
0.030	0.0205	141		
0.040	0.0259	151	12.1	10.4
0.050	0.0287	145		
0.060	0.0306	142	11.3	8.3
0.080	0.0362		10.9	6.7

a. Measured at the completion of the formation of the 3-adduct. A Benesi-Hildebrand type plot[76] gives an optical density for complete conversion to the 3-adduct of 0.0366.

b. Calculated using $K_{c,3} = \frac{OD_3(455)\ [AmH^+]}{[0.0366-OD_3(455)][Am]^2}$

c. Calculated using k_1 840 l mol^{-1} s^{-1}, k_{Am}/k_{-1} 1575 l mol^{-1}, k_{AmH^+} 320 l mol^{-1} s^{-1}, $K_{c,3}$ 146 l mol^{-1} and equation 8.17.

$$k_{obs} = \frac{k_1 k_{Am}[Am]^2/k_{-1}}{(1+k_{\frac{Am}{k_{-1}}}[Am])(1+K_{c,3}[Am]^2/[AmH^+])} + \frac{k_{AmH^+}[AmH^+]}{1+k_{\frac{Am}{k_{-1}}}[Am]}$$ (equation 8.

Using the calculated value for $K_{c,3}$ of 146 l mol^{-1} the data for n-butylamine concentrations <0.02M are best fitted using the values: k_1 840 l mol^{-1} s^{-1}, k_{Am}/k_{-1} 1575 l mol^{-1} and k_{AmH^+} 320 l mol^{-1} s^{-1}. For n-butylamine concentrations ≥0.02M k_{obs}, the observed rate coefficient, is found to be larger than k_{calc}, the calculated rate coefficient. In these solutions the optical density data indicate the presence of appreciable amounts of the di-adduct, which probably accounts for this discrepancy. The equilibrium constant $K_{c,1}$ calculated from the kinetic parameters gives a value of 4200 l mol^{-1} which is in good agreement with that calculated from the optical density measurements in Table 8.11.

The kinetic and equilibrium data measured in the presence of 0.1M n-butylammonium chloride are given in Table 8.14. No independent value for $K_{c,3}$ was measured, but a value of $K_{c,3}$ of 292 l mol^{-1} was used by assuming, as found previously, that equilibrium constants for adducts of 1:1 stoichiometry are about twice as large in solutions containing substituted ammonium chloride ions than those containing substituted ammonium perchlorate ions.[92,151] Using the parameters k_1 840 l mol^{-1} s^{-1}, k_{Am}/k_{-1} 1575 l mol^{-1}, k_{AmH^+} 176 l mol^{-1} s^{-1} and the value for $K_{c,3}$ of 292 l mol^{-1} with equation 8.17, good agreement between k_{calc} and k_{obs} is obtained. It is observed that $k_{obs} > k_{calc}$ for the last two n-butylamine concentrations which again suggests that at these n-butylamine concentrations there may be some formation of the 1:2 adduct.

TABLE 8.14 Kinetic and equilibrium data for the σ-adduct forming reactions of HNS (1×10^{-5}M) with n-butylamine in DMSO containing 0.1M n-butylammonium chloride at 25°C

[n-butylamine]/M	k_{obs}/s^{-1}	k^{a}_{calc}/s^{-1}	OD[b] (455nm)
0.0006	9.28	9.29	0.0016
0.0008	8.15	8.16	0.0028
0.001	7.50	7.35	0.0037
0.002	5.24	5.50	0.0109
0.004	5.02	5.18	0.0308
0.006	5.96	5.81	0.0400
0.008	6.82	6.54	0.0448
0.010	8.06	7.16	0.0467

a. Calculated using k_1 840 l mol^{-1} s^{-1}, k_{Am}/k_{-1} 1575 l mol^{-1}, k_{AmH^+} 176 l mol^{-1} s^{-1}, $K_{c,3}$ 292 l mol^{-1} and equation 8.17.

b. Measured at completion of the colour forming process.

8.3.6 Reaction with benzylamine

Visible spectra for the reaction of HNS with benzylamine in DMSO are similar to those of HNS with n-butylamine. In solutions without added benzylammonium salts the visible spectra of HNS (1×10^{-5}M) with benzylamine (0.001-0.1M) are typical of σ-adducts[92] and appear to be very stable. The maxima as the amine concentrations increase move from 450nm and 540nm with 0.001M benzylamine to 458 and 510nm with 0.1M benzylamine as shown in Figure 8.3. The first is probably the visible spectrum of the 1:1 adduct (8.4; R´RN = $C_6H_5CH_2NH$) while the second is that of the 1:2 adduct (8.5; R´RN = $C_6H_5CH_2NH$). In solutions containing 0.1M benzylammonium chloride, HNS (1×10^{-5}M) and benzyl-

Figure 8.3 Visible spectra of the σ-adduct formation reaction between HNS (1×10^{-5} M) and A 0.001M benzylamine; B 0.1M benzylamine in DMSO.

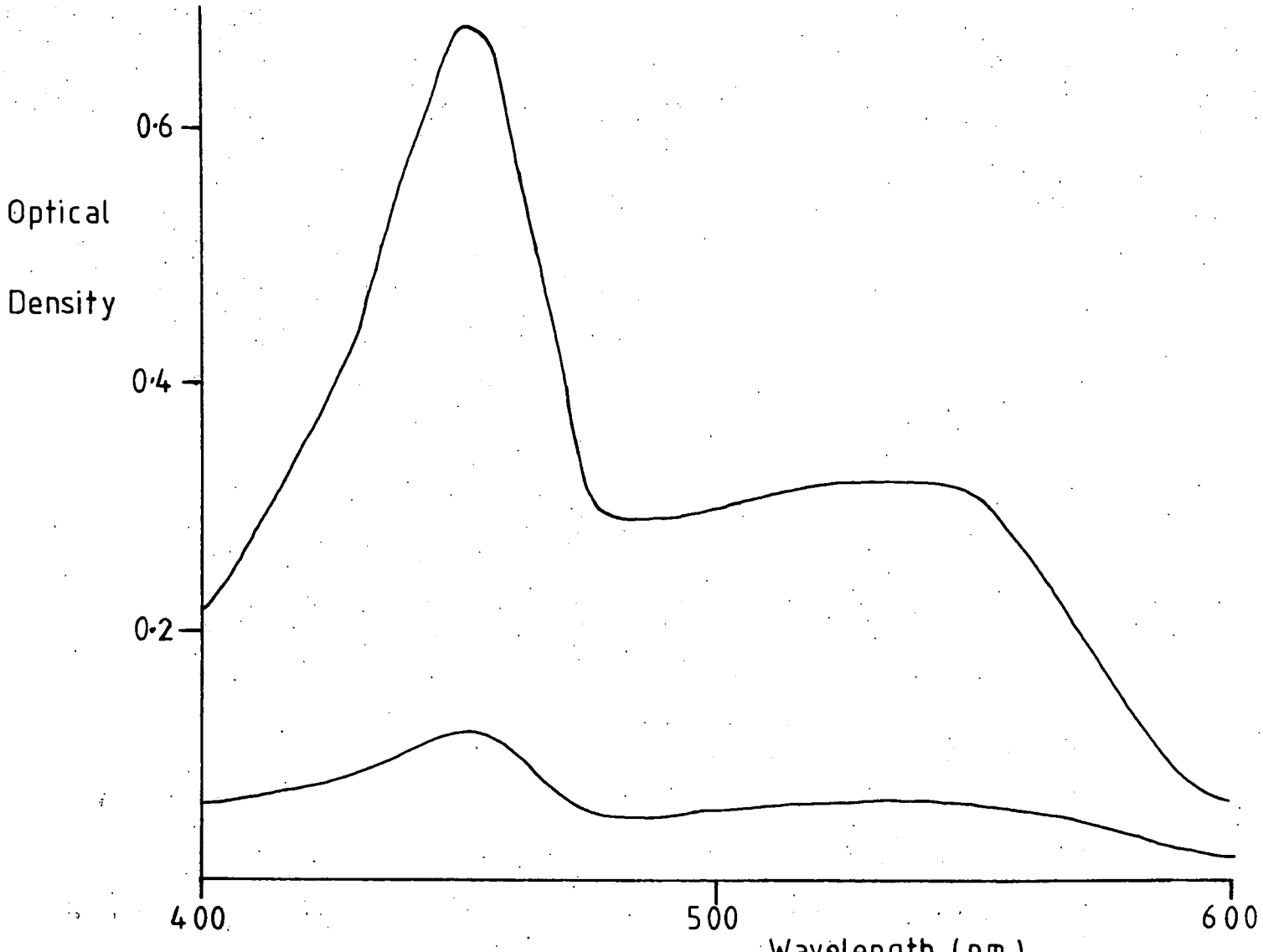

TABLE 8.15 Equilibrium data for σ-adduct formation from HNS (4×10^{-5} M) in DMSO containing 0.1 M benzylammonium perchlorate at 25°C

[Benzylamine]/M	OD_{obs} (530nm)	OD^{a}_{calc} (530nm)
0.00195	0.007	0.004
0.00396	0.020	0.015
0.00594	0.034	0.033
0.00790	0.058	0.055
0.00985	0.086	0.081
0.0195	0.210	0.219
0.0383	0.365	0.389
0.0603	0.470	0.468
0.0804	0.513	0.507
0.101	0.540	0.533
0.201	0.648	0.641
0.402	0.777	0.812
0.603	0.904	0.907
0.804	0.963	0.956
0.979	0.990	0.980
1.175	1.005	0.997

a. Calculated using $K_{c,1}$ 190 l mol^{-1}, $K_{D,1}$ 0.8 l mol^{-1} and optical densities for complete conversion for the 1:1 adduct of 0.52, and for the 1:2 adduct of 1.04.

amine (0.001-0.1M), σ-adduct formation is observed with maxima at 450 and 530-540nm. Very slowly a maximum at *ca* 500nm appears to replace the σ-adduct maxima. This is probably amine attack on the olefinic bond to produce the adduct (8.6; $C_6H_5CH_2NH{=}RR'N$).

Table 8.15 shows optical density data of the σ-adduct formation reactions in solutions containing 0.1M benzylammonium perchlorate. Using equations 8.12, 8.13 and 8.14 the values for $K_{c,3}$ of 190 l mol^{-1} and $K_{D,1}$ of 0.8 l mol^{-1} are calculated.

Kinetic studies have once again been limited to adducts of 1:1 stoichiometry. In solutions containing no added benzylammonium ions a value for k_3 of 1200±150 l $mol^{-1}s^{-1}$ has been calculated using equation 8.15 for the data in Table 8.16.

TABLE 8.16 Kinetic and equilibrium data for the reaction of HNS (1×10^{-5}M) with benzylamine in DMSO at 25°C

[Benzylamine]/M	k_{obs}/s^{-1}	k_3^a/l mol^{-1} s^{-1}	OD(455nm)
0.015	16.2±0.5	1100	0.040
0.020	21.4	1100	0.041
0.025	25.9	1050	0.040
0.030	38.5	1300	0.042
0.035	45.8	1300	0.042
0.040	48.7	1200	0.041

a. $k_3 = k_{obs}/[Am]$.

Table 8.17 contains the data for the formation of the 1-adduct in solutions containing 0.1M benzylammonium perchlorate. The data are best fitted using equation 8.17 and values for K_1k_{Am} of 6.8×10^4 l^2 mol^{-2} s^{-1}, for k_{AmH^+} of 310 l mol^{-1} s^{-1}, for k_{Am}/k_{-3} of 245 l mol^{-1} and $K_{c,3}$ 7.3±0.2 l mol^{-1}. $K_{c,3}$ is calculated from equilibrium optical densities at the higher amine

TABLE 8.17 Kinetic and equilibrium data for σ-adduct formation from HNS (1×10^{-5} M) and benzylamine in DMSO containing 0.1M benzylammonium perchlorate at 25°C

[Benzylamine]/M	OD_3^a(450nm)	$K_{c,3}^b$/l mol^{-1}	k_{obs}/s^{-1}	k_{calc}^c/s^{-1}	OD_1(450nm)
0.004			17.7	16.2	0.0019
0.006			13.3	13.5	0.0036
0.008			12.9	11.9	0.0062
0.01			11.2	10.9	0.0087
0.02			10.2	9.7	0.0106
0.04			11.7	11.9	0.0438
0.06			14.5	14.3	0.0526
0.08			17.0	15.9	0.0565
0.10	0.0177	7.3	17.8	16.6	0.0595
0.15	0.0259	7.2	19.5	16.2	0.0655
0.20	0.0315	7.5	19.0	14.5	0.0706
0.25	0.0343	7.1	18.5	12.8	0.0757

a. Measured at completion of the 3-adduct formation reaction. A Benesi-Hildebrand type plot[76] yields OD_3 for complete conversion to the 3-adduct of 0.0420.

b. Calculated from $K_{c,3} = OD_3(450)[AmH^+]/[0.0420-OD_3(450)][Am]^2$.

c. Calculated using K_1k_{Am} 6.8×10^4 l^2 mol^{-2} s^{-1}, k_{AmH^+} 310 l mol^{-1} s^{-1}, k_{Am}/k_{-1} 245 l mol^{-1}, $K_{c,3}$ 7.3 l mol^{-1} and equation 8.17.

d. Measured at completion of the 1-adduct formation reaction.

concentrations. From the rate coefficients $K_{c,1}$ is calculated as 220 l mol^{-1}. At the higher benzylamine concentrations a mixture of 1:1 and 1:2 adducts will be present thus causing k_{obs} to be larger than k_{calc}. Table 8.18 shows data measured in solutions containing 0.01 and 0.006M benzylamine. At these amine concentrations the concentration of the 1:2 adduct is very small. The rate and equilibrium coefficients calculated above fit these data using equation 8.18. The $K_{c,1}$ value calculated using the optical density data is found to be 213±15 l mo which is in good agreement with the $K_{c,1}$ value calculated from the kinetic data.

Table 8.19 contains the data for the formation of the 1-adduct in solutions containing 0.1M benzylammonium chloride. the data are best fitted using values for K_1k_{Am} of 7.4 x 10^4 l^2 mol^{-2} s^{-1}, k_{AmH^+} of 160 l mol^{-1} s^{-1}, k_{Am}/k_{-1} of 160 l mol^{-1}, $K_{c,3}$ of 16.9±1.5 l mol^{-1} (again measured from optical densities of the 3-adduct at high benzylamine concentrations) and equation 8.17. Again at the high benzylamine concentrations there will be appreciable amounts of the 1:2 adduct formed and this probably accounts for the discrepancy between the observed and calculated rate coefficients at these concentrations.

TABLE 8.18 Kinetic and equilibrium data for σ-adduct formation from HNS (2×10^{-5} M) and benzylamine in DMSO containing benzylammonium perchlorate at 25°C

[Benzylamine]/M	[Benzylamine perchlorate]/M	k_{obs}/s^{-1}	k^{a}_{calc}/s^{-1}	OD(450nm)[b]	$K^{c}_{c,1}$/ l mol^{-1}
0.01	0.01	2.8	2.7	0.0820	191
0.01	0.02	3.7	3.7	0.0635	207
0.01	0.04	5.5	5.5	0.0419	202
0.01	0.06	7.4	7.3	0.0334	219
0.01	0.08	8.9	9.1	0.0278	229
0.01	0.10	11.2	10.9	0.0214	207
0.006	0.01	2.2	2.2	0.0555	222
0.006	0.02	3.4	3.5	0.0348	214
0.006	0.04	5.9	6.0	0.0200	212
0.006	0.06	8.6	8.5	0.0144	217
0.006	0.08	10.9	11.0	0.0111	217
0.006	0.10	13.3	13.5	0.0092	221

a. Calculated using $K_1 k_{Am}$ 6.8×10^4 l^2 mol^{-2} s^{-1}, k_{AmH^+} 310 l mol^{-1} s^{-1}, k_{Am}/k_{-1} 245 l mol^{-1}, $K_{c,3}$ 7.3 l mol^{-1} and equation 8.17.

b. Measured at completion of the process. A Benesi-Hildebrand type plot[76] gives an optical density for complete conversion of 0.125.

c. Calculated using $K_{c,1} = OD(450)[AmH^+]/[0.125-OD(450)][Am]^2$.

TABLE 8.19 Kinetic and equilibrium data for σ-adduct formation from HNS (1×10^{-5} M) and benzylamine in DMSO containing 0.1M benzylammonium chloride at 25°C

[Benzylamine]/M	OD_3(450nm)[a]	$K^b_{c,3}$/l mol^{-1}	k_{obs}/s^{-1}	k^c_{calc}/s^{-1}	OD^d_1(450nm)
0.002			11.6±0.8	10.9	0.0014
0.004			8.2	8.7	0.0041
0.006			7.5	7.6	0.0078
0.008			7.0	7.0	0.0120
0.01			6.7	6.8	0.0164
0.02			6.9	7.4	0.0334
0.04			10.0	10.1	0.0477
0.06	0.0123	14.6	12.2	11.6	0.0526
0.07	0.0168	18.1			0.0565
0.08	0.0186	17.0	13.4	11.8	0.0585
0.10	0.0223	16.6			0.0605
0.15	0.0287	18.2	14.1	9.6	0.0655

a. Measured at completion of the formation of the 3-adduct. A Benesi-Hildebrand type plot[76] gives a OD_3 for complete conversion to the 3-adduct of 0.0357.

b. Calculated using $K_{c,3} = OD_3(450)[AmH^+]/[0.0357-OD_3(45C)][Am]$

c. Calculated using K_1k_{Am} 7.4×10^4 l^2 mol^{-2} s^{-1}, k_{AmH^+} 160 l mol^{-1}s^{-1} k_{Am}/k_{-1} 245 l mol^{-1}, $K_{c,3}$ 16.9 l mol^{-1} and equation 8.17.

d. Measured at completion of the 1-adduct formation reaction.

8.4 Discussion

As observed in the previous two chapters, and in agreement with previous work[86,151], the equilibrium constants $K_{c,1}$ and $K_{c,}$ have values *ca* twice as large in solutions containing 0.1M substituted ammonium chloride as in solutions containing 0.1M substituted ammonium perchlorate. Also the values of k_{AmH}^{+} are reduced by a factor of two. These observations have been attributed to the stabilising ability of the substituted ammoniu ions with the chloride ions.[86,151] Unless specifically stated this discussion will concentrate on the data obtained in the presence of perchlorate salts. Also the values of k_3, $K_{c,3}$, K_3k_{Am}, k_1 and $K_{c,1}$ for HNBB and HNS have been statistically corrected. This correction is necessary to allow for the presence of two picryl rings in these compounds and is achieved by dividing the afore-mentioned constants by two.

8.4.1 Attack at the unsubstituted positions

Table 8.20 compares the kinetic and equilibrium data for amine attack at the unsubstituted or 3-position of HNS, HNBB TNBCl and 1,3,5-trinitrobenzene (TNB). The assumption that the rate and equilibrium data for the reaction of HNS with piperidin and pyrrolidine refers to attack at the 3-position is justified by the way they fit regularly into the pattern for reaction at unsubstituted positions. In particular the values of k_{AmH}^{+} are those expected for attack at the 3-position,[152] as shown in Chapters Six and Seven.

The equilibrium constant $K_{c,3}$ increases in the order HNBB < HNS, TNBCl < TNB, after statistical correction, for each amine used. The reduction in values of $K_{c,3}$ for the substitute

TABLE 8.20 Comparison of kinetic data and equilibrium data (statistically corrected) for reaction at unsubstituted ring positions[a] in DMSO at 25°C

		Benzylamine	n-Butylamine	Pyrrolidine	Piperidine
k_3 (l mol^{-1}s^{-1})	HNBB	275	850	4000_4	>2500
	HNS	800	2700	1.8×10^4	>4000
	TNBCl	1000	3000	1.7×10^5	1.3×10^5
	TNB	13000	45000	7.5×10^5	$>2 \times 10^5$
$K_{c,3}$ (l mol^{-1})	HNBB	0.6	13	40	13
	HNS	3.7	73	180	75
	TNBCl	5	73	240	93
	TNB	105	1000	3500	2140
K_3k_{Am} (l^{2}mol^{-2}s^{-1})	HNBB			1.5×10^5	6000
	HNS			3.7×10^5	2×10^4
	TNBCl			5.8×10^5	2.6×10^4
	TNB			1.0×10^7	6×10^5
k_{Am}/k_{-3} (l mol^{-1})	HNBB			40	< 2
	HNS			21	< 5
	TNBCl			34	< 2
	TNB			14	<10
k_{AmH^+} (l mol^{-1}s^{-1})	HNBB			3900	420
	HNS			2100	270
	TNBCl			2400	280
	TNB			3000	280
$k_{-3}k_{AmH^+}/k_{Am}$ (s^{-1})	HNBB	450	70	100	>200
	HNS	160	37	97	> 55
	TNBCl	200	41	70	>140
	TNB	125	45	210	> 90

a. Data for HNBB from Chapter Seven; for TNBCl from Chapter Six; and for TNB from reference 152 and 153.

The measured values of HNBB and HNS have been statistically corrected to allow for the presence, in these compounds, of two picryl rings. Measured values of k_3, $K_{c,3}$, K_3k_{Am} have been divided by two.

compounds relative to TNB is probably due to the steric bulk of the 1-substituent which will force the ortho nitro-groups from the ring plane thus reducing their electron withdrawing ability.

The ratio k_{Am}/k_{AmH}^+ reflects the acidity of the zwitterionic intermediate relative to the acidity of the substituted ammonium ion and is unlikely to show a large variation with the nature of the substrate:[152] (also shown in Chapters Six and Seven). Values of k_3, the rate coefficient for attack at the 3-position, increase in the same order as values of $K_{c,3}^c$. However the $k_{-3}k_{AmH}^+/k_{Am}$ term changes relatively little with substrate and hence as neither does the ratio k_{Am}/k_{AmH}^+, then the values of k_{-3} are insensitive to substrate structure. Value of k_3 and $K_{c,3}$ decrease in the order pyrrolidine > piperidine, n-butylamine > benzylamine but the values of k_{-3} do not vary much with the nature of the amine. These observations may indicate that the transition states for amine attack at the 3-position on these compounds are "product like".

In the results section values of k_{AmH}^+, the rate coefficient for proton transfer between the anionic adduct and the zwitterion, have been directly measured for the secondary amines. The ratio k_{Am}/K_{AmH}^+ has previously been estimated[152,15] to have a value of 500. Therefore it is possible to calculate a value for k_{Am} of *ca* 10^6 l mol^{-1} s^{-1} for pyrrolidine and a value for k_{Am} of *ca* 10^5 l mol^{-1} s^{-1} for piperidine. The values of k_{Am} are significantly smaller than those expected for diffusion-controlled proton transfer reactions between nitrogen atoms. This is attributed to steric hindrance, particularly severe with piperidine, when the bulky amine approaches the zwitterion reaction centre.[152]

8.4.2 Attack at the substituted position

The formation of σ-adducts by amine attack at the substituted or 1-position of HNS was only observed for the primary amines n-butylamine and benzylamine. These amines, at high amine concentrations, also form the di-adducts by attack at the 1- and 1′-positions of HNS. The kinetic and equilibrium data for these processes are collected together in Table 8.21. Values of the equilibrium constants $K_{c,1}$ are larger than $K_{c,3}$ by factors of 29 for n-butylamine and 26 for benzylamine. The values of the rate coefficients k_1 are smaller than k_3 by a factor of *ca* 5. These changes reflect the steric and electronic effects of the CH=CHPic group. The 1-adduct is more stable than the 3-adduct because of the relief of steric strain, present in the parent molecule, when the CH=CHPic group is bent from the ring plane. The nitro-groups at the 2- and 6-positions are then able to become co-planar with the ring and exert their maximum electron withdrawal. An additional factor may be the inductive electron withdrawing effect of the Ch=CHPic group at the 1-position. The attack at the 1-position is slower than attack at the 3-position which may be attributed to F-strain,[160] (steric hindrance to the approach of the reagent). Once again it is necessary to note that k_{Am}/k_{AmH^+} will not vary greatly with the position of amine attack. Therefore from comparison of the third line and final line of data in Table 8.21 the ratios of k_{-3}/k_{-1} are 100-200, indicating very much slower expulsion of amine from the 1-position than from the 3-position.

The failure to observe attack at the 1-position in the reaction between HNS and secondary amines is probably once again due to the large steric requirements of such amines.[103,16]

TABLE 8.21 Kinetic and equilibrium data (statistically corrected) for σ-adduct formation between HNS and primary amines in DMSO at 25°C

	n-Butylamine	Benzylamine
$K_{c,3}$(1 mol^{-1})	73	3.7
k_3(1 mol^{-1} s^{-1})	2700	800
$k_{-3}k_{AmH^+}/k_{Am}$(s^{-1})	37	160
$K_{c,1}$(1 mol^{-1})	2300	1000
$K_{D,1}$(1 mol^{-1})	65	0.8
k_1(1 mol^{-1} s^{-1})	420	140
$k_{-1}k_{AmH^+}/k_{Am}$(s^{-1})	0.20	1.5

The sterically crowded 1-position due to the presence of two bulky groups would make the formation of the 1-adduct kinetically and/or thermodynamically unfavourable.

The values of $K_{D,1}$ for conversion of 1:1 adducts to 1:2 are lower than the $K_{c,1}$ values by factors of 350 for n-butylamine and 1250 for benzylamine. For comparison in Chapter Five it was reported that the corresponding factor for reaction with ethoxide ions is 80. Therefore, it is shown that even tho the picryl rings are well separated formation of the 1-adduct by attack at the 1-position inhibits attack at the 1′-position.

Table 8.21 compares data for the reactions of primar amines and HNBB, TNBCl and 2,4,6-trinitrophenetole (TNP) with those of HNS. The data for TNP are taken from the next chapter where the reactions of TNP with aliphatic amines in DMSO are reported. It is convenient for comparison purposes to report some of the TNP data here. $K_{c,1}$ values increase in the order

HNBB < HNS < TNBCl < TNP. Regarding the substrates as 1-substituted-2,4,6-trinitrobenzenes the order is the same as the inductive electron-withdrawal of the 1-substituent, with the ethoxy group being the most powerful.[137] However the $K_{c,1}$ values also are controlled by steric effects, as energy is gained when the 1-substituent rotates out of the plane of the ring on formation of the 1-adduct. It is impossible to estimate quantitatively the individual contribution of the electronic and steric effects to $K_{c,1}$. There is the possibility that adducts formed by attack at the 1-position of HNS and HNBB are still subject to steric strain so that the ortho nitro-groups are not coplanar with the ring. This is implied by the fact that the values of $K_{c,3}$ for TNB in Table 8.20, that is for amine attack at an unsubstituted position, are similar, for a given amine, to those observed for $K_{c,1}$ for HNS and are larger than $K_{c,3}$ values for HNBB.

Values of k_1 for HNBB, HNS and TNBCl increase in the same order as do values for $K_{c,1}$. However the value of k_1 for TNP is lower than expected on this basis. Electrostatic repulsion between the electronegative entering group and the ethoxy-substituent may be responsible.[171] Values of k_1 show a smaller variation, both with change in substrate and with amine, than do values of the ratio $k_{-1}k_{AmH^+}/k_{am}$. As before, values of the ratio K_{Am}/k_{AmH^+} are not expected to vary widely, so that the latter ratios give a measure of k_{-1} values. These values necessarily effect the k_{Am}/k_{-1} ratios which measure the susceptibility of adduct formation to base catalysis. Relatively low values are observed for HNS and TNBCl indicating a high susceptibility to catalysis. Values of k_{AmH^+} are in Table 8.22

TABLE 8.22 Comparison of kinetic and equilibrium data (statistically corrected) for the reaction at the substituted ring position[a] in DMSO at 25°C

		Benzylamine	n-Butylamine
$K_{c,1}$ (l mol^{-1})	HNBB	37	580
	HNS	95	2100
	TNBCl	1000	23000
	TNP	4700	50000
$K_{D,1}$ (l mol^{-1})	HNBB	0.6	17
	HNS	0.8	65
k_1 (l mol^{-1}s^{-1})	HNBB	30	75
	HNS	140	420
	TNBCl	230	630
	TNP	95	250
$k_1 k_{AmH^+}/k_{Am}$ (s^{-1})	HNBB	0.8	0.14
	HNS	1.5	0.20
	TNBCl	0.23	0.028
	TNP	0.02	0.005
k_{Am}/k_{-1} (l mol^{-1})	HNBB	> 1000	> 5000
	HNS	245	1600
	TNBCl	200	2000
	TNP	> 3000	> 1000
k_{AmH^+} (l mol^{-1}s^{-1})	HNBB	> 800	> 700
	HNS	310	320
	TNBCl	46	55
	TNP	> 60	> 50

a. Data for HNBB from Chapter Seven; for TNBCl from Chapter Six; and for TNP from Chapter Nine.

The measured values of $K_{c,1}$ and k_1 for HNBB and HNS have been divided by two to allow for the presence of two picryl rings (statistical correction).

Values of k_{Am} will be expected to be *ca* 500 times larger.[152] Nevertheless the values will be several orders of magnitude lower than those expected for diffusion-controlled reaction. This is attributed to the steric difficulties to the approach of the amine molecule to take off the excess proton from the zwitterionic intermediate. There are several other examples in the literature of slow proton transfers involving nitrogen centres.[172-174] Exactly the same explanation was used above for the same processes involving proton transfer between the anionic 3-adduct and its zwitterion.

8.4.3 Attack at the olefinic bond

Following σ-adduct formation HNS was observed, most clearly with pyrrolidine but also with the other amines reported in this chapter, to undergo a very slow reversible reaction to give a species with a maxima at *ca* 500nm. This species appears to be very thermodynamically stable and by analogy with related systems,[146,175,176] and because of similar observations for the reaction of HNS with methanolic methoxide ions in Chapter Five, it would seem probable that the species formed is (8.6), resulting from amine attack on the olefinic bond as shown by Scheme 8.4. Kinetic data were obtained for reaction of HNS with pyrrolidine and indicate that the rate-limiting step is reaction of HNS with amine. A rate constant of 0.52 l mol^{-1} was obtained.

8.5 Derivation of the Rate Expressions

The rate expressions for the formation of the 1- and 3-amido-adducts from HNS are derived in an analogous way to those formed from TNBCl, shown in Chapter Six.

(a) Formation of the σ-adduct by attack at the olefinic bond.

$$(\underline{8.1}) + 2Am \underset{k_{-b}}{\overset{k_b}{\rightleftharpoons}} (\underline{8.6.Z}) + Am \underset{k_{AmH^+}}{\overset{k_{Am}}{\rightleftharpoons}} (\underline{8.6}) + AmH^+$$

$$(\underline{8.1}) + 2Am \overset{K_{c,3}}{\rightleftharpoons} (\underline{8.2}) + AmH^+$$

$$\frac{d[8.6]}{dt} = k_{Am}[8.6.Z][Am] - k_{AmH^+}[8.6][AmH^+] \qquad (\underline{1})$$

$$\frac{d[8.6.Z]}{dt} = k_b[8.1][Am] + k_{AmH^+}[8.6][AmH^+] - k_{-b}[8.6.Z] - k_{Am}[8.6.Z][Am]$$

If (8.6.Z) is treated as a steady-state intermediate then $\frac{d[8.6.Z]}{dt} = 0$.

$$[8.6.Z] = \frac{k_b[8.1][Am] + k_{AmH^+}[8.6][AmH^+]}{k_{-b} + k_{Am}[Am]} \qquad (\underline{2})$$

Substituting (2) into (1).

$$\frac{d[8.6]}{dt} = k_{Am}[Am]\left(\frac{k_b[8.1][Am] + k_{AmH^+}[8.6][AmH^+]}{k_{-b} + k_{Am}[Am]}\right) - k_{AmH^+}[8.6][AmH^+] \qquad (\underline{3})$$

Multiplying the term $k_{AmH^+}[8.6][AmH^+]$ by $\frac{k_{-b}+k_{Am}[Am]}{k_{-b}+k_{Am}[Am]}$

and re-arranging,

$$\frac{d[8.6]}{dt} = \frac{k_b k_{Am}[8.1][Am]^2 - k_{-b}k_{AmH^+}[8.6][AmH^+]}{k_{-b} + k_{Am}[Am]} \qquad (\underline{4})$$

$$[8.1]_o = [8.1] + [8.2] + [8.6] + [8.6.Z] \quad (5)$$

[8.6.Z] ∿ 0 as (8.6.Z) is treated as a steady-state intermediate.

$$K_{c,3} = \frac{[8.2][AmH^+]}{[8.1][Am]^2} \quad (6)$$

Substituting (6) into (5) and re-arranging,

$$[8.1] = \frac{[8.1]_o - [8.6]}{1+K_{c,3}[Am]^2/[AmH^+]} \quad (7)$$

Substituting (7) into (4)

$$\frac{d[8.6]}{dt} = \frac{k_b k_{Am}[Am]^2([8.1]_o-[8.6])}{(k_{-b}+k_{Am}[Am])(1+K_{c,3}[Am]^2/[AmH^+])} - \frac{k_{-b}k_{AmH^+}[8.6][AmH^+]}{k_{-b}+k_{Am}[Am]}$$

At equilibrium, $\frac{d[8.6]}{dt} = 0$.

$$0 = \frac{k_b k_{Am}[Am]^2([8.1]_o-[8.6]_e)}{(k_{-b}+k_{Am}[Am])(1+K_{c,3}[Am]^2/[AmH^+])} - \frac{k_{-b}k_{AmH^+}[8.6]_e[AmH^+]}{k_{-b}+k_{Am}[Am]} \quad (9)$$

Subtracting (9) from (8) and re-arranging,

$$\frac{d[8.6]}{dt} \cdot \frac{1}{([8.6]_e-[8.6])} = \frac{k_b k_{Am}[Am]^2}{(k_{-b}+k_{Am}[Am])(1+K_{c,3}[Am]^2/[AmH^+])} + \frac{k_b k_{AmH^+}[AmH^+]}{k_{-b}+k_{Am}[Am]} \quad (10)$$

Relating [8.6] to OD.

The parent does not absorb at the wavelength chosen to study the reaction. At the wavelength chosen (8.6) is the major absorbing species and (8.2) may also have a significant absorption, while the species (8.6.Z) being a steady-state intermediate will have a very small negligible absorption. Therefore,

$$OD = \varepsilon_{8.6}[8.6] + \varepsilon_{8.2}[8.2] \quad (11)$$

Substituting (6) into (10), then (7),

$$OD = \varepsilon_{8.6}[8.6] + \varepsilon_{8.2}\left(\frac{[8.1]_o-[8.6]}{1+K_{c,3}[Am]^2/[AmH^+]}\right)\frac{K_{c,3}[Am]^2}{[AmH^+]}$$

Re-arranging,

$$OD = [8.6]\left(\varepsilon_{8.6} - \frac{\varepsilon_{8.2}K_{c,3}[Am]^2/[AmH^+]}{1+K_{c,3}[Am]^2/[AmH^+]}\right) + A \qquad (12)$$

$$\text{where } A = \frac{\varepsilon_{8.2}[8.1]_o K_{c,3}[Am]^2/[AmH^+]}{1+K_{c,3}[Am]^2/[AmH^+]}$$

Differentiating (12)

$$\frac{d\ OD}{dt} = \frac{d[8.6]}{dt}\left(\varepsilon_{8.6} - \frac{\varepsilon_{8.2}K_{c,3}[Am]^2/[AmH^+]}{1+K_{c,3}[Am]^2/[AmH^+]}\right) \qquad (13)$$

At equilibrium, (12) becomes (14).

$$OD_e = [8.6]_e\left(\varepsilon_{8.6} - \frac{\varepsilon_{8.2}K_{c,3}[Am]^2/[AmH^+]}{1+K_{c,3}[Am]^2/[AmH^+]}\right) + A \qquad (14)$$

Subtracting (12) from (14) and combining with (13)

$$\frac{d\ OD}{dt} \cdot \frac{1}{OD_e-OD} = \frac{d[8.6]}{dt} \cdot \frac{1}{[8.6]_e-[8.6]}$$

By definition,

$$k_{obs} = \frac{d\ OD}{dt} \cdot \frac{1}{OD_e-OD}$$

Therefore,

$$k_{obs} = \frac{k_b k_{Am}[Am]^2}{(k_{-b}+k_{Am}[Am])(1+K_{c,3}[Am]^2/[AmH^+])} + \frac{k_{-b}k_{AmH^+}[AmH^+]}{k_{-b}+k_{Am}[Am]}$$

CHAPTER NINE

THE REACTIONS OF 2,4,6-TRINITROPHENETOLE WITH ALIPHATIC AMINES IN DIMETHYL SULPHOXIDE

9.1 Introduction

Important evidence for the S_NAr mechanism of aromatic substitution has come from studies of base catalysis of reactions with amine nucleophiles.[79,177,178] The base catalysed step, $k_B[B]$ in Scheme 9.1, may involve rate-limiting proton transfer[179,180] from the zwitterionic intermediate (9.1), or rapid interconversion of (9.1) into its deprotonated form followed by general acid-catalysed leaving group departure (SB-GA mechanism).[102,103] The latter mechanism is likely to hold in dipolar aprotic solvents such as dimethyl sulphoxide (DMSO) where leaving group expulsion is difficult.[181] Thus

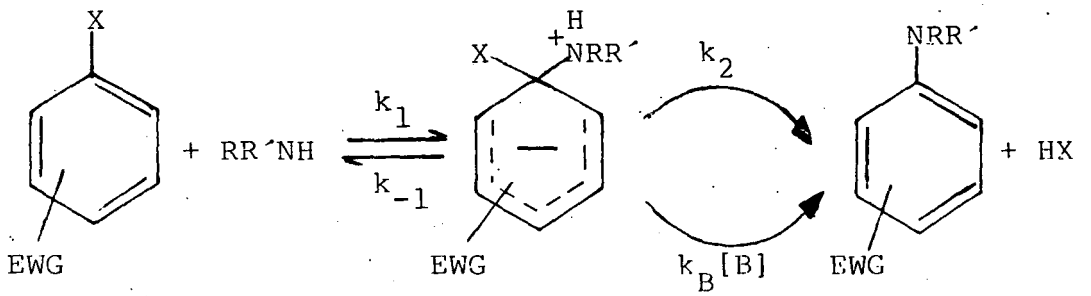

(9.1)

Scheme 9.1

in an elegant study of the reactions of 1-ethoxy-2,4-dinitronaphthalene with n-butylamine and t-butylamine in DMSO Orvik and Bunnett[182] were able to observe in separate steps formation of intermediates with the structure (9.1), and their acid catalysed conversion to substitution products. The structure (9.2; R = $CH_2CH_2CH_2CH_3$) has since been confirmed by flow-n.m.r. spectroscopy.[183,187] The adducts (9.3; R = $CH_2CH_2CH_2CH_3$) and

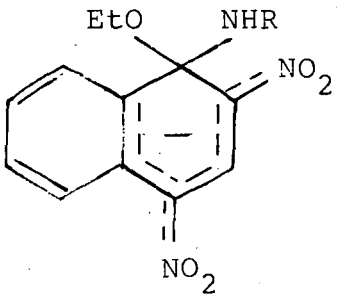

(9.2)

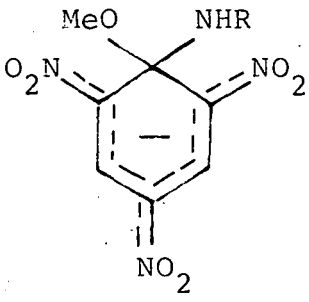

(9.3)

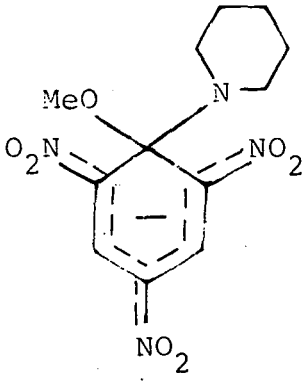

(9.4)

(9.3; R = Me) have also been observed by n.m.r. as a transient intermediate during reactions of 2,4,6-trinitroanisole (TNA) with primary aliphatic amines.[64,184] When reaction involves secondary amines the anionic adducts, such as (9.4) formed from TNA and piperidine, may have long lifetimes and in some cases do not yield the expected substitution products.[185,186]

Previously the kinetics of the reaction of 1,3,5-trinitrobenzene (TNB)[151-153] and 2,4,6-trinitrobenzyl chloride (TNBCl), reported in Chapter Six, with primary and secondary aliphatic amines have been examined. Here relatively stable σ-adducts are formed by attack at ring-carbon atoms carrying hydrogen or, in the case of TNBCl, CH_2Cl groups and nucleophilic substitution is not observed. It has been shown that in these reactions proton transfer from zwitterionic adducts to amines may be rate-limiting. Reduction below the values expected for diffusion controlled reaction of the rates of proton transfer were attributed to steric effects which are particularly severe (i) when reaction involves secondary amines, or (ii) when the bulky CH_2Cl

group is at the reaction site.

In this chapter the reactions of 2,4,6-trinitrophenetole (1-ethoxy-2,4,6-trinitrobenzene) (TNP) with n-butylamine, benzylamine and piperidine in DMSO have been examined. The results provide evidence for three types of process as shown in Scheme 9.2. These are the reversible formation of σ-adducts by attack at the 3-position or 1-position and, in the case of reaction with primary amines, acid catalysed expulsion of ethoxide to yield N-substituted picramides. It is known that the reaction products may undergo further reaction with excess amine either by proton transfer[182] or by base addition[64,161,184] but these reactions have not been studied here.

The results allow comparison of the effects of H, CH_2Cl and OEt ring-substituents on the rates and equilibria for reaction with amines, and also comparison of the 2,4,6-trinitrophenetole system with the 1-ethoxy-dinitronaphthalene system.

Scheme 9.2

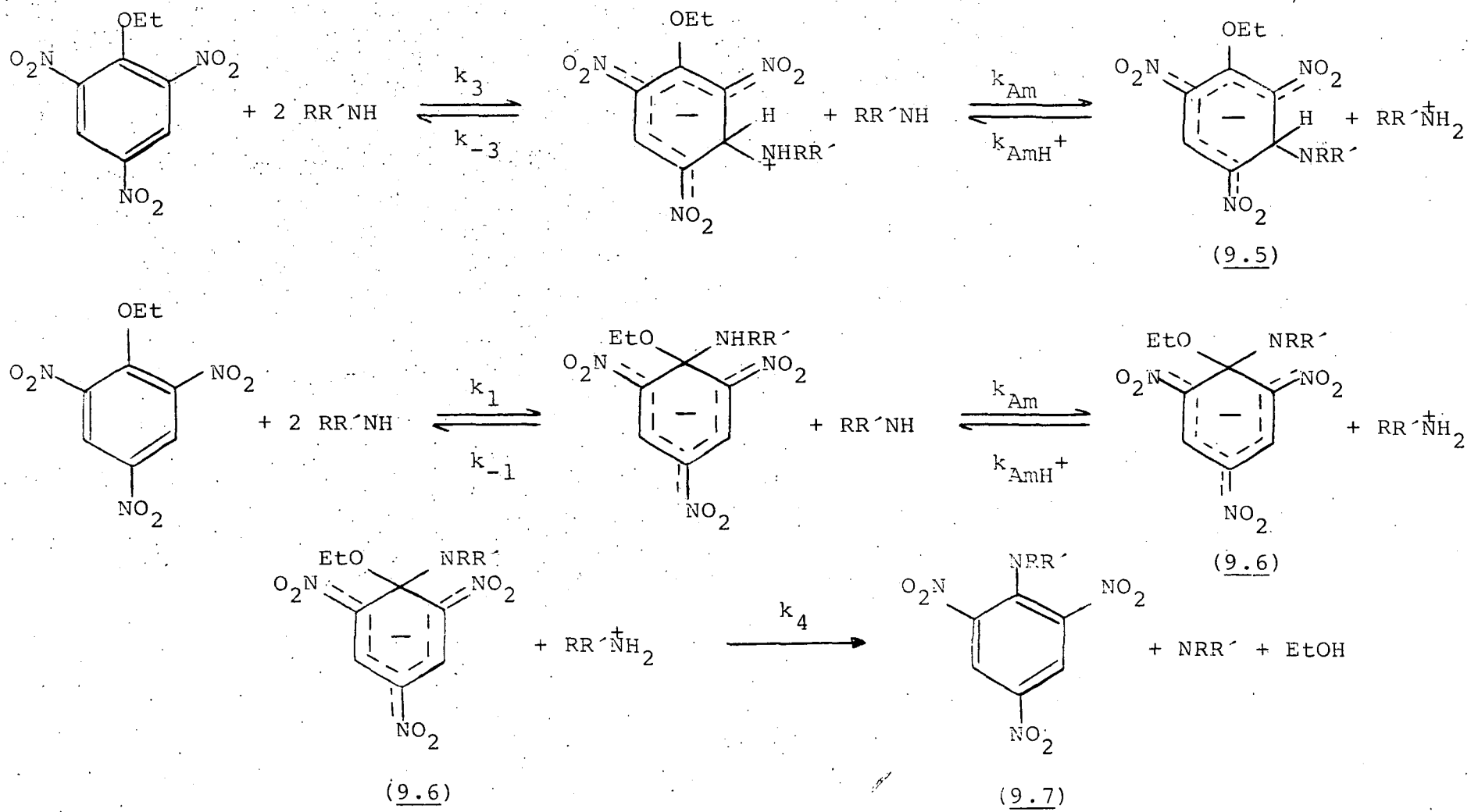
OEt
O_2N
NO_2
NO_2
+ 2 RR´NH
k_3
k_{-3}
H
$NHRR´^+$
k_{Am}
k_{AmH^+}
NRR´
$RR´\overset{+}{N}H_2$
(9.5)
EtO
NHRR´
NRR´
(9.6)
(9.7)
k_1
k_{-1}
k_4
+ NRR´ + EtOH

9.2 Experimental

Visible spectral measurements were made with Pye-Unicam SP 8005, Pye-Unicam SP 8100, or Hi-Tech SF-3L stopped-flow spectrophotometers.

Kinetic and equilibrium measurements were made on the latter two instruments at 25°C using freshly prepared solutions of reagents. Examples of the rate measurements are given in Tables 9.1, 9.2 and 9.3. Rate coefficients are the mean of at least five separate determinations, measured on the stopped-flow spectrophotometer, and at least two separate determinations, measured on the Pye-Unicam SP 8100, and are precise to ±5%.

^{1}H n.m.r. measurements were made on 0.1M solutions of the substrate in [$^{2}H_{6}$] dimethyl sulphoxide (DMSO) using a Varian EM 360L instrument.

A Kent EIL 7055 pH meter was used to check the acidity of the ammonium salts. Solutions were adjusted so as to contain less than 0.1% of free amine or acid.

TABLE 9.1 Typical results from rate measurements

(i) TNP (1×10^{-5} M), n-butylamine (0.005 M). σ-adduct formation; slow process. Measured at 435nm in DMSO.

(ii) TNP (1×10^{-5} M), n-butylamine (0.008 M). σ-adduct formation; fast process. Measured at 435nm in DMSO.

(i)		(ii)	
t/s	ΔV^a	t/ms	ΔV^a
0	4.2	10	3.2
2	3.4	20	2.4
4	2.6	30	1.9
6	2.2	40	1.5
8	1.8	50	1.1
10	1.5	60	0.9
12	1.2		

A plot of $\ln\Delta V$ versus t is linear and yields $k_{obs} = 0.104\ s^{-1}$

A plot of $\ln\Delta V$ versus t is linear and yields $k_{obs} = 26.40\ s^{-1}$

a. $\Delta V = V_\infty - V_t$

TABLE 9.2 Typical results from rate measurements

(i) TNP (1×10^{-5}M), benzylamine (0.02M). σ-adduct formation; slow process. Measured at 434nm in DMSO containing 0.01M benzylammonium chloride.

(ii) TNP (9.34×10^{-5}M), benzylamine (0.06M). Substitution process, measured at 380nm in DMSO containing 0.01M benzylammonium chloride.

(i)

t/s	ΔV^a
0.0	4.5
0.1	3.8
0.2	3.1
0.3	2.6
0.4	2.2
0.5	1.8
0.6	1.5

A plot of $\ln\Delta V$ versus t is linear and yields $k_{obs} = 1.83\ s^{-1}$

(ii)

t/s	ΔOD^b
0	0.312
5	0.281
10	0.251
15	0.224
20	0.203
25	0.181
30	0.160
40	0.129

A plot of $\ln\Delta V$ versus t is linear and yields $k_{obs} = 0.022\ s^{-1}$

a. $\Delta V = V_\infty - V_t$

b. $\Delta OD = OD_\infty - OD_t$

TABLE 9.3 Typical results from rate measurements

(i) TNP (2×10^{-5}M), piperidine (0.015M). σ-adduct formation; fast process. Measured at 434nm in DMSO containing 0.01M piperidinium perchlorate.

(ii) TNP (1×10^{-5}M), piperidine (0.015M). σ-adduct formation; slow process. Measured at 434nm in DMSO containing 0.01M piperidinium chloride.

(i)		(ii)	
t/ms	ΔV^a	t/s	ΔV^a
0	2.90	0.2	5.3
10	2.20	0.4	4.5
20	1.80	0.6	3.8
30	1.40	0.8	3.3
40	1.10	1.0	2.8
60	0.65	1.2	2.4
		1.6	1.8
A plot of $\ln\Delta V$ versus t is linear and yields $k_{obs} = 25.33\ s^{-1}$		A plot of $\ln\Delta V$ versus t is linear and yields $k_{obs} = 0.793\ s^{-1}$	

a. $\Delta V = V_\infty - V_t$

9.3 Results

9.3.1 Spectroscopic measurements

The visible spectra, recorded one minute after mixing, of solutions of TNP (2×10^{-5} M) in DMSO containing n-butylamine (0.001 - 0.1M) show maxima at 435nm (ε 2.7 l mol^{-1} cm^{-1}) and 505nm (ε 1.8×10^{4} l mol^{-1} cm^{-1}). The spectrum is typical[25-27,188] of a 1:1 σ-adduct. Very similar spectra are observed for TNP in the presence of benzylamine (λ_{max} 435,505nm) and piperidine (λ_{max} 435,495nm). Examination by stopped-flow spectrophotometry showed that for each amine there were two distinct colour forming reactions whose rate coefficients were separated by at least an order of magnitude. This is interpreted as fast formation of the 3-adducts followed by conversion to the 1-adducts, as shown in Scheme 9.2. The spectra recorded one minute after mixing correspond to the thermodynamically more stable (but more slowly formed) 1-adducts. The justificati for this interpretation is:

(i) that nucleophilic attack at unsubstituted ring positior is almost always faster than at substituted positions;[25-27,]

(ii) that the rate parameters calculated for the faster process correlate well with those determined[152] for attack at the unsubstituted position in TNB, and

(iii) in the case of piperidine the ^{1}H n.m.r. spectrum of the thermodynamically more stable adduct indicates attack at the 1-position.

With n-butylamine and benzylamine the visible absorption (λ_{max} 435, 505nm) gradually fades and a new band is formed at *ca* 360nm. This change, whose rate is greatly enhanced by the addition of ammonium salts, is attributed to the acid

catalysed departure of ethoxide (step 4 in Scheme 9.2). Spectra are shown in Figure 9.1. With piperidine the adduct formed is very stable and fading is very slow in the presence of added piperidinium ions.

The ^{1}H n.m.r. spectrum of TNP in [$^{2}H_{6}$] DMSO shows bands at δ9.2 (ring protons), 4.3,(q), J = 7Hz, (OCH_2) and 1,35,(t),(CH_3). This spectrum is unchanged after several hours. In the case of reaction with n-butylamine conversion to the product, N-butyl-2,4,6-trinitroaniline is relatively fast and the spectrum obtained in the presence of one equivalent of base shows a singlet at δ8.95 due to ring protons of the product and bands due to liberated ethanol.

9.3.2 Kinetic analysis

Rates of reaction were measured under first-order conditions. For reactions with buffers (amine plus amine salt) the buffer components were in large excess of the TNP concentration which was usually 1 x 10^{-5} M. For reactions with amines in the absence of added amine salts sufficient excess of amine was used so that >95% conversion to adduct was achieved at equilibrium. Under these conditions equation 9.1 applies.[152]

$$\ln\left(\frac{OD_\infty}{OD_\infty - OD}\right) = k_{obs}.t \qquad \text{(equation 9.1)}$$

By assuming that zwitterionic forms may be treated as steady-state intermediates,[15] so that the general rate expression for reaction at the unsubstituted 3-position is given by equation 9.2. When $k_{-3} >> k_{Am}[Am]$ then this simplifies to equation 9.3. If $k_{Am}[Am] >> k_{-3}$ and when no added salt, AmH^+, is initially present equation 9.2. becomes equation 9.4.

FIGURE 9.1 Visible spectra of TNP (2×10^{-5} M) in DMSO containing (A) 0.01M n-butylamine and (B) 0.01M n-butylamine and 0.01M n-butylamine perchlorate. The spectra were recorded two minutes after mixing and correspond to (A) the adduct (9.6;R=H,R=n-But), and (B) the reaction product (9.7;R=H,R´=n-But)

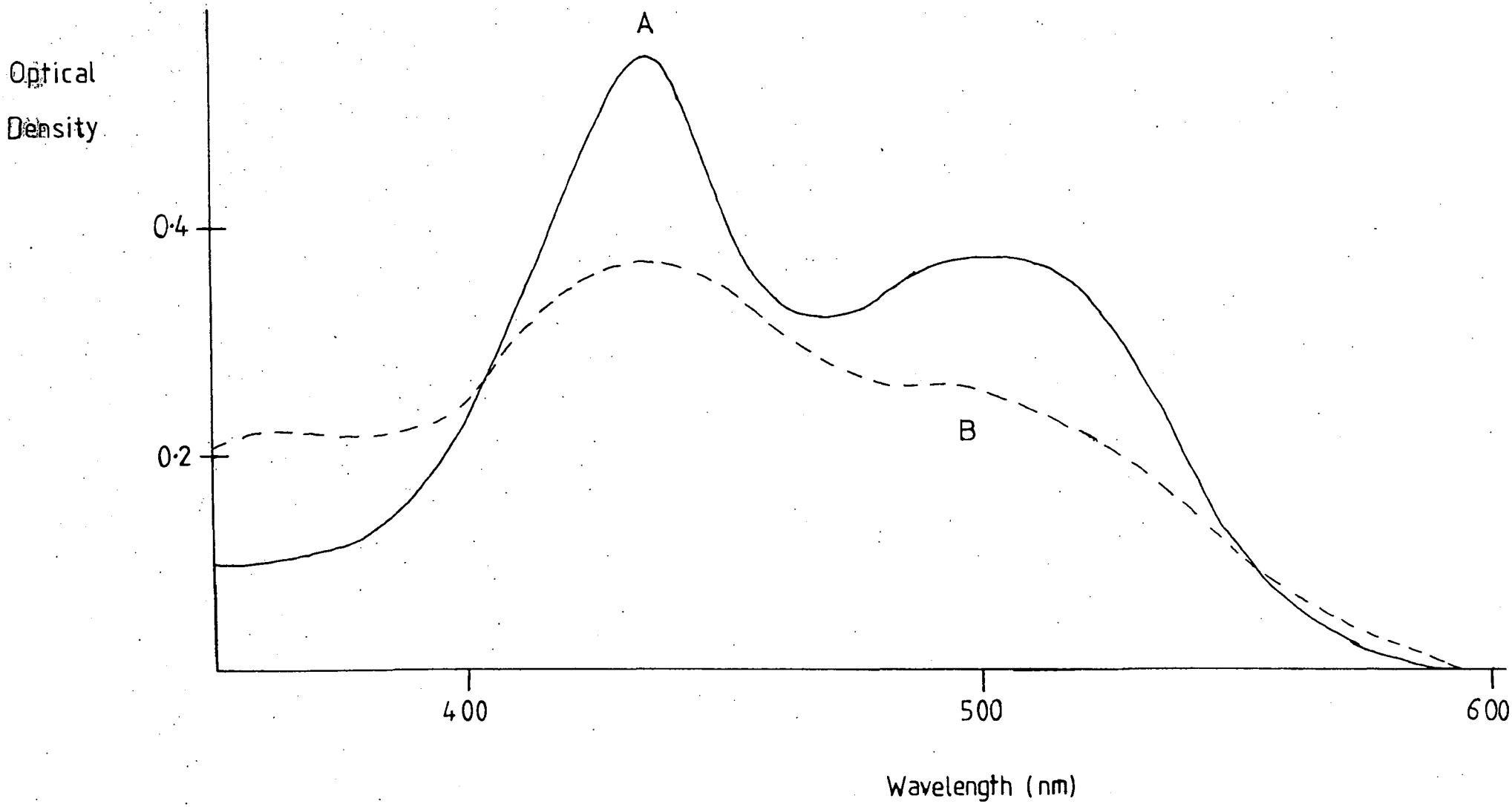

$$k_{obs} = \frac{k_3 k_{Am}[Am]^2 + k_{-3} k_{AmH^+}[AmH^+]}{k_{-3} + k_{Am}[Am]} \quad \text{(equation 9.2)}$$

$$k_{obs} = K_3 k_{Am}[Am]^2 + k_{AmH^+}[AmH^+] \quad \text{(equation 9.3)}$$

$$k_{obs} = k_3[Am] \quad \text{(equation 9.4)}$$

The reactions yielding 1-adducts were, for each amine, considerably slower than those giving the 3-adducts so that the rates could be measured consecutively. Also the formation of the 3-adducts may be treated as a mobile equilibrium[75] compared to the attack at the 1-position. Equation 9.5 expresses the rate of reaction in terms of coefficients for the forward and reverse reactions. Using standard methods[75] it can be shown that the general expression for reaction at the 1-position is given by equation 9.6. If the condition $k_{Am}[Am] >> k_-$ applies then equation 9.7 is obtained. It is also convenient to use equation 9.8 which applies in the absence of added amine salt, where k_r will be negligible, and where the fractionation of parent and 3-adduct is expressed in terms of $(OD)_3$, the absorption observed for the 3-adduct, and $(OD_\infty)_3$, the absorption for complete conversion of parent to 3-adduct.

$$k_{obs} = k_f + k_r \quad \text{(equation 9.5)}$$

$$k_{obs} = \frac{k_1 k_{Am}[Am]^2}{(k_{-1} + k_{Am}[Am])(1 + K_{c,3}[Am]^2/[AmH^+])} + \frac{k_{-1} k_{AmH^+}[AmH^+]}{k_{-1} + k_{Am}[Am]} \quad \text{(equation}$$

$$k_{obs} = \frac{k_1[Am]}{1 + K_{c,3}[Am]^2/[AmH^+]} + \frac{k_{-1} k_{AmH^+}[AmH^+]}{k_{Am}[Am]} \quad \text{(equation 9.7)}$$

$$k_{obs} = \frac{k_1[Am]}{\frac{1 + (OD)_3}{(OD_\infty)_3 - (OD)_3}} \quad \text{(equation 9.8)}$$

The rate expression appropriate to the conversion of adducts (9.6) to products (9.7) catalysed by substituted ammonium salts has been derived previously[182] and is given by equation 9.9. When the equilibrium between parent and adduct (9.6) is almost entirely in favour of the adduct equation 9.9 simplifies to equation 9.10.

$$k_{obs} = \frac{k_4 K_{c,1} [Am]^2 [AmH^+]}{K_{c,1} [Am]^2 + [AmH^+]} \qquad \text{(equation 9.9)}$$

$$k_{obs} \; k_4 [AmH^+] \qquad \text{(equation 9.10)}$$

9.3.3 Equilibrium constants

$K_{c,3}$, the equilibrium constant for the overall conversion of TNP into its 3-adduct (9.5), is defined by equation 9.11. Equation 9.12 relates $K_{c,3}$ to K_3 ($=k_3/k_{-3}$) and to the acid dissociation constants of the zwitterion, $K_a^{9.1}$, and protonated amine $K_a^{AmH^+}$. The rate coefficients associated with formation of the 3-adduct are related to $K_{c,3}$ by equation 9.13.

$$K_{c,3} = \frac{[9.5][AmH^+]}{[TNP]\;[Am]^2} \qquad \text{(equation 9.11)}$$

$$K_{c,3} = \frac{K_3 K_a^{9.1}}{K_a^{AmH^+}} \qquad \text{(equation 9.12)}$$

$$K_{c,3} = \frac{k_3 k_{Am}}{k_{-3} k_{AmH^+}} \qquad \text{(equation 9.13)}$$

Expressions exactly analogous to equations 9.11, 9.12 and 9.13 apply to $K_{c,1}$ the equilibrium constant for formation of the 1-adduct (9.6).

9.3.4 Reaction with n-butylamine

Data for the reaction in the absence of added n-butylammonium ions are given in Table 9.4. The rate data for the more rapid reaction giving the 3-adduct conform to equation 9.4 and yield a value for k_3 of 3200 l mol^{-1} s^{-1}. The invariance with base concentration of the calculated values of k_3 allow an estimate for the ratio k_{Am}/k_{-3} > 200 l mol^{-1}. The data for the slower reaction giving the 1-adduct yield, using equation 9.8, a value for k_1 of 220 l mol^{-1} s^{-1} and allow an estimation of a lower limit for the ratio k_{Am}/k_{-1} of 1000 l mol^{-1}.

Measurements were also made, Table 9.5, in the presence of varying concentrations of amine and with 0.01$\underline{M}$ n-butylammonium perchlorate. The reaction at the 3-position was too rapid to allow rate measurements but optical density measurements at the completion of this reaction gave a value for $K_{c,3}$ of 15±1 l mol^{-1}. The rate of reaction at the 1-position was measurable and the results show that $k_{Am}[Am] >> k_{-1}$ so that equation 9.7 applies. At amine concentrations >0.002$\underline{M}$ the second term in equation 9.7 (the k_r term) will be negligibly small, hence knowing the value of $K_{c,3}$ a value of k_1 of 250 l mol^{-1} s^{-1} can be calculated. This is quite close to the value obtained in the absence of salt. Calculation of values for the first term in equation 9.7 (the k_f term) is now possible for the four lowest amine concentrations and hence determine values, by difference, for the k_r term. These give a value for the ratio $k_{-1}k_{AmH^+}/k_{Am}$ of 0.005±0.001 s^{-1}. Combination of this value with the value of k_{-1} gives value for $K_{c,1}$ $(=k_1k_{Am}/k_{-1}k_{AmH^+}$ of 50,000 l mol^{-1} which is in agreement with that obtained from

TABLE 9.4 Kinetic data for reactions of TNP with n-butylamine in DMSO at 25° giving 3-adduct and 1-adduct

$[BuNH_2]/M$	k_{fast}/s^{-1}	$k_3^a/\ell\ mol^{-1}s^{-1}$	$(OD)_3^b$	k_{slow}/s^{-1}	$k_1^c/\ell\ mol^{-1}s^{-1}$
0.0005			0.0017	0.10	210
0.00075			0.0040	0.14	220
0.001			0.0057	0.19	230
0.002			0.014	0.27	210
0.003			0.022	0.28	220
0.004			0.025	0.27	200
0.006	21.5	3600	0.035		
0.008	26	3200	0.037		
0.010	31	3100	0.038		
0.015	48	3200	0.038		

a. Calculated from equation 9.4 .

b. Optical density, 435nm, at completion of the faster colour forming reaction.

c. Calculated from equation 9.8 .

TABLE 9.5 Kinetic and equilibrium data for the σ-adduct forming reactions of TNP with n-butylamine in DMSO containing 0.01M n-butylammonium perchlorate at 25°C

$[BuNH_2]/M$	$(OD)_3^a$	$K_{c,3}/\ell\ mol^{-1}$	k_{obs}^b/s^{-1}	k_{calc}^c	OD_1^d	$K_{c,1}/\ell\ mol^{-1}$
0.0006			0.22	0.23	0.029	53,000
0.0008			0.26	0.26	0.033	47,000
0.001			0.30	0.30	0.036	45,000
0.002			0.53	0.53	0.042	-
0.006			1.44	1.44	-	
0.008	0.0042	16	1.80	1.83	-	
0.01	0.0055	15	2.20	2.2	0.044	
0.02	0.016	14	3.3	3.1	0.044	
0.03	0.026	16	-	-	-	
0.04	0.031	15	3.0	3.0	0.044	
0.05	0.034	14	-	-	-	

a. Optical density, 435nm, at completion of the reaction forming the 3-adduct. A Benesi-Hildebrand type plot gives a value for complete conversion $(OD_\infty)_3$ of 0.044.

b. For attack at the 1-position.

c. Calculated from equation 9.7 with k_1 250 $\ell\ mol^{-1}s^{-1}$, $K_{c,3}$ 15 $\ell\ mol^{-1}$ and $k_{-1}k_{AmH^+}/k_{Am}$ 0.005 s^{-1}.

d. Optical density, 435nm, at completion of the slower adduct-forming reaction.

the equilibrium optical density data.

The product forming reaction was measured at 360nm using a conventional spectrophotometer and the data, Table 9.6, accord well with equation 9.9 with k_4 8.3 l mol^{-1} s^{-1}, $K_{c,1}$, 50,000 l mol^{-1}.

9.3.5 Reaction with benzylamine.

The behaviour and treatment of data is very similar to that observed with n-butylamine. The data in Table 9.7 obtained in the absence of added salt give values for k_3 of 900±100 l mol^{-1} s^{-1} and k_1 of 100±10 l mol^{-1} s^{-1}. At the benzylamine concentrations used, the proton transfer steps are not rate-limiting in the formation of either 3-adduct or 1-adduct, and it is estimated that $k_{Am}/k_{-3} > 100$ l mol^{-1} and $k_{Am}/k_{-1} > 3000$ l mol^{-1}.

Measurements were also made in solutions containing 0.01M benzylammonium perchlorate or benzylammonium chloride. It has been shown previously[86,151] and in Chapter Six that the anion present may affect the values of rate and equilibrium constants obtained. However, at the low salt concentration used here the effects are not large. The data in Tables 9.8 and 9.9 were treated independently using the approach outlined for the n-butylamine data. The rate data yield a value for k_1 of 95±5 l $mol^{-1}s^{-1}$ and values for the ratio $k_{-1}k_{AmH^+}/k_{Am}$ of 0.02 s^{-1} in the presence of perchlorate and 0.018 s^{-1} with the chloride salt. The values of $K_{c,1}$ obtained from combination of these values, 4700 l mol^{-1} (perchlorate) and 5300 l mol^{-1} (chloride) are in good agreement with those determined independently from equilibrium optical densities.

TABLE 9.6 Rate data for formation of N-(n-butyl)picramide from TNP and butylamine containing n-butylammonium perchlorate, 0.01M, in DMSO at 25°C

$[BuNH_2]$/M	k^a_{obs} /s^{-1}	k^b_{calc}
0.0002	0.015	0.014
0.0004	0.038	0.037
0.0006	0.053	0.053
0.0008	0.057	0.063
0.001	0.071	0.069
0.002	0.075	0.078
0.01	0.083	0.083
0.02	0.081	0.083
0.04	0.083	0.083
0.05	0.084	0.083
0.06	0.086	0.083

a. Measured on Pye-Unicam spectrophotometer at 360 nm.

b. Calculated from equation 9.9 with k_4 8.3 $\ell\ mol^{-1}\ s^{-1}$, $K_{c,1}$ 50,000 $\ell\ mol^{-1}$.

TABLE 9.7 Kinetic data for reaction of TNP with benzylamine in DMSO at 25°C giving 3-adduct and 1-adduct

$[PhCH_2NH_2]$/M	k_{fast}/s^{-1}	k_3^a/ℓ $mol^{-1}s^{-1}$	$(OD)_3^b$	k_{slow}/s^{-1}	k_1^c/ℓ $mol^{-1}s^{-1}$
0.0010				0.093	93
0.0016			0.0015	0.143	93
0.0020			0.0023	0.183	97
0.0040			0.0083	0.345	108
0.0060			0.0141	0.437	109
0.0080			0.0186	0.487	110
0.010			0.0259		
0.020	18	900	0.0357		
0.040	32	800	0.0400		
0.050	44	900	0.0419		
0.060	52	900	0.0410		
0.070	65	900	0.0419		
0.080	72	900	0.0429		

a. Calculated from equation 9.4.

b. Optical density, 434 nm, at completion of the faster colour-forming reaction.

c. Calculated from equation 9.8.

TABLE 9.8 Kinetic and equilibrium data for the σ-adduct forming reactions of TNP with benzylamine in DMSO containing 0.01M benzylammonium perchlorate at 25°C

$[PhCH_2CH_2]$/M	OD_3[a]	$K_{c,3}$/ℓ mol^{-1}	k_{obs}[b]/s^{-1}	k_{calc}[c]	$(OD)_1$[d]	$K_{c,1}$/ℓ mol^{-1}
0.001			0.26	0.29	0.017	5700
0.0015					0.023	4400
0.002			0.31	0.29	0.031	5000
0.003					0.037	4400
0.004			0.42	0.43	0.040	3900
0.006			0.57	0.60	0.044	
0.008			0.79	0.78	0.047	
0.01			0.92	0.95	0.046	
0.02			2.0	1.9	0.046	
0.04			3.5	3.4	0.047	
0.06	0.0088	0.75			0.046	
0.08	0.0150	0.87			0.047	
0.10	0.0195	0.87			0.047	
0.15	0.0278	0.87			0.046	
0.20	0.0334	0.97			0.047	

a. Optical density, 434nm, at completion of the reaction forming the 3-adduct. A Benesi-Hildebrand type plot gives a value for complete conversion, $(OD_\infty)_3$ of 0.042.

b. For attack at the 1-position.

c. Calculated from equation 9.7 with k_1 95 ℓ mol^{-1}s^{-1}, $K_{c,3}$ 0.87 ℓ mol^{-1}, and $k_1 k_{AmH^+}/k_{Am}$ 0.02 s^{-1}.

d. Optical density, 434 nm, at completion of the slower colour forming reaction.

TABLE 9.9 Kinetic and equilibrium data for the σ-adduct forming reaction of TNP with benzylamine in DMSO containing 0.01M benzylammonium chloride at 25°C

$[PhCH_2NH_2]/M$	$(OD)_3^a$	$K_{c,3}/\ell\ mol^{-1}$	k_{obs}^b/s^{-1}	k_{calc}^c	$(OD)_1^d$	$K_{c,1}/\ell\ mol^{-1}$
0.0008					0.012	5500
0.001			0.28	0.28	0.018	6300
0.0015					0.026	5600
0.002			0.29	0.28	0.033	6100
0.003					0.038	5000
0.004			0.43	0.42	0.042	5800
0.006			0.59	0.60	0.046	
0.008			0.77	0.78	0.047	
0.01			0.94	0.95	0.047	
0.02			1.80	1.8	0.046	
0.04	0.0062	1.08	3.50	3.3	0.047	
0.05	0.0092	1.12			0.047	
0.06	0.0114	1.03			0.046	
0.08	0.0164	1.00			0.046	
0.10	0.0214	1.04			0.047	

a. Optical density, 435nm, at completion of the reaction forming the 3-adduct. A Benesi-Hildebrand type plot gives a value for complete conversion, $(OD_\infty)_3$, of 0.042.

b. For attack at the 1-position.

c. Calculated from equation 9.7 with k_1 95 $\ell\ mol^{-1}\ s^{-1}$, $K_{c,3}$ 1.05 $\ell\ mol^{-1}$, and $k_{-1}k_{AmH}^+/k_{Am}$ 0.018 s^{-1}.

d. Optical density, 435nm, at completion of the slower colour forming reaction.

Rate data for the formation of the product N-benzylpicramide were measured at 380nm and are in Table 9.10. They yield values for k_4 of 2.6 l mol^{-1} s^{-1} in the presence of 0.01M perchlorate and 2.2 l mol^{-1} s^{-1} with the chloride salt.

9.3.6 Reaction with piperidine

Examination by stopped-flow spectrophotometry of the reactions of TNP with piperidine 0.008-0.04M, without added salts indicated two processes. The more rapid was colour forming and resulted in nearly complete conversion of TNP to adduct at all amine concentrations used. This is taken to be the formation of the 3-adduct (9.5; R´RN = $C_5H_{10}N$). A very much slower reaction, representing isomerisation to the 1-adduct (9.6; R´RN = $C_5H_{10}N$), gave inconveniently small changes in optical density. Data for the faster process, giving the 3-adduct, are in Table 9.11. Since no added piperidinium ions are present the term in equations 9.2 and 9.3 involving $[AmH^+]$ will be negligibly small. These data, in contrast to those observed to primary amines, conform to the case where $k_{-3} >> k_{Am}[Am]$ and yield a value for K_3k_{Am} of 44000±3000 l^2 mol^{-1} s^{-1}. Our results allow a limit of $k_{Am}/k_{-3} < 5$ to be set.

Data obtained in the presence of 0.01M piperidinium salts are in Tables 9.12 and 9.13. Here two processes were measurable giving rise to 3-adduct and 1-adduct respectively. The rate data for the faster reaction lead to values for $K_{c,3}$ $(=K_3k_{Am}/k_{AmH^+})$ of 27±5 l mol^{-1} with perchlorate salt and 30±5 l mol^{-1} with chloride salt. These values are in good agreement with those obtained from equilibrium optical densities.

TABLE 9.10 Rate data for formation of N-benzylpicramide from TNP and benzylamine containing benzylammonium salts, 0.01M, in DMSO at 25°C

$[PhCH_2NH_2]$/M	$[PhCH_2NH_3^+ClO_4^-]$/M	$[PhCH_2NH_3^+Cl^-]$/M	k^a_{obs} /s^{-1}	k^b_4/ℓ $mol^{-1}s$
0.0008		0.01	0.0055	2.2
0.0009		0.01	0.0065	2.2
0.001		0.01	0.0077	2.2
0.0015		0.01	0.012	2.2
0.002		0.01	0.015	2.2
0.003		0.01	0.020	2.4
0.004		0.01	0.020	2.2
0.005		0.01	0.022	2.4
0.01		0.01	0.023	2.3
0.02		0.01	0.022	2.2
0.04		0.01	0.025	2.5
0.06		0.01	0.022	2.2
0.08		0.01	0.021	2.1
0.10		0.01	0.021	2.1
0.01	0.01		0.026	2.6
0.02	0.01		0.026	2.6
0.04	0.01		0.026	2.6
0.06	0.01		0.026	2.6
0.08	0.01		0.025	2.5
0.10	0.01		0.025	2.5

a. Measured at 380 nm using a Pye-Unicam 8100 instrument.

b. Calculated from equations 9.9 and 9.10 using a value for $K_{c,1}$ of 5300 ℓ mol^{-1} (chloride salt).

TABLE 9.11 Rate data for formation of the 3-adduct from TNP and piperidine in DMSO at 25°C

[Piperidine]/M	k_{obs}/s^{-1}	k^a_{obs}/[piperidine]^2
0.008	3.0	47,000
0.01	4.8	48,000
0.015	10.3	46,000
0.02	17.5	44,000
0.025	27.2	43,000
0.03	37.7	42,000
0.035	52.2	43,000
0.04	67.8	42,000

a. This column gives values for K_3k_{Am}/ℓ^2 mol^{-2} s^{-1}.

TABLE 9.12 Kinetic and equilibrium data for adduct formation from TNP and piperidine in DMSO containing 0.01M piperidinium perchlorate at 25°C

[Piperidine]/M	k^a_{fast}/s^{-1}	k^b_{calc}	$(OD)^c_3$	$K_{c,3}/\ell\ mol^{-1}$	k^d_{slow}/s^{-1}	k^e_{calc}	$(OD)^f_1$	$K_{c,1}/\ell\ mol^{-1}$
0.006					0.27	0.27	0.032	610
0.008					0.38	0.38	0.037	610
0.010	20	20	0.0072	21	0.50	0.51	0.040	610
0.015	25	26	0.0141	23			0.043	560
0.020	32	33	0.0205	24	1.12	1.10	0.046	-
0.025	44	44	0.0259	26			0.046	-
0.030	52	55	0.0297	27	1.43	1.43	0.047	-
0.040					1.62	1.59	0.047	-
0.060					1.66	1.67	0.046	-

a. Represents attack at the 3-position.

b. Calculated from equation 9.3 with K_3k_{Am} 44,000 $\ell^2\ mol^{-2}s^{-1}$

c. Optical density, 434 nm, at completion of rapid colour-forming reaction. Value for complete conversion $(OD_\infty)_3$ is 0.042.

d. Represents attack at the 1-position.

e. Calculated from equation 9.6 with K_1k_{Am} 5.6×10^3 $\ell^2\ mol^{-2}s^{-1}$, k_{AmH^+} 9 $\ell\ mol^{-1}s^{-1}$, $K_{c,3}$ 27 $\ell\ mol^{-1}$, k_{Am}/k_{-1} 3 $\ell\ mol^{-1}$.

f. Optical density, 434 nm, at completion of slower colour-forming reaction. Value for (OD_∞), is 0.0465.

TABLE 9.13 Kinetic and equilibrium data for adduct formation from TNP and piperidine in DMSO containing 0.01M piperidinium chloride at 25°C

[Piperidine]/M	k^a_{fast}/s^{-1}	k^b_{calc}	$(OD)^c_3$	$K_{c,3}/\ell\ mol^{-1}$	k^d_{slow}/s^{-1}	k^e_{calc}	$(OD)^f_1$	$K_{c,1}/\ell\ mol^{-1}$
0.004							0.027	720
0.006					0.25	0.25	0.035	630
0.008					0.35	0.36	0.040	600
0.010	16	18	0.011	31	0.48	0.48	0.049	-
0.015	23	24	0.018	30	0.79	0.77	0.050	-
0.020	31	31	0.025	31	1.02	1.01	0.050	-
0.025	43	42	0.030	30	1.18	1.17	0.051	-
0.030	55	53	0.033	30	1.29	1.29	0.051	-
0.040			0.038	32	1.36	1.40	0.050	-

a. Represents attack at the 3-position.

b. Calculated from equation 9.3 with K_3k_{Am} 44,000 $\ell^2\ mol^{-2}s^{-1}$, k_{AmH^+} 1400 $\ell\ mol^{-1}s^{-1}$.

c. Optical density, 434nm, at completion of rapid colour-forming reaction. Value for complete conversion $(OD_\infty)_3$ is 0.0455.

d. Attack at 1-position.

e. Calculated from equation 9.6 with K_1k_{Am} $5.6 \times 10^3\ \ell^2\ mol^{-2}s^{-1}$, k_{AmH^+} 7 $\ell\ mol^{-1}s^{-1}$, $K_{c,3}$ 30 $\ell\ mol^{-1}$ and k_{Am}/k_1 4 $\ell\ mol^{-1}$.

f. Optical density, 434 nm, at completion of slower colour-forming reaction. Value for $(OD_\infty)_1$ is 0.0505.

The interpretation of the rate data for isomerisation to the 1-adduct requires the use of the complete rate expression, equation 9.6. However at sufficiently low amine concentrations the condition $k_{-1} >> k_{Am}[Am]$ applies so that equation 9.14 is obtained.

$$k_{obs}(1+K_{c,3}[Am]^2/[AmH^+]) = K_1 k_{Am}[Am]^2 + k_{AmH^+}[AmH^+](1+K_{c,3}[Am]^2/[AmH^+])$$

(equation 9.14

Plots of the left hand side of this equation *versus* $[Am]^2$ were linear at low amine concentrations. For the data measured with perchlorate salt, the slope gave a value for $K_1 k_{Am}$ of (5.6±0.2) x 10^3 l^2 mol^{-2} s^{-1} and the intercept a value for k_{AmH^+} of 10±2 l mol^{-1} s^{-1}. An alternative method for calculating k_{AmH^+} is to combine the value of $K_{c,1}$, 600 l mol^{-1}, obtained from equilibrium densities with the value for $K_1 k_{Am}$; this gives k_{AmH^+} 9 l mol^{-1} s^{-1}. Using the known values for these parameters, values of the ratio k_{Am}/k_{-1} were calculated for each experimental value using equation 9.6. The value obtained was 3±1 l mol^{-1}. The rate coefficients calculated with these parameters agree with the experimental values over the whole concentration range. The value for k_1 ($=K_1 k_{Am} . k_{-1}/k_{Am}$ is calculated to be 1800 l mol^{-1} s^{-1}. Similar treatment for the run containing the chloride salt yielded values for $K_1 k_{Am}$ of 5.6 x 10^3 l^2 mol^{-2} s^{-1}, k_{AmH^+} 7 ℓ mol^{-1} s^{-1} and the ratio k_{Am}/k_{-1} of 4 l mol^{-1}.

It should be noted that while the values obtained for $K_1 k_{Am}$ and k_{AmH^+} have relatively low error limits, the values

for the ratio k_{Am}/k_{-1} and hence also k_1 depend critically on the value used for $K_{c,3}$. The values given above represent the 'best' values, however the data in Table 9.13 values for k_{Am}/k_{-1} are calculated to be 10 l mol^{-1} if $K_{c,3}$ were 25 l mol^{-1} instead of 30 l mol^{-1}, and 0 if $K_{c,3}$ were 35 l mol^{-1}.

The visible and ^1H n.m.r. spectra indicate that the 1-adduct (9.6; R´RN = $C_5H_{10}N$) is stable in solution for several hours. Hence conversion to the product of nucleophilic substitution is very slow even in the presence of piperidinium ions.

9.4 Discussion

9.4.1 The effects of chloride ions

A salt concentration of 0.01M was used for the work presented in this chapter, using either the perchlorate or chloride anions. Comparisons of values obtained with benzylammonium and piperidinium salts are in Table 9.14. The data show that values of the equilibrium constants $K_{c,1}$ and $K_{c,3}$ are significantly higher when measured in the presence of chloride ions. A similar effect has been observed in the previous three chapters and in related work[86,151] and has been attributed to association of the chloride ions with substituted ammonium ions as shown in Scheme 9.3. The effects observed here are smaller than those observed with the substrate 2,4,6-

$$TNP + 2R'RNH + Cl^- \underset{}{\overset{K_c}{\rightleftharpoons}} (TNP.NRR') + R'R\overset{+}{N}H_2 + Cl^-$$

$$R'R\overset{+}{N}H_2 \;\; \underset{}{\overset{K_{Cl^-}}{\rightleftharpoons}} \;\; R'R\overset{+}{N}H_2 \ldots . Cl^-$$

Scheme 9.3

trinitrobenzyl chloride, reported in Chapter Six, where 0.1M chloride ions were used. The value for K_{Cl^-} of *ca* 10 l mol^{-1} obtained previously (reported in Chapter Six) would with a chloride concentration of 0.01M give rise to a 10% increase in values of $K_{c,1}$ and $K_{c,3}$. This is in line with the increases observed in Table 9.14. The main effect of chloride ions on rate coefficients is to lower values for the rate coefficients, k_{AmH^+}, for reaction of substituted ammonium ions with anionic adducts. In the following discussion we shall use values obtained using perchlorate salts.

TABLE 9.14 Effects of chloride ions on equilibrium and rate constants

	$K_{c,3}$/ℓ mol^{-1}	$K_{c,1}$/ℓ mol^{-1}	k_1/ℓ mol^{-1}s^{-1}	$k_{-1}k_{AmH^+}/k_{Am}$ (s^{-1}_1)	k_{AmH^+}/ℓ mol^{-1}s^{-1}
Benzylammonium perchlorate	0.87	4700	95	0.020	-
Benzylammonium chloride	1.05	5300	95	0.018	-
Piperidine perchlorate	27	600	-	-	9
Piperidine chloride	30	650	-	-	7

9.4.2 Reaction at unsubstituted ring-positions

In Table 9.15 the data for formation of adducts of the structure (9.5) are compared with those for formation of adducts (9.8) and (9.9) formed respectively from 2,4,6-trinitrobenzyl chloride (TNBCl) and 1,3,5-trinitrobenzene (TNB). Since reaction occurs in each case at an unsubstituted ring-position steric factors at the reaction centre should be simila for the three substrates. Thus values of k_3 measuring the

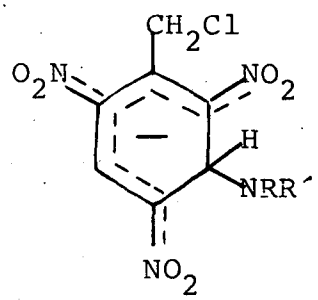

(9.8)

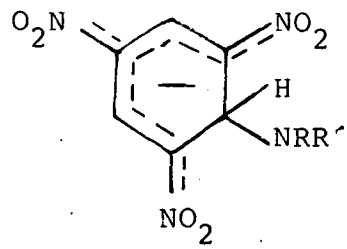

(9.9)

rate of amine attack and values of $K_{c,3}$ measuring the stabilitie of the adducts decrease in the order piperidine > n-butylamine > benzylamine which is that expected from the relative basicities of the amines.[157,158,189] Before comparing the values of these parameters for the three different nitro-compounds it must be stated that the data for TNP refers to an ionic strength of 0.01M while those for TNB and TNBCl were measured with 0.1M salt. Values of k_3 will not be expected to vary with ion strength[151,152] but the values of $K_{c,3}$, which relate to the information of ionic products from neutral reagents, will increase with increasing ionic strength. We estimate that if

TABLE 9.15 Comparison of kinetic and equilibrium data for reaction at unsubstituted ring positions of 2,4,6-trinitrophenetole (TNP)[a], 2,4,6-trinitrobenzyl chloride (TNBCl)[b] and 1,3,5-trinitrobenzene (TNB)[c]

		n-Butylamine	Benzylamine	Piperidine
$k_3/\ell\ mol^{-1}s^{-1}$	TNP	3200	900	> 9000
	TNBCl	3000	1000	>13000
	TNB	45000	13000	$>2 \times 10^5$
$K_{c,3}/\ell\ mol^{-1}$	TNP	15	0.87	27
	TNBCl	73	5	93
	TNB	1000	105	2140
$\frac{k_{-3}k_{AmH^+}}{k_{Am}}$ (s^{-1})	TNP	210	1000	>320
	TNBCl	41	200	>140
	TNB	45	120	>900
$k_{Am}/k_{-3}(\ell\ mol^{-1})$	TNP	> 200	>100	< 5
	TNBCl	>1000	>140	< 2
	TNB	1200	120	<10
$k_{AmH^+}/\ell\ mol^{-1}s^{-1}$	TNP	$>4.2 \times 10^4$	$>10^5$	1600
	TNBCl	$>4 \times 10^4$	3×10^4	280
	TNB	6×10^4	1.5×10^4	280

a. Data for TNP measured with 0.01M salt.

b. Data for TNBCl, measured with 0.1M salt, from Chapter Six.

c. Data for TNB, measured with 0.1M salt, from references 151,1

activity coefficients follow Debye-Hückel theory changing the salt concentration from 0.01 to 0.1 M will increase K_c values by a factor of 2. Values of k_{Am} will be increased and values of k_{AmH^+} reduced as the ionic strength is increased.

Taking account of ionic strength effects values of k_3 and $K_{c,3}$ are, for a given amine, very similar for TNP and TNBCl. Both sets of values are lower by at least an order of magnitude than corresponding values for reaction with TNB. The inductive electron-withdrawal of the ethoxy group (or CH_2Cl group) might be expected to enhance the stabilities of the 3-adducts formed from TNP (or TNBCl) relative to TNB. However, the steric effect of the substituent is probably the major factor. Thus the crystal structure[47] of TNP shows the ortho nitro-groups are rotated from the ring-plane by 32° and 61° respectively so that they cannot exert their maximum electro withdrawing influence.

Comparison for a given amine, of the values (or inequalities) of k_{AmH^+} and the ratio k_{Am}/k_{-3} show that there is not a wide variation with the nature of the nitro-compound. This probably results from the fact that in each case addition is occurring at an unsubstituted ring position. Nevertheless the values of k_{AmH^+} are *ca* two orders of magnitude smaller for reactions involving piperidine. This is attributable[152] to the greater steric bulk of piperidine which reduces the rate of proton transfer from the piperidinium ion to the anionic adduct. Similarly values of k_{Am} for proton transfer from the zwitterioni intermediate to amine will be reduced when reaction involves the secondary amine. This is a major factor in the lower values of the ratio k_{Am}/k_{-3} observed for piperidine relative to the primary amines, and accounts for the observation that in the

overall equilibrium the proton transfer step remains rate-determining at much higher amine concentrations for secondary than for primary amines.

9.4.3 Reaction at the substituted position

In Table 9.16 the values of parameters for the reaction at the ethoxy substituted ring-position are summarised. For a given amine the value of the equilibrium constant $K_{c,1}$ is considerably higher than the value of $K_{c,3}$. The ratios $K_{c,1}/K_{c,3}$ are 3300 for n-butylamine, 5500 for benzylamine and 22 for piperidine. The polar effect of the ethoxy group at the reaction centre will be expected to increase the value of K_1 relative to K_3 and there may also be a small increase in the ratio, $K_a^{9.1}/K_a^{AmH^+}$, of acidities of zwitterion and substituted ammonium ion. However the major factor is likely to be the relief of steric strain present in the parent[47] when the ethoxy group is twisted from the ring-plane during formation of the 1-adducts. This will manifest itself in a large value for the ratio K_1/K_3. That the value of the ratio is very much lower for the reaction with the secondary amine piperidine than for reaction with the primary amines probably indicates that the adduct (9.6; R´RN = $C_5H_{10}N$), where two bulky groups are at the C-1 position, is itself subject to steric strain. It is noteworthy that in the reaction of TNBCl with piperidine, reported in Chapter Six, attack at the 1-position was not observed presumably because of steric strain.

As has been noted in Chapter Six and in related systems[25-27,140] rate coefficients, k_1, for attack at the 1-position are considerably lower than corresponding values of k_3 for attack at the unsubstituted 3-position. Since values of

TABLE 9.16 Summary of kinetic and equilibrium data for amine attack at the 1-position of 2,4,6-trinitrophenetole in DMSO at 25°C

	n-Butylamine	Benzylamine	Piperidine[a]
$k_1/\ell\ mol^{-1}s^{-1}$	250	95	(1800)
$K_{c,1}/\ell\ mol^{-1}$	50,000	4700	600
$k_{-1}k_{AmH^+}/k_{Am}(s^{-1})$	0.005[b]	0.020[b]	(3)[b]
$k_{AmH^+}/\ell\ mol^{-1}s^{-1}$	>50	>60	9
$K_1k_{Am}/\ell^2\ mol^{-2}s^{-1}$	$>2.5 \times 10^6$	$>3 \times 10^5$	5600
$k_{Am}/k_{-1}(\ell\ mol^{-1})$	>10,000	>3000	(3)
$k_4/\ell\ mol^{-1}s^{-1}$	8.3	2.6	very slow reacti

a. Values in parentheses depend critically on value taken for $K_{c,3}$, and should be regarded only as "best estimates".

b. Since values of the ratio k_{AmH^+}/k_{Am} will not vary greatly with the nature of the amine (ref.152) these values give approximately the ratios of k_{-1} values for the three amines

K_1/K_3 are large this indicates that for a given amine values of k_{-1} will be several orders of magnitude smaller than values of k_{-3}.

The susceptibility to base catalysis of adduct formation depends upon the value of the ratio k_{Am}/k_{-1}. If at a given amine concentration $k_{Am}[Am] >> k_{-1}$ then base catalysis is not observed. This is the situation which applies to our measurements with the primary amines n-butylamine and benzylamin and may be attributed to the low values of k_{-1}. Nevertheless with piperidine our results indicate that formation of the 1-adduct is subject to catalysis by piperidine and we estimate that the value of k_{Am}/k_{-1} is reduced to *ca* 3. The data in row 3 of Table 9.16 indicate that the value of k_{-1} for reaction with piperidine will be much greater than for reaction with the prima amines; the bulky piperidine being expelled more rapidly. There is also evidence that the proton transfer between zwitterion and amine, k_{Am}, is considerably reduced for the reaction with secondary amine. Thus it was possible to determine a value of 9 l mol^{-1} s^{-1} for k_{AmH^+}, the rate coefficient for protonation of (9.6; R´RN = $C_5H_{10}N$) by piperidinium ions. This very low value, *ca* 20 times smaller than the corresponding value for reaction at the unsubstituted position (Table 9.15), results from the severe steric congestion around the 1-position. The value is lower than those for reaction involving primary amines. Hence since the value of the ratio $K_a^{9.1}/k_a^{AmH^+}$ is not expected to show large variations with the nature of the amine,[152] the value of k_{Am} ($=k_{AmH}+K_a^{9.1}/K_a^{AmH^+}$) will be smaller for the reaction with piperidine than with primary amines.

As has been observed in related systems[103,166,182] the value of k_4, the rate coefficient for acid catalysed expulsi

of the leaving group, is very much lower for the reaction with piperidine than for the reaction with primary amines. The result is that the adduct (9.6; R´RN = $C_5H_{10}N$) remains in solution for several hours with little decomposition. The reason for this increased stability is almost certainly steric in origin. The k_4 step involves proton transfer to the ethoxy group of the anionic intermediate coupled with rotation of the piperidine-moiety into the ring plane. The rate of proton transfer will be reduced by steric congestion and there is evidence[103,182] for unfavourable stereoelectronic/conformational effects when the transition state contains the piperidine group.

9.4.4 Comparison with related reactions

In Table 9.17 the data reported in this chapter is compared with those for reaction with amines of 1-ethoxy-2,4-dinitronaphthalene[103] and 1-methoxy-2,6-dinitro-4-methoxycarbonyl-benzene.[166] In each case nucleophilic substitution of the alkoxy group proceeds through detectable intermediates whose structures are respectively (9.6), (9.10) and (9.11). The values of the equilibrium constant $K_{c,1}$ decreases in the order (9.6) > (9.10) > (9.11), largely reflecting the electron

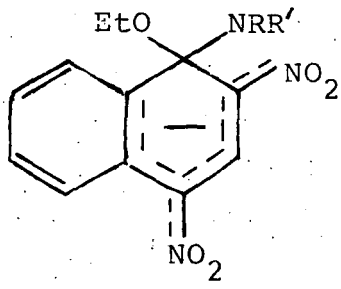

(9.10)

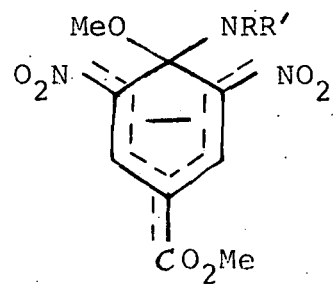

(9.11)

TABLE 9.17 Comparison of data for attack at the 1-position of 2,4,6-trinitrophenetole, 1-ethoxy-2,4-dinitronaphthalene and 1-methoxy-2,6-dinitro-4-methoxycarbonylbenzene

			Adduct	
		(9.6)	(9.10)[a]	(9.11)[b]
$k_1/\ell\ mol^{-1}s^{-1}$	n-Butylamine	250	31.8	-
	Piperidine	1800	240	100
$k_{c,1}/\ell\ mol^{-1}$	n-Butylamine	50,000	540	-
	Piperidine	600	1.55	0.083
$k_{-1}k_{AmH^+}/k_{Am}(s^{-1})$	n-Butylamine	0.005	0.059	-
	Piperidine	3	154	1200
$k_{Am}/k_{-1}(\ell\ mol^{-1})$	n-Butylamine	>10,000	-	-
	Piperidine	3	>20[c]	0.28

a. From references 103 and 182.

b. From reference 166.

c. Estimated from reference 103.

withdrawing ability of the ring substituents.[25-27] Values of k_1 decrease in the same order and it is expected that k_{-1} values will increase in this order. The value of the ratio k_{Am}/k_{AmH^+} ($\equiv K_a^{9.1}/K_a^{AmH^+}$) reflects the acidity of the zwitterionic intermediates relative to that of the corresponding substituted ammonium ions and will also depend on the electron withdrawing ability of ring substituents. Previously a value of 500 has been estimated for this quantity in a trinitro-activated compound,[152] and lower values are expected in the formation of (9.10) and (9.11). These changes coupled with the increases in the ratio $k_{-1}k_{AmH^+}/k_{Am}$ along the series (9.6), (9.10), (9.11).

Values of the ratio k_{Am}/k_{-1} are lower in the formation of (9.6) and (9.11) than in the formation of (9.10). A major factor here is likely to be a reduction in the value of k_{Am} as the reaction centre becomes increasingly sterically crowded.[166] The consequence is that the formation of (9.6) and (9.11) is more susceptible to base than is the formation of (9.10).

In conclusion the results reported in this chapter indicate that increased steric crowding at the reaction centre, engendered for example, by a change from primary amines to piperidine, results in (i) a reduction in the rate of proton transfer from zwitterionic intermediates to amine catalyst; and (ii) slower leaving group departure. There is evidence[151] that the first of these factors may be less severe in aqueous or partially aqueous media where proton transfer may proceed *via* interstitial water molecules. However both these factors will increase the probability of the observation of base catalysis during nucleophilic substitution reactions.

9.5 Derivation of the Rate Expressions

The rate expressions for the formation of the 3-adduct and 1-adduct of TNP with amines are derived in an analogous way to those for TNBCl shown in Chapter Six.

(i) The rate expression for the acid catalysed expulsion of ethoxide from the 1-adduct to give the N-substituted picramide.

$$TNP + 2Am \underset{}{\overset{K_{c,1}}{\rightleftharpoons}} (\underline{9.6}) + AmH^+$$

$$(\underline{9.6}) \xrightarrow{k_4} (\underline{9.7}) + Am + EtOH$$

The reaction is followed by measuring the formation of (9.7). Therefore,

$$\frac{d[9.7]}{dt} = k_4[9.6]\,[AmH^+] \qquad (\underline{1})$$

$$[TNP]_o = [TNP] + [9.6] + [9.7] \qquad (\underline{2})$$

$$K_{c,1} = \frac{[9.6][AmH^+]}{[TNP][Am]^2} \qquad (\underline{3})$$

Substituting for [TNP] in (2)by using (3).

$$[TNP]_o = [9.6]\left(1 + \frac{[AmH^+]}{K_{c,1}[Am]^2}\right) + [9.7] \qquad (\underline{4})$$

Re-arranging,

$$[9.6] = ([TNP]_o - [9.7])\,\frac{K_{c,1}[Am]^2}{K_{c,1}[Am]^2+[AmH^+]} \qquad (\underline{5})$$

Substituting (5) into (1)

$$\frac{d[9.7]}{dt} = ([TNP]_o - [9.7])\,\frac{k_4K_{c,1}[Am]^2[AmH^+]}{K_{c,1}[Am]^2+[AmH^+]} \qquad (\underline{6})$$

At equilibrium, $\frac{d[9.7]}{dt} = 0$

$$0 = ([TNP]_o - [9.7]_e) \frac{k_4 K_{c,1} [Am]^2 [AmH^+]}{K_{c,1} [Am]^2 + [AmH^+]} \quad (7)$$

Subtracting (7) from (6)

$$\frac{d[9.7]}{dt} = \frac{k_4 K_{c,1} [Am]^2 [AmH^+]}{K_{c,1} [Am]^2 + [AmH^+]} ([9.7]_e - [9.7]) \quad (8)$$

Relating [9.7] to OD

(9.7) is the only absorbing species at the wavelength used to follow the reaction. Hence,

$$OD = \varepsilon_{9.7} [9.7] \quad (9)$$

At equilibrium,

$$OD_e = \varepsilon_{9.7} [9.7]_e \quad (10)$$

Subtracting (9) from (10)

$$OD_e - OD = \varepsilon_{9.7} ([9.7]_e - [9.7]) \quad (11)$$

Differentiating (9),

$$\frac{d\ OD}{dt} = \varepsilon_{9.7} \frac{d[9.7]}{dt} \quad (12)$$

Substituting (12) into (11)

$$\frac{d\ OD}{dt} \cdot \frac{1}{OD_e - OD} = \frac{d[9.7]}{dt} \cdot \frac{1}{[9.7]_e - [9.7]} \quad (13)$$

The definition of k_{obs} is

$$k_{obs} = \frac{d\ OD}{dt} \cdot \frac{1}{OD_e - OD} \quad (14)$$

Hence combining (8), (13) and (14)

$$k_{obs} = \frac{k_4 K_{c,1} [Am]^2 [AmH^+]}{K_{c,1} [Am]^2 + [AmH^+]}$$

CHAPTER TEN

MISCELLANEOUS RESULTS

10.1 Introduction

This chapter is a collection of miscellaneous results, often incomplete, which could not be reported in the previous chapters. These results will be given under the following headings:

(a) The reaction of 2,4,6-trinitrobenzyl chloride with sodium hydroxide in water and in 30:70 (v/v) DMSO-water;

(b) Preliminary studies of the interactions between 2,4,6-trinitrobenzyl chloride and hydroxide ions in mixed solvents;

(c) Preliminary studies of the interactions of 2,2′,4,4′,6,6′-hexanitrobibenzyl with sulphite ions in water; and

(d) Kinetic and equilibrium studies of the interactions of 1,3,5-trinitrobenzene with thioglycollic acid in water.

10.2 Experimental

Visible spectral measurements were made using a Pye-Unicam SP 8005, SP 8100 or Hi-Tech SF-3L stopped-flow spectrophotometer. All rate measurements were made using the latter instrument at 25°C with the concentration of nucleophiles always in large excess over the substrate concentration so that first-order kinetics were observed. The rate coefficients are the mean of at least five separate determinations and are precise to ±5%. Examples of rate measurements are given in Table 10.1.

A Kent pH EIL 7055 pH meter and a combination electrode were used for pH measurements.

^{1}H n.m.r. measurements were made using a Varian EM 360L instrument using tetramethylsilane as an internal reference.

TABLE 10.1 Typical results from rate measurements

(i) TNBCl (1×10^{-5}M), sodium hydroxide (0.04M). First process. Measured at 455nm in water.

(ii) TNB (1×10^{-5}M), thioglycollic acid (0.006M). Measurable process. Measured at 500nm in water containing 0.026M sodium hydroxide and 0.0274M sodium chloride.[a]

(i)		(ii)	
t/s	ΔV^b	t/ms	ΔV^b
0.0	4.70	0	5.1
0.5	3.60	10	3.2
1.0	2.80	20	2.4
1.5	2.20	30	1.9
2.0	1.60	40	1.5
2.5	1.20	50	1.2
3.0	0.85	60	0.9
A plot of $\ln\Delta V$ versus t is linear and yields $k_{obs} = 0.55\ s^{-1}$		A plot of $\ln\Delta V$ versus t is linear and yields $k_{obs} = 24.0\ s^{-1}$	

a. Ionic strength I = 0.3M

b. $\Delta V = V_\infty - V_t$

10.3 The Reaction of 2,4,6-Trinitrobenzyl Chloride with Sodium Hydroxide in Water and in 30:70 (v/v) DMSO-water

10.3.1 Introduction

As stated previously, 2,2′,4,4′,6,6′-hexanitrostilbene (HNS) can be prepared by the reaction of 2,4,6-trinitrobibenzyl chloride (TNBCl) with base.[2,12] The reaction mechanism postulated[2] for this preparation requires the formation of the conjugate base (10.1) by removal of a side chain proton (see Chapter One). As the side chain proton could be removed by hydroxide ions, present in the reaction

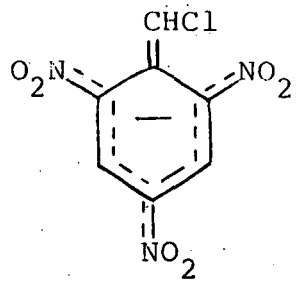

(10.1)

mixture, it is of interest to study the interactions of TNBCl with hydroxide ions. In this section the initial reversible reactions of TNBCl with sodium hydroxide in water, and in 30:70 (v/v) DMSO-water are reported.

10.3.2 Reactions with hydroxide ions in water

Figure 10.1 shows the visible spectra of TNBCl (2×10^{-5} M) in aqueous sodium hydroxide measured with a conventional spectrophotometer. In the more dilute solutions [NaOH] < 0.1 M the spectrum is similar to those of 1:1 σ-adducts formed from trinitro-activated substrates[25-27,82] showing a maximum at 445 nm with shoulder at 500 nm. In more concen-

Figure 10.1

Visible spectra of TNBCl, recorded one minute after mixing, in water containing the following concentrations of sodium hydroxide, A, 0.01M; B, 0.05M; C, 0.1M D, 0.5M

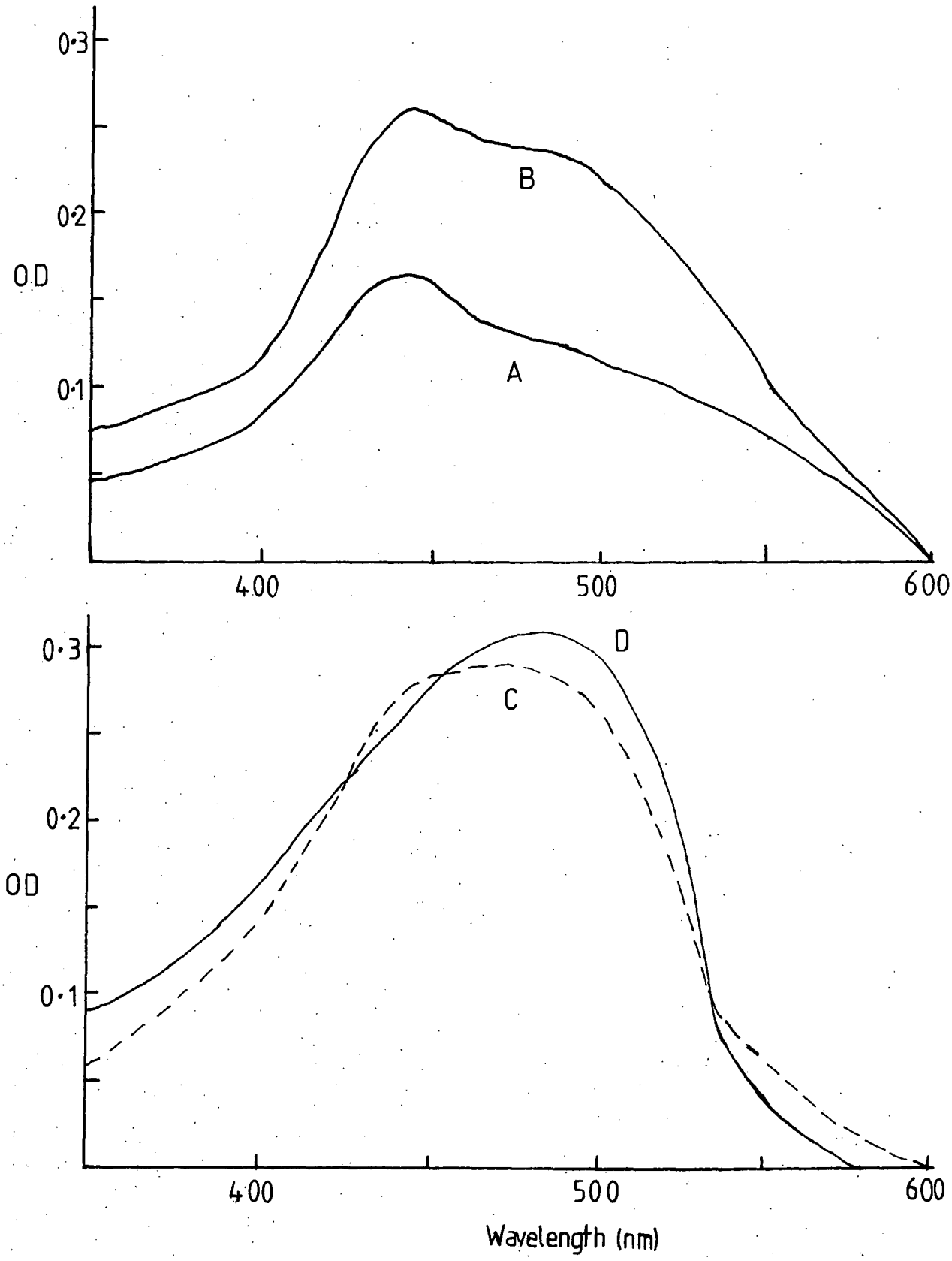

trated solutions a single broad maximum at 490 nm is observed indicating some further mode of reaction. By use of stopped-flow spectrophotometry the initial spectrum of a solution containing 0.1M base was measured within five seconds of mixing. It showed two absorption maxima at 455 nm and 500 nm and was similar to that of the time-stable species observed in more dilute solutions.

Two processes were observed using the stopped-flow spectrophotometer. Only the fast process was measured and the rate and equilibrium data are given in Table 10.2. As the hydroxide concentration was in large excess over TNBCl concentration the reaction was first order. The data are interpreted using Scheme 10.1. Evidence that the 1-hydroxy-adduct is formed rather than the 3-hydroxy-adduct will be given later. The data fits equation 10.1, derived using

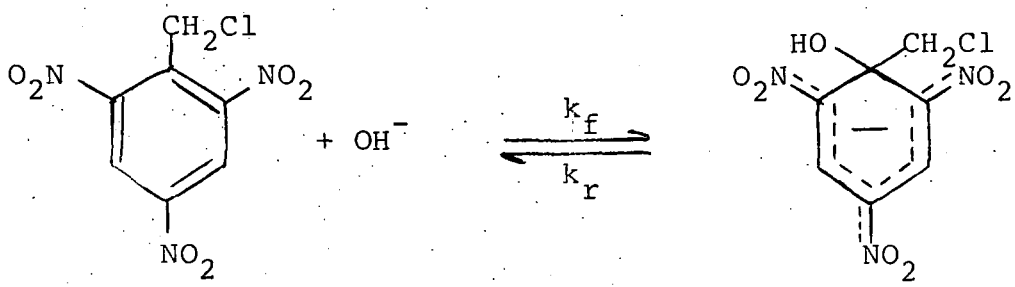

(10.2) (10.3)

$$k_{obs} = k_f[OH^-] + k_r \qquad \text{(equation 10.}$$

standard methods,[75] and gives a value for k_f of 11±0.1 ℓ $mol^{-1}s^{-1}$ and k_r of 0.1±0.02 s^{-1}. Combining these values gives an equilibrium constant $K(=k_f/k_r)$ of 110 ℓ mol^{-1}, which is in good agreement with that obtained from the optical densities.

^1H n.m.r. measurements in deuterium oxide would be the best technique to distinguish between the possible

TABLE 10.2 Kinetic and equilibrium data for the fast colour forming reaction of TNBCl (1×10^{-5}M) with sodium hydroxide in water[a] at 25°C

[NaOH][b]/M	k_{obs}/s^{-1}	OD[c](445 nm)	K[d]/ ℓ mol^{-1}
0.01	0.21	0.016	110
0.02	0.33	0.022	120
0.04	0.55	0.024	90
0.06	0.74	0.027	110
0.08	1.05	0.028	117
0.10	1.17	0.028	-

a. The solvent contains 1% by volume of DMSO.

b. I = 0.1M with sodium chloride.

c. A Benesi-Hildebrand plot[76] gives a value of 0.031 for complete conversion to adduct.

d. Calculated using K = OD(445)/[0.031-OD(445)][NaOH].

---

structures (10.3) and (10.4), but due to the low solubility of TNBCl in water this technique cannot be used. However, comparison of the rate and equilibrium data with those for reaction of 1,3,5-trinitrobenzene (TNB)[78] strongly suggests that these measurements relate to the formation of the 1-hydroxy adduct (10.2). The argument is as follows. It is known that the

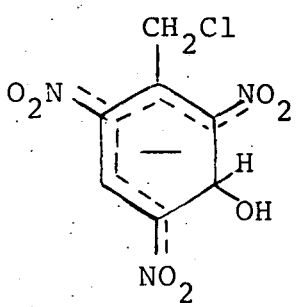

(10.4)

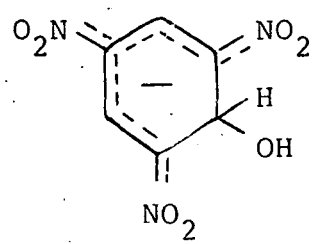

(10.5)

thermodynamic stabilities of adducts formed by attack of methoxide,[82] ethoxide,[82] sulphite[162] or amine (reported in Chapter Six) nucleophiles at the 3-position of TNBCl are lower than those of the corresponding adducts formed from TNB. This is probably due to the steric bulk of the CH_2Cl substituent which forces the ortho nitro-groups from the ring plane, thus reducing their electron withdrawal ability. However the value of 110 $\ell\ mol^{-1}$ observed for hydroxide attack on TNBCl is much higher than the value of 3.7 $\ell\ mol^{-1}$ for the reaction of hydroxide with TNB to give (10.5). The value is however compatable with the formation of (10.3) since attack at the 1-position will result in rotation of the CH_2Cl substituent from the ring plane with a consequent reduction in steric interaction. Since nucleophilic attack at unsubstituted ring positions is generally a faster process[140] than attack at substituted positions the failure to observe (10.4) can be attributed to the relatively low thermodynamic stability expected for this adduct in water.

The kinetic preference for attack at unsubstituted positions, and higher thermodynamic stability for the adducts formed by attack at the substituted position, is confirmed by comparing the data for reaction of TNBCl and TNB with hydroxide and methoxide ions given in Table 10.3. The ratios of equilibrium constants for the two substrates are 30 and 18 for the reaction with hydroxide and methoxide ions respectively.

Measurements for compounds[140,190] related to TNBCl with hydroxide ions have shown that ionisation of added hydroxyl groups can occur to give a di-anionic species. When this type

TABLE 10.3 Comparison of rate and equilibrium data for reactions of TNB and TNBCl with hydroxide ions in water and methoxide ions in methanol

	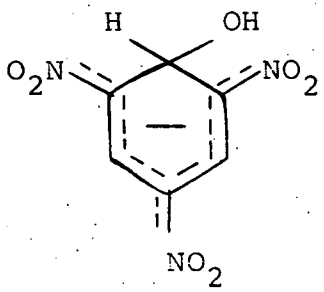	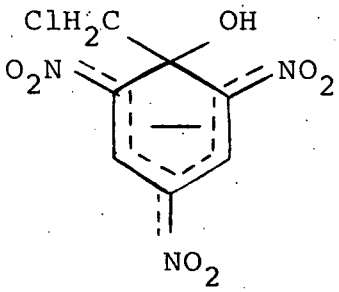	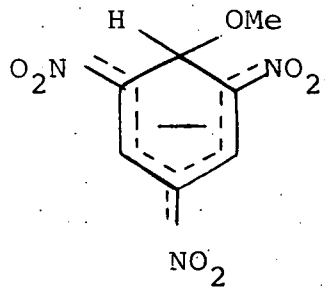	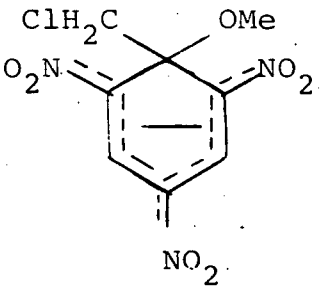
k_f	37.5	11	7300	770
k_r	9.8	0.1	330	2.2
K	3.7	110	20	350
Reference	78	This chapter	78	82

of di-anionic species is formed its spectrum usually differs only slightly from that of the 1:1 hydroxy-adduct. Also the equilibrium between the hydroxy adduct and its di-anionic form would be expected to be established very rapidly,[140,190] as it would involve proton transfer between two oxygen atoms. It has been found that in 0.1M base the spectrum recorded by stopped-flow spectrophotometry is different from that obtained at equilibrium. This is not in accord with rapid deprotonation. Therefore the spectral change observed in solutions where [NaOH] ≥0.1M is reasonably attributed[140,191] to formation of a di-adduct by hydroxide attack at the 1- and 3-positions and/or the 3- and 5- positions.

No evidence for the production of the conjugate base of TNBCl (10.1) is provided by these results. (10.1) is observed in methanol[82] where it gives a distinctive visible spectrum. Thus it can be presumed that in water or in media composed of a large water content the formation of (10.1) is unlikely, and therefore such solvents are not suitable for HNS synthesis.[2]

10.3.3 Reaction with hydroxide ions in 30:70 (v/v) DMSO-water

Visible spectra of TNBCl (2×10^{-5}M) and sodium hydroxide (0.001 - 0.1M) in 30:70 (v/v) DMSO-water were recorded on a conventional spectrophotometer. At sodium hydroxide concentrations ≤0.2M a spectrum typical of a σ-adduct was observed.[25-29] When [NaOH] = 0.001M maxima were observed at 440 and 512 nm which with increasing [NaOH] = 0.02M they were observed at 448 and 490 nm (shoulder). As [NaOH] was further increased the spectrum started to resemble those of 1:2 σ-adducts. Thus at

[NaOH] = 0.1M a single broad maxima was observed at 490 nm. The interpretation of these spectra is that applied to the spectra of the same reaction in water. That is formation of the 1:1 adduct (10.3) followed by formation of the 1:2 adduct, probably (10.6). Once again the distinctive visible spectrum of the conjugate base of TNBCl (10.1) was not observed.

^{1}H n.m.r. measurements in 70:30 (v/v) [$^2H_6$] DMSO-D_2O were attempted to try to discover the structure of the adducts formed. On addition of sodium deuterioxide the bands at δ9.08 (ring protons) and δ5.00 (CH_2 protons) due to TNBCl[92] disappeared and were not replaced. As the spectrum was recorded one minute after mixing it is believed that the σ-adduct formed is very unstable even in 70:30 DMSO-water solution. A further difficulty encountered during the ^{1}H n.m.r. measurements was a solid precipitating from the solution. This may be TINS.

Using stopped-flow spectrophotometry two well separated colour forming processes are observed and both were measurable. The rate and equilibrium data are in Table 10.4. Both processes produce reasonably linear plots for k_{obs} *versus* [NaOH]. Therefore the data will be interpreted using Scheme 10.2 The rate expressions derived from Scheme 10.2 are

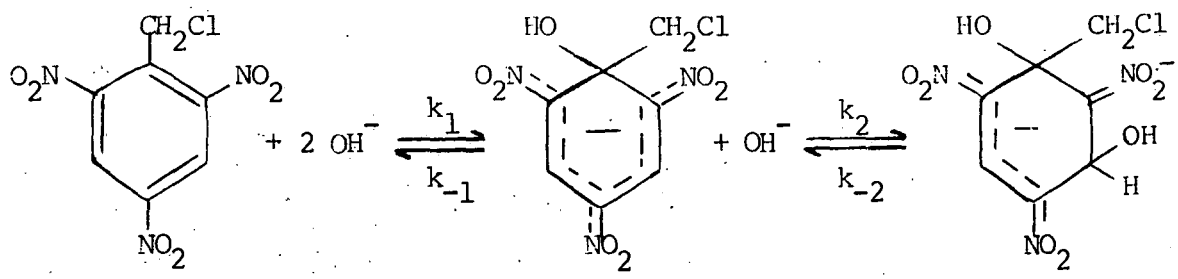

(10.2) (10.6)

Scheme 10.2

TABLE 10.4 Kinetic and equilibrium data for the σ-adduct formation reactions of TNBCl (1×10^{-5}M) with sodium hydroxide in 30:70 (v/v) DMSO-water at 25°C

[NaOH]^a/M	k_{fast}/s^{-1}	k^b_{fast}(calc)	OD_{fast}(490nm)	$10^2 k_{slow}/s^{-1}$	$10^2 k^c_{slow}$(c
0.01	0.60	0.70	0.020		
0.02	1.25	1.40	0.022		
0.03	2.09	2.10	0.024		
0.04	2.56	2.80	0.025	6.2	5.8
0.06	4.56	4.20	0.025	6.4	6.9
0.08	5.70	5.60	0.025	8.2	8.1
0.10	7.78	7.00	0.025	9.0	9.2

a. I = 0.1M using sodium chloride.

b. Calculated using k_1 0.70 ℓ mol^{-1} s^{-1} and equation 10.2.

c. Calculated using k_2 0.57 ℓ mol^{-1} s^{-1}, k_{-2} 0.035 s^{-1} and equation 10.2.

---

equations 10.2 and 10.3.

$$k_{fast} = k_1 [OH^-] + k_{-1} \qquad \text{(equation 10.}$$

$$k_{slow} = \frac{k_2 K_1}{1+K_1[OH^-]} + k_{-2} \qquad \text{(equation 10.}$$

A plot of k_{fast} *versus* $[OH^-]$ is linear with a zero or near zero intercept and gives a value for k_1 of 70 ℓ $mol^{-1}s^{-1}$. The optical density values show that complete conversion for the 1:1 adduct is attained at lower sodium hydroxide concentrations in 30:70 DMSO-water than in water. An approximate value of *ca.* 500 ℓ mol^{-1} for the equilibrium constant K_1 can be calculated from the optical densities. It is known[25-29] 1:1 σ-adducts are more stable in aprotic solvents or media containing an aprotic solvent, due to the ability of aprotic solvents to solvate the

large polarisable 1:1 σ-adduct and desolvate the small nucleophile.

As K_1 is large (estimated as *ca* 500 ℓ mol^{-1} from equilibrium optical densities) it can be assumed that $K_1[OH^-] >> 1$ and therefore equation 10.3 is modified to give equation 10.4. Thus a plot of k_{slow} *versus* $[OH^-]$ is linear. A value for k_{-2} of 0.57 ℓ mol^{-1} s^{-1} calculated from the slope

$$k_{slow} = k_2[OH^-] + k_{-2} \qquad \text{(equation 10}$$

and a value for k_{-2} of 0.035 s^{-1} from the intercept. However, these rate coefficients are likely to be subject to large errors due to them being based on limited data. A value for $K_2 (=k_2/k_{-2})$ of 16 is calculated.

Another possibility for the second process is shown by Scheme 10.3 below. This is hydroxide attack on the CH_2Cl group resulting in nucleophilic displacement reaction to form 2,4,6-trinitrobenzyl alcohol (TNBOH).

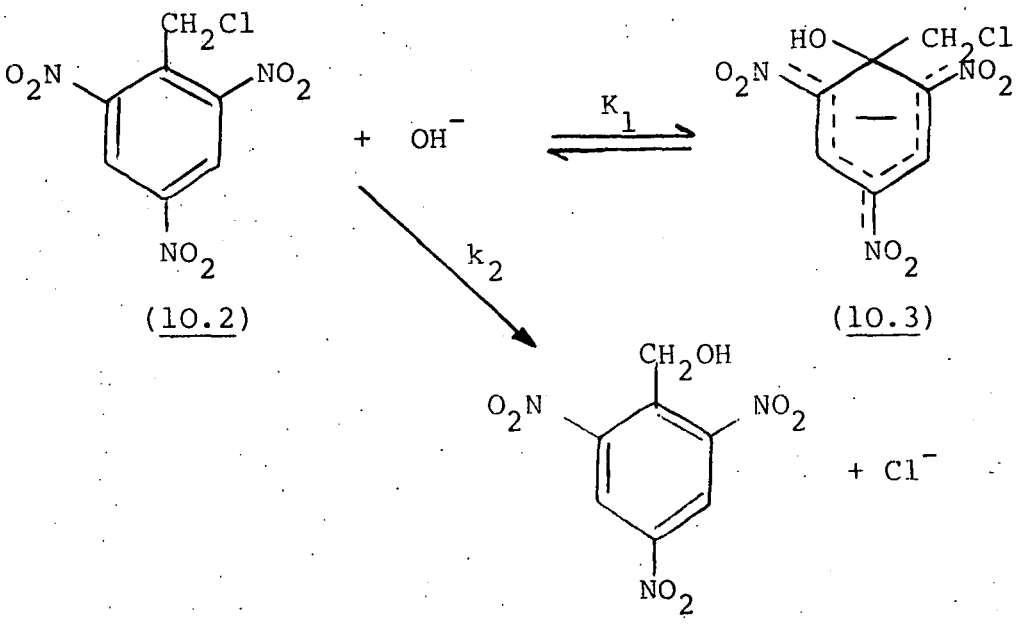

The rate expression is given by equation 10.5(a). Again if $K_1 \sim 500\ \ell\ mol^{-1}$ then $K_1[OH^-] >> 1$ and equation 10.5(a) is reduced to equation 10.5(b).

$$k_{obs} = \frac{k_2[OH^-]}{1+K_1[OH^-]} \qquad \text{(equation 10.5}$$

$$k_{obs} = \frac{k_2}{K_1} \qquad \text{(equation 10.5}$$

Equation 10.5(b) showsthat k_{obs} is a constant when $K_1[OH^-] >> 1$. The limited kinetic data does not allow the formation of TNBOH to be discounted but it appears unlikely. However, TNBOH will not be strongly coloured and as the visible spectra show a strongly coloured species is formed then the formation of TNBOH as a major reaction can be eliminated.

10.4 Preliminary Studies of the Interactions between 2,4,6-trinitrobenzyl chloride and hydroxide ions in mixed solvent

10.4.1 Introduction

The Shipp-Kaplan[2] reaction, *i.e.* the conversion of 2,4,6-trinitrotoluene (TNT) to HNS using alkaline hypochlorite, uses a 2:1:2 (v/v/v) tetrahydrofuran (THF)-methanol-(MeOH)-water solvent. It is well known that the first step of the reaction converts TNT to TNBCl but the intermediate via which TNBCl is converted to HNS, and hence the reaction mechanism, is unknown. (A fuller description of the Shipp-Kaplan reaction is given in Chapter One).

Previous kinetic studies[8,82,83,92,94,117,118,142] (which includes the data in Chapter Six) of the reactions of TNT and TNBCl have been made with a variety of bases in different solvent systems, but kinetic studies of the Shipp-Kaplan

reaction itself in the solvent system 2:1:2 THF-MeOH-water have been made. This section is a record of the preliminary visible spectra of the interaction of TNBCl with base in 2:1:2 THF-MeOH-water, which are a necessary precursor for kinetic studies. These spectra are incomplete and the information gained from them unsatisfactory. It should be stressed that the interpretations of the reactions are generally subjective as conclusive evidence can rarely be obtained from visible spectra.[25-29]

In the solvent 2:1:2 THF-MeOH-water the methoxide ions are in equilibrium as shown by Scheme 10.4. The equilibrium constant K'_{ha} is defined by equation 10.6. The value

$$MeOH + OH^- \underset{}{\overset{K'_{ha}}{\rightleftharpoons}} MeO^- + H_2O$$

Scheme 10.4

for K'_{ha} of 4.5, at 25°C, is known.[134] The equilibrium concen-

$$K'_{ha} = \frac{X_{H_2O}[MeO^-]}{X_{MeOH}[OH^-]} \qquad \text{(equation 10.6}$$

where X_{H_2O} = the mole fraction of water,
and X_{MeOH} = the mole fraction of methanol.

trations of methoxide ions and hydroxide ions can be changed by the addition of sodium hydroxide ions. Equations 10.7, 10.8 and 10.9 allows the calculation of the equilibrium concentrations of the methoxide ions $[MeO^-]_e$ and hydroxide ions $[OH^-]_e$ from the original concentration of hydroxide ions $[OH^-]_o$ added. When the concentrations used to measure the visible spectra are reported they will be given in terms of added sodium

$$[OH^-]_e + [MeO^-]_e = [OH^-]_o \qquad \text{(equation 10.}$$

$$[OH^-]_e = \frac{X_{H_2O}[MeO^-]_e}{X_{MeOH}K'_{ha}} \qquad \text{(equation 10.}$$

$$[OH^-]_o = [MeO^-]_e \left\{ 1 + \frac{X_{H_2O}}{X_{MeOH}K'_{ha}} \right\} \qquad \text{(equation 10.}$$

hydroxide with the methoxide concentrations at equilibrium given in brackets immediately afterwards.

In previous chapters very dilute substrate concentrations were used. Here higher concentrations, 0.001-0.01M were used. This required the use of a variable pathlength (usually *ca* 0.4mm) microcell.

10.4.2 Results and discussion

Using a 10mm pathlength cells visible spectra of solutions with TNBCl (2×10^{-5}M) and 0.001-0.01M NaOH (5.5×10^{-4} - 5.5×10^{-3}M methoxide ions) in 33/67 (v/v) MeOH-water were recorded. Initial spectra after about one minute show two maxima at 438nm and 510nm. At added sodium hydroxide concentrations $\leq$0.008M the lower wavelength maximum decays rapidly and the higher wavelength maximum decays slowly. At added sodium hydroxide concentrations of 0.01M the decay of the initial spectrum coincides with the growth of a maximum of *ca* 478 nm. The initial spectrum would suggest σ-adduct formation of 1:1 stoichiometry[25-29] while the single maximum at an added sodium hydroxide concentration of 0.1M would suggest a σ-adduct of 1:2 stoichiometry.[25-29] There are two nucleophiles present; MeO^- and OH^-. The 1:1 σ-adduct of TNBCl and methoxide ions in methanol[82] has maxima at 430 and 510nm while in the

previous section it has been reported that the spectrum of the 1:1 σ-adduct formed by TNBCl and hydroxide ions in water give maxima at 445 nm and 500 nm. In their own solvents the 1-methoxy-adduct is ninety-five times more stable than the 1-hydroxy-adduct and k_1 is twenty times larger. Changing to a 33:67 MeOH-water solvent should not change the relative values too much[192] and therefore the adduct observed in 33:67 MeOH-water is probably the 1-methoxy-adduct of TNBCl.

Visible spectra of 0.001$\underline{M}$ TNBCl in 50:50 (v/v) MeOH-water $5 \times 10^{-5}\underline{M}$ - 0.1$\underline{M}$ added sodium hydroxide (3.6×10^{-5} - $7.17 \times 10^{-3}\underline{M}$ methoxide ions) have been recorded using a cell with a pathlength of 5mm. At added hydroxide ion concentration $\geq 4 \times 10^{4}\underline{M}$ ($2.87 \times 10^{-4}\underline{M}$ methoxide ions) show double maxima, typical of σ-adduct formation,[25-29] at 430 and 510 nm. These maxima decay very slowly. At added hydroxide concentration of $4 \times 10^{-3}\underline{M}$ ($2.87 \times 10^{-3}\underline{M}$ methoxide ions) a maximum started to show after about an hour at 472 nm, which continued to grow very slowly. The initial species is presumably that assumed to be formed in 33:67 MeOH-water, the 1-methoxy-adduct. For comparison, it has previously been observed[193] in methanol that maxima at 424 nm and 500 nm were formed in the reaction of 0.0001$\underline{M}$ TNBCl with 0.001$\underline{M}$ NaOH. The species that produces this spectrum slowly decays. With 0.1$\underline{M}$ NaOH the species formed has maxima at about 430nm and 500nm, which is very stable. After eighteen hours a new species with a single maximum at 478nm is observed.

The next set of visible spectra to be recorded were for 2:1:2 THF-MeOH-water solutions containing $2 \times 10^{-5}\underline{M}$ TNBCl and 0.001-0.01$\underline{M}$ added hydroxide ions (4.41×10^{-4} - $5.59 \times 10^{-3}\underline{M}$ methoxide ions). Initial spectrum measured two minutes after

mixing of the red species formed show two maxima at 432nm and 512nm. At the added sodium hydroxide concentration of 0.01$\underline{M}$ ($5.59 \times 10^{-3}\underline{M}$ methoxide concentration) these maxima have extinction coefficients of 2.25×10^{4} $\ell\ mol^{-1}\ cm^{-1}$ and 1.6×10^{4} $\ell\ mol^{-1}\ cm^{-1}$ respectively. After about thirty minutes spectra of a purple species, formed from the red species had maxima of 600-650nm (very broad), 480nm (with shoulder at 430nm) and 370nm. An example of these spectra is shown in Figure 10.2. The initial spectrum of the red species is interpreted as σ-adduct formation by methoxide attack at the 1-position. In methanol this produces maxima at 430nm and 510nm. The purple species is interpreted as formation of the conjugate base of TNBCl which in methanol produces spectra at 650, 500 and 370 nm.[92] THF is an aprotic solvent and should therefore increase the stability of the σ-adduct in a THF-MeOH-water solvent compared to a MeOH-water solvent. Thus the visible spectra indicate that the red species is more thermodynamically stable in a THF-MeOH-water solvent than in MeOH-wate As the type of solvent is expected[25-29] to change the wavelength of absorption maxima the differences of the absorption maxima of the red species in MeOH-water compared to THF-MeOH-water is not surprising. When 0.001$\underline{M}$ TNBCl reacts with 0.01$\underline{M}$ NaOH ($5.59 \times 10^{-3}\underline{M}$ methoxide ions) in 2:1:2 THF-MeOH-water the spectrum indicates that the same species are formed but the maxima are more intense.

The Shipp-Kaplan reaction[2] produces the best yields of HNS if a pH of *ca* 10.2 is maintained. The buffer used to maintain a pH of 10.2 was a sodium bicarbonate buffer.[124] However after the visible spectra to be reported below were measured, a pH study of the reaction of $10^{2}\underline{M}$ TNBCl with $10^{-2}\underline{M}$

FIGURE 10.2 Visible spectrum of 2×10^{-5} M TNBCl and added 0.006M NaOH (3.35×10^{-3} M MeO^-) in 2:1:2 THF-MeOH-water; A, 2 minutes; B, 32 minutes after mixing

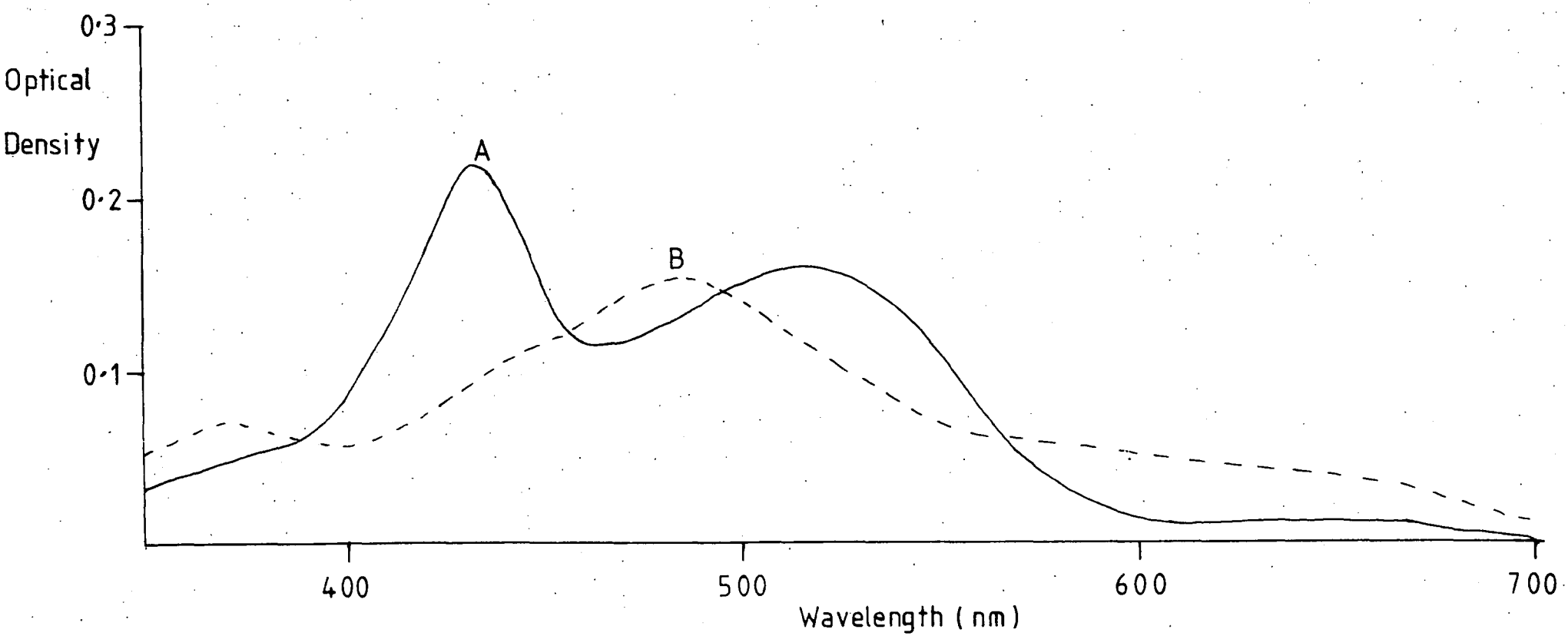

added NaOH (5.59×10^{-3} M methoxide) in 2:1:2 THF-MeOH-water, initially buffered at a pH of 10.18, showed that the pH of the solution decreased slowly to 9.05 after two hours before starting to increase. For some reason the bicarbonate/carbonate buffer was not maintaining pH.

The visible spectra of the red/brown solution measured while the pH was falling showed maxima at 432nm (OD_{max} 0.665) and 514nm (OD_{max} 0.460). The absorption slowly faded with the maxima moving slightly to 428 and 502nm. A 0.4mm pathlength cell was used. After ten minutes solid precipitated from solution, and is likely to be HNS as this is very insoluble in 2:1:2 THF-MeOH-water. Solid precipitated from a similar reaction system was filtered and dried. After dissolving in [$^2H_6$] DMSO its ^1H n.m.r. spectrum was recorded. Bands at δ9.10(s) and 7.13(s) were observed which can be assigned to the ring protons and olefinic protons of HNS respectively. This shows the solid precipitated is HNS.

The reactions of 2×10^{-5} M TNBCl in solutions of 2:1:2 THF-MeOH-water with an initial pH of 10.2, 10.68 and 11.2 were studied. The spectra all showed that three species were formed over eighteen hours after mixing. The first specie was red and gave maxima at 432-434 and 505-515nm. These maxima decayed to give a purplish species with maxima at 370, 436, 500 and 600-650nm. Finally after about eighteen hours a visible spectrum of a second red species shows absorption maxima at 465 and 525nm (shoulder). Figure 10.3 shows an example of these spectra. As the pH was increased the conversion to the σ-adduct was increased and in each case solid was observed to precipitate from the solution after about one and a half hours.

FIGURE 10.3 Visible spectra of 2 x 10^{-5} M TNBCl in 2:1:2 THF-MeOH-water at an initial pH of 10.2; A, 2 minutes, B, 31 minutes, C, 19 hours after mixing

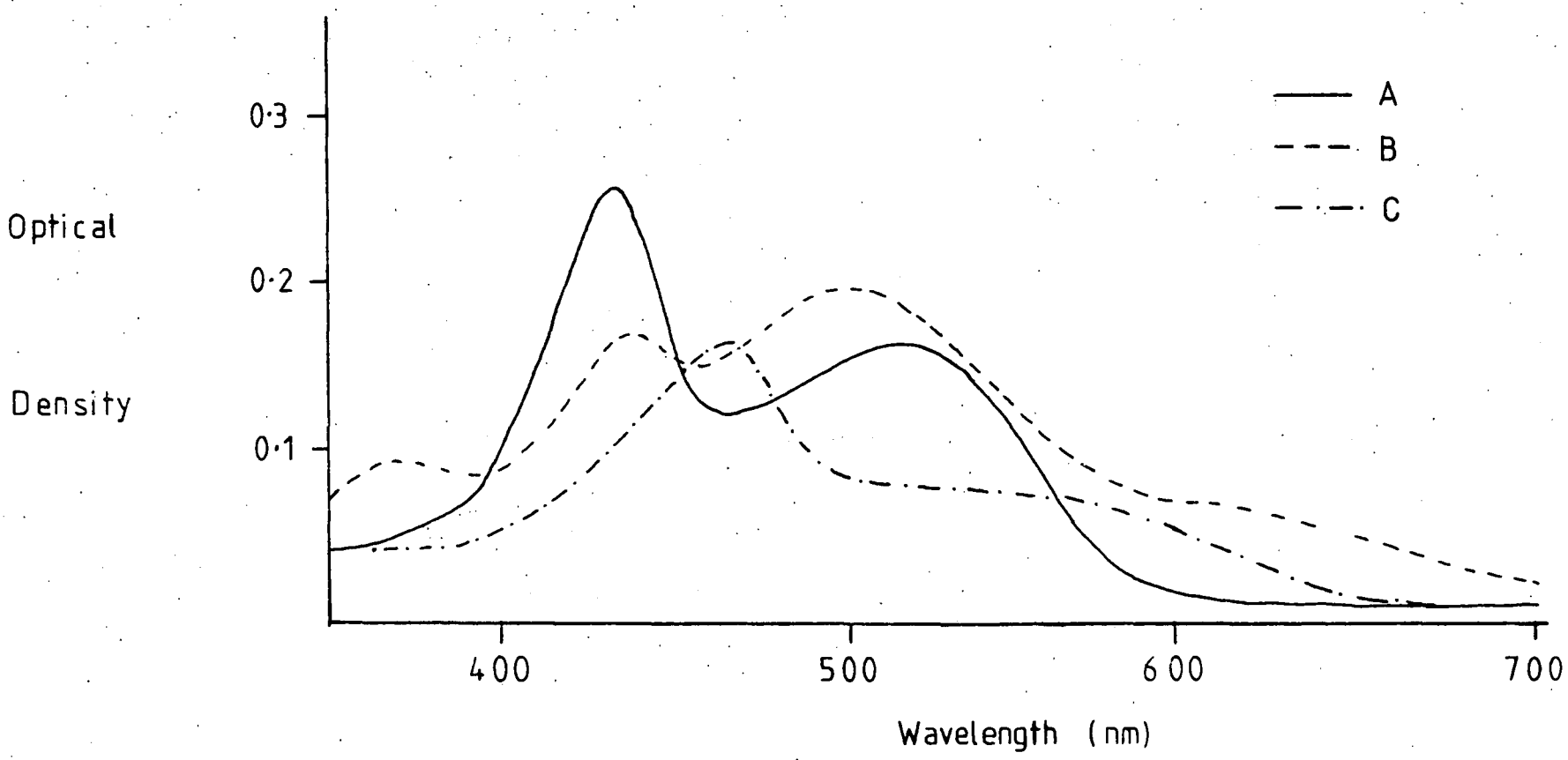

These spectra can be interpreted as formation of the 1-methoxy-adduct of TNBCl followed by its conversion to the conjugate base of TNBCl. The conjugate base of TNBCl then attacks a TNBCl molecule displacing Cl^- to form (10.8) which rapidly eliminates HCl to form HNS. The third species could then be some interaction of HNS with MeO^- or OH^-.

The visible spectra of 2×10^{-5}M HNS in 2:1:2 THF MeOH-water containing 0.1M added sodium hydroxide (5.59×10^{-2}M methoxide). Two maxima at 430nm and 480nm(shoulder) are record

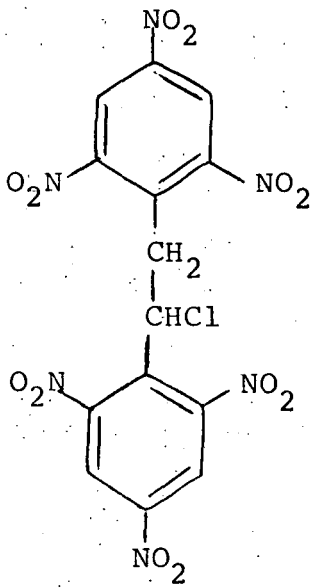

(10.8)

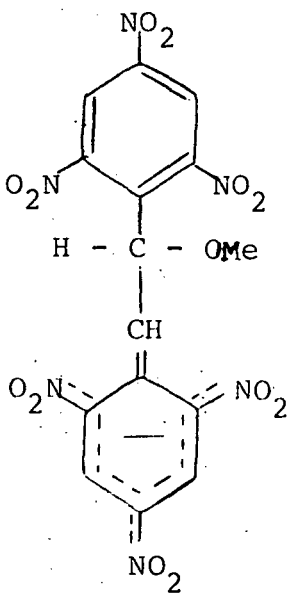

(10.9)

two minutes after mixing which after fifty-five minutes was a single maximum at 480nm. This is probably the formation of the 1-methoxy-adduct followed by the formation of (10.9) by methoxide attack at the olefinic bond. Allowing for the difference in solvent these species are found for the reaction between HNS and methoxide ions in methanol (reported in Chapter Five). The reactions of HNS and hydroxide ions, hydroxide ion being the other nucleophile present in the solvent, have not been studied.

10.5 Preliminary Studies of the Interactions of 2,2′,4,4′,6,6′-Hexanitrobibenzyl with Sulphite Ions

10.5.1 Introduction

Sulphite ions can form σ-adducts with trinitroaromatic compounds but because they are "soft" bases are not known to abstract any side-chain proton that might be available. Sulphite ions, due to their bulk tend to form 1:1 and 1:2 σ-adducts by addition at the unsubstituted positions of trinitroaromatic substrates containing a bulky substituent at the 1-position.[25-29] For example it has been shown that sulphite ions react with TNBCl[162] to form the adducts (10.10) and (10.11)

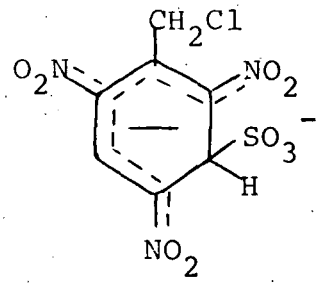

(10.10)

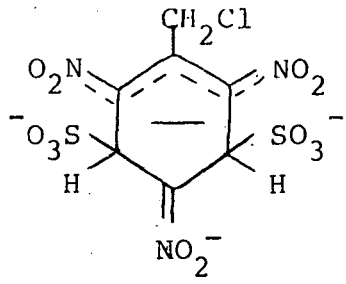

(10.11)

Throughout this thesis it has been shown that 2,2′,4,4′,6,6′-hexanitrobibenzyl (HNBB) reacts with nucleophiles in an analogous way to TNBCl. Therefore the σ-adducts (10.12) and (10.13) would be expected to be formed by nucleophili attack of sulphite ions on HNBB. Once again because there are two picryl rings per molecule of HNBB there is also the possibility of the σ-adducts (10.14), (10.15) and (10.16) being formed Isomerism may exist for some of the adducts shown.

It is known that 1:1 σ-adducts like (10.10) are more stable in aprotic solvents than protic solvents while 1:2 σ-adducts like (10.11) are more stable in protic solvents than

in aprotic solvents.[25] It would therefore be of interest to discover if (10.14) is more stable in DMSO, a dipolar aprotic solvent, than (10.12). Both are 1:2 σ-adducts but (10.14) could be described as a double 1:1 σ-adduct, as both picryl rings are well separated, and therefore better solvated in DMSO than (10.12). The opposite case would be expected in water, a protic solvent.

10.5.2 Visible Spectra

Visible spectra of HNBB (4×10^{-5} M) and sulphite ions (0.001 - 0.1M) in water containing 1% DMSO were attempted, but due to the insolubility of HNBB no useful results were obtained. At sulphite concentrations ≥ 0.1M a red species was observed and the spectra suggested 1:1 and 1:2 σ-adducts were responsible for the colour.

Visible spectra of HNBB (2×10^{-5} M) and sulphite ions (0.001 - 0.1M) in 30:70 (v/v) DMSO-water were recorded. They are very similar to those spectra previously observed between sulphite ions and trinitrobenzene compounds.[25-29] The actual structures of the 1:1 and 1:2 σ-adducts might be determined by using ^{1}H n.m.r. spectroscopy.

10.6 Kinetic and Equilibrium Studies of the Interactions of 1,3,5-Trinitrobenzene and Thioglycollic Acid in Water

10.6.1 Introduction

The reactions of 1,3,5-trinitrobenzene (TNB) with sulphite,[63,194-196] thiolate[197] and thiophenoxide[155,197] ions in water have previously been studied. It is found sulphur

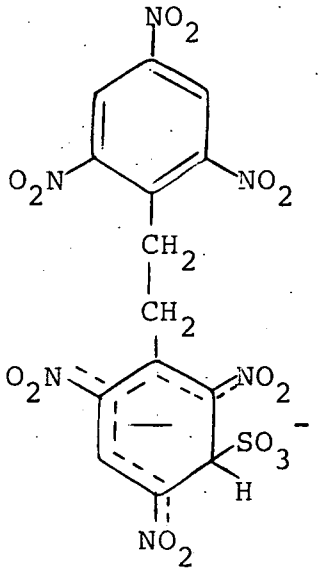

(10.12)

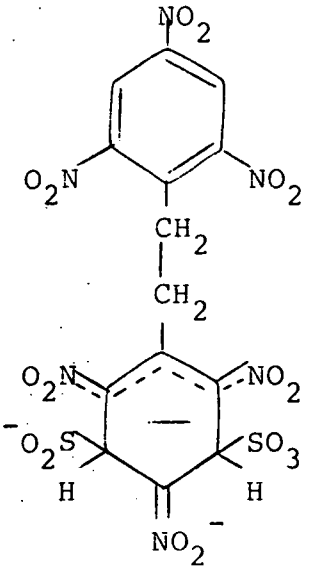

(10.13)

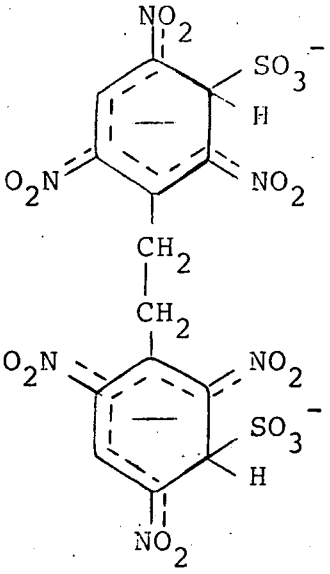

(10.14)

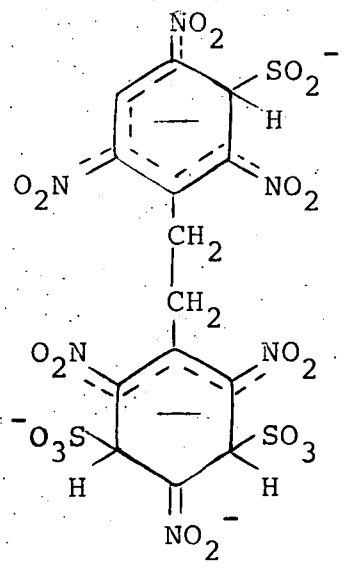

(10.15)

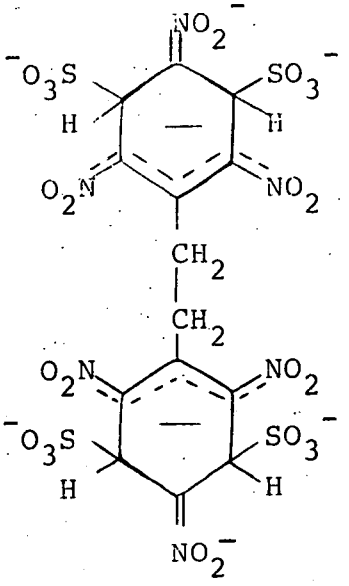

(10.16)

nucleophiles are more reactive than oxygen nucleophiles,[27] an unexpected fact on the basis of their pK_a values.

In this section the interactions of TNB with thioglycollic acid will be reported, although the study is incomplete and the results poor. This reaction is of interest because in water thioglycollic acid exists mainly as the di-anion, $^{-}SCH_2COO^{-}$, which is capable of reacting as a sulphur or oxygen nucleophile. The pK_a value for Scheme 10.5 as defined by equation 10.10 is reported[124] as 10.6±0.08.

$$HSCH_2COO^{-} \underset{}{\overset{K_a}{\rightleftharpoons}} {}^{-}SCH_2COO^{-} + H^{+}$$

Scheme 10.5

$$K_a = \frac{[{}^{-}SCH_2COO^{-}][H^{+}]}{[HSCH_2COO^{-}]} \qquad \text{(equation 10.1C}$$

10.6.2 Results and discussion

Visible spectra of TNB (4×10^{-5}M) with thioglycollic acid (0.001 - 0.1M) in water were recorded on a conventional spectrophotometer. At thioglycollic acid concentrations ≤0.004M spectra typical[25-29] of 1:1 adducts were observed with maxima at 464 and 540-570 nm (shoulder). At thioglycollic acid concentrations ≥0.4M spectra typical[25-29] of 1:2 σ-adducts were observed with a maximum *ca* 490nm. At the intermediate thioglycollic acid concentrations, between the stated limits, spectra were obtained that indicated that 1:1 and 1:2 σ-adducts were present. These spectra were very similar to those obtained for 1:1 and 1:2 σ-adducts formed between TNB and sulphite ions.[63,195] This indicates that thioglycollic

acid is behaving as a sulphur nucleophile forming a sulphur bonded σ-adduct. If it were forming an oxygen bonded σ-adduct the spectra would show maxima at shorter wavelengths, at *ca*, 410nm and 500nm.[25]

No ^1H n.m.r. spectra of the adducts formed by the reaction of TNB and $^-SCH_2COO^-$ have been recorded. However, the structures of the σ-adducts formed by the reaction of TNB with sulphite ions[195] and TNB with thiophenoxide ions,[197] are known. By analogy the 1:1 and 1:2 σ-adducts formed between TNB and $^-SCH_2COO^-$ can be predicted to have the structures (10.17) and (10.18).

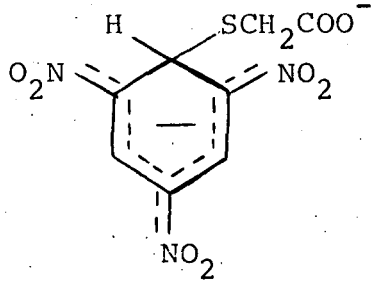

(10.17)

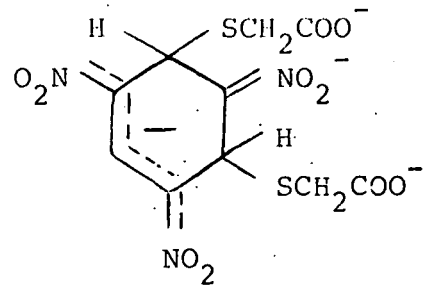

(10.18)

By the addition of sodium hydroxide in excess of thioglycollic acid concentration the thioglycollic acid will be present very largely in the form of the dianion, $^-SCH_2COO^-$. Visible spectra of TNB (4×10^{-5}M) and thioglycollic acid (0.001M) with [NaOH] in excess of [thioglycollic acid], in water, were recorded. These spectra indicate that provided [NaOH] was ≥0.008M, in exess of thioglycollic acid concentration then there is maximum conversion to the 1:1 σ-adduct for that particular thioglycollic acid concentration. Because the [NaOH

is present in large excess over TNB concentration in these aqueous TNB/thioglycollic acid solutions, formation of the 1:1 σ-adduct between TNB and hydroxide ions (10.3) must be considered. The equilibrium constant for formation of (10.3), K_{TNB/OH^-}, has previously[78] been measured as 3.8. Using equation 10.11 it can be shown that the concentration of (10.3)

$$K_{TNB/OH^-} = \frac{[10.3]}{[TNB]\,[OH^-]} \qquad \text{(equation 10.1}$$

present in solutions containing 0.01 or 0.02M excess sodium hydroxide will be small.

Stopped-flow spectrophotometry showed that the reaction of TNB and thioglycollic acid produced what appeared to be two colour forming species. Observation of the reaction at a wavelength of 490nm showed that a rapid colour forming process, completed almost instantaneously the reactants were mixed, was followed by a measurable colour forming process. At a wavelength of 550nm the same reaction gave a rapid colour forming process followed by a rapid colour fading process. These observations are in accord with the visible spectral evidence.

The reaction between TNB and thioglycollic acid in water was measured under three different experimental conditions on the stopped-flow spectrophotometer. Kinetic and equilibrium data measured with ionic strength, I = 0.1M and 0.01M [NaOH] in exesss of thioglycollic acid concentration are given in Table 10.5; with I = 0.1M and 0.02M [NaOH] in excess of thioglycollic acid concentration are given in Table 10.6; and with I = 0.3M and 0.02M [NaOH] in excess of thioglycollic acid concentration are given in Table 10.7. The excess sodium hydroxide concentration was added to ensure the majority of thioglycollic

TABLE 10.5 Kinetic and equilibrium data for the reaction of TNB (2×10^{-5} M) thioglycollic acid in water[a] containing 0.01 excess sodium hydroxide at 25°C

$[^{-}SCH_2COO^{-}]$/M	k_{obs}/s^{-1}	OD_1^b(500nm)	$K_1^c/\ell\ mol^{-1}$	OD_2^d(500nm)
0.001	6.9±0.2	0.0063	104	0.0129
0.002	8.0	0.0123	113	0.0250
0.004	11.5	0.0214	118	0.0391
0.006	15.7	0.0278	119	0.0458
0.008	18.9	0.0334	125	0.0496
0.01	22.5	0.0372	126	0.0525
0.02	29.1	0.0477	125	0.0545
0.04	33.5	0.0487	68	0.0555

a. I = 0.1M made up using sodium chloride.

b. Measured at completion of the first process. A Benesi-Hildebrand plot yields an optical density for complete conversion to adduct of 0.0561.

c. Calculated using $K_1 = OD_1(500)/[0.0561-OD_1(500)][^{-}SCH_2COO^{-}]$

d. Measured at the completion of the second process.

TABLE 10.6 Kinetic and equilibrium data for the reaction of TNB (2×10^{-5} M) with thioglycollic acid in water[a] containing 0.02 M excess sodium hydroxide at 25°C

$[^-SCH_2COO^-]$/M	k_{obs}/s^{-1}	OD_1^b(500nm)	$K_1^c/\ell\ mol^{-1}$	OD_2^d(500nm)
0.001	7.4±0.3	0.0063	104	0.0137
0.002	7.8	0.0123	113	0.0264
0.004	11.2	0.0205	111	0.0400
0.006	15.9	0.0278	119	0.0458
0.008	20.5	0.0362	148	0.0496
0.010	25.3	0.0391	141	0.0526
0.020	35.9	0.0467	117	0.0535
0.040	36.8	0.0487	68	0.0516

a. I = 0.1 M made up with sodium chloride.

b. Measured at the completion of the first process. A Benesi-Hildebrand plot yields an optical density for complete conversion to the adduct of 0.0667.

c. Calculated using $OD_1(500)/[0.0667-OD_1(500)][^-SCH_2COO^-]$

d. Measured at completion of the second process.

TABLE 10.7 Kinetic and equilibrium data for the reaction of TNB (2×10^{-5}M) with thioglycollic acid in water[a] containing 0.02M excess sodium hydroxide at 25°C

$[^{-}SCH_2COO^{-}]$/M	k_{obs}	OD_1(500nm)[b]	K_1^c/ℓ mol^{-1}	OD_2(500nm)
0.001	7.6±0.3	0.0070	44	0.0237
0.002	10.1	0.0150	49	0.0419
0.004	17.8	0.0306	56	0.0615
0.006	24.9	0.0372	48	0.0645
0.008	30.6	0.0438	45	0.0655
0.01	33.3	0.0516	45	0.0716

a. I = 0.3 made up with sodium chloride.

b. Measured at the completion of the first process. A Benesi-Hildebrand plot yields an optical density value for complete conversion to the adduct of 0.1667.

c. Calculated using $K_1 = OD_1(500)/[0.1667-OD_1(500)][^{-}SCH_2COO^{-}]$

d. Measured at completion of the second process.

acid was present as the $^{-}SCH_2COO^{-}$ ion. Data in Table 10.6 are a repetition of data in Table 10.5 but with the excess [NaOH] doubled. This does appear to change the rate coefficients for the measured process, especially at high thioglycollic acid concentrations, suggesting that not all the thioglycollic acid is converted into $^{-}SCH_2COO^{-}$ ion when 0.1M excess sodium hydroxide is present.

The data was first interpreted using Scheme 10.6. From this scheme the general rate expression, given in equation 10.12, can be derived.

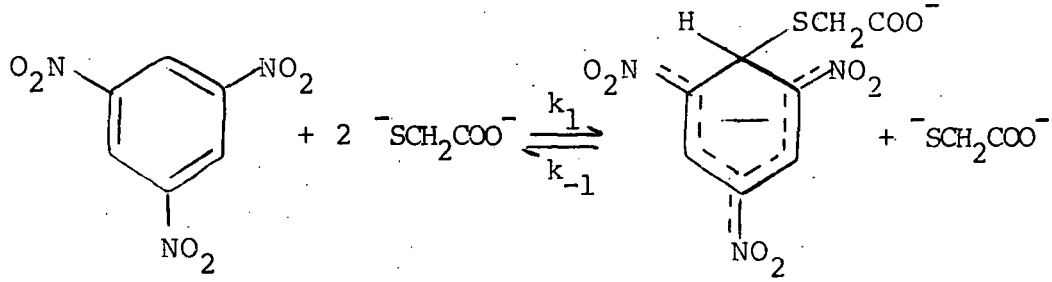

(10.2) (10.17)

Scheme 10.6

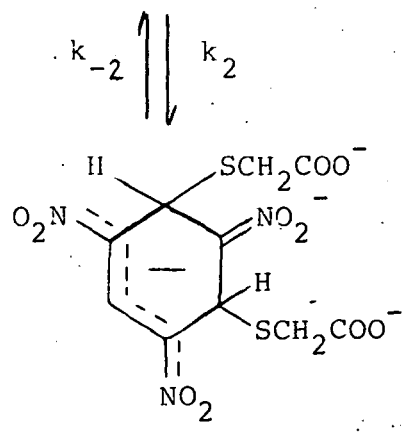

(10.18)

$$k_{obs} = \frac{k_2 K_1 [S]^2}{1+K_1[S]} + k_{-2}$$ (equation 10.1

where [S] = [$^{-}SCH_2COO^{-}$]. This notation will be used throughout this chapter.

Although too fast for rate measurements the first processes equilibrium constant K_1 can be calculated from the optical density measurements. It is found for the data in Tables 10.5 and 10.6 that K_1 has a value of 120±20 ℓ mol^{-1}. Using this value in equation 10.12 a plot of k_{obs} *versus* $K_1[S]/(1+K_1[S])$ is not linear as would be predicted, (see Figures 10.4 and 10.5). k_{obs} tends towards a maximum. This observation suggests that the $[^-SCH_2COO^-]$ is not as expected; possibly $^-SCH_2COO^-$ decays in water.

In water the thioglycollic acid dianion produces an absorption maximum at 233nm. The decay of this maximum was measured every thirty minutes for five hours. It was found the maximum decays slowly and linearly with time. After thirty minutes the $[^-SCH_2COO^-]$ had fallen by *ca* 1%.

Table 10.7 consists of data using freshly prepared solutions of $^-SCH_2COO^-$ for each $[^-SCH_2COO^-]$, and by completing rate and equilibrium measurements within thirty minutes of preparation of each $[^-SCH_2COO^-]$ the $[^-SCH_2COO^-]$ should be reasonably accurate. From the optical densities a value for K_1 of 48±8 ℓ mol^{-1} is calculated. Once again a plot of k_{obs} *versus* $K_1[S]^2/(1+K_1[S])$ is curved with k_{obs} tending towards a maximum.

Scheme 10.6 does not appear to interpret the data very successfully. There are two other schemes that can be regarded as sensible possible explanations for the data. Scheme 10.7 shows the formation of the bicyclic complex (10.19). In order for this scheme to comply with the processes observed by stopped-flow spectrophotometry it is necessary to assume that

FIGURE 10.4 Plot of k_{obs} *versus* $K_1[^-SCH_2COO^-]^2/(1+K_1[^-SCH_2COO^-])$ for the data in Table 10.5 using K_1 118 ℓ mol^{-1}

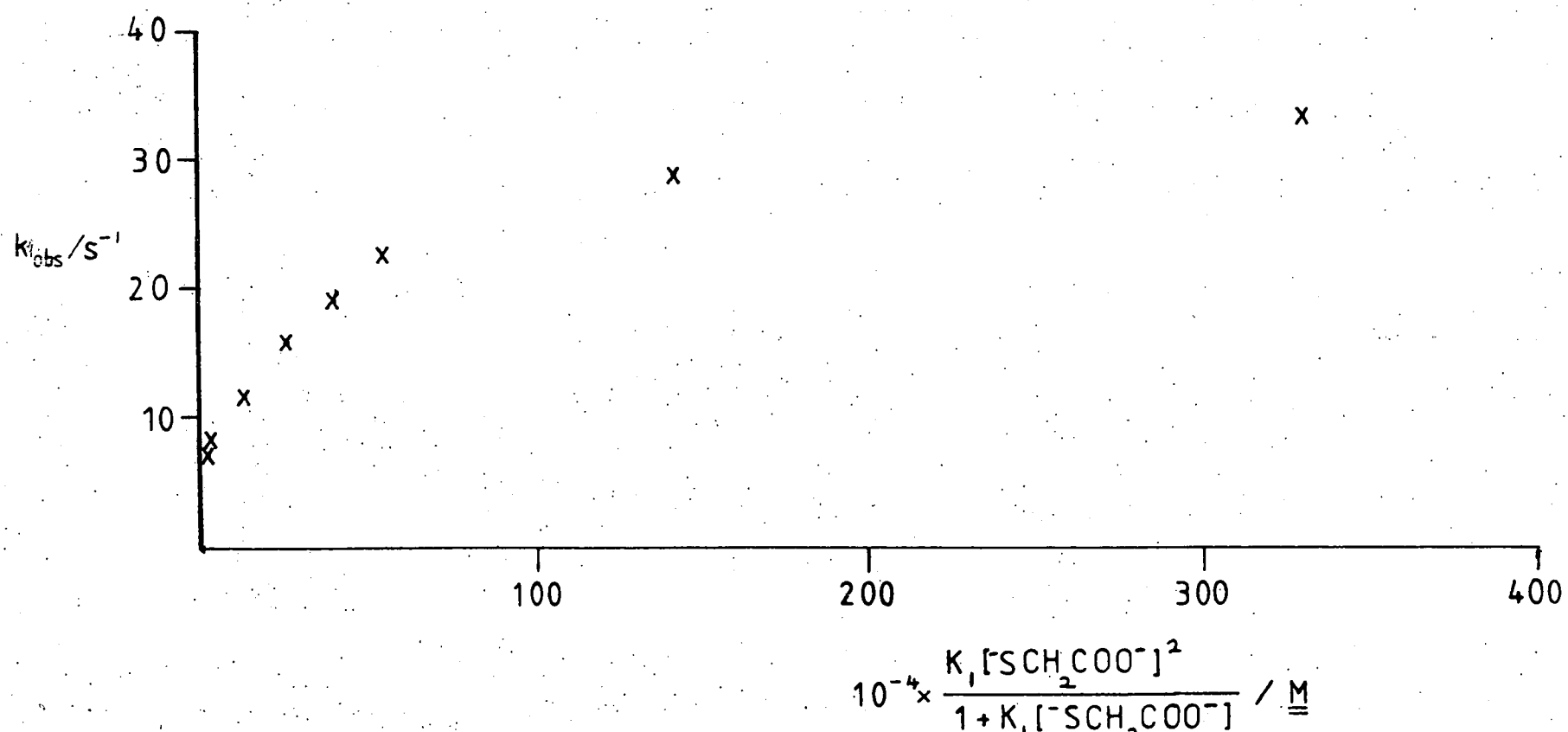

FIGURE 10.5 Plot of k_{obs} *versus* $K_1\,[^-SCH_2COO^-]^2/(1+K_1[^-SCH_2COO^-])$ for the data in Table 10.6 using K_1 118 ℓ mol^{-1}

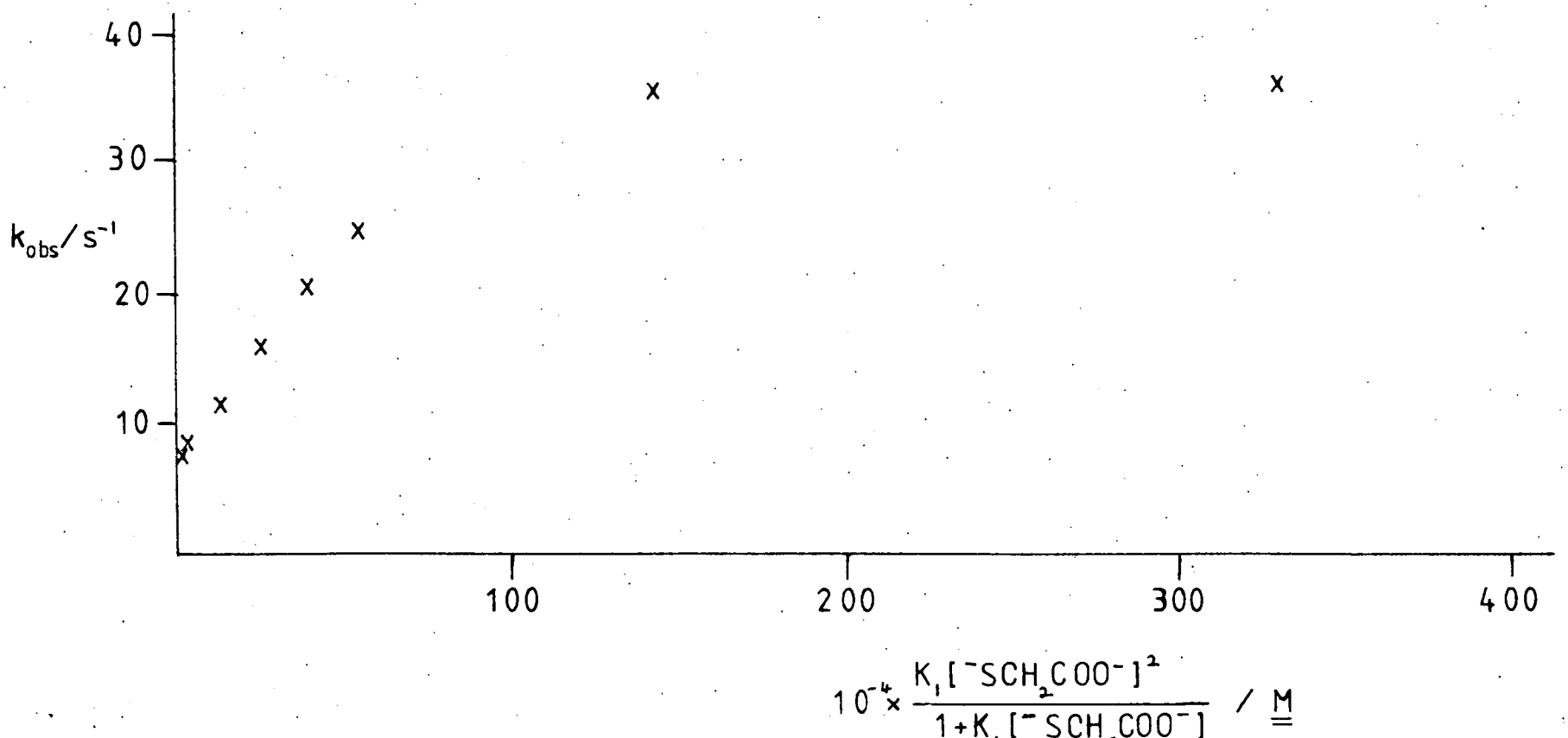

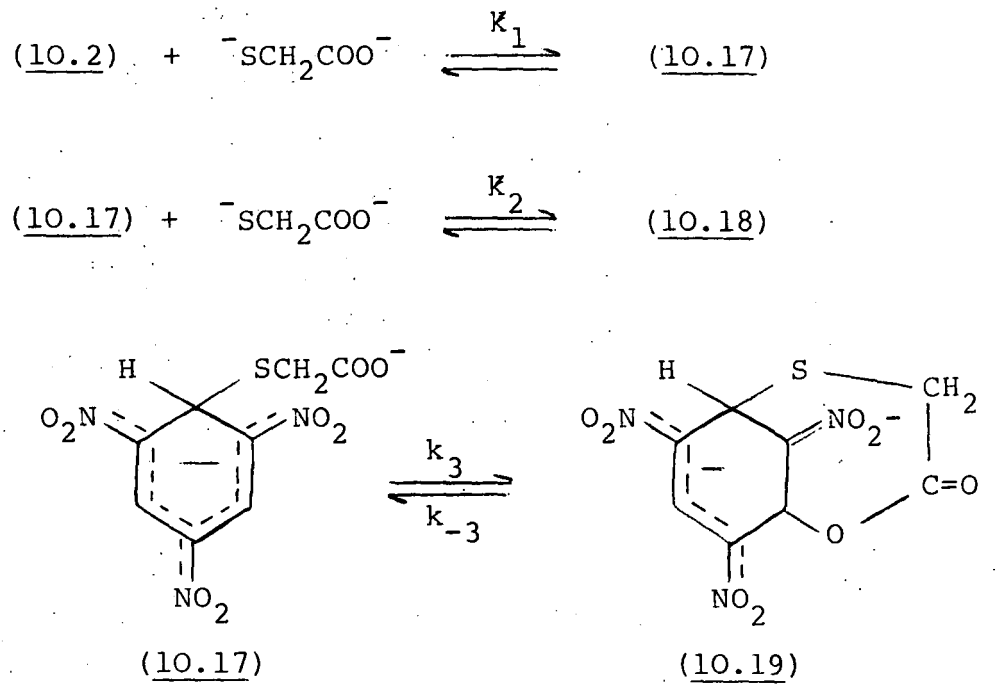

Scheme 10.7

the formation of (10.17) and (10.18) are rapid followed by the formation of (10.19) which is the measurable process by stopped-flow spectrophotometry. The rate expression for Scheme 10.7 is given by equation 10.13. If this scheme is

$$k_{obs} = \frac{k_3 K_1 [S]}{1+K_1[S](1+K_2[S])} + k_{-3} \qquad \text{(equation 10.13}$$

correct it will require further study to provide the evidence. ^1H n.m.r. spectroscopy would be able to determine whether (10.19) is formed. The visible spectra tend to suggest a 1:2 σ-adduct is being formed rather than a bicyclic complex.

Scheme 10.8 shows the possibility that after the formation of the 1:1 adduct there is formation of the cis (10.18c and trans (10.18t) 1:2 adducts.

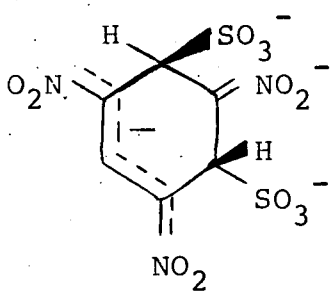

(10.18t)

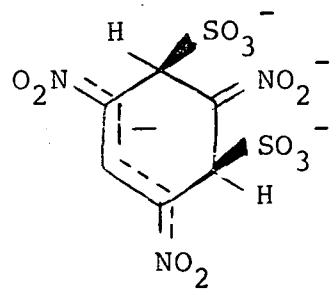

(10.18c)

$$(10.2) + {}^{-}SCH_2COO^{-} \underset{}{\overset{K_1}{\rightleftharpoons}} (10.17)$$

Scheme 10.8

$$(10.17) + {}^{-}SCH_2COO^{-} \underset{k_{-2}}{\overset{k_2}{\rightleftharpoons}} (10.18t)$$

$$\underset{k_{-3}}{\overset{k_3}{\rightleftharpoons}} (10.18c)$$

The formation of cis and trans adducts of TNB has only previously been observed for its reaction with sulphite ions.[195] In this study three relaxation times were observed corresponding to the formation of the 1:1 σ-adduct, the cis 1:2 σ-adduct and the trans 1:2 σ-adduct were possible. The visible spectra of the cis and trans 1:2 σ-adducts were, when measured using a stopped-flow spectrophotometer, found to be slightly different.[195] The maximum for the cis 1:2 adduct (10.18c) was at 490nm and for the trans 1:2 adduct (10.18t) was at 500nm. Previously [63,194] conventional spectrophotometric measurements had just reported one equilibrium for a 1:2 adduct and this has been explained[195] as a summed spectra of the cis and trans 1:2 adduct. Therefore the observation of a single 1:2 adduct by conventional spectrophotometry for TNB and ${}^{-}SCH_2COO^{-}$ may be misleading. Studies by ^1H n.m.r. spectroscopy have not provided

any evidence for the formation of cis and trans 1:2 adducts for the reactions between the activated aromatic molecules and nucleophiles.[63] However this may be due to the isomers having very similar spectral properties that the experimental techniques are not sensitive enough to distinguish between the isomers, or that one isomer is much more stable than the other.[194] The rate expression derived from Scheme 10.8 is given by equation 10.14.

$$k_{obs} = \frac{k_3 K_1 [S]^2}{1+K_1[S](1+K_2[S])} + k_{-3} \qquad \text{(equation 10.14)}$$

Once again it is necessary to assume the first two processes are rapid and the third process is the only one measurable by stopped-flow spectrophotometry. The rate coefficient, k_3, is assumed to be that for formation of the cis 1:2 adduct following Bernasconi's interpretation that the cis 1:2 adduct is the final process in the reaction between TNB and sulphite ions.[194] However there is the possibility that the third process reported here may be the formation of the trans 1:2 adduct.

It was shown[194] for the reaction of TNB with sulphite ions that a plot of k_{obs} *versus* [S], where [S] = SO_3^{2-}, is sigmoid in shape. If k_{obs} *versus* [S], where [S] = $^-SCH_2COO^-$, is plotted for the data in Tables 10.5 and 10.6, then a sigmoid plot is obtained. Where the plot is linear the conditions $K_1[S] >> 1$ and $K_2[S] << 1$ could apply producing equation 10.15. Using equation 10.15 values for k_3 and k_{-3} can be estimated

$$k_{obs} = k_3[S] + k_{-3} \qquad \text{(equation 10.15)}$$

from the slope and intercept respectively. For the data in Table 10.5 a value for k_3 of 1810±200 $\ell\ mol^{-1}\ s^{-1}$ and for k_{-3}

of 4.4±0.4 s^{-1} are calculated. This gives a value for K_3 ($=k_3/k_{-3}$) of 410 ℓ mol^{-1}. Data in Table 10.6 give values of k_3 2160±200 ℓ mol^{-1} s^{-1}, k_{-3} 3±0.5 s^{-1} and K_3 720 ℓ mol^{-1}. The differences in the rate coefficients and the equilibrium constants derived from them is perhaps an indication that not all the thioglycollic acid concentration was present as $^-SCH_2COO^-$ ions when 0.1M excess sodium hydroxide was present.

It has already been mentioned that k_{obs} tends towards a maximum value. If $K_1[S]>>1$ and $K_2[S]>>1$ then equation 10.14 becomes equation 10.16. This new rate expression predicts a rate maximum equivalent to $k_{-3} + k_3/K_2$.

$$k_{obs} = \frac{k_3}{K_2} + k_{-3} \qquad \text{(equation 10.16}$$

To estimate a value for K_2 it is assumed that the data in Table 10.5 tend to a maximum rate of 36 s^{-1}. Then using the known values of k_3 and k_{-3} a value for K_2 of 57 ℓ mol^{-1} is obtained. For the data in Table 10.6 the maximum value of k_{obs} is 38 s^{-1} leading to a value for K_2 of 62 ℓ 1 mol^{-1}.

Data in Table 10.7, when I = 0.3M, gives a linear plot which can be interpreted using equation 10.15. Values for k_3 of 3450 ℓ mol^{-1} s^{-1} and for k_{-3} of 3.5 s^{-1} are calculated yielding a value for K_3 of 986 $l.mol^{-1}$. At the concentrations studied it is difficult to determine a maximum k_{obs} value but it is estimated as *ca* 38 s^{-1}, giving a value for K_2 of 100 ℓ mol^{-1} s^{-1}, using equation 10.16.

Comparison of the data for the reactions at I = 0.3M of TNB and $^-SCH_2COO^-$ in water with TNB and sulphite ions in water is given in Table 10.8. Here it is seen that for the reaction between TNB and sulphite ions the

ratio k_2/k_3 is *ca* 163 and the ratio k_{-2}/k_{-3} is *ca* 161. If these ratios were applied to the reactions of TNB with $^-SCH_2COO^-$ then the half life for the second process, formation of the cis 1:2 adduct, at the concentrations studied would be *ca.* 0.1ms. This would mean the reaction would be too fast for measurement by stopped-flow spectrophotometry. If this explanation of the data is correct, *i.e.* using Scheme 10.8, then one 1:2 adduct, (nominally called the trans adduct), formed between TNB and $^-SCH_2COO^-$ ions is ten times more stable than the other. This is not found[194] for the 1:2 adducts formed between TNB and sulphite ions where they are of almost equal stability.

It must be stressed that there is no definite evidence for the formation of cis/trans isomers of 1:2 stoichiometry from TNB and $^-SCH_2COO^-$ ions. The kinetic analysis given is highly speculative. This section has shown that there is need for further study of the interactions between TNB and $^-SCH_2COO^-$ ions to identify the species involved.

TABLE 10.8 Comparison of data for the cis and trans 1:2 σ-adducts formed between TNB and sulphur nucleophiles in water at I = 0.3M

	k_2/ℓ $mol^{-1}s^{-1}$	k_{-2}/s^{-1}	K_2/ℓ mol^{-1}	k_3/ℓ $mol^{-1}s^{-1}$	k_{-3}/s^{-1}	K_3/ℓmol^{-1}
[a] SO_3^{2-}	195	21	9.3	1.2	0.13	9.2
$^-SCH_2COO^-$			100	3450	3.5	986

a. Data from reference 194.

10.7 Derivation of the Rate Expressions

(i) σ-adduct formation.

$$(\underline{10.2}) + OH^- \underset{k_r}{\overset{k_f}{\rightleftharpoons}} (\underline{10.3})$$

$$\frac{d[10.3]}{dt} = k_f[10.2][OH^-] - k_r[10.3] \quad (\underline{1})$$

$$[10.2]_o = [10.2] + [10.3]$$

$$[10.2] = [10.2]_o - [10.3] \quad (\underline{2})$$

Substituting (2) into (1).

$$\frac{d[10.3]}{dt} = k_f[OH^-]([10.2]_o - [10.3]) - k_r[10.3] \quad (\underline{3})$$

At equilibrium, $\frac{d[10.3]}{dt} = 0$

$$0 = k_f[OH^-]([10.2]_o - [10.3]_e) - k_r[10.3]_e \quad (\underline{4})$$

Subtracting (4) from (3).

$$\frac{d[10.3]}{dt} = (k_f[OH^-] + k_r)([10.3]_e - [10.3]) \quad (\underline{5})$$

Relating OD to [10.3]

(10.3) is the only absorbing species.

$$OD = \varepsilon_{10.3}[10.3] \quad (\underline{6})$$

At equilibrium,

$$OD_e = \varepsilon_{10.3}[10.3]_e \quad (\underline{7})$$

Subtracting (6) from (7).

$$OD_e - OD = \varepsilon_{10.3}([10.3]_e - [10.3]) \quad (\underline{8})$$

Differentiating (6)

$$\frac{d\,OD}{dt} = \varepsilon_{10.3}\frac{d[10.3]}{dt} \quad (\underline{9})$$

Substituting (9) into (8).

$$\frac{d\ OD}{dt} \cdot \frac{1}{OD_e - OD} = \frac{d[10.3]}{dt} \cdot \frac{1}{([10.3]_e - [10.3])} \qquad (10)$$

As k_{obs} is defined

$$k_{obs} = \frac{d\ OD}{dt} \cdot \frac{1}{OD_e - OD} \qquad (11)$$

Combining (11), (10) and (5) gives

$$k_{obs} = k_f[OH^-] + k_r.$$

$$(10.2) + 2OH^- \underset{k_{-1}}{\overset{k_1}{\rightleftharpoons}} (10.3) + OH^- \underset{k_{-2}}{\overset{k_2}{\rightleftharpoons}} (10.6)$$

$$\frac{d[10.6]}{dt} = k_2[10.3][OH^-] - k_{-2}[10.6] \qquad (12)$$

$$[10.2]_o = [10.2] + [10.3] + [10.6] \qquad (13)$$

$$K_1 = \frac{[10.3]}{[10.2][OH^-]} \qquad (14)$$

Substituting (14) into (13) and re-arranging.

$$[10.3] = \frac{[10.2]_o + [10.5]}{1+K_1[OH^-]} \qquad (15)$$

Substituting (15) into (12).

$$\frac{d[10.6]}{dt} = k_2[OH^-]\left(\frac{[10.2]_o - [10.6]}{1+K_1[OH^-]}\right) - k_{-2}\ [10.6] \qquad (16)$$

At equilibrium, $\frac{d[10.6]}{dt} = 0$

$$0 = k_2[OH^-]\left(\frac{[10.2]_o - [10.6]_e}{1 + K_1[OH^-]}\right) - k_{-2}[10.6]_e \qquad (17)$$

Subtracting (17) from (16)

$$\frac{d[10.6]}{dt} = \left(\frac{k_2[OH^-]}{1+K_1[OH^-]} + k_{-2}\right)\ ([10.6]_e - [10.6]) \qquad (18)$$

Relating OD to [10.6]

At the wavelength at which the reaction was studied, (10.3) and (10.6) are the species that absorb.

$$OD = \varepsilon_{10.3}[10.3] + \varepsilon_{10.6}[10.6] \qquad (19)$$

Substituting (15) into (19).

$$OD = \varepsilon_{10.3} \frac{[10.2]_o - [10.6]}{1+K_1[OH^-]} + \varepsilon_{10.6}[10.6]$$

Re-arranging,

$$OD = [10.6]\left(\varepsilon_{10.6} - \frac{\varepsilon_{10.3}}{1+K_1[OH^-]}\right) + A \qquad (20)$$

$$\text{where } A = \frac{\varepsilon_{10.3}[10.2]_o}{1+K_1[OH^-]}$$

At equilibrium,

$$OD_e = [10.6]_e\left(\varepsilon_{10.6} - \frac{\varepsilon_{10.3}}{1+K_1[OH^-]}\right) + A \qquad (21)$$

Differentiating (20)

$$\frac{d\ OD}{dt} = \frac{d[10.6]}{dt}\left(\varepsilon_{10.6} - \frac{\varepsilon_{10.3}}{1+K_1[OH^-]}\right) \qquad (22)$$

Subtracting (20) from (21) and combining with (22)

$$\frac{d\ OD}{dt} \cdot \frac{1}{OD_e - OD} = \frac{d[10.6]}{dt} \cdot \frac{1}{([10.6]_e - [10.6])} \qquad (23)$$

k_{obs} is defined thus,

$$k_{obs} = \frac{d\ OD}{dt} \cdot \frac{1}{OD_e - OD} \qquad (24)$$

Combining (18), (23) and (24) gives

$$k_{obs} = \frac{k_2[OH^-]}{1+K_1[OH^-]} + k_{-2}$$

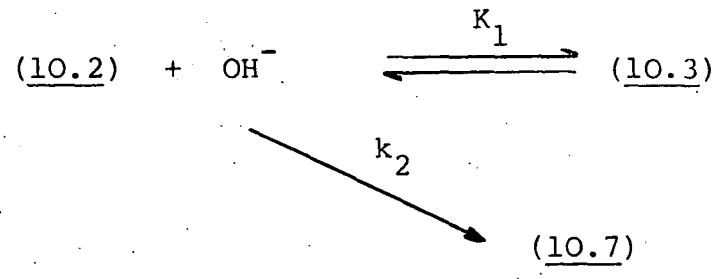

$$\frac{d[10.7]}{dt} = k_2[10.2][OH^-] \qquad (25)$$

$$[10.2]_o = [10.2] + [10.3] + [10.7] \qquad (26)$$

Substituting (14) into (26) and re-arranging

$$[10.2] = \frac{[10.2]_o - [10.7]}{1+K_1[OH^-]} \qquad (27)$$

Substituting (27) into (25)

$$\frac{d[10.7]}{dt} = k_2[OH^-]\left(\frac{[10.2]_o - [10.7]}{1 + K_1[OH^-]}\right) \qquad (28)$$

At equilibrium, $\frac{d[10.7]}{dt} = 0$

$$0 = k_2[OH^-]\left(\frac{[10.2]_o - [10.7]_e}{1 + K[OH^-]}\right) \qquad (29)$$

Subtracting (29) from (28)

$$\frac{d[10.7]}{dt} = \frac{k_2[OH^-]}{1+K_1[OH^-]} ([10.7]_e - [10.7])$$

[10.7] is related to OD in an analogous way as above. Therefore,

$$k_{obs} = \frac{k_2[OH^-]}{1+K_1[OH^-]}$$

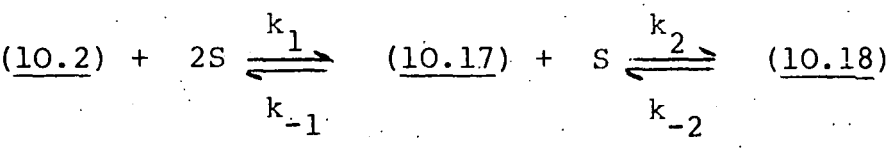

$$\frac{d[10.18]}{dt} = k_2[10.17][S] - k_{-2}[10.18] \qquad (30)$$

$$[10.2]_o = [10.2] + [10.17] + [10.18] \qquad (31)$$

$$K_1 = \frac{[10.17]}{[10.2][S]} \qquad (32)$$

Substituting (32) into (31) and re-arranging,

$$[10.17] = ([10.2]_o - [10.18]) \frac{K_1[S]}{1+K_1[S]} \qquad (33)$$

Substituting (33) into (30)

$$\frac{d[10.18]}{dt} = \frac{k_2K_1[S]^2}{1+K_1[S]} ([10.2]_o-[10.18]) - k_{-2}[10.18] \qquad (34)$$

At equilibrium, $\frac{d[10.18]}{dt} = 0$

$$0 = \frac{k_2K_1[S]^2}{1+K_1[S]} ([10.2]_o - [10.18]_e) - k_{-2}[10.18]_e \qquad (35)$$

Subtracting (35) from (34)

$$\frac{d[10.18]}{dt} = \left(\frac{k_2K_1[S]^2}{1+K_1[S]} + k_{-2}\right) ([10.18]_e-[10.18]) \qquad (36)$$

Using a method analogous to that described earlier [10.18] can be related to OD. Therefore it can be shown

$$k_{obs} = \frac{k_2K_1[S]^2}{1+K_1[S]} + k_{-2}.$$

$$(10.2) + S \underset{}{\overset{K_1}{\rightleftharpoons}} (10.17)$$

$$(10.17) + S \underset{}{\overset{K_2}{\rightleftharpoons}} (10.18)$$

$$(10.17) \underset{k_{-3}}{\overset{k_3}{\rightleftharpoons}} (10.19)$$

$$\frac{d[10.19]}{dt} = k_3[10.17] - k_{-3}[10.19] \qquad (37)$$

$$[10.2]_o = [10.2] + [10.17] + [10.18] + [10.19] \qquad (38)$$

Substituting (32) into (38)

$$[10.2]_o = \frac{[10.17]}{K_1[S]} + [10.17] + [10.18] + [10.19] \qquad (39)$$

$$K_2' = \frac{[10.18]}{[10.17][S]} \qquad (40)$$

Substituting (40) into (39)

$$[10.2]_o = [10.17]\left(\frac{K_1[S] + 1}{K_1[S]}\right) + K_2[S][10.17] + [10.19]$$

Re-arranging

$$[10.17] = ([10.2]_o - [10.19])\left(\frac{K_1[S]}{1+K_1[S](1+K_2[S])}\right) \quad (41)$$

Substituting (41) into (37)

$$\frac{d[10.19]}{dt} = \frac{k_3K_1[S]}{1+K_1[S](1+K_2[S])}([10.2]_o-[10.19])-k_{-3}[10.19] \quad (4$$

At equilibrium, $\frac{d[10.19]}{dt} = 0$

$$0 = \frac{k_3K_1[S]}{1+K_1[S](1+K_2[S])}([10.2]_o-[10.19]_e) - k_{-3}[10.19]_e \quad (43)$$

Subtracting (43) from (42).

$$\frac{d[10.19]}{dt} = \left(\frac{k_3K_1[S]}{1+K_1[S](1+K_2[S])} + k_{-3}\right)([10.19]_e-[10.19])$$

By analogous methods to those shown previously [10.19] can be related to OD in the following way,

$$\frac{d\ OD}{dt} \cdot \frac{1}{OD_e-OD} = \frac{d[10.19]}{dt} \cdot \frac{1}{([10.19]_e-[10.19])}$$

As k_{obs} is defined thus,

$$k_{obs} = \frac{d\ OD}{dt} \cdot \frac{1}{OD_e-OD}$$

Therefore,

$$k_{obs} = \frac{k_3K_1[S]}{1+K_1[S](1+K_2[S])} + k_{-3}$$

(10.2) + S $\underset{}{\overset{k_1}{\rightleftharpoons}}$ (10.17)

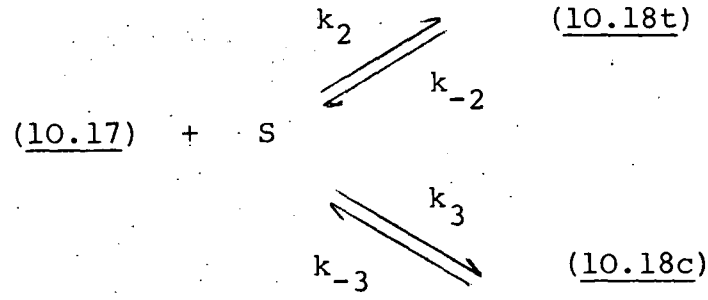

$$\frac{d[10.18c]}{dt} = k_3[10.17][S] - k_{-3}[10.18c] \quad (44)$$

$$[10.2]_o = [10.2] + [10.17] + [10.18c] + [10.18t] \quad (45)$$

$$K_1 = \frac{[10.17]}{[10.2][S]} \quad (46)$$

$$K_2 = \frac{[10.18t]}{[10.17][S]} \quad (47)$$

Substituting (46) and (47) into (45) and re-arranging,

$$[10.17] = \frac{([10.2]_o - [10.18c])\ K_1[S]}{1+K_1[S](1+K_2[S])} \quad (48)$$

Substituting (48) into (44)

$$\frac{d[10.18c]}{dt} = \frac{k_3K_1[S]^2}{1+K_1[S](1+K_2[S])}([10.2]_o-[10.18c])-k_{-3}[10.18c] \quad (49$$

At equilibrium, $\frac{d[10.18c]}{dt} = 0$

$$0 = \frac{k_3K_1[S]^2}{1+K_1[S](1+K_2[S])}([10.2]_o-[10.18c]_e)-k_{-3}[10.18c]_e \quad (50)$$

Subtracting (50) from (49),

$$\frac{d[10.18c]}{dt} = \left(\frac{k_3K_1[S]^2}{1+K_1[S](1+K_2[S])} + k_{-3}\right)([10.18c]_e-[10.18])$$

By analogous methods to those shown previously [10.18c] can be related to OD in the following way,

$$\frac{d\ OD}{dt} \cdot \frac{1}{OD_e-OD} = \frac{d[10.18c]}{dt}\ \frac{1}{([10.18c]_e-[10.18c])}$$

As k_{obs} is defined thus,

$$k_{obs} = \frac{d\ OD}{dt} \cdot \frac{1}{(OD_e - OD)}$$

Therefore,

$$k_{obs} = \frac{k_3 K_1 [S]}{1+K_1[S](1+K_2[S])} + k_{-3}.$$

APPENDIX

a. Research Colloquia and Seminars organised by the Department of Chemistry during the period 1980-1983

(* denotes those attended)

*
7 October 1980

Professor T. Fehler (Notre Dame University, Indiana, U.S.A.) "Metalloboranes - Cages or Coordination Compounds?"

15 October 1980

Dr. R. Alder (University of Bristol), "Doing Chemistry Inside Cages - Medium Ring Bicyclic Molecules".

*
12 November 1980

Dr. M. Gerloch (University of Cambridge), "Magnetochemistry is about Chemistry".

*
19 November 1980

Dr. T. Gilchrist (University of Liverpool), "Nitroso olefins as Synthetic Intermediates".

*
3 December 1980

Dr. J.A. Connor (University of Manchester), "Thermochemistry of Transition Metal Compounds".

18 December 1980

Dr. R.F. Evans, "Some Recent Communications to the Editor of the Australian Journal of Failed Chemistry".

*
18 February 1981

Professor S.F.A. Kettle (University of East Anglia), "Variations in the Molecular Dance at the Crystal Ball".

*
25 February 1981

Dr. K. Bowden (University of Essex), "The Transmission of Polar Effects of Substituents".

*4 March 1981

Dr. S. Craddock (University of Edinburgh), "Pseudo-linear pseudohalides".

11 March 1981

Dr. J.F. Stoddart (I.C.I. Ltd./University of Sheffield), "Stereochemical Principles in the Design and Function of Synthetic Molecular Receptors".

*17 March 1981

Professor W. Jencks (Brandeis University, Massachusetts), "When is an intermediate not an intermediate?".

18 March 1981

Dr. P.J. Smith (International Tin Research Institute), "Organotin Compounds - A Versatile Class of Organometallic Derivatives".

9 April 1981

Dr. W.H. Meyer (RCA Zurich), "Properties of Aligand Polyacetylene".

*6 May 1981

Professor M. Szware, F.R.S. "Ions and Ion pairs".

10 June 1981

Dr. J. Rose (I.C.I. Plastics Division), "New Engineering Plastics".

17 June 1981

Dr. P. Moreau (University of Montpellier), "Recent Results in Perfluoroorganometallic Chemistry".

26 June 1981

Professor A.P. Schaap (U.S. Office of Naval Research, Londc "Mechanisms of Chemiluminescence and Photooxygenation".

14 October 1981

Professor E. Kluk (University of Katowice, Poland), "Some Aspects of the Study of Molecular Dynamics in Simple Molecular Liquids".

*28 October 1981

Dr. R.J.H. Clark (University College, London), "Resonance Raman Spectroscopy - A New Technique for Chemical, Spectroscopic and Structural Studies".

*6 November 1981

Dr. W. Moddeman (Monsanto Research Laboratories, St. Louis, Missouri), "High Energy Materials".

*18 November 1981

Professor M.J. Perkins (Chelsea College), "Spin Trapping and Nitroxide Radicals".

25 November 1981

Dr. M. Baird (University of Newcastle), "Intramolecular Reactions of Carbenes and Carbenoids".

2 December 1981

Dr. G. Beamson (University of Durham), "Photoelectron Spectroscopy in a Strong Magnetic Field".

20 January 1982

Dr. M.R. Bryce (University of Durham), "Organic Metals".

*27 January 1982

Dr. D.L.H. Williams (University of Durham), "Nitrosation of Nitrosamines".

*3 February 1982

Dr. D. Parker (University of Durham), "Modern Methods for the Determination of Enantiometric Purity".

10 February 1982

Dr. D. Pethrick (University of Strathclyde), "Conformational Dynamics of Small and Large Molecules".

*17 February 1982

Professor D.T. Clark (University of Durham), "Structure, Bonding, Reactivity and Synthesis of Surfaces as revealed by E.S.C

24 February 1982

Dr. L. Field (University of Oxford), "The Application of N.M.R. Methods to the Study of Penicillin Biosynthesis".

3 March 1982

Dr. P. Bamfield (I.C.I. Organics Division), "Computer Aided Synthesis Design: A View from Industry".

*17 March 1982

Professor R.J. Haines (University of Cambridge/University of Nata "Clustering around Ruthenium, Iron and Rhodium".

7 April 1982

Dr. D.A. Pensak (E.I. Dupont de Nemours and Company, Delaware, U.S.A.), "Computer Aided Synthesis".

*23 April 1982

Mr. R.S. Crespi (Patents Controller, British Technology Grou "Patents in Chemistry and Related Disciplines".

*5 May 1982

Dr. G. Tennant (University of Edinburgh), "Exploitation of the Aromatic Nitro-group in the Design of New Heterocyclisation Reactions".

12 May 1982

Dr. C.D. Garner (University of Manchester), "The Structure and Function of Molybden Centres in Enzymes".

*19 May 1982

Professor R.D. Chambers (University of Durham), "Fluorocarbanions - Some Alice in the Looking Glass Chemistry".

26 May 1982

Dr. A. Welch (University of Edinburgh), "Conformation Patterns and Distortions in Carbometallaboranes".

*14 June 1982

Professor C.J.M. Stirling (University College of Wales, Bang "How much does Strain affect Reactivity?".

28 June 1982

Professor D.J. Burton (University of Iowa, U.S.A.), "Some Aspects of the Chemistry of Fluorinated Phosphonium Salts and Phosphates".

*2 July 1982

Professor H.F. Koch (Ithaca College, U.S.A.), "Proton Transfer to and Elimination Reactions from Localised and Delocalised Carbanions".

*27 September 1982

Dr. W.K. Ford (Xerox Research Centre, Webster, New York), "The Dependence of Electronic Structure of Polymers on their Molecular Architecture".

13 October 1982

Dr. W.J. Feast (University of Durham), "Approaches to the Synthesis of Conjugated Polymers".

14 October 1982

Professor H. Suhr (University of Tübingen), "Preparative Chemistry in Non-Equilibrium Plasmas".

*27 October 1982

Dr. C.E. Housecroft (Oxford High School and Notre Dame University), "Bonding Capabilities of Butterfly-shaped Fe_4 Units Implications for C-H Bond Activation in Hydrocarbon Complexes".

28 October 1982

Professor M.F. Lapport, F.R.S. (University of Sussex), "Approaches to Asymmetric Synthesis and Catalysis using Electron-rich Olefins and Some of their Metal Complexes".

15 November 1982

Dr. G. Betrand (Universite Paul Sabatier, Toulouse), "Curtius Rearrangement in Organometallic Series: A Route for New Hybridised Species".

*24 November 1982

Professor F.R. Hartley (R.M.C.S., Shrivenham), "Supported Metal Complex Hydroformylation Catalysts: A Novel Approach using γ-radiation".

*24 November 1982

Professor G.G. Roberts (Department of Applied Physics, University of Durham), "Langmuir - Blodgett Films".

*2 December 1982

Dr. G.M. Brooke (University of Durham), "The Fate of the Ortho-fluorine in 3,3-sigmatropic Reactions involving Polyfluoro-aryl and heteroaryl-systems".

*8 December 1982

Dr. G. Woolley (Trent Polytechnic), "Bonds in Transition Metal Cluster Compounds".

12 January 1983

Dr. D.C. Sherington (University of Strathclyde), "Polymer-supported Phase Transfer Catalysts".

*9 February 1983

Dr. P. Moore (University of Warwick), "Mechanistic Studies in Solution by Stopped-Flow F.T. N.M.R. and High Pressure N.M.R. Line Broadening".

21 February 1983

Dr. R. Lyndon-Bell (University of Cambridge), "Molecular motion in the Cubic Phase of NaCN".

2 March 1983

Dr. D. Bloor (Queen Mary College, University of London), "The Solid-State Chemistry of Diacetylene Monomers and Polymers".

8 March 1983

Professor D.C. Bradley, F.R.S. (Queen Mary College, University of London), "Recent Developments in Organo-Imido-Transition Metal Chemistry".

*9 March 1983

Dr. D.M.J. Lilley (University of Dundee), "DNA, Sequence, Symmetry, Structure and Supercooling".

11 March 1983

Professor H.G. Viehe (University of Louvain), "Oxidation of Sulphur".

16 March 1983

Dr. I. Gosney (University of Edinburgh), "New Extrusions Reactions: Organic Synthesis in a Hot Tube".

25 March 1983

Professor F.G. Baglin (University of Nevada), "Interaction Induced Raman Spectroscopy in Supracritical Ethane".

21 April 1983

Professor J. Passmore (University of New Brunswick), "Novel Selenium - Iodine Cations".

4 May 1983

Professor P.H. Plesch (University of Keele), "Binary Ionisation Equilibria between Two Ions and Two Molecules. What Ostwald never thought of".

*10 May 1983

Professor K. Berger (University of Munich), "New Reaction Pathways from Trifluoromethyl-Substituted Keterodienes to Partially Fluorinated Heterocyclic Compounds".

*11 May 1983

Dr. N. Isaacs (University of Reading), "The Application of High Pressures to the Theory and Practice of Organic Chemistry".

*13 May 1983

Dr. R. de Kock (Calvin College, Grand Rapids, Michigan/ The Free University, Amsterdam), "Electronic Structural Calculations on Organometallic Cobalt Cluster Molecules: Implications for Metal Surfaces".

13 May 1983

Dr. T.B. Marder (U.C.L.A./University of Bristol), "The Chemistry of Metal-Carbon and Metal-Metal Multiple Bonds".

16 May 1983

Dr. D.M. Adams (University of Leicester), "Spectroscopy at Very High Pressures".

18 May 1983

Professor R.J. Lagow (University of Texas), "The Chemistry of Polylithium Organic Compounds: An Unusual Class of Matter".

*
25 May 1983

Professor J.M. Vernon (University of York),
"New Heterocyclic Chemistry Involving Lead Tetra-acetate".

15 June 1983

Dr. A. Pietrzykowski (Technical University of Warsaw/ University of Strathclyde),
"Synthesis, Structure and properties of Aluminoxanes".

22 June 1983

Dr. D.W.H. Rankin (University of Edinburgh),
"Floppy Molecules - The Influence of Phase on Structure".

*
5 July 1983

Professor J. Miller (University of Campinas, Brazil),
"Reactivity in Nucleophilic Substitution Reactions".

b. Conferences attended during the period 1980-1983

(i) The Royal Society of Chemistry Fast Reactions in Solutions Group, University of Cardiff, 9-11 September 198

(ii) Graduate Symposium, University of Durham, 21 April 1982.

(iii) The Royal Society of Chemistry Third International Conference on the Mechanisms of Reactions in Solution, University of Kent, 5-9 July 1982.

(iv) Graduate Symposium, University of Durham, 15 April 1983.

(v) The Royal Society of Chemistry Tenth Anniversary Meeting of the Reaction Mechanisms Group on the Selectivity, Reactivity and Structure in Organic Reactions, St. Patrick's College, Maynooth, Ireland, 12-15 July 1983.

c. First year induction course (6 October - 7 November 1980)

A series of one hour presentations on the services available in the Department of Chemistry.

(i) Departmental Organisation.

(ii) Safety Matters.

(iii) Electrical Appliances and Infrared Spectroscopy.

(iv) Chromatography and Microanalysis.

(v) Library Facilities.

(vi) Atomic Absorptiometry and Inorganic Analysis.

(vii) Mass Spectrometry.

(viii) Safety Lecture.

(ix) N.M.R. Spectroscopy.

(x) Glassblowing Technique.

REFERENCES

1. K.G. Shipp, J.Org.Chem., 1964, 29, 2620.

2. K.G. Shipp and L.A. Kaplan, J.Org.Chem., 1966, 31, 857.

3. J.S. Back, J.L. Soderburg and C.L.Hakanson, U.K. Patent 1,249,038, 1971.

4. E.E. Kilmer, J. Spacecraft 10, 1973, 7, 463.

5. D.F. Hoeg and D.I. Lusk, J.Am.Chem.Soc., 1964, 86, 928.

6. D. Bethell and R. Bird, J.Chem.Soc., Perkin Trans.2, 1977, 1856.

7. K.L. Servis, J.Am.Chem.Soc., 1967, 89, 1508

8. R. Bird, unpublished M.o.D. (P.E.R.M.E.) report.

9. P. Golding, Personal Communication.

10. R. Bird and A.E. Webb, U.K. Patent Appl.No. 9077/78, March 1978.

11. D.A. Salter, N.F. Scilly and K.E. Watson, U.S. Patent 1,513,221, June 1978.

12. G.P. Sollot, J.Org.Chem., 1982, 47, 2471.

13. P. Golding and G.F. Hayes, U.K. Patent Appl.No. 7,910,361,19

14. P. Hepp, Ann., 1882, 215, 344.

15. C.A. Lobry de Bruyn and F.H. van Leent, Rec.Trav.Chim., 1895, 14, 89, 150.

16. F.H. van Leent, Rec.Trav.Chim., 1896, 15, 89.

17. C.L. Jackson and W.F. Boos, Amer.Chem.J., 1898, 20, 444.

18. A. Hantzsch and H. Kissel, Ber., 1899, 32, 3137.

19. C.L. Jackson and F.H. Gazzolo, Amer.Chem.J., 1900, 23, 376.

20. J. Meisenheimer, Justus Liebigs.Ann.Chem., 1902, 323, 205.

21. C.L. Jackson and R.B. Earle, Amer.Chem.J., 1903, 29, 89.

22. J.F. Bunnett and R.E. Zahler, Chem.Rev., 1951, 49, 273.

23. J.F. Bunnett, Q.Rev.Chem.Soc., 1958, 12, 1.

24. R. Foster and C.A. Fyfe, Rev.Pure and Appl.Chem., 1966, 16, 61.

25. M.R. Crampton, Adv.Phys.Org.Chem., 1969, 7, 211.

26. M.J. Strauss, Chem.Rev., 1970, 70, 667.

27. F. Terrier, Chem.Rev., 1982, 82, 78.

28. G. Artamkina, M.P. Egorov and I.P. Beletskaya, Chem.Rev., 1982, 82, 427.

29. "Electron Deficient Aromatic- and Heteroaromatic-Base Interactions. The Chemistry of Anionic Sigma Complexes", Elsevier Scientific Publishing Company, 1984.

30. S. Sekiguchi, Yuki Gosei Kagaku Kyokaishi, 1979, 36, 633.

31. S. Carra, M. Raimondi and M. Simonetta, Tetrahedron, 1966, 22, 2673; P. Beltrame, P.L. Beltrame and M. Simonetta, Tetrahedron, 1968, 24, 3403.

32. P. Caveng, P.B. Fischer, E. Heilbronner, A.L. Miller and H. Zollinger, Helv.Chim.Acta., 1967, 50, 848.

33. R. Destro, C. Cramaccioli and M. Simonetta, Acta.Crystallogr., 1968, B24, 1369.

34. H. Hosaya, S. Hosaya and S. Nagakura, Theor.Chim.Acta., 1968, 12, 117.

35. H. Wennerström and O. Wennerström, Acta.Chem.Scand., 1972, 26, 2883.

36. S. Sekiguchi, T. Hirose, K. Tsutsumi, T. Aizawa and H. Shizuka, J.Org.Chem., 1979, 44, 3921.

37. K.B. Lipkowitz, J.Am.Chem.Soc., 1982, 104, 2647.

38. L. Radom, "Modern Theoretical Chemistry, vol.4, Applications of Electronic Structure Theory", Ed.H.F. Shafer, Plenum, New York, 1977, 333.

39. W.J. Here, R.F. Stewart and J. Pople, J.Chem.Phys., 1969, 51, 2657.

40. A.J. Birch, A.L. Hinde and L. Radom., J.Am.Chem.Soc., 1980, 102, 6430.

41. J. Burdon, I.W. Parsons and E.J. Avramides, J.Chem.Soc., Perkin Trans.1, 1979, 1268.

42. J. Burdon, I.W. Parsons and E.J. Avramides, J.Chem.Soc., Perkin Trans.2, 1979, 1201.

43. R.D. Gandour, Tetrahedron, 1980, 36, 1001.

44. A. Counotte-Potman, H.C. van der Plas and B. van Velhiuzen, J.Org.Chem., 1981, 46, 2138.

45. H. Veda, N. Sakabe, J. Tanaka and A. Fursisaki, Bull.Chem. Soc.Jap., 1968, 41, 2866.

46. G.G. Messmer and G.J. Palenik, Chem.Commun., 1969, 470.

47. C.M. Gramaccioli, R. Destro and M. Simonetta, Acta Crystallogr. 1968, 24, 129.

48. A.R. Norris, J.Org.Chem., 1969, 34, 1486.

49. R.A. Henry, J.Org.Chem., 1962, 27, 2637.

50. A.R. Norris, Can.J.Chem., 1967, 45, 175.

51. M. Kimura, M. Kawata, M. Nakadate, N. Obi and M. Kawazoe, Chem.Pharm.Bull.Jap., 1968, 16, 634.

52. A.R. Norris and H.F. Shurvell, Can.J.Chem., 1969, 47, 4267.

53. S.S. Gitis and A. Ya. Kaminski, J.Gen.Chem.U.S.S.R., 1964, 34, 3974.

54. R. Foster and R.K. Mackie, J.Chem.Soc., 1963, 708.

55. R. Foster and D.L. Hammick, J.Chem.Soc., 1954, 2153.

56. L.K. Dyall, J.Chem.Soc., 1960, 5160.

57. L.K. Dyall, Spectrochem.Acta., 1966, 22, 467.

58. L.P. Olekhnovich, I.E. Mikhailov, V.I. Minkin, N.G.Furmanova, O.E. Kompan, Yu.T. Struchov and A.V. Lukash, Zh.Org.Khim., 1982, 18, 484.

59. M.R. Crampton and V. Gold, J.Chem.Soc., 1964, 4293.

60. M.R. Crampton and V. Gold, J.Chem.Soc.(B), 1966, 893.

61. V. Gold and C.H. Rochester, J.Chem.Soc., 1964, 1687.

62. R. Foster and R.K. Mackie, J.Chem.Soc., 1963, 3796.

63. M.R. Crampton, J.Chem.Soc.(B), 1967, 1341.

64. J.F. McGarrity, J. Prodolliet and T. Smyth, Org.Magn. Resonance, 1981, 17, 59.

65. G.A. Olah and H. Mayr, J.Org.Chem., 1976, 41, 3448.

66. V. Macháček, V. Štěrba, A. Lyčka and D. Snobl, J.Chem.Soc., Perkin Trans.2, 1982, 355.

67. N.V. Ignat'ev and V.N. Boiko, Zh.Org.Khim., 1981, 17, 1948.

68. K.G. Shipp, L.A. Kaplan and M.E. Sitzman, J.Org.Chem., 1966, 37, 1972.

69. S.S. Kravtsova, G.L. Ryzkova and T.T. Kuryaeva, Deposited Doc., 1980, SPSTL 797 khp-D80.

70. S. Ohsawa and M. Takeda, Ibarski Daigaku Kogakubu Kenkyu Shuho, 1980, 28, 101.

71. S.S. Gitis, A.Ya.Kaminski, A.I. Glaz, L.N. Savinova and T.V. Golopolosova, Dokl.Akad.Nauk.U.S.S.R., 1981, 260, 365.

72. T. Abe, Bull.Chem.Soc.Japan, 1964, 37, 508.

73. T. Abe, Bull.Chem.Soc.Japan, 1966, 39, 627.

74. M.J. Willison, Ph.D. Thesis (Durham), 1975, 49.

75. C.F. Bernasconi, "Relaxation Kinetics", Academic Press, New York, 1976.

76. H.A. Benesi and J.H. Hildebrand, J.Am.Chem.Soc., 1949,71,2703.

77. W.A. Shepherd, J.Am.Chem.Soc., 1963, 85, 1314.

78. C.F. Bernasconi, J.Am.Chem.Soc., 1970, 92, 4682.

79. J. Miller, "Aromatic Nucleophilic Substitution", Elsevier, Amsterdam,19

80. J.H. Fendler, E.J. Fendler and C.E. Griffin, J.Org.Chem., 1969, 34, 689.

81. J.H. Fendler, E.J. Fendler, C.E. Griffin and J.W. Larsen, J.Org.Chem., 1970, 35, 287.

82. D.N. Brooke, M.R. Crampton, G.C. Corfield, P. Golding and G.F.Hayes, J.Chem.Soc., Perkin Trans.2, 1981, 526.

83. D.N. Brooke and M.R. Crampton, J.Chem.Res., 1980 (S) 340, (M) 4401.

84. M.R. Crampton, J.Chem.Soc.(B), 1968, 1208.

85. M.R. Crampton and H.A. Khan, J.Chem.Soc., Perkin Trans.2, 1972, 2286; *ibid*, 1973, 1103.

86. E. Buncel and W. Eggiman, J.Chem.Soc., Perkin Trans.2, 1978, 673.

87. E. Buncel, A.R. Norris and K.E. Russell, Quart.Rev.(London), 1968, 22, 123.

88. V. Meyer, Ber., 1894, 27, 3153; V. Meyer, Ber., 1896,29, 848.

89. R.J. Politt and B.C. Saunders; Proc.Chem.Soc., 1962, 176.

90. E. Buncel and E.A. Symons, Can.J.Chem., 1966, 44, 771.

91. M.R. Crampton and V. Gold, J.Chem.Soc.B., 1966, 498.

92. D.N. Brooke and M.R. Crampton, J.Chem.Soc., Perkin Trans.2, 1982, 231.

93. E. Buncel, A.R. Norris, K.E. Russell, P. Sheridan and H. Wilson, Can.J.Chem., 1974, 52, 1750, 2306; C.F. Bernasconi, J.Org.Chem., 1971, 36, 1671.

94. E. Buncel, A.R. Norris, K.E. Russell and R. Tucker, J.Am.Chem.Soc., 1972, 94, 1646.

95. R.S. Mulliken, J.Am.Chem.Soc., 1952, 74, 811.

96. J. Weiss, J.Chem.Soc., 1942, 245.

97. G. Briegleb, "Elektronnen Donator-Akzeptor Komplexe", Springer Verlag, Berlin; G. Briegleb, Angew.Chemie. Internat.Edn., 1964, 3, 617.

98. G.A. Russell and E.G. Janzen, J.Am.Chem.Soc., 1962, 84, 4153

99. G.A. Russell, E.G. Janzen and E.T. Strom, J.Am.Chem.Soc., 1964, 86, 1807.

100. G.A. Russell and E.G. Janzen, J.Am.Chem.Soc., 1967, 89, 300.

101. I.I. Bilkis and S.M. Shein, Tetrahedron, 1975, 31, 969.

102. J.F. Bunnett and A.V. Carteno, J.Am.Chem.Soc., 1981, 103, 48

103. J.F. Bunnett, S. Sekiguchi and L.A. Smith, J.Am.Chem.Soc., 1981, 103, 4865.

104. N. Marendi and A.R. Norris, Can.J.Chem., 1973, 95, 3927.

105. F. Terrier, C. Ah-Khow, M.J. Pouet and M.P. Simonnin, Tett.Let., 1976, 227.

106. Full reference list contained in reference 28.

107. E.G. Kaminskaya, S.S. Gitis and A.Ya.Kiminsky, Zh.Org.Khim., 1979, 15, 793.

108. P.P. Onys'ko and Yu.G. Gololobov, Zh.Obsch Khim., 1980, 50, 729

109. Full reference list contained in reference 27.

110. K.A. Kovar, Pharm., Unserer Z., 1972, 1, 17.

111. P.J. Atkins and V. Gold, J.Chem.Soc., Chem.Commun., 1983, 140.

112. S.S. Gitis, A.Ya. Kiminsky, Yu.D. Grudtsyn and E.E.Gol'teuzen Dokl.Akad.Nauk.U.S.S.R., 1972, 206, 102.

113. E.E. Gol'teuzen, Yu.D. Grudtsyn, S.S. Gitis and A.Ya Kiminsky, Zh.Org.Khim., 1972, 8, 1916.

114. M.P. Egorov, G.A. Artamkina, I.P. Beletskaya and O.A.Reutov, Izv.Akad.Nauk.U.S.S.R. Ser.Khim., 1978, 2431.

115. R.D. Taylor, J.Chem. Soc., Chem.Commun., 1970, 1463.

116. G.A. Artamkina, M.P. Egorov, I.P. Beletskaya and O.A. Reutov, Zh.Org.Khim., 1978, 14, 1350; G.A.Artamkina M.P. Egorov, I.P. Beletskaya and O.A. Reutov, J.Organomet.Chem., 1979, 182, 185.

117. E.F. Caldin and G. Long, Proc.R.Soc.(London), Ser.A, 1955, 226, 263.

118. J.B. Ainscough and E.F. Caldin, J.Chem.Soc., 1956, 2540.

119. V.N. Knyazev, V.N. Drozd and V.M. Minov, J.Org.Chem.U.S.S.R., 1978, 14, 95.

120. D.V. Roberts, "Enzyme Kinetics", Cambridge University Press, 136.

121. "Dictionary of Organic Compounds", 4th Edn., London, Eyre and Spottiswoode, 1965.

122. A. Hantsch and H. Gorke, Ber., 1906, 39, 1097.

123. J.A. Orvik and J.F. Bunnett, J.Am.Chem.Soc., 1960, 82, 665.

124. R.C. Weast (Ed.), "Handbook of Chemistry and Physics", 60th Edn., CRC Press, 1979.

125. E.A. Guggenheim, Phil.Mag., 1926, 2, 538.

126. J.W. Moore and R.G. Pearson, "Kinetics and Mechanism", 3rd Edn., John Wiley and Sons, 1981, 70.

127. F.J. Kezdy, J. Jaz and A. Bruylants, Bull.Soc.Chim.Belg., 1958, 67, 687.

128. E.S. Swinbourne, J.Chem.Soc., 1960, 2371.

129. M.R. Crampton and V. Gold, J.C.S.Chem.Commun., 1965, 543.

130. M.R. Crampton and M.J. Willison, J.Chem.Soc., Perkin Trans.2, 1976, 155.

131. M.R. Crampton and M.J. Willison, J.Chem,Soc., Perkin Trans.2, 1974, 1681, 1686.

132. C.F. Bernasconi and J.R. Gandler, J.Org.Chem., 1977, 42, 3387

133. J.H. Fendler, E.J. Fendler, W.E. Byrne and C.E. Criffin, J.Org.Chem., 1968, 33, 977, 4141.

134. J. Murto, "Chemistry and the Hydroxyl Group", Interscience, New York, 1971, part 2, 1087.

135. M.R. Crampton, P.J. Routledge and P.M. Wilson, J.Chem,Res., 1981, (S) 152 (M) 1972.

136. P. Ballinger and F.A. Long, J.Am.Chem.Soc., 1960, 82, 795.

137. G.B. Barlin and D.D. Perrin, Quart Rev., 1966, 20, 75.

138. B. Capon and S.P. McManus, "Neighbouring Group Participation' Vol.1, Plenum, New York, 1976.

139. N.L. Allinger and V. Zalkov, J.Org.Chem., 1960, 25, 701.

140. B. Gibson and M.R. Crampton, J.Chem.Soc., Perkin Trans.2, 1979, 648.

141. G.P. Sollott, M. Warman and E.E. Gilbert, J.Org.Chem., 1979, 44, 3329.

142. C.A. Fyfe, C.D. Malkiewich, S.W.H. Damji and A.R. Norris, J.Am.Chem.Soc., 1976, 98, 6983.

143. E.E. Kilmer, J. Spacecraft, 1968, 5, 1216.

144. D.J. Kroeger and R. Stewart, Can.J.Chem., 1967, 45, 2163.

145. C.A. Fyfe, "Chemistry of the Hydroxyl Group", ed. S. Patai, Wiley-Interscience, New York, 1971, vol.1, 51.

146. C.A. Fyfe, Can.J.Chem., 1969, 47, 2331.

147. R.M. Silverstein, G.C. Bassler and T.C. Morrill, "Spectrometric Identification of Organic Compounds", Wiley, New York, 1976.

148. C.H. Rochester and B. Rossall, J.Chem.Soc.B, 1967, 743.

149. I thank Dr. B.C. Gilbert (University of York) for these measurements made at the request of the author and his supervisor.

150. G.P. Sollott, J.Org.Chem., 1966, 31, 857.

151. M.R. Crampton and C. Greenhalgh, J.Chem.Soc., Perkin Trans.2 1983, in the press.

152. M.R. Crampton and B. Gibson, J.Chem.Soc., Perkin Trans.2, 1981, 533.

153. C.F. Bernasconi, M.C. Muller and P. Schmid, J.Org.Chem., 1979, 44, 3189.

154. E. Buncel and W. Eggiman, J.Am.Chem.Soc., 1977, 99, 5958.

155. M.R. Crampton, J.Chem.Soc.(B), 1971, 2112.

156. E. Buncel and J.G.K. Webb, Can.J.Chem., 1974, 52, 630.

157. D.D. Perrin, "Dissociation Constants of Organic Bases", I.U.P.A.C. supplement 1972.

158. A. Mucci, R. Domain and R.L. Benoit, Can.J.Chem., 1980, 58, 953.

159. H.K. Hall, J.Org.Chem., 1964, 29, 3539.

160. G. Baldini, G. Doddi, G. Illuminati and F. Stegel, J.Org.Chem., 1976, 41, 2153.

161. S. Sekiguchi and J.F. Bunnett, J.Am.Chem.Soc., 1981, 103,487

162. D.N. Brooke and M.R. Crampton, J.Chem.Soc., Perkin Trans.2, 1980, 1850.

163. M.R. Crampton, B. Gibson and F.W. Gilmore, J.Chem.Soc., Perkin Trans.2, 1979, 91.

164. D.N. Brooke and M.R. Crampton, J.Chem.Soc., Perkin Trans. 2, 1982, 533.

165. H.C. Duffin and A.M. Jayaweera-Bandara, Kingston Polytechnic unpublished data.

166. Y. Hasegawa, Bull.Chem.Soc. Japan, 1983, 56, 1314.

167. A. Streitweiser Jr., Int.Symp.on Org.React.Mech., Kyushu University, Fukuoka, Japan, August 1982.

168. M. R. Crampton, J.Chem.Soc.(B), 1971, 2112.

169. T. Kompolthy, G. Bencz, J. Deres and L. Hajos, Hung.Teljes 9, 639 (Cl CO6 f), 28, April 1975.

170. Dr. B.C. Gilbert, personal communication; "Electron Spin Resonance in Chemistry", Peter B. Ayscough, Methuen, London, 1969, 270.

171. G. Bartoli and D.E. Todesco, Acc.Chem.Research, 1977, 10, 125.

172. M.M. Kreevoy and Y. Wang, J.Phys.Chem., 1977, 81, 1924.

173. J.J. Relpuech and B. Bianchiv, J.Am.Chem.Soc., 1979, 101, 383

174. C.D. Ritchie, J.Am.Chem.Soc., 1983, 105, 3573.

175. S. Patai and Z. Rappoport, "Chemistry of the Alkenes, Wiley Interscience, New York, 1974, 469.

176. C.F. Bernasconi and D.J. Carré, J.Am.Chem.Soc.,1979, 101, 2698

177. J.F. Bunnett and J. Randall, J.Am.Chem.Soc., 1958, 80, 6020.

178. C.F. Bernasconi, "MTP Int.Rev.Sci.: Org.Chem.,Ser.One", Butterworths, London, 1973, vol.3, 33.

179. C.F. Bernasconi, R.H. de Rossi and P. Schmid, J.Am.Chem.Soc. 1977, 99, 4090.

180. C.F. Bernasconi, Acc.Chem.Research, 1978, 11, 147.

181. D. Ayediran, T.O. Bamkole and J. Hirst, J.Am.Chem.Soc., 1981, 103, 1013.

182. J.A. Orvik and J.F. Bunnett, J.Am.Chem.Soc., 1970, 92, 2417.

183. C.A. Fyfe, A. Koll, S.W.H. Damji, C.D. Malkiewich and P.A. Forte, Chem.Comm., 1977, 335.

184. C.A. Fyfe, S.W.H. Damji and A. Koll, J.Am.Chem.Soc., 1979, 101, 951.

185. C.A. Fyfe, S.W.H. Damji and A. Koll, J.Am.Chem.Soc., 1979, 101, 956.

186. S. Sekiguchi, T. Itagaki, T. Hirose, K. Matsui and K. Sekine, Tettrahedron, 1973, 29, 3527.

187. C.A. Fyfe, A. Koll, S.W.H. Damji, C.D. Malkiewich and P.A. Forte, Can.J.Chem., 1977, 55, 1468.

188. M.R. Crampton and V. Gold, J.Chem,Soc.B, 1967, 23.

189. J.I. Brauman and L.K. Blair, J.Am.Chem.Soc., 1968, 90, 6561.

190. M.R. Crampton, J.Chem.Soc., Perkin Trans.2, 1978, 343.

191. C.F. Bernasconi and R.G. Bergstrom, J.Am.Chem.Soc., 1974, 96, 2397.

192. C.F. Bernasconi and R.G. Bergstrom, J.Org.Chem., 1971, 36, 1325.

193. D.N. Brooke, unpublished work.

194. F. Cuta and E. Beranek, Collect.Czech.Chem.Commun., 1958, 23, 1501.

195. C.F. Bernasconi and R.G. Bergstrom, J.Am.Chem.Soc., 1973, 95, 3603.

196. M. Sasaki, Chem.Lett., 1973, 205.

197. M.R. Crampton and M.A. El. Ghariani, J.Chem.Soc. (B), 1971, 1043.